# Investigating antagonism of innate immunity by HIV-1 accessory protein Vpr

Hataf Khan

Division of Infection and Immunity

University College London

A thesis submitted for the degree of

Doctor of Philosophy

July 2019

# Declaration

I, Hataf Khan, confirm that the work presented in this thesis is my own. Where information has been derived from other sources, I confirm that this has been indicated in the thesis.

# Acknowledgements

First and foremost, I would like to thank my supervisor Prof Greg Towers for all the guidance and support, and for the opportunity to undertake my PhD in his lab. I would like to acknowledge my thesis committee members Prof Prof Mahdad Noursadeghi, Dr Clare Jolly and Prof Ravi Gupta, who have also helped to guide this project. I would like to thank Dr Rebecca Sumner for teaching me all the lab skills and for being an outstanding mentor.

I would like to thank present and past members of the lab who supported me and patiently answered all my questions. Big thanks go to Petra, Lucy, Lorena, Jane, Chris and Che. I thank Doug for the positivity, late-night science discussions and “debriefing sessions”. I thank Stephen, Lauren, Liane and David for all the entertainment and fun times. I thank Liora and Lara, who I supervised for their research projects, for giving me the most rewarding moments during my PhD.

Most importantly, I would like to thank my family and friends, particularly my parents for their constant support and encouragement throughout my PhD, which made it all possible.

# Abstract

The role of the HIV-1 accessory protein Vpr has been obscure. Recent studies suggested that HIV-1 is sensitive to type-I Interferon stimulated by activation of cytoplasmic DNA sensor cGAS. Given that Vpr is packaged into HIV-1 particles and present during early stages of the viral lifecycle when its DNA is prone to detection by cGAS, it was hypothesised that Vpr may antagonise cGAS activation of innate immune responses. Consistent with this hypothesis, HIV-1 replication was Vpr dependent in macrophages activated with cGAMP, a product of activated cGAS. High dose infection of THP-1 cells by HIV-1 triggered a Vpr sensitive ISG response, which depended on cGAS but not MAVS. Vpr expression inhibited interferon stimulated genes (ISGs) mRNA and protein expression stimulated by cGAMP. Vpr mutants revealed that this activity required interaction with the DCAF1 E3 ubiquitin ligase complex and importin-α but is independent of Vpr cell cycle arrest function. DCAF1 requirement was further confirmed by DCAF1 depletion. Surprisingly, Vpr expression also inhibited LPS or Sendai virus activated ISG expression suggesting that Vpr targets a conserved step downstream of several innate immune sensors. Indeed, Vpr potently inhibited nuclear translocation of IRF3 without affecting IRF3 phosphorylation at serine386 which is necessary and sufficient for IRF3 activation. In addition to IRF3, Vpr also inhibited NF-κB nuclear translocation downstream of DNA sensing. Immunofluorescence analysis of Vpr correlated antagonism of immune signalling with localisation of Vpr to the nuclear envelope, suggesting that Vpr may target nuclear translocation of IRF3 and NF-κB at the nuclear pore.

In parallel, investigation of Vpr in HEK293T cells revealed that Vpr inhibits mRNA expression from various promoters except the ubiquitin or EF1α promoter which lack NF-κB binding sites. This function correlated with Vpr localisation to the nuclear envelope and was independent of the cell cycle arrest function of Vpr. Interestingly, Vpr did not inhibit HIV-1 gene expression or infectivity. Moreover, nucleofection or integration of a reporter overcame the Vpr-mediated block to expression, suggesting that Vpr may inhibit nuclear import of co-transfected plasmids.

In conclusion, I propose that during infection Vpr acts to suppress cGAS activation induced by inappropriately exposed HIV-1 DNA in infected cells and Vpr mediated block to expression from the co-transfected plasmids is a consequence of Vpr inhibition of IRF3 and NF-κB nuclear import.

# Impact statement

All pathogens are subject to inhibition by the cell autonomous innate immune system. My research suggests a role for the last HIV-1 orphan gene, Vpr, against the innate immune system. It suggests that Vpr, a virion associated protein, may target importin-α to inhibit translocation of activated transcription factors, IRF3 and NF-κB, into the nucleus, which results in inhibition of ISG and proinflammatory gene expression. Molecular characterisation of this Vpr function has wide implications for disease biology extending beyond infection to inflammation, cancer and gene therapy.

A detailed knowledge of IRF3 and NF-κB nuclear translocation and its regulation by phosphorylation is lacking. Molecular characterisation of how Vpr targets and modulates activity of the importin-α will broaden our understanding of IRF3 and NF-κB nuclear translocation. Identification of the importin-α targeted by Vpr and characterisation of their interactions may allow development of compounds that can be used therapeutically to prevent inhibition of innate immunity by Vpr during HIV-1 infection. Similarly, therapeutic compounds can also be designed to disrupt Vpr localisation to the nuclear envelope, which was found to be essential for its activity against the innate immune system. Given the differential effects of Vpr on IRF3 phosphorylation, Vpr can also be used to discern the role played by IRF3 phosphorylation sites in nuclear translocation of IRF3. Furthermore, the activity of Vpr against expression from transfected plasmids and not from lentiviral vector transduction can be used to further our understanding of non-viral gene therapy.

# Table of contents

# List of figures

# List of tables

# Abbreviations

| | |
|---|---|
| 6HB | 6-helix bundle |
| Ab | antibody |
| AIDS | acquired immune deficiency syndrome |
| APC | antigen presenting cell |
| APOBEC3 | Apolipoprotein B mRNA-editing enzyme catalytic polypeptide-like 3 |
| APS | ammonium persulfate |
| ART | Antiretroviral therapy |
| AZT | azidothymidine |
| BLAST | Basic Local Alignment Search Tool |
| BSA | bovine serum albumin |
| CA | capsid |
| cART | combined ART |
| CCL | chemokine ligand |
| CCR5 | C-C chemokine receptor 5 |
| CD4 | cluster of differentiation 4 |
| CD8 | cluster of differentiation 8 |
| CDK | cyclin-dependent kinase |
| cDNA | Complementary DNA |
| cGAMP | cyclic GMP-AMP or cyclic [G(2'-5')pA(3'-5')p] |
| cGAS | cyclic GMP-AMP synthase |
| CHR | C-terminal helical region |
| CLR | C-type lectin receptors |
| CMV | Cytomegalovirus |
| cPPT | central PPT |
| CPSF6 | cleavage and polyadenylation specificity factor 6 |
| CsA | cyclosporine A |
| Ct | cycle threshold |
| CTD | C-terminal domain |
| CTL | cytotoxic T lymphocyte |
| CXCR4 | C-X-C chemokine receptor 4 |
| CypA | cyclophilin A |
| DBP | DNA binding protein |
| DC | dendritic cell |
| DC-SIGN | dendritic cell-specific intercellular adhesion molecule-3-grabbing |
| DMEM | Dulbecco's Modified Eagle Medium |
| DMSO | dimethyl sulphoxide |

| | |
|---|---|
| EDTA | ethylenediaminetetraacetic acid |
| EIAV | Equine Infectious Anaemia Virus |
| ELISA | enzyme-linked immunosorbent assay |
| EM | electron microscopy |
| Env | envelope |
| ER | endoplasmic reticulum |
| ESCRT | endosomal sorting complexes required for transport FBS foetal bovine serum |
| FISH | fluorescent in situ hybridisation |
| FIV | Feline Immunodeficiency Virus |
| FoC | fate of capsid |
| FRAP | fluorescence recovery after photobleaching |
| FSC-H | forward scatter height |
| Gag | Group specific antigen |
| GALT | gut associated lymphoid tissue |
| GFP | green fluorescent protein |
| gp120 | glycoprotein 120kDa |
| gp160 | glycoprotein 160kDa |
| gp41 | glycoprotein 41kDa |
| GPI | glycophosphatidylinositol |
| GWAS | Genome-wide association study |
| HA | hemagglutinin |
| HAART | highly active ART |
| HIV | Human Immunodeficiency Virus |
| HLA | human leukocyte antigen |
| HTLV | Human T-Lymphotropic Virus |
| ICAM-1 | Intracellular adhesion molecule 1 |
| IF | immunofluorescence |
| IFN | interferon |
| IFNAR2 | IFNα/β receptor 2 |
| IL-2 | interleukin 2 |
| IN | integrase |
| ISG | IFN-stimulated gene |
| IU | infectious unit |
| Jun | Jun proto-oncogene |
| kb | Kilobase |
| LB | lysogeny broth |
| LEDGF/p75 | lens epithelium-derived growth factor |
| LTNP | Long-term non-progressor |

| | |
|---|---|
| LTR | long terminal repeat |
| MA | matrix |
| MDM | Monocyte-derived macrophage |
| MFI | mean fluorescence intensity |
| MHC | major histocompatibility complex |
| MLV | Murine Leukaemia Virus |
| MOI | multiplicity of infection |
| MxB | Myxovirus resistance protein B |
| NC | nucleocapsid |
| Nef | negative regulatory factor |
| NES | nuclear export signal |
| NFAT | nuclear factor of activated Tcells |
| NF-κB | nuclear factor κB |
| NHEJ | Non-homologous end joining |
| NHR | N-terminal helical region |
| NLS | nuclear localisation signal |
| NMR | nuclear magnetic resonance |
| NPC | nuclear pore complex |
| NTD | N-terminal domain |
| Nup | nucleoporin |
| ORF | Open reading frame |
| OWM | Old world monkey |
| p-TEFb | positive transcription elongation factor b |
| PAGE | polyacrylamide gel electrophoresis |
| PAMP | Pathogen-associated molecular pattern |
| PBMC | peripheral blood mononuclear cells |
| PBS | phosphate buffered saline |
| PBS | primer binding site |
| PCP | Pneumocystis carinii pneumonia |
| PEG | polyethylene glycol |
| PFA | paraformaldehyde |
| PHA | phytohemagglutinin |
| PI | prpidium iodide |
| PIC | pre-integration complex |
| POD | peroxidase |
| PPIase | peptidyl-prolyl isomerase |
| PPT | polypurine tract |
| PR | protease |
| PRR | pattern recognition receptor |

| | |
|---|---|
| PVDF | polyvinylidene difluoride |
| qPCR | quantitative/real time PCR |
| RANBP2 | Ran binding protein 2 |
| Rev | regulator of expression of virion proteins |
| RING | Really Interesting New Gene |
| RLU | relative light units |
| RNAPII | RNA polymerase II |
| RPMI | Roswell Park Memorial Institute Medium Rev responsive element |
| RRE | Rev response element |
| RRM | RNA recognition motif |
| RS | arginine/serine-rich |
| RT | reverse transcriptase |
| RTC | reverse transcription complex |
| SAMHD1 | sterile α motif and HD domain-containing protein 1 |
| SDM | site directed mutagenesis |
| SDS | sodium dodecyl sulphate |
| SGA | single genome analysis |
| SIV | Simian Immunodeficiency Virus |
| SP | spacer peptide |
| SR | serine/arginine-rich |
| SSC-H | side scatter height |
| STING | stimulator of IFN genes |
| SV40 | Simian Virus 40 |
| TAE | Tris acetate EDTA |
| TAK-1 | tumour growth factor-β activated kinase 1 |
| TAR | transactivation responsive region |
| Tat | trans-activator of transcription |
| TCR | T cell receptor |
| TE | Tris EDTA |
| TEMED | tetramethylethylenediamine |
| Tm | melting temperature |
| TNFα | tumour necrosis factor α |
| TNPO3 | transportin 3 |
| TRIM | tripartite motif |
| UTR | untranslated region |
| V3 | variable loop 3 |
| Vif | viral infectivity factor |
| VLP | Virus-like particle |
| Vpr | viral protein r |

| | |
|---|---|
| Vpu | Viral protein u |
| Vpx | Viral protein x |
| VS | Virological synapse |
| VSV | Vesicular stomatitis virus |
| VSV-g | VSV G envelope protein |
| WHO | World Health Organisation |
| WT | Wild type |
| Ψ | HIV-1 packaging signal |

# 1 Chapter 1: Introduction

## 1.1 Human Immunodeficiency virus 1

HIV is the causative agent of the acquired immune deficiency syndrome (AIDS) (1,2). It belongs to the genus Lentivirus of the family Retroviridae (3). Lentiviruses are characterised by their ability to infect dividing as well as non-dividing cells (4). HIV primarily infects CD4+ T lymphocytes and macrophages by binding CD4 and engaging a co-receptor, CXCR4 or CCR5 (5–7). Different HIV strains have different preference for the co-receptor usage. CCR5 tropic viruses dominate early stages of infection whereas late stages of infection are characterised by CXCR4 tropic viruses (8).

In 2017, approximately 36.9 million people were living with HIV and 1.8 million new cases of HIV were reported globally (9). So far 35 million people have died due to HIV with 940 000 deaths reported in 2017 (9). Natural history of HIV infection involves infection of target cells in the mucosal tissues which spreads to the lymphoid tissues (10). Virus replication peaks at about day 30. After peak viremia, HIV replication drops due to adaptive immune responses and stays relatively stable for several years (11). During this period CD4+ T-cells are progressively lost and the resultant immunodeficiency manifests into characteristic infectious or oncological complications which define AIDS (12). AIDS can develop in 2-15 years depending on the individual. There is no cure however effective antiretroviral drugs can suppress the virus and prevent transmission.

### 1.1.1 HIV-1 classification and origin

HIV belongs to the genus Lentivirus of the family Retroviridae (3). There are two main types of HIV, HIV-1 and HIV-2. HIV-1 is the cause of most infections worldwide whereas HIV-2 is less transmitted and is less pathogenic. Several independent zoonotic transmissions of Simian immunodeficiency virus (SIV) gave rise to HIV. HIV-1 is closely related to SIVs isolated from African apes whereas HIV-2 is thought to be originated from SIV that infects sooty mangabeys (13). HIV-1 is further classified into four groups, M, N, O, and P, each originated from a zoonotic transmission event (14–16). HIV-1 group M is the cause of the pandemic whereas groups O, N, and P are restricted to West Central Africa. Chimpanzees in southern Cameroon are thought to be the source of viruses that gave rise to group M and N whereas group O and P are thought to have originated from gorillas. So far two cases of group P and fifteen cases of group N have been identified (14,17). The mechanism of cross species transmission event is unclear but likely involved contact with animal blood during butchering and hunting. Overtime, genetic diversification in the *env* and *gag* gene of HIV-1 group M has given rise to nine subtypes A, B, C, D, F, G, H, J, and K. The diversity of subtypes varies geographically with greatest subtype

diversity seen in the Sub-Saharan Africa. North America is dominated by subype B however infections with non B subtypes and recombinant strains are on the rise in Europe (18,19).

### 1.1.2 HIV-1 genome organisation

The HIV-1 genome is 9.4kb long +ssRNA. It contains 9 open reading frames (ORFs) that encode for 15 protiens. Viral gene transcription is driven by long terminal repeats (LTR) which are present on each end of the genome and contain binding sites for several cellular transcription factors such as NF-κB (20). The *Gag* gene encodes for a myristoylated polyprotein, p55, which is processed into matrix (MA, p17), capsid (CA, p24), nucleocapsid (NC, p7), p6 and the spacer peptide 1 and 2 (sp1, sp2) by the viral protease during maturation. *Pol* encodes the enzymes reverse transcriptase, protease and integrase. Pol is produced as a Gag-Pol precursor due to ribosome frameshifting and is processed by the viral protease (21). *Env* encodes the polyprotein gp160 which is cleaved by the cellular protease, furin, into gp120 and gp41 (22). Regulatory proteins are encoded by the *rev* and *tat* genes whereas the accessory proteins are encoded by the *vif, vpr, vpu* and *nef* genes.

### 1.1.3 HIV-1 virion structure

The mature HIV particle is spherical about 145nm in size (23). Envelope, the outermost component, is a host cell derived lipid bilayer decorated with 10-20 spikes composed of trimers of viral surface glycoproteins, gp120, and transmembrane glycoproteins, gp41 (24). The inside of the envelope is lined with the matrix protein (MA). Underneath the matrix, the capsid shell contains two identical molecules of 9.4kB +ssRNA bound to the viral enzymes, integrase and reverse transcriptase. Viral accessory gene, Vpr, is also packaged into virions (25).

## 1.2 Life cycle

### 1.2.1 Fusion

HIV-1 entry into cells is a multistep process that involves virus attachment, receptor and coreceptor binding, conformational changes in the viral envelope glycoprotein (Env) and eventual fusion of the viral and cellular lipid membranes that results in delivery of the viral capsid into cell cytoplasm (Fig. a1.1).

#### 1.1.1.1 Envelope glycoprotein

Env is the key viral protein that orchestrates HIV-1 entry into target cells. It is expressed as a precursor protein, gp160. GP160 undergoes proteolytic processing in the trans-Golgi

network by the cellular furin protease into gp120 and gp41 hetrodimers (22). After proteolysis the heterodimers are transported to the cell membrane where trimers of gp120-gp40 hetrodimers are incorporated into budding virions. Each virion contains about 10-20 Env trimers on its surface (24). Gp120 is a globular glycoprotein that forms the surface subunit of Env. It is highly glycosylated on the outer surface. It contains five conserved (C1-C5) domains interspersed with five highly variable (V1-V5) domains. The conserved domains, especially C1, C3 and C4, determine binding to the receptor. Each variable domain, except for V5, forms a disulphide bond at its base resulting in the formation of the variable loops (26). The variable loops, in particular the V3 loop, are important determinants for coreceptor binding and sensitivity to antibody neutralisation (27). GP41 is a transmembrane glycoprotein that anchors Env in the lipid bilayer. It contains three major domains: an N-terminal extracellular domain, a transmembrane domain and a C-terminal cytoplasmic tail (28). The extracellular domain contains the fusion peptide and two heptad-repeat domains (HR1 and HR2) that form α-helices.

#### 1.1.1.2 Mechanism of HIV-1 fusion

To bring Env closer to its receptor and coreceptor the virus first attaches to the cell. Specific attachment occurs via interaction between Env and the cellular integrin α4β7 or the pattern recognition receptor, DC-SIGN (29). Interactions between negatively charged hepran sulphate proteoglycan moieties and positively charged side chains of Env results in non-specific attachment (30). Attachment can also be mediated by cellular proteins that enter virion membrane during budding. For example, ICAM-1 binds to its cognate receptor LFA-1 on lymphocytes. Virus attachment is thought to bring Env closer to its receptor and coreceptor however it is not essential for virus entry and its role in vivo is unclear (31).

CD4 is the receptor for HIV-1 Env (6) . It belongs to the immunoglobulin superfamily and functions in T cell receptor (TCR) signalling. Binding of CD4 to gp120 triggers a conformational change in V1, V2 and V3 domains and formation of the 4-stranded β sheet known as the bridging sheet (32). These changes reveal the coreceptor binding site. HIV-1 Env uses G-protein coupled chemokine receptors, CXCR4 and CCR5, as coreceptors (5,7). Different HIV strains have different preference for coreceptor binding. R5 viruses use CCR5, X4 viruses use CXCR4 and R5/X4 viruses can use CCR5 and CXCR4 (33). In the absence of coreceptor binding, the fusion peptide in gp41 is hidden in the Env quaternary structure. Upon coreceptor binding conformational changes reveal the hydrophobic fusion peptide which is immediately inserted into the target cell membrane (34). A six-helix bundle is formed as the fusion peptide from each gp41 folds and brings the N- and C-terminal helical regions (HR1 and HR2) antiparallel to each other (35). Formation of the six-helix bundle brings the viral membrane closer to the cell membrane,

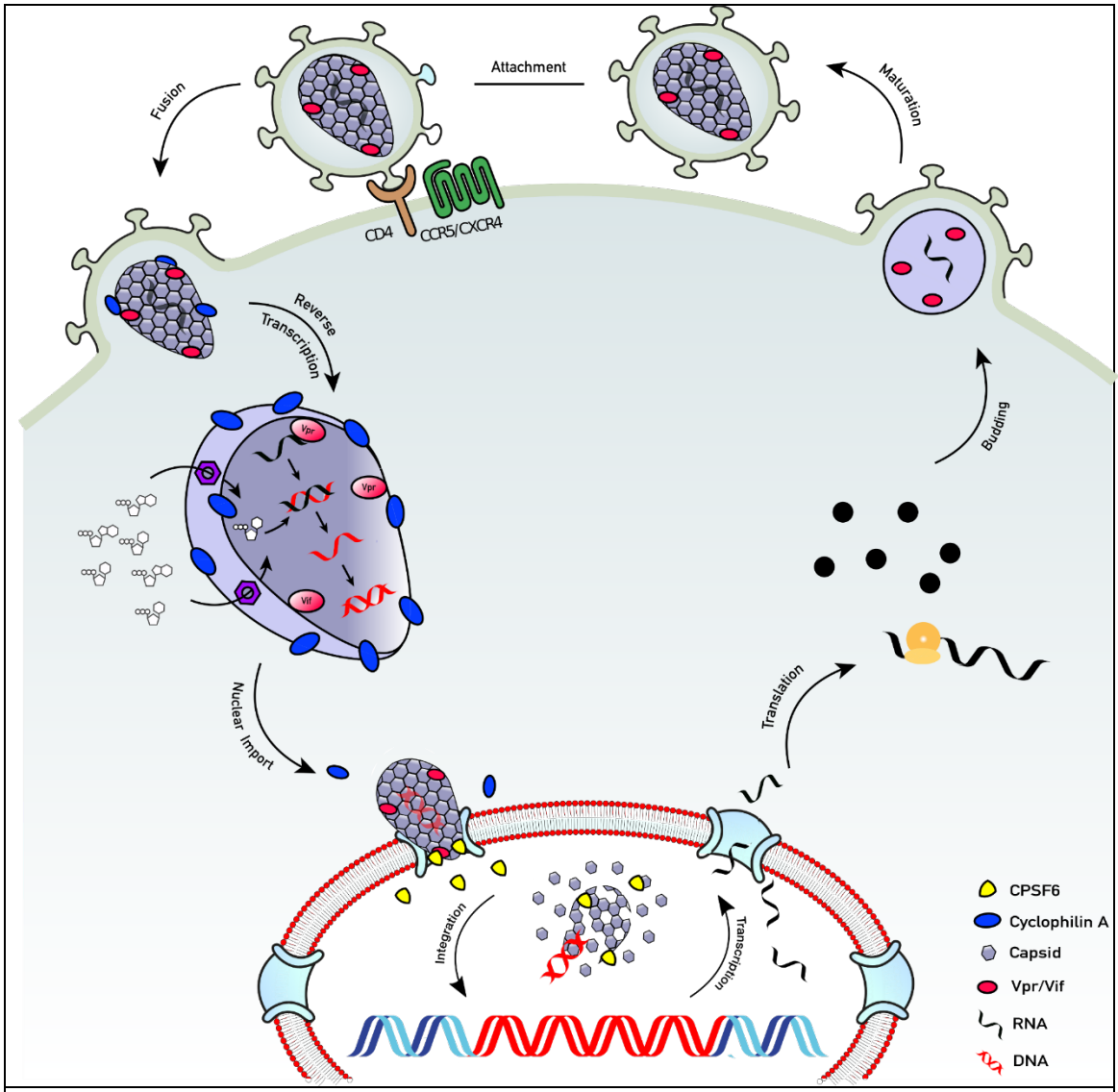


**Figure 1.1 HIV life cycle**

HIV life cycle is a complex series of immune evasion strategies that allow successful infection and transmission. To enter cells HIV engages its envelope glycoprotein gp120 with cell surface protein CD4 and a co-receptor (CXCR4 or CCR5). Upon fusion, the capsid is released into the cytoplasm. Nucleotides are pumped into the capsid cone through an electrostatic pump to fuel reverse transcription. Capsid recruits cellular proteins cyclophilin A (blue) and CPSF6 (yellow) to prevent detection of the viral reverse transcribed products by DNA sensors. Partial or complete uncoating may happen in the nucleus and the viral DNA is integrated into the cellular genome. Once integrated the provirus is invisible to the host cell defences and may become latent. Transcription and translation of the provirus results in viral proteins that assemble at the cell surface. Immature virions bud off and are released. Finally, during maturation, the protease enzyme cleaves the structural polyprotein to form mature Gag proteins, resulting in the production of new infectious virions.

resulting in lipid mixing and formation of the fusion pore which delivers the capsid core to the cell cytoplasm (36).

#### 1.1.1.3 Location of HIV-1 fusion

Location or the site of HIV-1 fusion has been controversial. It appears to be cell type and viral strain specific. HIV-1 entry is pH-independent suggesting that it does not require the acidic endosomal environment to activate fusion (37). In CD4+ T cells, cell surface fusion is the main site of virus entry (38). Genetic and pharmacological approaches have been employed to show that disruption of the endocytic pathway in CD4+ T cells does not inhibit productive infection by HIV-1 (38,39). Consistently, fusion by the endocytosed viruses has not been observed (38). Dynamin 2, a GTPase involved in clathrin mediated endocytosis, has been shown to be important for HIV-1 entry into T-cells (40). However, it has been demonstrated that Dynamin 2 allows HIV-1 entry by stabilising the fusion pore independent of its function in the endocytic pathway (41). Macrophages, on the other hand, have a higher endocytic potential compared to T cells and may readily uptake attached virions into the endocytic compartment (42). Entry of HIV-1 into macrophages has been shown to require a Dynamin 2, Rac1 and PaK1 dependent endocytic pathway (39). Retention of CD4 at the cell surface allowed virus fusion and reverse transcription but not productive infection suggesting that productive infection relied on the endocytic pathway (39). Virus fusion may start at the plasma membrane but complete in the endocytic compartment due to the high endocytic rate of macrophages (43). Elucidating the role of the endocytic pathway in HIV-1 entry is crucial because endocytic entry of HIV-1 can minimise the exposure of viral epitopes to the neutralising antibodies and reduce efficiency of fusion inhibitors.

#### 1.1.1.4 HIV-1 fusion inhibitors

Two inhibitors of HIV-1 entry have been developed. Enfuvirtide targets the gp41 subunit of Env and inhibits formation of the 6-helix bundle (44). It is expensive and needs to be injected due to its low oral bioavailability, limiting its clinical application. Maraviroc targets the transmembrane domain of the coreceptor, CCR5, and prevents binding to the gp120 subunit of Env. It is not active against X4 tropic viruses. Intriguingly, Maraviroc resistant viruses do not switch coreceptor usage but instead gain ability to use the drug bound CCR5 for fusion (45).

### 1.2.2 Capsid structure and function

HIV-1 capsid core is a closed ultrastructure that is released into the cytoplasm after virus fusion. It contains two copies of the viral genome, reverse transcriptase, integrase,

accessory protein Vpr and nucleocapsid. The building block of the capsid core is the capsid protein (CA). The capsid core is a fullerene-like conical structure made up of approximately 1200 CA monomers assembled into hexamers and pentamers (46,47). Hexamers forms the length of the cone whereas five pentamers are present at the narrow end and seven are present at the wide end. Pentamers provide curvature at the cone ends resulting in a closed capsid shell. CA consists of an 80 amino acid long C-terminal (CA-CTD) domain and 150 amino acids long N-terminal domain (CA-NTD). In an assembled capsid CA-NTD forms the outer surface and CA-CTD forms the inner surface of the capsid. Recent molecular dynamic simulations and atomic force microscopy have revealed that capsid is a dynamic structure in which each CA experiences tilting and twisting movements due to a hinge region between CA-NTD and CA-CTD resulting in different hexamer and pentamer conformations (48). These allosteric changes are thought to be influenced by binding of cellular proteins which, depending on the context, can stabilise or destabilise the capsid structural integrity and trigger CA dissociation, a process known as uncoating (49).

For a long time, HIV-1 capsid was thought to disassemble in the cytoplasm immediately after fusion. However, increasing amounts of recent data suggest that HIV-1 capsid is a metastable structure which encapsidates and protects the viral genome as it traverses the cellular cytoplasm. In addition, it plays important roles during reverse transcription, nuclear import and integration.

### 1.2.3 Reverse transcription

Capsid uncoating and reverse transcription have been shown to be coupled events that influence virus nuclear import and integration site selection. Recent studies show that uncoating is triggered by reverse transcription. Second strand transfer of RT and DNA flap formation have been associated with initiation of capsid uncoating (50,51). Inhibition of RT by chemical inhibitors such as neverapine stabilised the capsid and resulted in delayed uncoating (52). Similarly, an immunofluorescence based tracking of HIV-1 single particles showed that initiation of RT accelerated disassembly of the capsid (53). Recent atomic force microscopy of HIV-1 capsids during in vitro reverse transcription revealed that as reverse transcription progresses newly synthesised viral DNA exerts a mechanical force on the interior of the capsid core which eventually overcomes structural integrity of the capsid core and results in breakdown of the capsid lattice (48,54).

Reverse transcription is a process that converts an RNA template into a double stranded DNA. A study by Jacques et a. (2016) suggests that reverse transcription occurs inside intact capsids (55). It was found that the N-terminal β-hairpin can adopt at least two distinct conformations in the capsid hexamer, termed open and closed. Movement of the β-hairpin

revealed or obscured a pore or channel at the center of each hexamer. The pore or channel contained six R18, one from each capsid monomer, arranged in a ring. The positively charged arginine ring was shown to bind negatively charged dNTPs via electrostatic interactions which resulted in dNTP import into intact capsids and fuelled reverse transcription, a process termed encapsidated DNA synthesis.

HIV-1 reverse transcriptase (RT) is encoded by the *pol* gene. It is produced as a GagPol precursor protein due to programmed frameshift during translation. Fusion of Pol with Gag ensures incorporation of RT into budding virions. RT is a heterodimer of p66 and p51 subunits. P66 subunit contains two catalytic activities. The N-terminal polymerase activity allows copying of either an RNA or a DNA template and the C-terminal RNase H activity causes degradation of RNA in a RNA:DNA hybrid (56,57). HIV-1 contains two copies of positive sense single stranded RNA (+ssRNA) genome which is used by RT as a template for DNA synthesis. Cellular tRNALys3 act as a primer for synthesis of the minus-strand DNA (58). tRNALys3 binds to a complementary sequence at the 5' end of the RNA genome known as the primer binding sequence (PBS). Polymerase activity of RT results in the formation of DNA:RNA hybrid, generating a substrate for the RNase H subunit of the RT. RNase H cleaves the 5' end of the viral RNA in the RNA:DNA hybrid, releasing the newly synthesised minus-strand DNA (59). Since the 5' and 3' ends of viral genome are exact copies of each other, the newly synthesised minus-strand DNA anneals to the 3' end of the viral RNA which is then extended along the rest of the RNA (60). The resulting minus-strand DNA contains the PBS region which is critical for the formation of the plus-strand DNA. Since HIV-1 contains two copies of the RNA, the minus-strand DNA can be transferred to either of the two RNAs.

HIV-1 contains two purine-rich sequence known as the polypurine tract (ppt), one at the 3' end and one in the middle of the genome. The 3'ppt is essesntial for reverse transcription whereas the central ppt is not essential but can increase the efficiency of the plus-strand DNA synthesis (61). Ppt regions are resistant to the RNase H activity and are not digested during synthesis of the minus-strand DNA (62). 3'ppt act as the primer for plus-strand DNA synthesis which extends to the 18 nucleotides of the tRNALys3 primer. Since the minus-strand DNA contains the PBS and the plus-strand DNA contains the complementary tRNALys3 primer sequence, annealing of the plus and minus strand DNA results in production of double stranded DNA.

### 1.2.4 Nuclear import

CA is the main regulator of nuclear entry and determines integration site selection (63), (64). Studies showed that chimeric HIV-1 with MLV CA was defective for nuclear entry and certain capsid mutations can result in a virus that can infect dividing cells but is unable to

infect non-dividing cells (65,66). The CA has been shown to interact with members of the NPC which allow nuclear import of the virus (63,64). Recent microscopy based studies of single HIV-1 particles revealed that in primary macrophages CA is imported into the nucleus along with viral DNA, suggesting a nuclear function of CA (67,68). Consistent with a nuclear function of CA, preventing interaction of CA with certain cellular cofactors has consequences for HIV-1 integration site selection in the host genome (63,69). Nuclear import of HIV-1 is orchestrated by sequential interactions of HIV-1 CA with cellular cofactors as described below.

#### 1.1.1.5 CypA

CypA was the first HIV-1 cellular co-factor to be identified (70). It is packaged into HIV-1 virions and influence infectivity in the target cells (71,72). It is a peptidyl-prolyl cis-trans isomerase which catalyses the interconversion of *cis* and *trans* forms of proline imidic peptide bonds (73). It binds to a loop between helix 4 and 5 of the CA-NTD known as the CypA binding loop and catalyses isomerisation of the Gly89-Pro90 bond at the apex of the loop (74). Interaction between CA and CypA can be disrupted by capsid mutations G89V and P90A or by CypA inhibitors, cyclosporines.

The role of CypA in promoting HIV-1 infection seems to be cell type dependent (75). Abrogation of CA and CypA interaction by CypA depletion, G89V and P90A CA mutations or cyclosporine treatment have shown that CypA is required at an early step in infection that influences reverse transcription (71). It is not clear whether the isomerase activity is required for CypA function during HIV-1 infection due to inability to separate CypA catalytic activity from CA binding (73).

There are conflicting reports for a role of CypA in virus uncoating. One study observed in vitro stabilization of CA cores by CypA and a different study showed destabilization of CA by CypA (76,77). CypA recruitment to the capsid has been shown to be an innate immune evasion mechanism employed by the virus (78). Perturbing the interaction of CA with CypA by mutating CA (P90A) or using CypA inhibitor, cyclosporine, resulted in exposure of the viral DNA to the DNA sensor, cGAS, resulting in type I interferon production and suppression of viral replication in primary macrophages.

CypA has also been shown to regulate HIV-1 nuclear import (63). Unlike WT virus which relies on nuclear pore proteins Nup358 and Nup153 for nuclear import, cyclophilinA binding mutant viruses (P90A and G89V) were found to be imported into the nucleus in the absence of Nup358 and Nup153. This favored integration of the virus into higher gene density regions than the wild type virus.

#### 1.1.1.6 Nup358

Nup358 is located on the cytoplasmic side of the nuclear pore complex. It forms the cytoplasmic filaments that protrude into the cytoplasm. It contains several FG-repeats that form a hydrophobic gel-like matrix and regulates transport across the nuclear pore (79). Depletion of Nup358 reduces HIV-1 2-LTR circle formation without affecting reverse transcription suggesting that it is involved in virus nuclear import (80). Nup358 contains a cyclophilin-like domain which has *cis–trans* isomerisation activity. NMR studies using CA-NTD have shown that CA-NTD binds to the cyclophilin-like domain of Nup358 which then catalyses *cis–trans* isomerisation of G89-P90 bond in CA-NTD (81). This suggested that HIV-1 CA interaction with the cyclophilin-like domain in Nup358 docks the virus at the nuclear pore where it may undergo uncoating and nuclear import. However, the role of cyclophilin-like domain of Nup358 during HIV-1 infection has been challenged by observations showing HIV-1 infection of cells lacking the Nup358 cyclophilin-like domain (82).

#### 1.1.1.7 Nup153

Nup153 is a member of the nuclear pore complex, located on the nuclear side of the NPC. It is required for formation of the nuclear pore basket which is involved in recruiting actively transcribed genes to the NPC for mRNA export (83). It was identified as a HIV-1 cofactor in a siRNA screen against HIV-1 infection (80,84). Nup153 depletion prevented HIV-1 infection by inhibiting nuclear import with no effect on reverse transcription (85). Nup153 is one of the FG-nucleoporin present in the nuclear pore complex. It contains phenylalanine-glycine (FG) dipeptides which form a hydrophobic gel-like matrix in the central transport channel and regulate transport of cargoes across the nuclear pore complex (86). C-terminus of Nup153 contains 21 FG-repeats. Structural studies show that HIV-1 CA specifically contacts the twentieth FG-repeat (87). Nup153 binds to an interface that is formed between two CA molecules (88). The FG repeat of Nup153 interacts with a pocket in NTD of one CA monomer whereas on the adjacent CA monomer Nup153 interacts with the hinge between the NTD and CTD. These observations suggest that when HIV-1 reaches nuclear pore, at least some CA is present as a hexameric lattice to allow Nup153 binding and nuclear import.

#### 1.1.1.8 CPSF6

Cleavage and polyadenylation specificity factor 6 (CPSF6) is an mRNA-processing protein that belongs to the family of Ser/Arg-rich (SR) proteins (89). It contains a serine/arginine (SR)-rich nuclear-localization signal (NLS) on its C terminus which allows nuclear import by recruiting transportin 3 (90). It was identified as a HIV-1 restriction factor in a murine

cDNA-expression screen (64). It inhibited HIV-1 infection by preventing RT and delaying uncoating. Interestingly, murine CPSF6 was unable to inhibit MLV infection which relies on cell division and nuclear envelope breakdown, suggesting that CPSF6 played a role in infection of non-dividing cells. The murine CPSF6 cDNA used in the screen lacked the NLS which resulted in its cytoplasmic accumulation. This cytoplasmic CPSF6 was responsible for inhibition of HIV-1 infection. Since then human CPSF6ΔNLS has been shown to be active against HIV-1 infection (91). Passage of HIV-1 in CPSF6ΔNLS expressing cells resulted in a CPSF6 independent virus with a single point mutation, N74D, in the capsid (64). N74 forms two hydrogen bonds with CPSF6 which are lost upon N74D mutation. Similarly, single point mutation in the CPSF6ΔNLS (F321N) relieves inhibition of HIV-1 infection (92).

In cells lines CPSF6 depletion or overexpression does not inhibit HIV-1 infection (64). Nonetheless, N74D mutation or CPSF6 depletion makes the virus independent of other cellular cofactors such as Nup358 and Nup153 which alters integration site selection. Unlike WT HIV-1 which integrates into gene dense and transcriptionally active regions of the genome, N74D mutant HIV-1 integrates into transcriptionally inactive regions (63). In primary macrophages N74D mutation or CPSF6 depletion resulted in activation of a viral DNA dependent innate immune response that suppressed viral replication (78).

A recent study has provided new insights into CPSF6 function. Bejarano et al. (2019) showed that CPSF6 was essential for HIV-1 nuclear import in primary macrophages (68). The authors showed that CPSF6 co-localised with the CA only in the nucleus. Since CPSF6 binding interface is present in the CA hexamer and absent from CA monomers this suggested the presence of intact capsid cores in the nucleus. Furthermore, CA was found to be present in the nucleus with almost the same signal intensity as the cytoplasmic CA suggesting none or very little loss of the CA during cytoplasmic trafficking and nuclear import. By depleting CPSF6 or using a CPSF6 binding mutant, A77V, it was shown that virus was blocked at the nuclear pore complex without any effect on virus trafficking to the nuclear pore complex or reverse transcription. Since the binding interface of CPSF6 overlaps with that of Nup153 it was suggested that the viral CA first interacted with the Nup153 in the NPC and then CPSF6 displaced Nup153 resulting in the nuclear import of the virus. This model is consistent with the role of CPSF6 in directing HIV-1 towards gene rich transcriptionally active regions (93). In the absence of CPSF6 the virus is arrested at the nuclear pore which may allow integration near the nuclear envelope in gene-deficient heterochromatin as proposed by a recent study (93).

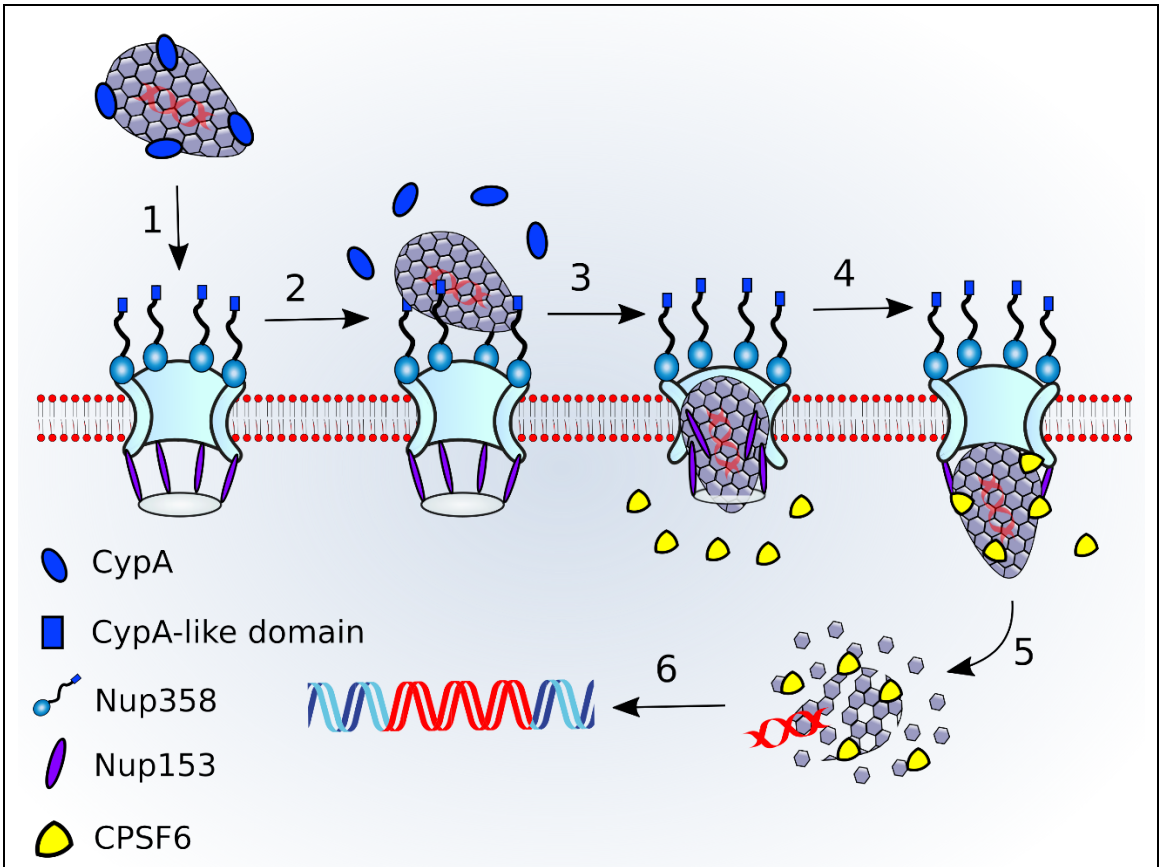


**Figure 1.2 HIV-1 nuclear import and uncoating**

**(1)** Intact or partially intact HIV-1 capsid cores, decorated with CypA and containing partially or fully reverse transcribed DNA, arrive at the nuclear pore complex. **(2)** The capsid core is docked at the nuclear pore complex by Nup358. Cyclophilin-like domain in Nup358 binds to the cyclophilin-binding loop in the capsid by displacing CypA. **(3), (4)** HIV-1 nuclear import is orchestrated by Nup153 and CPSF6. First Nup153 binds to the capsid core (3) which is then displaced by CPSF6, resulting in nuclear import of the capsid core (4). **(5), (6)** Partial or complete capsid uncoating occurs in the nucleus (5) and the viral DNA is integrated into the cellular genome (6).

### 1.2.5 Integration

Integration is a process by which viral DNA is inserted into the cellular genome by the viral integrase (IN). IN is encoded by the pol gene and packaged into budding virions as a GagPol precursor protein. Functional IN is produced after protease mediated processing of GagPol during virion maturation (94). IN can be divided into three domains (95). The N-terminal domain consists of three α-helices and regulates oligomerisation and catalytic activity (96). This domain also coordinate a Zn2+ ion via the “HHCC” motif containing two histidine and two cysteine residues (97). The catalytic activity and DNA binding site of IN is present in the central core domain (CCD) (95). The CCD domain is post-translationally modified by c-Jun N-terminal kinase (JNK) mediated phosphorylation followed by Pin1 mediated peptidyl-prolyl cis-trans isomerization (98). These modifications stabilize IN and enhance the efficiency of integration. During integration three key residues Asp64, Asp116 and Glu152 present in the active site form coordinate bonds with two Mg2+ ions (99). The C-terminal domain (CTD) is involved in IN multimerisation and DNA binding (100). It is regulated by posttranslational acetylation by histone acetyltransferases at specific lysine residues (K264, K266, K273) which promote DNA strand transfer activity of IN (101).

#### 1.1.1.9 Mechanism of integration

IN catalyses 3’ end processing and strand transfer of the viral DNA. Upon viral DNA synthesis, IN multimerises on the nascent DNA resulting in the formation of a DNA:IN complex known as intasome (102). A functional intasome contains four IN proteins in which only two IN molecules contact the DNA (102). 3’-end processing of the DNA by IN results in removal of two nucleotides from each 3’end of the blunt ended viral DNA, revealing 3’hydroxyl groups that can be joined to the target DNA. The second step of integration involves DNA strand transfer whereby the viral DNA ends are inserted into the target DNA. 3’hydroxyl groups carry out a nucleophilic attack on the phosphodiester bond in the opposite strands of the target DNA. 3’ends are then covalently joined to the 5’ends of target DNA. The sites of attack on the target DNA are separated by 5 nucleotides. This results in five nucleotides long single strand gaps on the target DNA and two nucleotides long overhangs at the 5’ ends of the viral DNA which are filled by the cellular DNA repair machinery.

After entry into nucleus the viral DNA can also undergo circularization into 2-LTR and 1-LTR circles. 2-LTR circle formation is dependent on the host cell non-homologous DNA end-joining components (NHEJ) components Ku70/80, ligase lV and XRCC4 (103). 1-LTR circles are formed by a recombination event between the LTRs and depend on the host MRN complex (Mre11, Rad50, and NBS1) (104).

### 1.2.6 HIV-1 transcription

Transcription from the integrated provirus marks the beginning of the late phase of the HIV-1 replication cycle. It is regulated by the viral transactivator protein (Tat). HIV-1 transcription results in about 40 differentially spliced species of mRNA transcripts which can be of three types: unspliced, spliced or partially spliced. Spliced mRNAs are readily exported form the nucleus whereas the partially spliced and unspliced mRNAs require the viral protein Rev for nuclear export.

#### 1.1.1.10 HIV-1 promoter

The HIV-1 genome contains two long terminal repeats (LTRs), one located at the 5' end and the other at the 3' end. The 5' LTR is dominant and acts as the promoter for transcription. The 3' LTR functions as the promoter only when the 5'LTR is defective (105,106). The HIV-1 LTR is divided into three regions, U3, R and U5. Transcription initiates from the R region in the 5'LTR and terminates in the R region of the 3'LTR. The U3 region contain four elements that regulates viral transcription. The modulatory and enhancer elements contain binding sites for cellular transcription factors such as NF-κB, Sp1 and NFAT (20). The core promoter element contains the TATA box. The TAR element binds the HIV-1 protein Tat which enhances proviral transcription.

#### 1.1.1.11 Transcription initiation and elongation

HIV-1 transcription is initiated when cellular transcription factors bind the 5'LTR and recruit histone modifying enzymes, allowing recruitment of the RNA polymerase II (RNAPII) (107). Shortly after initiation, transcription is halted by recruitment of repressive proteins such as negative elongation factor (NELF) and DRB sensitivity-inducing factor (DSIF) (108,109). The short-transcribed mRNA adopts a stem loop structure known as the transactivation region (TAR) (108,109). The viral Tat protein binds TAR and stimulates transcription elongation by recruiting the cellular positive transcription elongation factor b (P-TEFb) (110). P-TEFb contains a catalytic subunit, cyclin dependent kinase 9 (CDK9), and a regulatory subunit, cyclin T1. P-TEFb recruitment results in phosphorylation of NELF and DSIF (111). Phosphorylated NELF dissociates from the complex and DSIF phosphorylation blocks its inhibitory activity on transcription elongation (112). Furthermore P-TEFb phosphorylates serine residues at position 2 and 5 in the C-terminus of the RNAPII which enhances its processivity (113,114). These phosphorylation events result in a Tat dependent positive feedback loop resulting in accumulation of Tat and sustained HIV-1 transcription.

#### 1.1.1.12 HIV-1 mRNA processing

Like cellular mRNA, viral mRNA is capped at the 5' end, introns are removed by splicing and a poly-A tail is added at the 3' end before it is exported from the nucleus. HIV-1 mRNA processing is coupled with its transcription.

Capping of the viral mRNA is promoted by Tat due to RNAPII phosphorylation (115), (116). RNA guanylytransferase (RNA GT) is recruited to the viral transcript by the phosphorylated Ser2 in RNAPII (117). Phosphorylation of the Ser5 is required for activation of the RNA GT (117). RNA triphosphatase cleaves the 5' triphosphate into a diphosphate which is then capped with GMP by RNA GT and methylated by guanine N7methyltransferase.

HIV-1 contains two polyadenylation signals. One at the 5' end and one at the 3' end of the genome. The 5' polyadenylation signal is suppressed due to its close proximity to the transcription initiation site and by binding of U1 snRNP (118,119). The usage of the 3' signal is enhanced by the presence of an upstream enhancer motif. Cleavage and polyadenylation specificity factor (CPSF) binds to this enhancer motif and cleaves mRNA between the AAUAAA motif and the downstream U or GU rich region (120). A Poly A tail is then added by Poly(A) polymerase using ATP as a substrate.

Splicing is a process in which introns are removed from mRNA transcripts by a large multicomponent ribonucleoprotein complex known as the splicosome. Splicosomes contain five small nuclear ribonucleoprotein complexes (snRNPs), U1, U2, U4, U5, and U6, which assemble onto the transcript. U1 snRNP recognise the 5'splice site and U2 snRNP recognises the 3'splice site. Splicing is regulated by sequences in the exons and introns known as exonic and intronic splicing enhancers or silencers (ESE and ISE respectively) (121,122). Serine-arginine (SR) rich family of splicing activators are recruited by ESEs rich in purine. SR proteins bind ESEs and stabilize the binding of the core splicing factors at the splice sites.

HIV-1 transcript splicing results in about 40 differentially spliced mRNA transcripts due to alternative usage of the multiple 5' and 3' splice sites (123). Partially spliced transcripts are 4kb long and encode Env, Vpu, Vpr and Vif. 2kb transcripts are fully spliced and encode Tat, Rev and Nef. 50% of the viral mRNAs are unspliced of 9kb length. Unspliced mRNA codes for the Gag and GagPol precursor polyproteins that are packaged into budding virions alongside the viral genome.

#### 1.1.1.13 HIV-1 mRNA export

During early stages of HIV infection only fully spliced transcripts are expressed. Partially spliced or unspliced transcripts are retained in the nucleus (124). Nuclear export of the mRNAs to the cytoplasm occurs through the nuclear pore complex. Export of the fully spliced viral mRNAs is mediated by transport factors such as the conserved nuclear RNA export factor 1 (NXF1) and its cofactor p15 that bind and export fully spliced mRNAs like cellular mRNAs (125). The fully spliced mRNA encodes for Rev which overcomes the nuclear retention of partially spliced and unspliced viral mRNAs (126). Rev contains an N-terminal arginine-rich nuclear import signal as well as a C-terminal leucine-rich motif that acts as a nuclear export signal. Rev binds to the Rev response element (RRE) present in the Env coding region of both partially spliced and unspliced transcripts. The leucine-rich export sequence binds to an exportin known as chromosome region maintenance 1 protein homologue (CRM1) and the whole complex is exported to the cytoplasm in a Ran-GTP dependent manner. In the cytoplasm, Ran-GTP is converted into Ran-GDP and the complex dissociates releasing viral mRNAs in the cytoplasm (127).

### 1.2.7 HIV-1 mRNA translation

HIV-1 employs various strategies to exploit the cellular translation machinery for efficient synthesis of its proteins (128). Translation occurs mainly by the Cap-dependent scanning method in which the 5' end of the capped mRNA recruits the 40S ribosomal subunit (129). The 40S ribosomal subunit scans towards the 3' end and recruits the 60S ribosomal subunit when a start codon (AUG) is encountered. For translation of the Pol gene, a programmed frameshift occurs at the Gag stop codon resulting in the production of GagPol precursor protein (130). This event is crucial for production of the viral enzymes. Env and Nef genes are translated due to a leaky scanning mechanism of vpu and rev start codons by the ribosomes (131). Furthermore, HIV-1 uses structural RNA elements such as internal ribosome entry (IRES) to initiate translation (132). The IRES drives translation by directly recruiting the 40S ribosomal subunit in a cap-independent manner. Two IRES elements have been found in HIV-1 genome. The IRES present in the 5'UTR seems to be active under oxidative stress and when the cap-dependent translation is blocked (133,134). The IRES present in the Gag coding mRNA drives expression of a 40kDa Gag isoform in addition to the Pr55Gag (135).

## 1.2.8 Assembly

### 1.1.1.14 Gag trafficking to the plasma membrane

Gag is the building block of HIV-1 virions. Gag expression alone can drive production of virus like particles (VLPs). The N-terminus of Gag is myristylated by cotranslational modification. It contains four major domains, matrix (MA), capsid (CA), nucleocapsid (NC) and p6, and two spacer peptides (SP1 and SP2). HIV-1 particle assembly occurs at the plasma membrane. Gag is targeted to the plasma membrane by MA where it forms a curved lattice (136). A basic region in MA forms electrostatic interactions with the negatively charged inositol head group of phosphatidylinositol-4,-5-bisphosphate $PI(4,5)P_2$ (137). This interaction reveals the N-terminus myristic acid moiety in MA which is then inserted into the plasma membrane, resulting in tethering of Gag in the plasma membrane (138). Gag retention at the plasma membrane is followed by enrichment of the membrane with cholesterol and sphingolipid resulting in the formation of microdomains known as lipid rafts which act as platforms for viral particle assembly (139).

### 1.1.1.15 Genome encapsidation

A single HIV-1 virion contains two copies of the RNA genome (140). Dimerisation of the RNA is a prerequisite for packaging which can occur at the plasma membrane or in the cytosol (141,142) . The 5' untranslated region (UTR) of the RNA genome contains a dimer initiation signal and the packaging sequence known as the Ψ-element. Interaction between the dimer initiation signals of two RNA molecules results in the formation of an RNA dimer which then binds the two Cys-Cys-His-Cys zinc-finger-like regions present in the NC domain of Gag (143,144). Localisation of RNA at the plasma membrane triggers particle assembly around it.

### 1.1.1.16 Env incorporation

Env is synthesised as a gp160 precursor protein in the rough endoplasmic reticulum. After cotranslational glycosylation in the rough endoplasmic reticulum it is transported to the Golgi and then trans-Golgi where it is cleaved by furin protease into gp120 and gp41 (22). Heterodimers of gp120-gp41 traffic through the secretory pathway to the plasma membrane. Trimers of heterodimeric gp120-gp41 are incorporated into virions (24). The mechanism of Env incorporation into virions is not fully understood. Four models of Env incorporation into virions have been proposed (145). The passive incorporation model proposes non-specific incorporation of Env into budding virions. The direct Gag-Env interaction model claims that direct interaction between MA and the cytoplasmic tail of gp41 is responsible for Env incorporation. In contrast, the indirect Gag-Env interaction

model suggests that a host protein acts as a link between Env and Gag which results in Env incorporation into virions. The Gag-Env co-targeting model argues that Env and Gag are targeted to the same site in the plasma membrane such as the micro domains known as lipid rafts where virion assembly takes place.

### 1.2.9 Budding

HIV-1 usurps the ESCRT machinery for budding. The ESCRT complex is involved in multivesicular body biogenesis, cytokinesis, and macroautophagy (146). It contains four multiprotein complexes ESCRT-1, ESCRT-2, ESCRT-3 and several accessory proteins including AAA ATPase Vps4 (147). ESCRT-1 and ESCRT-2 are essential for the formation of the bud whereas ESCRT-3 is required for scission of the bud (148). Vps4 is involved in recycling of the ESCRT proteins after budding (149).

The P6 domain in Gag contains two late domains. The Pro-Thr/Ser-Ala-Pro [PT/SAP] domain recruits tumour susceptibility gene 101 (TSG101) and the Tyr-Pro-Xn-Leu (YPXnL, where X is any amino acid and n=1–3 residues) domain recruits ALG2-interacting protein X (ALIX) (150,151). ESCRT complexes and Vps4 are subsequently recruited. The ESCRT 3 complex proteins forms concentric rings (circular arrays or spirals) at the base of the bud that are then constricted resulting in scission of the bud (152). ESCRT complex mediated budding and scission is triggered by ubiquitination of the cargoes (153). Gag has been shown to be ubiquitinated but its role in HIV-1 budding and release is not yet clear (154).

### 1.2.10 Maturation

Maturation is essential for virion infectivity. It is driven by the protease packaged as a GagPol precursor. During translation of the Gag RNA very small amounts of GagPol precursor are produced due to a programmed frameshift event (130). After release of the virion, protease cleaves Gag and GagPol resulting in morphological changes in virion structure. HIV-1 protease belongs to the group of aspartyl proteases (155). It functions as a dimer and contains an active site at the dimer interface (155). Mutations in the protease specific cleavage sites in the Gag polyprotein results in formation of aberrant non-infectious particles (156).

In immature virions hexamers of Gag are arranged radially with N-termini contacting the membrane and the C-termini facing the centre of the virion. MA remains attached to the membrane and the capsid assembles into a fullerene-like conical core and surrounds the viral dimeric RNA genome in complex with the NC, RT and IN (46). Like the immature gag lattice, the mature CA lattice is composed of hexamers of CA. However, the interactions

between and within hexamers change. Furthermore, the mature CA lattice contains 12 pentamers at the narrow ends of the capsid cone that fully close the capsid shell (46,157).

### 1.2.11 Role of IP6 in assembly and maturation

IP6 been shown to promote in vitro assembly of HIV-1 into immature spherical VLPs. It is a highly negatively charged compound that is involved in various cellular metabolic processes. Recent studies have provided molecular details of IP6 action during HIV-1 assembly and maturation (158,159). During assembly about 300 molecules of IP6 are packaged in a single virus. In the immature virus, the six negatively charged phosphate groups in IP6 make contact with two rings of six positively charged lysine residues (K290 and K359) and stabilise the immature Gag lattice. Consistent with this, IP6 depletion or mutation at residues K290 or K359 in Gag decreases HIV-1 infection. During maturation, protease cleavage of Gag releases IP6 which then promotes assembly of the mature CA lattice inside virions by coordinating a ring of six positively charged arginine residues at position 18.

## 1.3 Innate immunity

Innate immunity provides the first line of defence against infections. It keeps the site of infection under control and conveys specific information about the pathogen to the cells of the adaptive immune system. Activation of adaptive immunity leads to global surveillance of the body for that pathogen and provides immunological memory if a reinfection occurs. Both, innate and adaptive, systems have humoral and cell-mediated components. Humoral immunity is regulated by soluble proteins that label the pathogenic antigens for efficient detection and clearance. On the other hand, cell-mediated immunity involves activation and cross-communication of cells which eventually leads to the clearance of infection.

Cell-mediated immunity in an innate response is regulated by phagocytes. Macrophages and neutrophils are the key phagocytes in initiating an innate response while the dendritic cells act as an interface between the innate and adaptive immune system. These cells can recognise highly conserved features of a pathogen called pathogen associated molecular patterns (PAMPs) by pattern recognition receptors (PRR). The PRRs are germline encoded (160). They detect and distinguish non-self-molecules from self-molecules and activate adaptive immune responses only to the non-self-molecules. They survey different cellular compartments such as the plasma membrane, endosomes or cytosol and recognise several structural and biosynthetic components of bacteria, fungi and viruses (161). The activation of a particular receptor determines the antiviral functions of the cell and its impact on the adaptive immune system.

PRRs are divided into five groups based on protein domain homology. These five groups comprise the Toll-like receptors (TLRs), C-type lectin receptors (CLRs), nucleotide-binding domain, leucine-rich repeat (LRR)-containing receptors (NLRs), RIG-I-like receptors (RLRs), and the AIM2-like receptors (ALRs) (162). Recently, the cGAS/STING pathway of DNA sensing has been identified. These PRRs can be further classified into membrane bound or unbound intracellular receptors. TLRs and CLRs localise to the plasma membrane and endosomal membranes whereas RLRs, NLRs, ALRs are located in the cytoplasm where they detect PAMPs (161). DNA receptors have been shown to be cytosolic and nuclear with recent reports of plasma membrane localisation (163,164).

Activation of PRRs by PAMPs results in a cascade of signalling events that culminate in activation and nuclear translocation of transcription factors such as NF-κB and IRF3. These transcription factors activate innate immune response genes (162). In an antiviral response, this is dominated by induction and secretion of soluble type 1 interferon. IFN-I binds to its receptors on the producer as well as the neighbouring cells activating JAK/STAT signalling pathway, resulting in a second line of gene expression changes that lead to development of the so-called antiviral state (165). In the antiviral state cells upregulate antiviral proteins called restriction factors which makes cells nonpermissive to viral replication. In addition to IFN-I induction, PRR activation results in expression of various proinflammatory cytokines such as CXCL-10, IL-8, and CCL-2 which promote recruitment of neutrophils, monocytes and lymphocytes to the site of infection. These cytokines drive differentiation of T-cells into effector T-cells resulting in a pathogen specific adaptive immune response (166).

### 1.3.1 cGAS/STING pathway of DNA sensing

To date, several proteins have been identified to be involved in detection of DNA. However, numerous recent studies indicate that cyclic GMP-AMP synthase (cGAS) is central to sensing of DNA in various cell types and infections.

#### 1.1.1.17 cGAS

cGAS belongs to the family of nucleotidyltransferases (NTase) (167). It contains a C-terminal NTase domain followed by a Mab21 domain and a highly positively charged N-terminal domain. The NTase and the Mab21 domains are highly conserved whereas the N-terminal domain is less conserved (167). cGAS detects double stranded DNA (dsDNA) in a sequence independent manner (168). It has been shown to induce IFN-β production when overexpressed and conversely cGAS depletion prevents DNA transfection or DNA virus infection stimulated IFN-β expression (167). Furthermore, cGAS knockout mouse

cells such as macrophages and DCs have been shown to be completely insensitive to DNA simulation (169).

Localisation of cGAS has been a controversial topic. cGAS was thought to be a cytosolic sensor of DNA however recent studies have challenged this view. Barnett et al. (2019) showed that under unstimulated conditions cGAS is localised to the plasma membrane via interactions between its N-terminal domain and phosphatidylinositol 4,5-bisphosphate (PI(4,5)P2) (164). In contrast, Gentili et al. (2019) showed that the N-terminal domain was responsible for nuclear localisation of cGAS in human and mice dendritic cells (163). Another study by Liu et al. (2018) demonstrated that cGAS is primarily cytosolic, however it contains an NLS which mediates its nuclear import in an importin-α dependent manner (170). B-lymphoid tyrosine kinase was identified to phosphorylate cGAS at tyrosine 215 for cytosolic retention after etoposide treatment (170). The discrepancy between these observations might be explained by the different cell types and experimental conditions used in these studies.

#### 1.1.1.18 cGAS structure

Analyses of cGAS structure in complex with or without dsDNA has provided important insights into activation of cGAS by dsDNA (168,171). Binding of dsDNA results in formation of cGAS dimers in which two cGAS molecules interact with two dsDNA molecules (172,173). The NTase domain forms two lobes with the catalytic active site present in a groove between the two lobes. The sugar-phosphate backbone of dsDNA contacts the two positively charged surfaces in the NTase which is stabilised by a zinc ribbon. Dimerisation is followed by formation of ladder-like networks along the dsDNA molecules which strengthen cGAS association with the dsDNA. A recent study by Du et al. (2018) showed that the cGAS dsDNA complex is concentrated in phase separated liquid droplets which promote cGAS dimerisation and activation (174).

#### 1.1.1.19 cGAMP production

dsDNA binding to cGAS results in conformational changes in the active site which reveal the catalytic residues and the nucleotide binding pocket resulting in the production of a secondary messenger molecule, cyclic GMP–AMP (cGAMP), from adenosine 5′-triphosphate (ATP) and guanosine 5′-triphosphate (GTP) (175). cGAMP synthesis occurs in a two-step reaction (176). First a linear dinucleotide pppGpA intermediate is formed which is then cyclised to 2′3′-cGAMP with two phosphodiester linkages, one between 2′-OH of GMP and 5′-phosphate of AMP and the other between 3′-OH of AMP and 5′-phosphate of GMP (177).

cGAMP has been shown to be a potent vaccine adjuvant as it can enhance antigen-specific T cell activation and antibody production (169). Recent studies show that cGAMP transfers antiviral immunity to bystander cells. cGAMP travels through gap junctions or HIV-1 envelope glycoprotein induced membrane fusion sites and activates innate immunity in the bystander cells (178,179). Furthermore, cGAMP can be packaged into viral particles which carry it to uninfected cells (180,181). These mechanisms of cGAMP transfer may provide an additional layer of protection to the host when signalling downstream of cGAMP production is inhibited by the invading pathogen in the infected cell.

#### 1.1.1.20 STING activation

cGAMP is a secondary messenger molecule that binds and activates an endoplasmic reticulum resident protein known as stimulator of interferon genes (STING) (182,183). Structural studies show that STING contains four transmembrane helices and a cytoplasmic domain (184). In an inactive state the cytoplasmic and the transmembrane domains interact to form a dimer. In a dimer, the cytoplasmic domains form a V-shaped binding pocket for cGAMP. Upon cGAMP binding, STING undergoes dramatic conformational changes (182). The V-shaped cGAMP binding pocket undergoes an inward rotation such that the STING monomers are brought closer and the cGAMP binding site becomes deeper (185). This is accompanied by the formation of four antiparallel β-sheets which form a “lid” over the cGAMP binding site. Furthermore, the transmembrane domains undergo $180^{o}$ rotation relative to the cGAMP binding site. This allows side-by-side packing of STING dimers and formation of tetramers resulting in formation of higher order oligomers (186). Activated STING translocates to the Golgi apparatus via the ER-Golgi intermediate compartment (ERGIC) (187). Localisation of STING to the Golgi is essential for interaction with downstream signalling proteins and signal transduction. In the Golgi, STING is palmytoilated at Cys88 and Cys91 which is thought to be involved in the formation of high order structures (188).

cGAMP binding to STING results in activation of transcription factors such as NF-κB and IRF3 (189). STING depletion in various cell types has been shown to inhibit IFN induction by DNA virus infection. Furthermore, STING is critical for antiviral responses to DNA viruses *in vivo* and STING knockout mice have been shown to be highly susceptible to HSV-1 infection (189). The activity of STING has been shown to be regulated by cGAMP in a negative feedback loop. cGAMP has been shown to activate Unc51-like autophagy activating kinase 1 (ULK1) by stimulating dephosphorylation of adenosine monophosphate–activated protein kinase (AMPK) (190). Activated ULK1 phosphorylates STING which inhibits downstream signalling (190).

#### 1.1.1.21 IRF3 and NF-κB activation by STING

Recent cryo-electron microscopy has revealed how higher order assembly of STING acts as a platform for recruitment and activation of downstream signalling proteins (191). First TBK1 is recruited to the C-terminal tail (CTT) of STING. CTT of STING forms a β-strand-like conformation and inserts into the kinase domain of first TBK1 subunit and the scaffold and dimerisation domain of the second subunit in the TBK1 dimer. In this complex TBK1 phosphorylates adjacent STING molecules at Serine366 present in a conserved motif pLxIS (p is a hydrophilic residue and x is any residue) (192). This allows recruitment of IRF3 to the STING CTT which is subsequently phosphorylated by TBK1. Phosphorylated IRF3 dissociates from the STING-TBK1 complex and homodimerises. Dimeric IRF3 translocates to the nucleus and upregulates IRF3 responsive genes which includes IFN-I and ISGs (193,194). In addition to IRF3, STING also activates NF-κB. Activation of IRF3 and NF-κB by STING has been shown to be spatially independent events (195,196). Mutational analysis of human and murine STING revealed that translocation of STING to the Golgi apparatus is essential for IRF3 activation but dispensable for activation of NF-κB. K224R and K288R mutations in human and murine STING, respectively, abrogated exit of STING from the ER which prevented IRF3 activation, however NF-κB activation was unaffected. Activated NF-κB tranlocated to the nucleus and activated expression of proinflammatory cytokines such as IL-6 (195,196).

### 1.3.2 RLRs

RLRs are a family of DExH/D box RNA helicases. Three RLRs have been identified: retinoic acid-inducible gene-I (RIG-I), melanoma differentiation gene 5 (MDA5) and laboratory of genetics and physiology 2 (LGP2) (197). RIG-I and MDA5 contain an N-terminal domain consisting of tandem caspase activation and recruitment domains (CARD), a central DExD/H box RNA helicase domain and a C-terminal repressor domain (RD). LGP2, on the other hand, lacks the N-terminal CARD domain but contains the helicase and C-terminal domain. It is involved in regulating RIG-I and MDA5 signalling with reports of both stimulatory and inhibitory effects (197–199).

RLRs detect non-self RNA in the cytosol. The specificity for non-self RNA is achieved by detection of specific features that are absent in self RNA but common in foreign RNA. RIG-I senses short dsRNA and binds to blunt-ended RNA with 5′ triphosphate groups whereas MDA5 binds to long dsRNA (200,201). In the absence of a PAMP RIG-I and MDA5 exist in an autorepressed conformation in which the CARD domain is bound by the helicase and the RD. Upon binding RNA conformational changes exposes the CARD domains which interact with CARD domains in an adaptor protein known as mitochondrial antiviral signalling protein (MAVS) (202). RIG-I activation results in its K63-linked ubiquitination by

TRIM25 and RNF135 (203,204). Activated RIG-I is translocated to MAVS containing membranes by a chaperone protein 14-3-3e (205). MAVS is located in the outer mitochondrial membrane, peroxisomes and mitochondria associated membranes via its C-terminal transmembrane domain. MAVS localisation to these sites is essential for its signal transduction ability as MAVS variants lacking the C-terminal transmembrane domain cannot activate signalling despite possessing the interaction domains for downstream signalling molecules (206). Activated MAVS oligomerises to form prion like aggregates resulting in formation of a signalsosome and recruitment of ubiquitin ligases, TRAF2, TRAF3 and TRAF6, which are required for activation of NF-κB and IRF3 (207). TRAF2 and TRAF6 activates NF-κB via IKK whereas TRAF3 activates IRF3 via TBK1 (208). Activation of IRF3 and NF-κB leads to expression of proinflammatory cytokines, IFN-I and interferon stimulated genes. Localisation of MAVS has been shown to determine the antiviral gene expression. MAVS signalling from the mitochondria results in IFN-I and IFN-III dependent ISG expression whereas signalling from the peroxisome resident MAVS results in ISG expression that is independent of IFN-I (209,210). However, these findings have been challenged by a study which showed activation of IFN-I and IFN-III response by mitochondrial and peroxisomal MAVS (211).

### 1.3.3 ALRs

In humans, ALRs are a family of four IFN inducible proteins which include AIM2 and IFI16. ALRs contain an N-terminal pyrin domain (PYD) which allows protein-protein interactions and a C-terminal DNA binding HIN-200 domain (212). Unlike AIM2, IFI16 contains two HIN-200 domains. AIM2 and IFI16 have been shown to detect intracellular DNA in a sequence independent manner (213,214). Detection of DNA leads to the formation of a multi-protein complex known as inflammasome. Upon binding DNA, AIM2 and IFI16 undergo conformational changes that allow the pyrin domain to interact with the pyrin domain of an adaptor protein apoptosis-associated speck-like protein containing CARD (ASC) (215,216). Subsequent ASC nucleation results in recruitment of caspase-1 via interaction between their CARD domains. Inflammasome activation results in secretion of bioactive IL-1β and IL-18. IL-1β and IL-18 belong to a groups of cytokines known as leaderless cytokines that lack protein trafficking signals for secretion (217). They are synthesised as inactive precursors. The inflammasome provides a platform for caspase-1 to process pro-IL-1β and pro-IL-18 into their active forms which are then secreted by lysosome exocytosis or exosome release from multivesicular bodies (218). They can also be released during inflammasome induced pyroptosis (219).

IFI16 has been shown to detect DNA of various viruses such as herpes simplex virus (HSV), Kaposi's sarcoma–associated herpesvirus (KSHV), cytomegalovirus, and HIV (216,220,221). IFI16 is predominantly nuclear however depending on the cell type, IFI16

can be found localised to the cytoplasm (222). Both nuclear and cytoplasmic forms of IFI16 have been shown to detect pathogenic DNA. Nuclear localisation of IFI16 is attributed to a multipartite nuclear localisation signal which is regulated by acetyltransferase p300 mediated post translational acetylation (223). Acetylation of the IFI16 NLS has been shown to inhibit its nuclear import and sensing of nuclear viral DNA (223). In addition to inflammasome activation, IFI16 has also been shown to be involved in modulation of the cGAS/STING activation of IFN-I (224,225). The role of IFI16 during HIV-1 infection is describe in section 1.4.2 and 1.4.3.

### 1.3.4 TLRs

The human genome encodes for 10 TLR proteins (TLR1-TLR10). TLRs are type 1 transmembrane glycoproteins that contain an N-terminal ectodomain, a hydrophobic transmembrane domain and a cytoplasmic C-terminal domain. The N-terminal ectodomain contains leucine rich motifs that allow recognition of various pathogen derived molecules (226). The C-terminal domain is involved in intracellular signal transduction (227). TLR1, TLR2 and TLR6 recognise lipoproteins and lipopeptides. TLR3 detects double stranded RNA (228). TLR4 binds to LPS whereasTLR5 binds flagellin. TLR7, TLR8 and TLR9 bind to nucleic acids (162). TLRs localise to the plasma membrane and endosomes. TLR1, TLR2, TLR4, TLR5 and TLR6 are mainly found in the plasma membrane whereas TLR3, TLR7, TLR8 and TLR9 are present in the endosomes (229–231).

TLR binding to its cognate ligand results in formation of homo- or heterodimers of TLRs with the ligand present between the two receptors (232). This brings the c-terminal domains closer to each other and activates intracellular signalling. The c-terminal domain of TLRs resembles the IL-1β receptor and contains a Toll-IL-1 resistance (TIR) domain (233). Dimerisation of TLRs results in conformational changes that reveal the TIR domain which then recruits the downstream adaptor proteins. There are 5 TIR-domain binding adaptor proteins: myeloid differentiation primary-response protein 88 (MyD88), TIR-associated protein (TIRAP), TIR-domain-containing adaptor protein-inducing IFN-β (TRIF) and TRIF-related adaptor molecule (TRAM) and sterile-α-and armadillo-motif-containing protein 1 (SARM1) (234). TLRs can activate NF-κB and IRF3 by differential recruitment of the adaptor proteins. MyD88 recruitment allows activation of the NF-κB complex and proinflammatory gene expression whereas TRIF recruitment results in activation of IRF3 and IFN-I induction (235,236). TRIF is only recruited by TLR3 and TLR4 in the endosomes (237).

### 1.3.5 CLRs

CLRs are a family of membrane bound or cytosolic receptors that contain a characteristic C-type lectin-like domain (CTLD). They can detect a variety of microbes and are divided into 17 groups based on structure homology (238). However, only a few CLRs are able to induce proinflammatory signalling against pathogens. Dectin1 and Dectin 2 are the best characterised.

Dectin-1 plays a major role against fungi and bacteria. It is expressed by DCs, macrophages, neutrophils and monocytes. It is a type two transmembrane protein that detects fungal and bacterial cell wall component such as β-glucan (239). It contains an extracellular CTLD and an intracellular domain called hemiTAM containing a single tyrosine motif (YxxL) (240). Upon binding β-glucan, Dectin-1 triggers phagocytosis resulting in microbe destruction and activation of a proinflammatory response. Activated Dectin-1 dimerises and translocates to lipid rafts where its hemITAM motif is phosphorylated by Src family kinases (SFKs) (241). This is followed by recruitment of Syk to the hemITAM motif which in turn results in a signalling cascade that leads to activation of MAPK, canonical and non-canonical NF-κB and NFAT. Canonical NF-κB is activated via TRAF6-TAK1 complex activation whereas the non-canonical NF-κB is activated via the kinase NIK (242,243).

Dectin-2 has been shown to bind alpha-mannose of hyphal *Candida* however it can also detect certain bacteria including *Schistosoma mansoni* and *Mycobacterium tuberculosis* (244,245) . In contrast to Dectin-1, Dectin-2 contains a short cytoplasmic tail that lacks the hemiTAM motif and therefore cannot activate signalling. To activate signalling it binds to a hemiTAM containing protein, FcRγ, which activates signalling in a SFK dependent manner like Dectin-1 signalling. Dectin 2 has also been shown to form heterodimers with Dectin-3 which increases the sensitivity of alpha-mannose detection however the molecular details are not yet clear (246).

### 1.3.6 NLRs

NLRs are a family of intracellular receptors which are critical for pathogenesis of a variety of inflammatory diseases. 22 NLR proteins are expressed by human immune and non-immune cells (247). NLRs are characterised by a tripartite structure containing N-terminal protein-protein interaction domain, central nucleotide binding domain (NOD) and a C-terminal leucine rich repeat (LRR). The N-terminal domain is further divided into a CARD domain, PYRIN domain and baculovirus inhibitor repeat (BIR) which are critical for intracellular signal transduction (247). The NOD domain is responsible for activation

induced oligomerisation of the receptors whereas the C-terminal is critical for recognising the PAMP.

NOD1 and NOD2 recognise components of the bacterial cell wall peptidoglycans, γd-glutamyl-meso-diaminopimelic acid (iE-DAP) and muramyl dipeptide (MDP) respectively (248,249). NOD1 recognises iE-DAP primarily on gram negative bacteria whereas NOD2 detects MDP that is found in a range of bacteria including *Streptococcus pneumoniae, L. monocytogenes, Mycobacterium tuberculosis, Salmonella*, and *Staphylococcus aureus* (250,251) .

Upon sensing the PAMP, NLRs activates a signalling cascade that culminates in the activation of NF-κB and MAPKs (252). PAMP binding causes oligomerisation of the NLR which then recruits a serine threonine kinase RICK (253,254). Polyubiquitination of RICK results in recruitment of TAK1 which activates IKK by phosphorylating the IKKβ subunit (255). Activated IKK phosphorylates IκBα resulting in its degradation and liberation of NF-κB for nuclear translocation. NF-κB activates transcription of inflammatory cytokines and chemokines such as TNF-α, IL-6 and IL-8. For NF-κb activation by NOD1 TRAF6 has been shown to be important whereas for NOD2 TRAF2 and TRAF5 are shown to be essential (255). NOD signal transduction is thought to occur by their recruitment to the endosomal membranes (256). Activation of NOD1 with iE-DAP has been shown to localise RICK kinase and NOD1 to the endosomes which correlates with cytokine production (257). NOD1 and NOD2 signalling also results in activation of MAPKs such as p38, extracellular signal–regulated protein kinase (ERK), and c-Jun N-terminal kinase (JNK). Unlike NF-κB activation by NODs, the signalling events that activate MAPKs are less well defined, however RICK1 and TAK1 have been shown to be required (254,258).

## 1.4 HIV-1 innate immune detection

### 1.4.1 HIV-1 RNA detection

The endosomal PRRs TLR7 and TLR8 have been shown to detect HIV-1 ssRNA. Heil et al. (2004) transfected HIV-1 derived guanosine (G)- and uridine (U)-rich ssRNA oligonucleotides into macrophages and dendritic cells which resulted in production of IFN-I and proinflammatory cytokines (259). In mice TLR7 was found to be essential for detection of HIV-1 derived GU-rich oligonucleotides whereas in human HEK293 cells overexpression of TLR8 was shown to detect HIV-1 derived GU-rich oligonucleotides and activate a NF- κb luciferase reporter (259). Another study found that TLR7 detects HIV-1 RNA in plasmacytoid dendritic cells (pDCs) which results in IFN-a production (260). TLR7 detection of HIV-1 RNA was dependent on HIV-1 entry via the endosomes. TLR7 inhibitor

treatment or infection with HIV-1 lacking genomic RNA prevented IFN- α production whereas transfection of HIV-1 genomic RNA induced INF-α in pDCs (260).

Cytosolic RLRs have also been implicated in detection of HIV-1 RNA. Berg et al. (2012) showed that transfection of full-length virion derived genomic RNA of HIV-1 triggers various ISGs in PBMCs which correlated with activation of NF-κB, p38, and IRF signaling pathways (261). Analysis of various HIV-1 genomic regions revealed that the regions that formed secondary structures were the most potent for inducing ISG expression. RIG-I and MAVS were found to be essential for this response in Huh7 cell lines and murine macrophages, respectively. In another study transfection of monomeric and dimeric forms of HIV-1 RNA triggered an ISG response in murine embryonic fibroblasts (MEFs) which was found to be RIG-I dependent but MDA5 independent (262).

These studies are limited by the lack of experimental data that show detection of HIV-1 RNA during infection. Most of the experiments were done with purified virion derived genomic RNA which was transfected into the cells. During natural infection of HIV-1 the viral RNA genome is associated with various viral proteins and is surrounded by the viral capsid core which may prevent activation of PRRs. Furthermore, transfection may deliver the RNA to compartments which are not accessed during infection. However, recent studies have shed some light on HIV-1 RNA detection during infection.

Recent work by Akiyama et al. (2018) showed that in primary macrophages HIV-1 is sensed at a post integration step which activates IFN-I dependent proinflammatory signalling (263). The PAMP for this IFN-I induction was identified to be the viral intron containing RNA (icRNA). HIV-1 icRNA mediated activation of IFN-I was found to be MAVS dependent but RIG-I and MDA5 independent. Furthermore, immune activation of macrophages by HIV-1 induced inhibitory receptor expression and functional immune exhaustion of co-cultured T-cells. In contrast, Gringhuis et al. (2017) showed that in DCs abortive HIV-1 RNA is sensed by an RNA helicase DDX3 which activates IFN-I responses via MAVS (264). In another report, MDA5 was shown to be able to detect HIV-1 genomic RNA during infection of DCs and macrophages (265).

### 1.4.2 HIV-1 DNA detection

HIV DNA has been shown to be detected by cGAS and IFI16. Evidence for the HIV-1 reverse transcribed DNA to activate innate immune responses came from a study which showed that depletion of the exonuclease TREX1 results in ISG expression upon HIV-1 infection in T-cells and macrophages(266). TREX1 was found to bind and degrade HIV-1 DNA. In TREX1 depleted cells accumulation of HIV-1 DNA correlated with activation of

IFN-I and inhibited virus replication. This observation led to the search for HIV DNA sensors.

Gao et al. (2013) found that HIV-1 activated cGAS dependent IFN-I production (267). IFN production was inhibited by RT inhibitors but not integrase inhibitors suggesting that the viral reverse transcribed DNA was the PAMP for cGAS. Furthermore, depletion of cGAS prevented activation of IFN-I by HIV-1 and other retroviruses such as SIV and MLV. Another study used a comparative approach and showed that both HIV-1 and HIV-2 activated cGAS dependent innate immune responses in DCs however HIV-2 was a more potent activator of cGAS (268). In contrast to the study by Gao et al. this study showed that the viral sensing was dependent on integration as the integrase mutant viruses were unable to activate innate signalling.

IFI16 has been reported to detect transfected ssDNA oligo nucleotides derived from HIV-1 and HIV-1 infection of macrophages (221). This resulted in an IFN-I and IFN-III response which inhibited virus spread. IFI16 depletion was shown to abrogate innate immune activation by HIV-1. A subsequent study by the same group showed that IFI16 modulated activity of cGAS/STING pathway (269). IFI16 depletion inhibited cGAMP production by cGAS, conversely IFI16 overexpression increased cGAMP production. In addition, IFI16 enhanced recruitment of TBK1 to STING. This suggested that IFI16 may not directly sense HIV-1 DNA but may act as a cofactor for the cGAS mediated innate immune activation.

Similar to the role of IFI16 in augmenting cGAS activity, PQBP1 has also been shown to contribute to cGAS detection of HIV-1 (270). It was identified in an siRNA screen for immune modulators that interfere with HIV-1 activation of innate immune responses in DCs. Unlike IFI16, PQBP1 was found to directly bind HIV-1 DNA and cGAS. Interestingly, PQBP1 was found to be essential for activation of ISGs by retroviruses including FIV and EIAV but was not required for ISG activation by transfected DNA or mouse hepatitis virus (MHV) infection. Figure 1.3 summarises HIV-1 nucleic acid sensing in a schematic diagram.

### 1.4.3 HIV-1 detection in T-cells

The DNA sensors, cGAS, IFI16 and DNA-PK, have been shown to detect HIV-1 in T-cells, however the step of the viral lifecycle required for detection and the outcome of detection are controversial. Some studies have shown reverse transcription to be required for detection whereas others have reported a requirement for integration. The outcome of HIV-1 detection in T-cells is also conflicted with some studies reporting IFN-I production and others showing cell death via apoptosis or pyroptosis.

The first report of HIV-1 sensing in T-cells came from a study that used *ex vivo* human lymphoid aggregated cultures (HLACs) prepared from tonsillar tissue infected with HIV-1. Doitsh et al (2010) found very low HIV-1 productive infection of CD4+ T-cells which coincided with a massive CD4+ T-cell death(271). The T-cell death was shown to be associated with abortive HIV-1 infection which did not require integration. Abortive infection resulted in accumulation of viral DNA before integration which induced proapoptotic and proinflammatroy responses. Using unbiased proteomic and biochemical approaches, subsequent studies by the same group showed that abortive infection of CD4+ T-cells was detected by IFI16 which activated inflammasome formation resulting in caspase-1 mediated pyroptosis(272,273). They also found that peripheral blood derived CD4+ T-cells were resistant to HIV-1 driven pyroptosis and this was associated with the resting state CD4+ T-cells, the lower HIV-1 reverse transcription and lower IFI16 expression(274). It was proposed that microenvironment of the lymphoid tissues program the T-cells to undergo pyroptosis upon HIV-1 abortive infection because the PBMC derived CD4+ T-cells could be made sensitive to pyroptosis by coculturing with lymphoid-derived T-cells(274).

In contrast to these studies, Cooper et al. (2013) showed that PBMC derived CD4+ T-cell death was due to HIV-1 productive infection which required integration(275). Integrase deficient HIV-1 did not cause cell death and treatment with Raltegravir, an integrase inhibitor, prevented CD4+ T-cell death. Cell death upon HIV-1 infection required DNA-PK which triggered a DNA damage response via p53 activation.

Evidence for HIV-1 detection by cGAS in T-cells comes from two studies, however the activation of the downstream pathway which results in IFN-l expression is not clear. Vermeire et al. (2016) showed that detection of HIV-1 in activated PBMC-derived CD4+ T-cells resulted in IFN-l production(276). This was dependent on integration and modulated by accessory proteins. Vpu was shown to inhibit and Vpr was shown to potentiate cGAS induction of IFN-l. On the other hand, Xu et al. (2016) found that HIV-1 infection of T-cells resulted in cGAMP production, however IFN was not detected from infected cell supernatants(179).

### 1.4.4 HIV capsid detection

HIV-1 capsid has been shown to be a PAMP that can activate innate immune responses. The role of TRIM5α in capsid recognition and activation of NF-κB is described in section 1.5.7. A recent study has identified a nuclear protein known as NONO which potentiates HIV activation of the DNA sensor, cGAS(277). Lahaye et al. (2018) carried out a yeast two-hybrid screen for potential HIV capsid interacting proteins. NONO was identified to bind HIV-1 and HIV-2 capsid NTD. Comparison of interaction strength showed that NONO

interacted more strongly with HIV-2 capsid than HIV-1 capsid. Although depletion of NONO did not affect HIV-1 or HIV-2 infection of myeloid cells it prevented activation of innate immune responses by HIV-1 and HIV-2 in dendritic cells and macrophages. NONO was found to interact with the viral capsid and cGAS in the nucleus. cGAS was shown to bind HIV-2 DNA in a NONO dependent manner as NONO depletion did not result in immunoprecipitation of HIV-2 DNA with cGAS. Finally, it was shown that HIV infection of dendritic cells from NONO deficient individuals resulted in a lower innate immune activation compared to cells from healthy individuals.

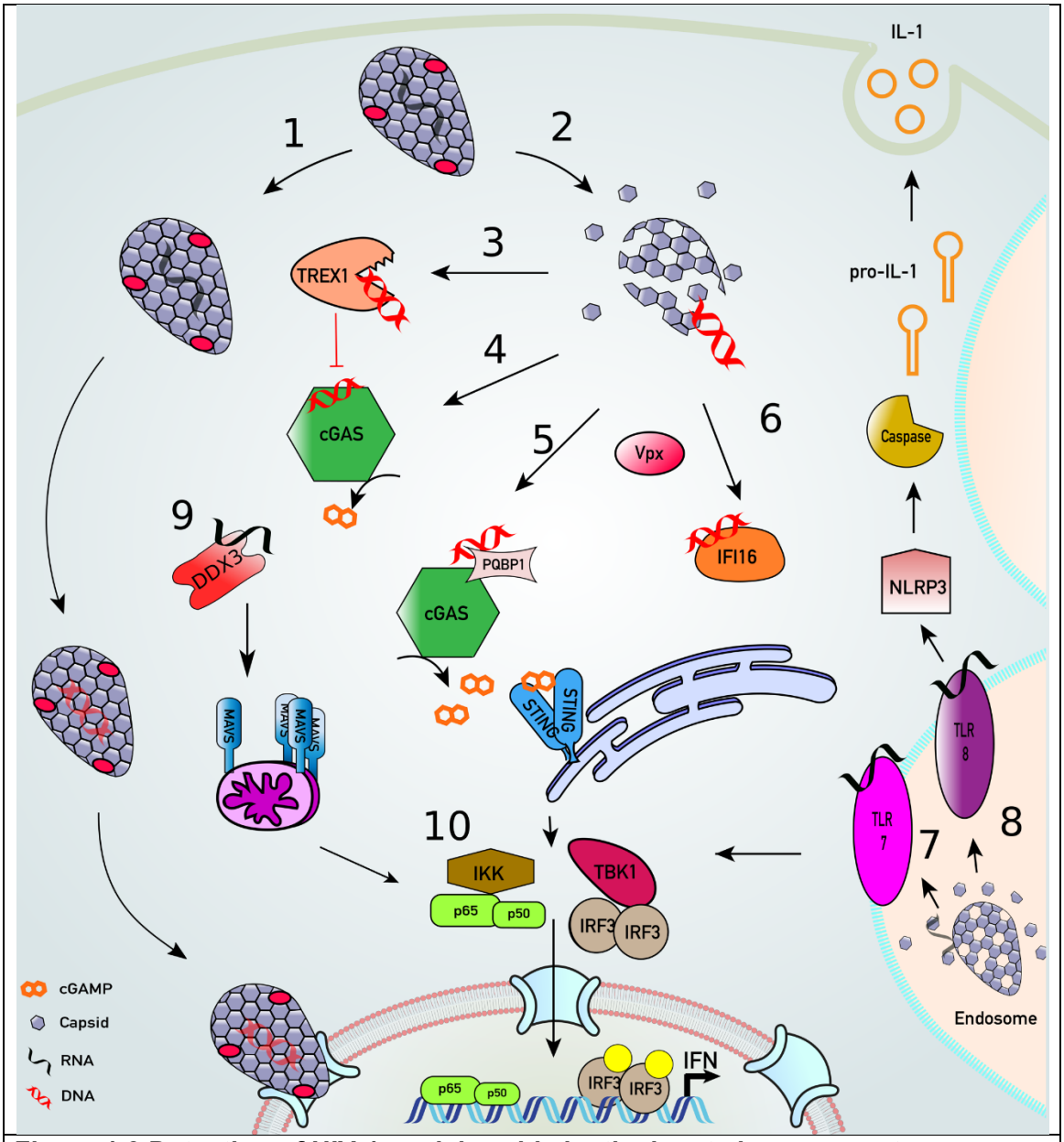


**Figure 1.3 Detection of HIV-1 nucleic acids by the innate immune system**

The HIV-1 capsid stays intact and shields the genomic RNA or the reverse transcribed DNA from the innate PRRs as it transverses the hostile cellular cytoplasm. It uncoates in the nucleus in a manner that does not lead to innate immune activation **(1)**. HIV-1 cytoplasmic uncoating may be stochastic or occur under certain conditions **(2)**. The Cytoplasmic exonuclease TREX1 digests cytosolic HIV-1 DNA **(3)** that would otherwise trigger DNA sensing through cGAS **(4)**. After SAMHD1 degradation by viral protein x (Vpx), HIV-1 DNA products are sensed by polyglutamine-binding protein 1/cGAS **(5)** or interferon-γ inducible protein 16 (IFI16) **(6)**. HIV-1 virions in endosomal compartments may reveal genomic RNA to toll-like receptor (TLR) 7 that triggers an innate immune response **(7)**. HIV-1 genomic RNA detection by TLR8 may lead to assembly of an NLRP3 inflammasome to activate caspase-1, which cleaves pro-interleukin-1β (IL-1β) into bioactive IL-1β **(8)**. HIV-1 abortive RNA may be detected by DDX3 which activates IFN-I via MAVS **(9)**. All sensing pathways described converge on activation of transcription factors IRF3 and NF-κB that drive IFN production **(10)**.

## 1.5 HIV-1 restriction factors

### 1.5.1 APOBEC3

APOBEC (apolipoprotein B mRNA editing enzyme, catalytic polypeptide-like) proteins belong to the family of cytidine deaminases which include APOBEC1, APOBEC2, APOBEC3 and AID (Activation-induced cytidine deaminase) (278). Human chromosome 22 encodes 7 APOBEC3 proteins: A3A, A3B, A3C, A3DE, A3F, A3G and A3H. A3 proteins contain one or two Z-domains (279). The Z-domains exhibit deaminase activity and coordinate a zinc ion via three cysteine or histidine residues (280). Structurally the Z-domains comprise five beta strands flanking alpha helices and connecting loops (280). A3A, A3C, and A3H have one and A3B, A3DE, A3F, and A3G have two Z-domains (281). Out of the seven A3 proteins A3G is the most studied and is the most potent inhibitor of HIV-1.

A3G packaged into HIV-1 virions is the major determinant of A3G mediated restriction of HIV-1. It is packaged into HIV-1 particles via interaction with the viral RNA and nucleocapsid in the Gag polyprotein (282). A3G has been shown to dimerise in an RNA dependent manner which is important for packaging and antiviral activity (283). In the target or infected cells A3G acts during viral reverse transcription. A3G deaminates cytidine residues in the newly formed minus single stranded DNA (284). This causes guanosine to adenosine hypermutation in the plus strand DNA resulting in defective proviruses. Hypermutated proviruses contain premature stop codons and missense mutations that produce non-functional proteins and defective particles which cannot sustain viral replication (285).

Another feature of A3G restriction of HIV-1 is reduction in viral reverse transcription products. The mechanism of this is not fully understood. It was postulated that the hypermutated viral DNA is degraded by cellular enzymes. The hypermutated DNA was shown to be recognised by the cellular uracil-DNA glycosylases (UDGs) involved in the uracil base excision pathway (UBER) which was thought to result in its degradation (286). However, inhibition of UBER does not rescue viral DNA levels (287). In addition, the reduction in viral DNA levels by A3G has been shown to be independent of its deaminase activity (288). Given that A3G is an RNA binding protein, several groups demonstrated A3G inhibition of reverse transcription at several steps. A3G has been shown to inhibit tRNA binding to the primer binding site in the viral RNA, minus and plus strand transfer and primer tRNA processing and DNA elongation (289–292). A recent study by Pollpeter et al. (2018) has provided another mechanism for reduction in reverse transcription products (293). They show that A3G can bind and inhibit HIV-1 reverse transcriptase (RT).

A point mutation prevented RT binding and reduced the antiviral effect. In addition, a double point mutant A3G that was defective for RT binding and deaminase activity was completely inactive against HIV-1. The mechanism by which A3G binding inhibited RT activity was not determined.

A3G is expressed in numerous cell types to varying levels including HIV-1 target cells, CD4+ T-cells and macrophages (294). Its expression can be enhanced by IFN-I stimulation (294). Analysis of hypermutated motifs has revealed A3G to be the most potent A3 deaminase against HIV-1 in CD4+ T cells and macrophages (295,296). A3G expression and hypermutation of viral DNA has been correlated with low viremia and increased CD4+ T-cell counts in HIV-1 infected individuals (297). Furthermore, there is evidence for A3G mediated restriction of HIV-1 in CD4+ T-cells by hypermutation as well as inhibition of reverse transcription (295). At least 6% and 10% of guanosines have been shown to be mutated in HIV-1 infected CD4+ T-cells and macrophages, respectively (298). Low levels of G to A hypermutations in HIV-1 infected cells suggest that inhibition of reverse transcription might be the dominant mechanism of HIV-1 restriction by A3 proteins. Dendritic cells which are refractory to HIV-1 productive infection but allow transfer to T-cells have also been shown to hypermutate viral cDNA after IFN-I stimulation and inhibit HIV-1 transmission to T-cells (299).

A3G has been shown to modulate innate and adaptive immune activation. In mice, A3G mediated suppression of reverse transcription limited detection of viral DNA by the DNA sensor, cGAS, and prevented IFN induction (300). Hypermutation of the viral DNA has been proposed to be both beneficial and detrimental for the virus. Sub lethal mutations by A3G may generate viral strains that are resistant to immune responses and antiretroviral drugs (301,302). In support of this, a study has shown reduced CD8+ T cell responses to HIV-1 infected T-cells due to hypermutation of the genomic regions that are associated with CTL escape (303). In contrast, lethal mutations in the viral genome have been shown to generate non-functional proteins that are processed and presented by the MHC-I on the cell surface which increased CTL response to HIV-1 infected T-cells (304). A3G also promotes detection of infected T-cells by NK cells (305). Hypermutation of viral DNA by A3G activates a DNA damage response which leads to upregulation of NK cell activating ligands such as ULBPs and PLAP and enhances NK cell detection and cell lysis (305).

### 1.5.2 IFITMs

Interferon-induced transmembrane (IFITM) proteins are a family of antiviral factors that prevent infection by enveloped viruses including members of the retro-, orthomyxo-, flavi- and filo- families of viruses (306–308). In humans, five loci have been identified on chromosome 11 that encode for IFITM proteins, 1, 2, 3, 5 and 10 (309). IFITM1, 2 and 3

are IFN inducible with antiviral activity. IFITM5 has been shown to be involved in bone mineralization in osteoblasts. It is not induced by IFN and lacks antiviral activity. The function of IFITM10 has not yet been identified. IFITMs localize to distinct cellular membranes where they inhibit virus membrane fusion with the target cell membranes (310). All IFITM proteins are targeted to the plasma membrane after synthesis. Unlike IFITM1, IFITM2 and 3 contains the endocytic motif, YxxΦ which results in their internalisation into endosomes (311,312). IFITM1 is mainly found at the plasma membrane (313). IFITM2 is found in early endosomes whereas IFITM3 is present in late endosomes (313). The specificity of IFITM antiviral activity is determined by its localisation. For example, IFITM3 is active against Influenza A virus (IAV), however IFITM3 relocalisation to the plasma membrane by mutating the endocytic motif has been shown to abolish its antiviral activity (312). IFITMs have also been shown to inhibit entry of non-enveloped viruses such as reoviruses which require endosomes for cell entry (314).

IFITMs belong to the dispanins superfamily of proteins (315). They contain a conserved intracellular loop (CIL) flanked by an N-terminal and a C-terminal hydrophobic domain. The CIL is cytoplasmic. Unlike the C-terminal hydrophobic domain in which the alpha helix is transmembrane, the N-terminal hydrophobic domain contains two alpha helices that are embedded into the inner leaflet of the membrane (310,316). The IFITMs structure is stabilized by posttranslational palmitoylation of the CIL domain (317). The N- terminal hydrophobic domain appears to regulate the curvature of the membrane which may modulate the antiviral activity (318). The C-terminal transmembrane domain is involved in IFITM oligomerisation into higher order structures which may influence the fluidity of the membrane (319).

IFITMs block fusion of enveloped viruses with target cell membranes but the exact mechanism is not fully understood. Most mechanistic studies have been done in the context of IAV infection and suggest that IFITMs prevent fusion by regulating the fluidity of the target membranes (320,321). Based on these studies three mechanisms have been proposed that all depend on interaction between IFITM proteins and formation of higher order complexes. It has been suggested that multimerisation of the IFITM reduces fluidity of the membranes which may hinder the movement of virus receptors along the membrane and limits interaction with the viral envelope glycoproteins, inhibit clustering of the viral glycoproteins in the viral membrane required for their role in fusion or induce a membrane curvature that counteracts the curvature forced by the virus membrane fusion (322). A recent study found a transmembrane zinc metallopeptidase STE24 (ZMPSTE24) to be required for the antiviral activity of IFITM (323). ZMPSTE24 inhibited infection by various enveloped viruses and immunoprecipitated with IFITM1, 2 and 3. ZMPSTE24 processes

lamin A on the inner nuclear membrane however the antiviral activity of ZMPSTE24 was found to be independent of its catalytic activity.

IFITM inhibitory activity against HIV-1 was identified in an ISG siRNA screen (308). IFITM1, 2 and 3 were found to suppress HIV-1 spreading infection. Subsequently it was shown that expression of IFITMs in producer cells results in IFITM localisation to the sites of virus assembly which does not affect virion production but reduces virion infectivity in the target cells due to IFITM virion incorporation (324,325). The authors concluded that the antiviral effect of IFITM comes from the IFITM present in the virion membrane and not from the target cell membrane associated IFITM. Another study found that IFITM expression inhibited processing and virion incorporation of the HIV-1 Env glycoprotein, gp160. It was shown that virus passage in IFITM expressing cells resulted in an IFITM resistant virus with mutations in the Env gene (326). A recent study found that HIV-1 transmitted founder (TF) viruses were resistant to IFITM mediated restriction (313). TF viruses are thought to be responsible for the establishment of de novo infections and known to be more resistant to the antiviral effects of IFN than viruses isolated during chronic phase. In this study Foster et al. (2016) compared TFs and chronic viruses from the same individual and found that TFs were more resistant to IFITM restriction than the chronic viruses. The increased susceptibility of chronic viruses to IFITMs, especially IFITM2 and 3 was associated with mutations that drive escape from neutralizing antibodies, positing IFITMs as a barrier to HIV-1 transmission. Using HIV-1 strains with different coreceptor usage, it was demonstrated that R5 tropic viruses were restricted by the plasma membrane associated IFITM1. In contrast X4-tropic viruses were found to be restricted by IFITM2 and IFITM3 present in the endosomes. Furthermore, the restrictive activity of IFITM2 and 3 against X4-tropic viruses could be abolished by their mislocalisation to the plasma membrane. These observations not only implicate the dependency of HIV-1 fusion site on the coreceptor usage but also demonstrates that IFITMs in the target cells provide the antiviral activity as the IFITM incorporation was not affected by different corecptor usage.

### 1.5.3 MxB

Human genome encodes for two Myxovirus resistance (Mx) genes, MxA and MxB, which were identified as IAV restriction factors (327,328). Mx proteins are IFN-I inducible guanosine triphosphatases (GTPases) belonging to the dynamin superfamily. MxA inhibits infection of various DNA and RNA viruses however antiviral activity of MxB is restricted to retroviruses, VSV and herpes viruses (327,329–331). Both Mx proteins contain a GTPase domain connected to a C-terminal stalk domain via tripartite bundle signaling element (BSE) (332). Unlike MxA, MxB contains a 25-amino acid long N-terminal domain that confers antiretroviral activity to MxB (333).

MxB has been shown to restrict HIV-1 infection in various cell lines such as CD4+CXCR4+U87 MG cells and SupT1 cells (334,335). MxB restricts HIV-1 infection by inhibiting integration without affecting reverse transcription (335). It is thought that MxB blocks nuclear import of HIV-1 preintegration complex because it Inhibits HIV-1 more potently in nondividing cells and reduces HIV-1 2-LTR circles which are only formed after nuclear entry. One study has shown a bigger defect in infection than in nuclear import suggesting that MxB may inhibit additional steps in viral life cycle (336).

Mutational analyses of MxB revealed that the GTPase domain is dispensable for its antiviral activity. This was shown by mutations in the GTPase domain that prevented GTP binding and hydrolysis (335). Recently, MxB has been shown to oligomerise into higher-order structures. Recombinant MBP-fused MxB has been shown to form helical assemblies in vitro (337). However abrogation of higher order assembly of MxB does not seem to be essential for HIV-1 restriction (338). On the other hand, the N-terminal domain of MxB is essential for HIV-1 restriction. Addition of the human MxB N-terminus to the canine MxB, which lacks anti-HIV-1 activity, made HIV-1 sensitive to the canine MxB (336). Similarly, two unrelated proteins, Fv1 and oligomerization competent leucine zippers, gained anti-HIV-1 activity when fused to MxB N-terminal domain (339). MxB mRNA translation results in synthesis of two isoforms, short and long, due to an internal initiation methionine at position 26. The long isoform contains the N-terminal domain that provides the antiviral activity and allows localisation to the nuclear envelope (336). Since antiviral activity correlated with the nuclear envelope localisation, initially it was proposed that nuclear envelope localisation is required for HIV-1 restriction. However, a study genetically separated the two activites of MxB by a single point mutation at K20. Mutation of K20 abrogated nuclear envelope localization but allowed HIV-1 restriction, suggesting that nuclear envelope localisation is not required for the antiviral activity of MxB (340).

HIV-1 capsid is targeted by MxB. A triple arginine motif, 11RRR13, in the N-terminal domain was identified to bind to the capsid and in vitro studies have shown MxB binding to the CA nanotubes (339,341,342). However, the relationship between CA binding and restriction seems to be complicated because mutations in MxB that abolished HIV-1 restriction did not prevent CA binding (342). Nonetheless, passage of HIV-1 in cells expressing MxB results in a point mutation in CA at position A88 that makes HIV-1 resistant to MxB (343). The occurrence of MxB resistance mutation at residue A88 which is present in the cypA binding loop implicated the role of HIV-1 cofactors in MxB meditated restriction of HIV-1. Further investigations showed that MxB antiviral activity was dependent on HIV-1 cofactor recruitment. Abolishing CypA recruitment by CypA depletion or CsA treatment inhibited MxB antiviral activity (334,335). Interaction between MxB and

CypA has also been reported (343). Consistently, HIV-1 capsid cofactor binding mutants, P90A and N74D, have been shown to be MxB insensitive (334,335).

Given the localisation of MxB to the nuclear rim and MxB insensitivity of HIV-1 mutants that show altered nuclear import mechanism, two recent studies investigated the role of nucleoporins in MxB antiviral activity. The first study carried out a yeast-two-hybrid screen for MxB N-terminal domain and identified interaction with seven nucleoporins (344). Depletion of these nucleoporins in cell lines and CD4+ T-cells inhibited MxB anti-HIV-1 activity. Nup214 and TNPO1 depletion was sufficient to completely inhibit MxB antiviral activity and nuclear envelope localisation. TNPO1 and Nup214 were found to interact with MxB in a triple arginine motif dependent manner. Consistent with these findings the second study carried out an siRNA screen against nucleoporins and found that changes in nucleoporin levels alter MxB activity (345). NPCs in different cell lines were found to be composed of different nucleoporins that differentially modulated MxB activity. Interestingly, MxB expression also inhibited non-viral NLS mediated nuclear entry. These studies demonstrated that nuclear pore proteins and nuclear import factors can regulate antiviral activity of MxB and extend its function in nuclear import of cargoes beyond HIV-1.

### 1.5.4 SAMHD1

Human sterile alpha motif and HD-domain-containing protein (SAMHD1) restricts HIV-1 in non-dividing cells including monocyte derived macrophages and resting CD4+ T-cells (346–348). SAMHD1 is a deoxynucleoside triphosphate triphosphohydrolase (dNTPase) (349). In the presence of dGTP or GTP SAMHD1 hydrolyses dNTPs into deoxynucleosides and inorganic triphosphate (350). It contains 626 amino acids that from N-terminal nuclear localisation signal, a sterile alpha motif (SAM) and an HD domain. The SAM domain is involved in protein-protein or protein-nucleic acid interactions whereas the HD domain contains the dNTP hydrolase activity. In non-cycling cells the dNTPase activity of SAMHD1 results in depletion of dNTPs to such a level that HIV-1 reverse transcription is inefficient and infection is blocked (346). It is highly expressed in HIV-1 target cells, macrophages and CD4+ T-cells (346–348).

Structural studies show that SAMHD1 can oligomerise. Monomers and dimers of SAMHD1 are catalytically inactive whereas a homotetramer of SAMHD1 has a catalytically active dNTPase domain (351–353). Tetramerisation is promoted by GTP and is essential for restriction of HIV-1. Binding of GTP to the first allosteric site (AL1) in a monomer results in conformational changes that allow dimer formation. This is followed by binding of dNTPs to the second allosteric site (AL2) and the catalytic site resulting in the formation of an active tetramer.

SAMHD1 catalytic activity and tetramerisation is regulated by cell cycle dependent phosphorylation. In cycling cells CDK1 and 2 have been shown to phosphorylate SAMHD1 at the C-terminal residue T592 in a cyclin A dependent manner that inhibits dNTPase activity (354,355). SAMHD1 dNTPase activity has also been shown to be sensitive to oxidation. It has been shown that cell proliferation results in oxidation of SAMHD1 which inhibits its tetramerisation and dNTPase activity (356). Unlike SAMHD1 phosphorylation, oxidation of SAMHD1 resulted in its cytoplasmic localisation. The tetramer formation can also be inhibited by binding of single stranded nucleic acids to the dimer-dimer interface (357).

A recent study by Mlcochova et al. (2017) has shed light into how HIV-1 exploits the regulation of SAMHD1 to infect macrophages (358). Primary macrophages were found to transition between two states, a G1-like and a G0-like state. In the G1-like state, macrophages expressed a cell cycle marker protein minichromosome maintenance complex component 2 (MCM2) but did not progress to DNA replication or cell division. The expression of MCM2 correlated with SAMHD1 phosphorylation and HIV-1 infection. On the other hand, in the G0-like state macrophages did not express MCM2 and SAMHD1 was not phosphorylated which correlated with HIV-1 restriction. These observations demonstrated how HIV-1 evaded SAMHD1 restriction in macrophages by exploiting a window during which SAMHD1 antiviral activity is turned off.

In addition to the dNTPase dependent restriction of HIV-1, some studies have suggested dNTPase independent restriction of HIV-1. In vitro studies have shown that SAMHD1 binds single stranded nucleic acids and contains a nuclease activity (359). Another in vitro study found the nuclease activity to be independent of the dNTPase activity (360). SAMHD1 was shown to bind and degrade the incoming HIV-1 genomic RNA in MDMs and CD4+ T-cells (361). These findings have been controversial and associated with contamination during protein purification and different experimental conditions in different studies.

Several lines of research have implicated SAMHD1 as a negative regulator of innate and adaptive immune responses. Mutations in SAMHD1 are associated with a rare hereditary autoimmune disease Aicardi-Goutières syndrome (AGS) (362). AGS is a severe inflammatory disease characterised by spontaneous IFN production and upregulation of ISGs. AGS associated mutations in SAMHD1 have been shown to prevent dNTP hydrolysis by SAMHD1 and result in IFN-I production (363).

Consistent with the role of SAMHD1 in AGS, depletion of SAMHD1 in THP-1 cells was shown to spontaneously induce IFN-I production and upregulate ISGs (364). This was found to be inhibited by TBK1 phosphorylation inhibitor, BX795, and treatment of cells with type I IFN receptor antibody. However, the stimulus for this spontaneous IFN-I induction

was not determined. In addition to restriction of exogenous viruses, SAMHD1 also restricts replication of endogenous retroviruses. LINE-1 is the only retrotransposon active in humans (365). SAMHD1 depletion increases LINE-1 expression in dividing cells (366). dNTPase activity and phosphorylation of T592 are essential for LINE-1 restriction. SAMHD1 was shown to interact with the LINE-1 RNP and sequester it in large cytoplasmic stress granules (367). Expression of LINE-1 in the absence of SAMHD1 is thought to drive IFN-I induction seen in AGS.

In contrast to these reports, a recent study by Chen et al. (2018) showed a direct inhibition of NF-κB and IRF7 signaling by SAMHD1 that prevented IFN-I induction (368). Silencing of SAMHD1 in primary macrophages and THP-1 cells resulted in a higher IFN-I response upon stimulation with viruses, including HIV-1, or inflammatory stimuli. Reconstitution of SAMHD1 knocked out THP-1 cells with SAMHD1 resulted in suppression of NF-κB activation and IFN-I induction upon stimulation. SAMHD1 was shown to interact with NF-κB and prevent phosphorylation of IκBα. SAMHD1 also prevented phosphorylation of IRF7 by interacting with IRF7 and its kinase IKKε. The HD domain of SAMHD1 was required for interaction with IRF7.

SAMHD1 restriction of HIV-1 reverse transcription has been shown to prevent activation of innate immune system and development of an adaptive immune responses (369). Since SAMHD1 prevents DNA synthesis by HIV-1, this was shown to limit activation of the DNA sensor cGAS and IFN-I induction. Lack of an innate immune response to HIV-1 prevented induction of virus specific cytotoxic CD8+ T-cells.

### 1.5.5 SERINCs

SERINCs are a group of transmembrane proteins with unknown cellular function. The human genome contains 5 loci that encode SERINC 1, 2, 3, 4, and 5 proteins. SERINCs contain 10 transmembrane domains flanked by cytoplasmic C- and N-termini. SERINCs (SERine INCorporator) are named after their function in serine incorporation in cellular membranes however these observations have been challenged by studies showing no impact on membrane phospholipids in the absence of SERINCs (370,371). Out of the five SERINCs, SERINC5 is the most abundant and potent inhibitor of HIV-1 whereas SERINC2 lacks the antiviral activity (372). SERINC1 and 3 show moderate antiviral activity against HIV-1(372). SERINC4 also shows potent antiviral activity against HIV-1 when expressed ectopically however in vivo relevance of SERINC4 is undermined by lack of expression in human tissues (373).

In HIV-1 producer cells SERINC5 localises to the detergent-resistant microdomains known as lipid rafts where virus assembly takes place, resulting in virion incorporation (372). The

determinants of localisation to these sites are not known. The antiviral activity of SERINC5 has been shown to correlate with virion incorporation suggesting that virion associated SERINC5 is the major determinant of virus inhibition (374,375).

Studies have shown that SERINC5 virion incorporation prevents delivery of reporter proteins into the target cell cytoplasm, suggesting a block to virus entry (374,375). Given that SERINCs have been shown to be involved in serine incorporation during phospholipid biosynthesis, SERINC5 was thought to restrict HIV-1 fusion by modulating the composition of the viral membrane. It was proposed that changes in membrane composition by SERINC5 would decrease the fluidity of the viral membrane, making it too rigid to fuse with the target cell membrane. However, no significant changes in lipid composition of the cellular or viral membranes were observed in the presence or absence of SERINC5 (371). Nonetheless, like IFITM proteins, it is possible that sole presence of SERINC5 in the viral membrane may decrease the propensity of membrane fusion.

Recent studies point towards the modulation of Env activity by SERINC5. SERINC5 has been shown to prevent formation of the fusion pore by inactivating the Env trimers (376,377). In addition to a block to fusion, this activity of SERINC5 makes HIV-1 sensitive to neutralization by antibodies raised against gp41 peptides. Furthermore, these studies found a bigger defect in infection than fusion suggesting that SERINC5 may inhibit a step after fusion pore formation.

### 1.5.6 Tetherin

Tetherin inhibits egress of several enveloped viruses including HIV-1 (378–380). Tetherin is a type II transmembrane protein. It contains an N-terminal domain, an alpha helical transmembrane domain, a coiled-coil ectodomain and a C-terminal glycosyl-phosphatidylinositol (GPI) anchor (381,382). The N-terminal domain is cytoplasmic. It contains a conserved dual tyrosine motif (YDYCRV) which interacts with clathrin adaptor proteins AP1 and AP2 resulting in clathrin dependent endocytosis of tetherin into endosomes (383). After synthesis, tetherin continuously cycles between the plasma membrane, endosomes and the trans-Golgi network. Tetherin is post-translationally modified in the ER and Golgi apparatus. Two asparagine residues in the coiled-coil ectodomain are N-linked glycosylated which allows transport to the plasma membrane (384,385). The coiled-coil ectodomain also contains three cysteine residues which form disulphide bonds and allow homodimerisation (385). The transmembrane domain has also been shown to be involved in homodimerisation (386). While in the ER, the C-terminus of tetherin is cleaved and a GPI anchor is added to a serine residue at position 161 (386). GPI anchors allow targeting of tetherin to specialised cholesterol rich microdomains known as lipid rafts where viral assembly occurs.

Tetherin exists as a dimer at the plasma membrane (385). The C-terminus is anchored in the lipid rafts, sites of viral budding, by GPI whereas the N-terminus is embedded into the plasma membrane by the transmembrane domain. During budding the GPI anchor of tetherin is incorporated into viral membranes leaving the N-terminus embedded in the plasma membrane. Scission of the particles tethers the viral particles to the producer cells as well as to each other which has been observed by electron microscopy (387).

Tetherin expression can be induced in an IFN dependent and independent manner (388,389). It has been shown to be induced by Type I, II and III IFNs in various cell types (389–391). In HIV-1 positive individuals tetherin expression has been found to be highest during the acute phase in peripheral blood mononuclear cells including CD4+ T-cells (392). In addition, tetherin can be induced in an IFN independent manner. Using STAT1 depleted cells, activation of TLR8 and TLR3 was shown to upregulate tetherin (388). Similarly, Il-27 stimulation induced tetherin expression in an IFN independent manner (393). Blockade of IFN signaling by the soluble vaccinia virus-encoded type I-IFN receptor (B18R) inhibited IFN signaling but not IL-27-mediated upregulation of tetherin in human monocytes and T-cells. In contrast, TGF beta has been shown to inhibit tetherin expression in epithelial cells (394).

Two isoforms, long and short, are expressed from the tetherin mRNA (395). Both isoforms have been shown to be able to dimerise and suppress virus release. The shorter isoform is produced due to leaky scanning of the mRNA that allows methionine at position 13 to act as an alternative start codon. The shorter tetherin isoform lacks the initial 12 amino acids that contain the tyrosine motif responsible for the clathrin mediated endocytosis and activation of innate signaling.

In addition to inhibiting release of budding virions, tetherin has also been shown to act like a PRR that activates innate immune responses and modulates adaptive immunity. Tetherin was identified to activate NF-κB in a cDNA expression screen for NF-κB activators (396). Subsequently, it was shown that virion budding results in NF-κB activation (397). Virion retention and NF-κB activation were found to be genetically separable (398). The GPI anchor which is essential for virion capture is dispensable for NF-κB activation. On the other hand, the dual tyrosine motif present in the cytoplasmic tail is essential for the NF-κB signaling activation however endocytosis of tetherin is not required. Further analysis of the tetherin cytoplasmic tail has revealed the presence of hemi-immunoreceptor tyrosine-based activation motifs (hemITAMs) which are a feature of C-type lectin pattern recognition receptors (399). Tethering of virions results in exposure of the SH2 domains in the cytoplasmic tails of tetherin. Tetherin is first phosphorylated by a Src-fiamily kinase (Src) at residue Y6 which is followed by phosphorylation of the residue

Y8 by the spleen tyrosine kinase (Syk) (399). This allows recruitment of TRAF2, TRAF6 and TAK1 complex that activates NF-κB. Activation of NF-κB is also dependent on tetherin interaction with the cortical actin cytoskeleton via the adaptor protein RICh2 (399,400). Tetherin mediated tethering of virions on the cell surface has been shown to enhance adaptive immune responses. Tethered viruses are targeted by neutralising antibodies which result in antibody dependent cell cytotoxicity (ADDC) mediated by myeloid and NK cells (401,402). Recently, tetherin has also been shown to be a ligand for leucocyte inhibitory receptor, immunoglobulin-like transcript (ILT7), present on plasmacytoid dendritic cells (403). Tetherin Interaction with ILT7 was shown to inhibit TLR signaling pathways. In the context of infection, tetherin incorporation into budding virions prevented this interaction and allowed activation of pDCs by activating TLR signals.

### 1.5.7 TRIM5α

TRIM5 was identified in a rhesus macaque cDNA expression screen as a retroviral restriction factor (404). It is IFN inducible and belongs to the TRIpartite Motif (TRIM) family of proteins (405). In the human genome about 100 genes encode for TRIM proteins which are involved in a wide variety of cellular functions including innate immunity. TRIM5 is the best studied for its antiviral function against HIV-1.

TRIM5 contains an N-terminal RING domain, a B-box domain, a coiled-coil domain and a C-terminal PRYSPRY domain (406). Among the TRIM5 isoforms, the alpha isoform contains the PRYSPRY domain and exhibits antiviral activity (407). The PRYSPRY domain of TRIM5α detects retroviral capsids that leads to the formation of a higher order hexagonal lattice on the surface of the capsid cores (408–410). This suppresses reverse transcription and blocks infection (411). Since TRIM5α has a low affinity for the capsid the higher-order complex formation stabilises the lattice by increasing the avidity. Expression of TRIM5α in the absence of capsid can also result in assembly of higher-order structures known as cytoplasmic bodies (412). These structures have been shown to be dynamic and can envelope the incoming viral capsid cores (413). The flexibility and dynamic nature of these structures are thought to be the reason why TRIM5α can assemble into lattices on diverse lentiviral capsids. Assembly of TRIM5α into higher order complexes depends on the B-box domain. Mutations of the residues in the B-box domain that form the oligomerisation interface prevent the formation of the hexagonal lattice on the capsid cores and abolishes the antiviral activity (414,415).

The RING domain contains an E3 ubiquitin ligase activity (416). TRIM5α is autoubiquitinated by the RING domain resulting in its turn over via the proteasome (417). During retroviral infection recruitment of TRIM5α to the capsid promotes the E3 ligase activity of the RING domain which correlates with its increased turnover in the infected

cells (418,419). First, Ube2W attaches mono-Ub to K63 in TRIM5α. Then poly-Ub chains are formed by the Ube2N/Ube2v2 complex. Mutations in the RING domain that abolish the ligase activity relieve the block to RT but not infection (418,420). This can be recapitulated by treating cells with the proteasome inhibitor, MG132. Based on these observations, two models of TRIM5a restriction have been proposed. One model of restriction depends on the ligase activity of the RING domain and results in a block to RT and infection. The second mechanism depends on the assembly of TRIM5α into a hexagonal lattice on the capsid surface that allows RT but may stabilise the cores or disassemble the cores prematurely, resulting in a block to infection.

Upon detecting retroviral capsids TRIM5α not only blocks infection but also initiates an innate immune response that drives adaptive immunity. TRIM5α has been shown to activate nuclear factor κB (NF-κB) and activator protein 1 (AP-1) via a tumour growth factor β activated Kinase 1 (TAK1) dependent signaling pathway (416). Higher-order assembly of TRIM5α on the viral capsid and the subsequent K63-Ub chain formation are essential for NF-κB and AP-1 activation. It has been suggested that TRIM5α mediated degradation of the capsid produces peptides for MHC presentation that enhances adaptive immune responses. Indeed, TRIM5α was shown to promote activation and cytotoxic activity of CD8+ T-cells (421). Furthermore, some CTL escape mutations in the capsid have been associated with TRIM5α sensitivity (422).

hTRIM5α has largely been described to be inactive against HIV-1 infection. A recent study by Jimenez-Guardeño et al. (2019) provide new insights into antiviral action of hTRIM5α against HIV-1. By using an siRNA library targeting ISGs in IFN-α treated U87-MG cells, hTRIM5α was identified as a HIV-1 restriction factor (423). hTRIM5α antiviral activity was then confirmed in IFN-α treated CD4+ T-cells, the main targets of HIV-1 infection in vivo. HIV-1 capsid was the target of hTRIM5α as replacing the HIV-1 capsid with SIV capsid abrogated the restriction. In addition, hTRIM5α lacking the PRYSPRY domain, the region that recognises the capsid, was unable to restrict HIV-1. Interestingly, this study showed that inhibition of the hTRIM5α ligase activity or the proteasome is sufficient to allow HIV-1 infection. The requirement of IFN-α treatment to induce hTRIM5a activity was associated with increased hTRIM5α turnover via the specialized proteasome known as the immunoproteasome.

In addition to TRIM5α mediated targeting of HIV-1 to the immunoproteasome, hTRIM5α has also been shown to direct HIV-1 to autophagosomes (424). Langerhans cells (LC) are a subset of dendritic cells that specifically express Langerin, a C-type lectin receptor. HIV-1 uptake by LCs via Langerin resulted in HIV-1 degradation. In LCs TRIM5a was found to be associated with the components of the autophagosomes. Depletion of hTRIM5α or

autophagosome components, ATG16L1 or ATG5, allowed HIV-1 infection of LCs. hTRIM5α dependent restriction of HIV-1 was specific to Langrin and not observed when HIV-1 used another C-type lectin receptor, DC-SIGN, for entry.

## 1.6 Antagonism and evasion of innate immunity by HIV-1

### 1.6.1 Vpu antagonism of tetherin and NF-κB signaling

Vpu is a type 1 transmembrane protein expressed from a bicistronic mRNA by HIV-1 but not HIV-2. Vpu deleted HIV-1 clusters on the cell surface as it is unable to detach after budding (425). Early studies showed that this was a cell-type specific effect which could be enhanced by IFN-I stimulation (426,427). A microarray screen for IFN-I inducible membrane associated factors specific to the non-permissive cell types revealed tetherin as the dominant factor that inhibited the release of Vpu deleted virus (427). Overexpression of tetherin was shown to inhibit Vpu deficient virus release whereas the wild type virus was unaffected (427).

Vpu localises to the endosomes where it gets access to the newly synthesized and recycling tetherin. A very highly conserved alanine and tryptophan domain in the transmembrane region of Vpu interacts with the transmembrane domain of tetherin (428). Phosphorylation of the cytoplasmic tail of Vpu allows formation of a complex with tetherin and clathrin adaptor proteins, AP1 and AP2 (429). Phosphorylation of a dual serine phosphorylation motif, DSGxxS, in Vpu recruits a Skip1-Cullin1-F-box protein (SCF) E3 ubiquitin ligase via interaction with the β-transducing repeat containing (βTrCP) adaptor protein resulting in tetherin ubiquitination and ESCRT mediated lysosomal degradation (430). The cytoplasmic tail of tetherin which recruits the clathrin adaptor proteins is critical for its sensitivity to Vpu. The short form of tetherin lacks the cytoplasmic tail and is insensitive to Vpu mediated degradation (431). However, it contains the transmembrane domain that allows interaction with Vpu and disrupts its incorporation into budding virions (431).

Downregulation of tetherin by Vpu not only allows virion egress but also prevents tetherin activation of NF-κB. However, Vpu has also been shown to inhibit NF-κB activation downstream of various other NF-κB activators such as TNF-a in a tetherin independent manner (432). Vpu inhibits TNF-a induced degradation of IκBα without inhibiting activation of the upstream kinase IKK (432). Interaction of Vpu with βTrCP is essential for inhibition of NF-κB downsteam of TNF-α as a βTrCP biding mutant is unable to inhibit NF-κB activation. Since βTrCP is involved in degradation of activated IκBα which allows NF-κB activation it has been proposed that Vpu sequesters βTrCP in the endosomes resulting in

IκBα stabilisation and inhibition of NF-κB signaling. Recent studies show that Vpu inhibition of IκBα degradation does not correlate with its ability to interact with βTrCP suggesting that there might be βTrCP independent mechanism of NF-κB inhibition (433).

### 1.6.2 Nef antagonism of SERINC5/3

Nef is a 27 kDa protein that is expressed early during infection (434). N-terminus of Nef is post-translationally myristoylated which allows interaction with lipid membranes (435). Nef is best characterised for its role in downmodulation of CD4 and MHC-I from the plasma membrane (436). Nef uses a di-leucine-based motif to recruit components of the endosomal sorting machinery such as AP-1 and AP-2 (437,438) . This results in endocytosis of CD4 and MHC-I molecules which are then degraded in the lysosomes via the multivesicular body pathway (439).

For a long time Nef has been known to enhance infectivity of HIV-1 (440). Nef has been shown to retain this activity during acute and chronic phases of infection suggesting that it is required for transmission and persistence (441). Increased infectivity of HIV-1 was associated with expression of Nef in the producer cells and required Nef mediated endocytosis via interactions with AP2 and dynamin 2 (442,443). These observations suggested that Nef overcame a virus restriction by targeting a plasma membrane associated restriction factor. Two groups showed that Nef counteracted SERINC5/3 in producer cells to enhance virion infectivity in the target cells (444,445). One group carried out transcriptomic analyses of various producer cells whereas the other group analysed the proteomic profile of virions produced in the presence or absence of Nef. Both studies revealed that in the absence of Nef SERINC5/3 was incorporated into HIV-1 virions which inhibited infectivity in the target cells. Nef was shown to inhibit cell surface expression of SERINC5/3 by promoting its endocytosis into endosomes which prevented its incorporation into virions. Like endocytosis of CD4, myristoilation and the di-leucine-based motif were shown to be essential for Nef mediated downregulaton of SERINC5/3. Endocytosis of SERINC5/3 has been shown to result in its lysosomal degradation. Endocytosed SERINC5/3 has been shown to colocalise with the lysosome marker LAMP1 and treatment with lysosome inhibitors, Bafilomycin A1 and ammonium chloride, inhibited degradation of SERINC5/3 (446). A recent study showed that Nef increased infectivity of HIV-1 when reduced SERINC5/3 incorporation and cell surface expression was not evident suggesting that there might be an additional endocytosis independent mechanism (447).

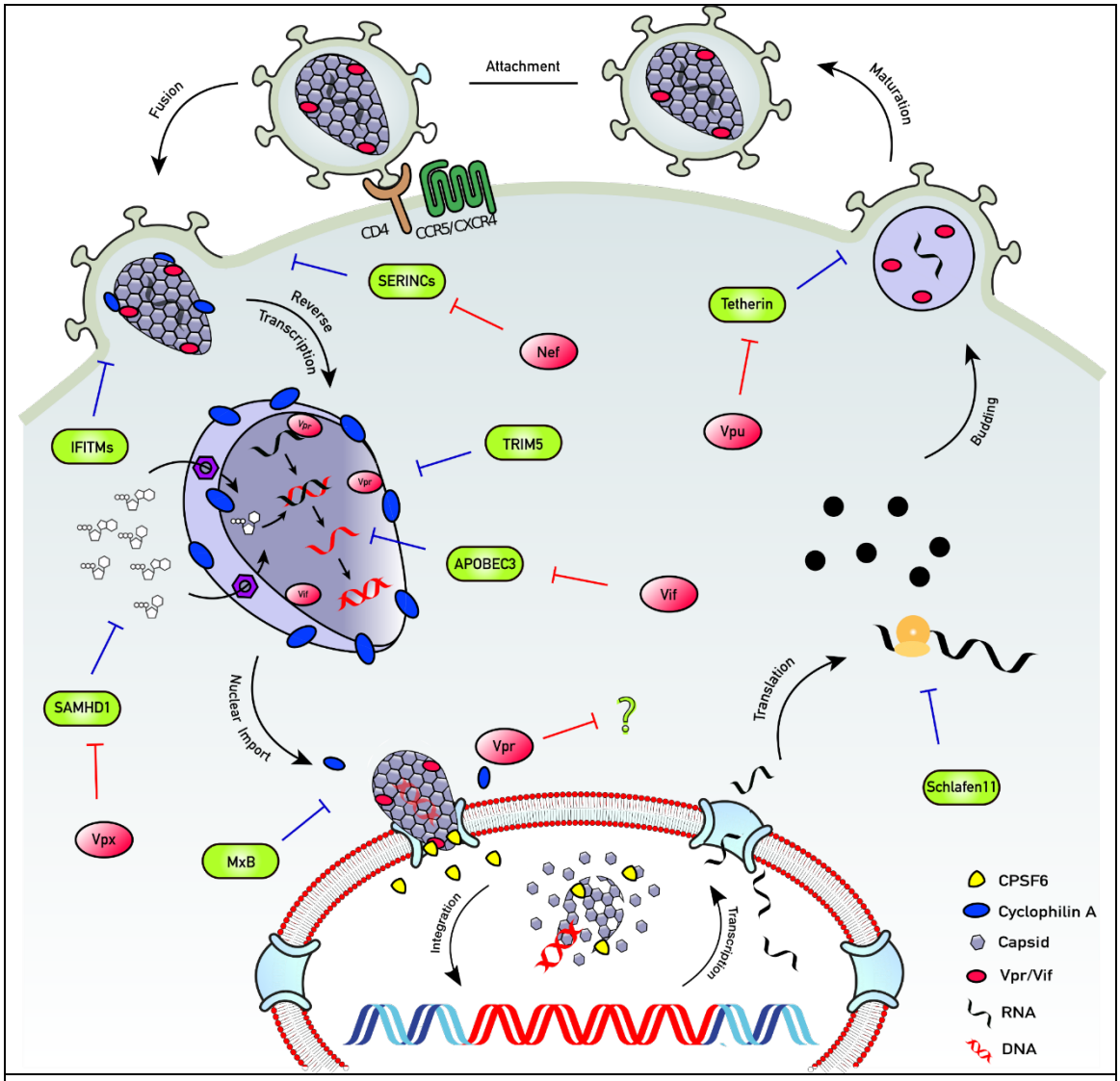


**Figure 1.4 Antagonism of innate restriction factors by HIV-1**

SERINC3/5: Inhibit fusion of viral particles with target cells. Antagonised by Nef. IFITMs: Impair virus entry into target cells. Antagonised by evolving IFITM3 insensitive Env proteins. TRIM5: Forms a hexagonal lattice around the capsids. Targets them for proteasomal degradation and activates innate signalling. Antagonised by evolving TRIM5 insensitive viral capsid proteins. APOBEC3s: Suppress viral DNA synthesis and induces mutations in the viral DNA. Antagonised by Vif mediated degradation. SAMHD1: Restricts infection by lowering nucleotide concentrations below those which support viral DNA synthesis. Antagonised by Vpx mediated degradation (SIVsm/HIV-2) or infection of cells with inactive SAMHD1 (HIV-1). MxB: Restricts HIV-1 nuclear entry and possibly integration. Schlafen 11: Restricts HIV-1 protein translation. Tetherin: Inhibits virus release from infected cells. Antagonised by Vpu mediated degradation.

### 1.6.3 Vif antagonism of APOBEC3s (A3)

HIV-1 viral infectivity factor (Vif) is essential for viral replication in CD4+ T-cells and some T-cell lines (448). Vif counteracts the antiviral activity of A3 enzymes by inducing their degradation in producer cells which prevents their virion incorporation (449). Vif recruits A3 enzymes to a Cullin5 (Cul5) E3 ubiquitin ligase complex by mimicking Cul5 cellular substrate recognition subunit suppressor of cytokine signaling (SOCS2) (450). This results in polyubiquination of A3 enzymes and proteasomal degradation.

Structural and biochemical analyses have revealed that Vif contains specific motifs that are responsible for recruiting different A3 enzymes. Structurally, Vif exhibits an elongated cone-like shape with two domains on either side of a Zn2+ ion (451). The αβ domain in the N-terminus has been shown to interact with various A3 proteins. The 40YRHHY44 motif allows interaction with A3G, 11WQxDRMR17 and 74TGERxW79 allow interaction with A3F, A3C and A3D and 39F and 48H have been shown to be involved in A3H interaction (452–455) . Vif expression is stabilized by interaction with a transcription factor (CBFβ) and the Vif structure is held together by Zn2+ coordination through the HCCH motif (456).

Counteraction of A3G by Vif has been shown to be species specific and acts as a cross-species infection barrier. Species specificity of A3G antagonism by Vif has been mapped to a single residue at position 128 in A3G (457). African green monkey (AGM) A3G contains a lysine (K) at position 128 whereas the human A3G contains a positively charged aspartic acid (D). This single point mutation makes AGM A3G resistant to HIV-1 Vif and mutating this residue in human A3G from 128D to 128K makes the human A3G insensitive to HIV-1 Vif. Furthermore, it has been shown that the charged amino acid rather than the identity of the amino acid governs the Vif sensitivity as mutation of residue 128 to alanine does not abrogate Vif sensitivity (457).

Vif can also antagonise A3G antiviral activity in a degradation independent manner. Vif has been shown to inhibit translation of A3G mRNA, virion incorporation of A3G and cytidine deaminase activity of A3G (458–460).

### 1.6.4 HIV-1 evasion of innate immunity

Current studies suggest that after fusion the capsid core stays intact as it traverses the hostile cytoplasm which not only allows encapsidated reverse transcription and nuclear import but also shields viral nucleic acids from detection by cellular PRRs.

HIV-1 evasion of DNA sensing has been shown to be orchestrated by the capsid which recruits cellular cofactors CypA and CPSF6 to cloak viral replication. Rasaiyaah et al.

(2013) showed that infection of MDMs by WT HIV-1 was silent and did not induce IFN-l however HIV-1 capsid mutants which were unable to recruit CypA (P90A) or CPSF6 (N74D) activated IFN-l production which suppressed viral replication (78). This effect was recapitulated by inhibition of CypA with a non-immunosuppressive cyclosporine A analogue, Smbz, and depletion of CPSF6. IFN-l induction was dependent on reverse transcription and independent of integration suggesting that viral reverse transcribed DNA was sensed by innate sensors. Critically, inhibition of IFN-l signaling by IFN-l receptor antibody treatment rescued replication of P90A and N74D mutant viruses. More cGAMP was detected from HIV-1 P90A infected MDMs suggesting that this mutant virus was detected by the DNA sensor cGAS. The exact mechanism of how recruitment of CypA and CPSF6 by capsid prevents viral detection by innate immune sensors in not fully understood. One hypothesis is that CypA and CPSF6 regulate capsid uncoating and disturbing their recruitment to the capsid results in premature uncoating in the cytoplasm which reveals viral DNA to cGAS.

Evasion of HIV-1 RNA sensing has recently been shown to be mediated by methylation of the viral RNA genome in the producer cells (265). 2'-O-methylation is one of the most common RNA modification in mammalian cells. The 5'guanosine cap of cellular mRNA is methylated by methyltransferases which allows cellular innate immune system to distinguish self RNA from non-self RNA (461). Various viruses including West Nile virus, Ebola virus and Flaviviruses encode a 2′-O-Methyltransferase (2′-O-MTase) to methylate their RNA and avoid detection by the innate immune system (462). In contrast, HIV-1 does not encode a 2′-O-MTase but hijack a cellular 2′-O-MTase known as FTSJ3 to carry out 2′-O-methylation of its genomic RNA to avoid detection by the innate immune sensors. Ringeard et al. (2019) showed that FTSJ3, a 2′-O-MTase, is recruited to HIV-1 RNA by TAR binding protein (TARBP) in producer cells. TARBP binds to the TAR sequence and Rev response element in HIV-1 RNA. Recruitment of FTSJ3 resulted in 2′-O-methylations at 17 residues in the viral genome. Production of virus in FTSJ3 depleted cells resulted in virions that induced an IFN-l response in primary dendritic cells and macrophages which inhibited viral replication. Furthermore, it was shown that IFN-l induction was partially MDA5 dependent but RIG-l independent. Finally, treatment with IFN receptor antibody partially restored replication of the virus produced in FTSJ3 depleted cells. These observations showed that HIV-1 hijacks a cellular 2′-O-MTase to methylate its genome to avoid MDA5 sensing and IFN-l production which explains why premature uncoating has never been reported to activate RNA sensors. One of the limitations of this study is that all the viruses were produced in 293T cells whereas in vivo virus is produced by HIV-1 target cells, CD4+ T-cells and macrophages. The role of FTSJ3 in methylating HIV-1 RNA in CD4+ T-cells and macrophages needs further investigation.

## 1.7 Viral protein R (Vpr)

Vpr is a 96 amino acid long protein encoded by all HIVs and SIVs (463). *In vitro*, Vpr is dispensable for HIV-1 replication (464). However, *in vivo* infection of macaque rhesus monkeys with Vpr deleted SIV results in poor viral replication and delayed disease progression (465). In humans, infection with a Vpr-defective HIV-1 has been reported to result in markedly delayed seroconversion, suppressed viremia and normal T-cell levels without treatment (466). Like other HIV accessory proteins, Vpr hijacks the cellular cullin4A-RING E3 ubiquitin ligase (CRL4) by interacting with its substrate recognition subunit DDB1- and CUL4A-associated factor 1 (DCAF1) (467). Vpr has been shown to recruit several cellular proteins to CRL4 resulting in their ubiquitination and subsequent proteasomal degradation (468–470). Vpr‘s molecular functions include nuclear import of the viral pre-integration complex (PIC), induction of G2 cell cycle arrest, modulation of T-cell apoptosis, transcriptional coactivation of viral and host genes, and regulation of nuclear factor kappa B (NF-κB) activity (276,468,471–473). Despite numerous reported functions of Vpr, its role in HIV-1 infection has remained poorly defined and its function is somewhat enigmatic. This is partly because under cell culture conditions Vpr is dispensable for replication in CD4+ T-cells and there are conflicting reports of Vpr-dependent HIV-1 replication in MDMs, suggesting that its function might only be apparent under certain conditions (464,474). A major challenge is to identify a reliable assay for Vpr function and a corresponding replication assay that links target degradation to viral replication as was the key to understanding the relationships between HIV-1 Vif and APOBECs, Vpu/Nef and Tetherin and Nef and SERINC3/5.

### 1.7.1 Structure of Vpr

The NMR structure of Vpr shows that it contains a central α-helical core, containing three alpha helices connected by loops, which is flanked by unstructured N- and C-terminal tails (475). The N-terminal tail is negatively charged whereas the C-terminal tail is positively charged. Vpr contains four proline residues at position 4, 10, 14 and 35 which are thought to undergo cis/trans isomerisation by the peptidyl-propyl isomerase cyclophilin A and allow correct folding of Vpr (476). The third α-helix is rich in leucine residues and is involved in the formation of a leucine-zipper like motif that allows assembly of Vpr into higher order oligomers (477).

The recently resolved crystal structure of Vpr confirmed the NMR structure and delineated interactions of Vpr with its cofactor, DCAF1 (478). It showed that Vpr interacted with DCAF1 primarily through the N-terminal tail and α-helix 3. Residues Arg62, Gln65, and Arg73 on the third α-helix of Vpr formed hydrogen bonds with Glu1088, Ser1136, and Thr1139 of DCAF1, respectively. Phe69 of Vpr was also found to make contact with a

small hydrophobic pocket in DCAF1 and mutating it to alanine abolished the interaction. In addition, DCAF1 residue Trp1156 was buried in a hydrophobic pocket made by the α-helix 1 and 3. The N-terminal tail of Vpr was found to be wrapped around DCAF1, however the C-terminal tail was unresolved suggesting that it is flexible and can adopt multiple conformations which might be stabilized by binding other cellular proteins.

### 1.7.2 Particle incorporation

Vpr is specifically packaged at a high copy number into virions (25). An estimate suggested 275 molecules of Vpr per virion (479). Vpr incorporation into budding virions is the result of Vpr interaction with the p6 domain in the Gag polyprotein (25). Phosphorylaion of p6 by cellular protein kinase C has been shown to be essential for Vpr packaging (480). Earlier reports suggested that a leucine rich motif in the p6 C-terminus directly bound Vpr (481). This was done with particles formed by chimeric Rous sarcoma virus (RSV) or murine leukemia virus (MLV) Gag polyproteins containing the HIV-1 p6 sequence fused to their C termini. Latter studies investigated Vpr incorporation in the context of full length HIV-1 Gag and found the leucine rich domain in p6 to be dispensable for Vpr incorporation (482). P6 region responsible for Vpr packaging was mapped to an FxFG motif, 15FRFG, commonly found in proteins of the nuclear pore complex. During maturation proteolytic cleavage of the Gag polyprotein generates NCp7 which has been shown to exhibit higher affinity for Vpr than the mature p6 (483,484). After maturation Vpr binds NCp7 which recruits it into the conical core where Vpr associates with the viral RNA genome (479,485)

A real-time study using a flow cytometry fluorescence resonance energy transfer has shown that Vpr self-assembles into dimers, trimers, tetramers and higher order oligomers (477). Oligomerisation of Vpr is required for interaction with the Gag polyprotein and is essential for virion incorporation. However, oligomerisation of Vpr does not seem to be essential for its function. Mutations in Vpr that prevent oligomerisation do not affect Vpr mediated cell cycle arrest. Similarly, mutations that abrogate Vpr cell cycle arrest function do not prevent oligomerisation of Vpr (486).

Virion incorporation of Vpr has been exploited in various ways to investigate HIV-1 infection. Beta-lactamase-Vpr chimeric protein (BlaM-Vpr) has been used extensively for the study of HIV-1 entry into cells (487). Vpr has been used to package various cellular and viral proteins into virions such as the integrase and the reverse transcriptase (488,489). Vpr tagged with a fluorescent protein such as mCherry or GFP has been used to study uncoating of the viral capsid and track viral particles as they traverse the cellular cytoplasm (490,491).

### 1.7.3 Cellular localisation

Localisation of Vpr is dynamic and depends on the step of the viral life cycle. Desai et al. (2015) used single virus tracking, confocal imaging and fluorescence correlation spectroscopy to investigate the localisation of virion delivered Vpr (492). Fluorescently-tagged Vpr was found to dissociate from HIV-1 cores to accumulate rapidly in the nucleus as monomers and large complexes with host proteins. Vpr shedding from the viral core did not correlate with capsid stability as HIV-1 mutants with hyperstable or unstable capsids did not affect kinetics of Vpr nuclear localisation. Shedding of Vpr from the viral cores was suggested to be an active process that did not occur when immobilized virions were treated with detergents in the presence or absence of cytosol. In contrast, a previous study by Campbell et al. did not observe GFP-tagged Vpr accumulation in the nucleus post fusion (493).

Exogenously expressed Vpr localises to the nucleus and shows accumulation around the nuclear envelope in various cell lines and primary macrophages (494). HIV-1 containing Vpr mutants that do not show nuclear envelope localisation replicate less in macrophages compared to WT HIV-1 (494,495). Localisaion of Vpr to the nuclear envelope has been associated with interaction with components of the nuclear pore complex (NPC). Vpr has been shown to interact with various members of the NPC. It interacts with FG-rich regions of Nup54, Nup58 and Pom121 (496,497). hCG1 has been shown to interact with Vpr in a FG-region independent manner (498). The relevance of Vpr interactions with nucleoporins is not clear.

Gag expression has been shown to change localisation of Vpr. Co-transfection of Vpr with Gag expressing plasmid resulted in localisation of Vpr to the plasma membrane and this inhibited the cell cycle arrest function of Vpr (477,486). This is consistent with the fact that Vpr interacts with the p6 domain of Gag for virion incorporation at the plasma membrane (25,484). These findings suggest that certain functions of Vpr that depend on nuclear envelope localisation may only be apparent during very early stages of infection when Gag is absent. Proviral expression of Gag may inhibit Vpr functions by changing Vpr localisation or by masking the target or co-factor binding sites.

### 1.7.4 Vpr and importins

Several studies have shown Vpr interaction with components of the nuclear import machinery which has been linked to nuclear import of the HIV-1 preintegration complex (499). Importins are a group of proteins involved in nuclear import of cellular proteins and nucleic acids. Different groups of importins recognise different classes of nuclear localisation signals (NLS) in proteins (500). The classical nuclear import pathway is

regulated by importin-α and importin-β. Importin-α contains an NLS binding site that recognises a canonical basic NLS in protein cargoes. Upon binding the NLS, importin- α recruits importin- β which carries the complex through the nuclear pore via interactions with nucleoporins in a Ran GTPase dependent manner.

Vpr does not contain a canonical NLS and Vpr mediated transport has been shown to be insensitive to NLS peptide (501–503). Nonetheless, there are numerous reports of Vpr interaction with importin-α. Vodicka et al. (1998) showed that GST-tagged Vpr co-purified with importin-α but not importin-β from yeast cell extracts (495). This was associated with localisation of Vpr to the nuclear envelope as the Vpr mutant (F34I) defective for nuclear envelope localisation did not co-purify with importin-α. Furthermore, the cell cycle arrest function of Vpr was found to be independent of importin-α interaction. Finally, the authors showed that HIV-1 encoding the Vpr mutant F34I was unable to replicate in primary human macrophages.

An in vitro transport assay using digitonin permeabilised HeLa cells has been used to characterize Vpr interaction with importin-α. In this assay, recombinant Vpr localises to the nuclear envelope and enters the nucleus upon addition of recombinant importin-α but not importin-β or transportin (504). Cytosolic extracts from macrophages have been shown to allow Vpr nuclear import whereas cytosolic extracts from monocytes do not which was correlated with lower expression of importin-α in monocytes (505). In vitro immunoprecipitation experiments have been used to show Vpr interaction with three importin-α Rch1, Qip1 and NPI-1 (506). Although biochemical analyses revealed identical binding affinities between Vpr and the importin-α isoforms, interaction with NPI-1 was responsible for its nuclear import. In vitro immunoprecipitation experiments showed that CAS/Exportin 2, a protein involved in importin-α export, prevented Vpr interaction with NPI-1 but not with Rch1 or Qip1 (506). Furthermore, in vitro transport assay showed that depletion of CAS prevented nuclear import of Vpr by NPI-1 which was rescued by addition of recombinant NPI-1 (506).

The Vpr C-terminal tail contains a cluster of basic residues ($^{87}$RRTRNGASKS$^{96}$). It is different from the canonical NLS but has been shown to interact with importin-α (507). Miyatake et al. (2016) resolved the crystal structure of the Vpr C-terminal tail and murine importin-α2 lacking the autoinhibitory importin-β binding domain (ΔIBB–m-importin-α2). ΔIBB–m-importin-α2 shares 94.5% amino acid sequence with human importin-α1 and yields crystals. They found that Vpr C-terminal tail makes a twisted β-turn that mimics a canonical NLS-binding motif. Upon binding importin-α it induces homodimerization of importin-α.

### 1.7.5 Vpr causes cell cycle arrest

Vpr hijacks the Cul4-DCAF1 E3 ubiquitin ligase complex to target proteins for proteasomal degradation (508). The most extensively studied function of Vpr is to cause cell cycle arrest at the G2 to mitosis (G2/M) transition. A study by Laguette et al. (2014) has provided some insight into this process. Taking a biochemical approach, the authors showed that Vpr manipulates an endonuclease complex to arrest the cell cycle (468). They proposed this prevents innate immune sensing of the viral DNA. The data suggested that Vpr interacts directly with SLX4, which is implicated in DNA damage repair pathways. SLX4 recruits structure-specific endonucleases (SSE) MUS81-EME1, ERCC1-ERCC4 and SLX1 to form a complex (SLX4com) that repairs DNA damage. The activity of SSEs is kept under tight control during cell cycle. They are only activated at the G2/M transition, for example, by kinases such as polo-like kinase 1 (PLK1) leading to resolution of stalled replication forks and maintenance of genomic integrity. Vpr recruits PLK1 to the SLX4com prior to the G2/M transition. PLK1 then prematurely activates SLX4com by phosphorylating EME1 resulting in abnormal processing of replication forks that eventually leads to replication stress and cell cycle arrest at the G2/M transition. This function of Vpr is dependent on Cul4-DCAF1 ubiquitin E3 ligase complex as the DCAF1 binding mutant, VprQ65R, is unable to interact with SLX4com to cause cell cycle arrest. Furthermore, SLX4 was found to bind HIV-1 reverse transcripts only in the presence of Vpr suggesting that Vpr may recruit SLX4 to process HIV-1 reverse transcripts and prevent innate sensing.

These findings raise important questions of how Vpr manipulates the SLX4com to degrade viral DNA and evade innate sensing without suppressing productive infection. Importantly, the significance of SLX4 activation by Vpr should be demonstrated during HIV-1 replication. The relevance of the Vpr interaction with SLX4 is undermined by the recent suggestion that specific HIV-1 Vpr isolates are unable to interact with SLX4 (509). However, species specific Vpr-SLX4 interactions support the validity of this interaction (510). The role of SLX4 in HIV-1 replication and Vpr activity certainly warrants further investigation.

### 1.7.6 Vpr and innate immunity

Various studies have shown that Vpr modulates innate immune activation by regulating activation of transcription factors, IRF3 and NF-κB. In Tzmbl cells reconstituted with STING, Vpr was found to inhibit sensing of HIV-1 by blocking translocation of IRF3 into the nucleus (511). On the other hand, in PBMCs, and the Jurkat T-cell line, Vpr was found to degrade IRF3 to suppress immune responses (512). In contrast to the effects of Vpr on IRF3, NF-κB has been described to be activated by Vpr, potentiating innate sensing of HIV-1 in CD4+ T-cells and dendritic cells (276,513).

### 1.7.7 Vpr drives global cellular proteome remodeling

A recent study by Greenwood et al. (2019) showed Vpr driven global cellular proteome remodelling (514). Comparison of total proteomes of uninfected CEM-T4 T-cell line with cells infected with either WT HIV-1 or an HIV-1 Vpr deletion mutant (HIV-1 ΔVpr) showed that 1,940 proteins changed significantly in wild-type HIV-1 infected cells whereas only 45 significant changes occurred in cells infected with HIV-1 ΔVpr (514). Vpr-dependent proteomic remodeling was found to be dependent on the interaction of Vpr with DCAF1/DDB/Cul4 ligase complex. Critically, depletion of DCAF1 alone did not phenocopy Vpr-mediated proteome remodeling, and the widespread effects of Vpr were therefore unlikely the result of DCAF1 depletion. Proteomics analysis using CEM-T4 T cells exposed to lentiviral particles lacking or bearing Vpr in the presence of reverse transcriptase inhibitors (RTIs) phenocopied the Vpr-dependent proteome remodeling seen in HIV-1 infection, suggesting that incoming Vpr is sufficient for remodeling of the proteome. Comparison of the proteomic profiles showed depletion of at least 302 proteins and upregulation of 413 proteins by Vpr. By combining data acquired from cell proteomics, MS co-IP with epitope-tagged Vpr, and pulsed SILAC, the authors proposed at least 38 direct targets for Vpr-dependent degradation, some of which were validated by immunoblotting.

These observations explain why effects of Vpr on cellular phenotypes and viral replication are complex and remain poorly understood. However, these observations are limited to the CEM-T4 T cell line model and need to be validated in primary CD4+ T-cells. Moreover, some functions of Vpr might be exclusive to other cell types such as macrophages or dendritic cells and may not be explained by protein targets identified in this study.

## 1.8 Project Aim

Demonstration of HIV-1 reverse transcribed DNA as a potent PAMP for the DNA sensor, cGAS, instigated efforts for identification of a DNA sensing antagonist encoded by HIV-1. Given the role of HIV-1 accessory proteins in antagonism of innate restriction factors and the presence of Vpr during early stages of the HIV-1 life cycle when its reverse transcribed DNA is prone to detection by cGAS, it was hypothesised that Vpr may play a role in antagonism of the cGAS signalling pathway. The aim of the project was to investigate and characterise the function of Vpr against innate immunity, particularly the cGAS/STING pathway of DNA sensing, in myeloid cells competent for mounting effective IFN-I responses.

# 2 Chapter 2: Methods and materials

## 2.1 Restriction enzyme digestion

Each digestion contained 1.5 µg DNA, 1 µl appropriate 10 x restriction enzyme buffer (Sigma/NEB), 1.0 µl of each restriction enzyme (Sigma/NEB) and made up to 30 µl with water. Restriction digests were incubated at 37 $^{o}$C for at least 2 hours. Digestion products were analysed by agarose gel electrophoresis and the DNA was purified from the gel.

## 2.2 Agarose gel electrophoresis

DNA was separated by agarose gel electrophoresis on a 1 % (w/v) agarose gel at 80-125 mV in TAE buffer (40 mM Tris, 20 mM acetic acid, and 1 mM EDTA). Ethidium bromide (0.2 µg/ml) (Sigma) was used to visualise the DNA by UV transillumination (UVP BioDocWIT).

## 2.3 Purification of DNA from agarose gel slices

DNA bands of interest were excised from agarose gels with a scalpel and the DNA was purified using the QIAgen gel extraction kit according to the manufacturer's protocol.

## 2.4 DNA ligation

Each ligation reaction contained 100 ng digested plasmid vector, an appropriate quantity of digested insert to achieve a 2:1 molar ratio of insert:vector, 10 x T4 DNA ligase buffer (Promega) and 1µl T4 DNA ligase (Promega), made up to 10 µl with water. Ligation reactions were incubated at 16 $^{o}$C for at least 2 hours.

## *2.5* Transformation of *E. coli*

50 µl of transformation competent HB101 *E. coli* were mixed with 10 µl of a ligation reaction. The bacteria were incubated on ice for 30 min. Bacteria were then heat shocked at 42 $^{o}$C for 45 seconds and then incubated on ice for 5 min. The bacteria were spread on Luria Broth (LB) agar plates containing ampicillin (100 µg/ml).

## 2.6 Site directed mutagenesis (SDM)

SDM PCRs were performed using Pfu Turbo DNA Polymerase (Agilent). For details of reaction setup, see Table 2.1. For cycling parameters, see Table 2.2. For each PCR, a negative control that contained no Pfu Turbo was included. 1µl DpnI (NEB) was added to each completed PCR and incubated at 37°C for 2hours. The DpnI digested PCR products were purified using a QIAquick PCR purification kit (QIAgen) and used to transform HB101 bacteria. Successful insertion of the desired mutations was confirmed by sequencing.

| Component | Amount per reaction |
|---|---|
| Pfu Turbo DNA Polymerase 2.5U/µl | 2µl |
| Pfu Turbo 10x Buffer | 5µl |
| dNTPs (Promega) 25mM each | 1µl |
| Forward primer (Sigma) 10µM | 2µl |
| Reverse primer (Sigma) 10µM | 2µl |
| Plasmid Template (30ng) | 3µl |
| $dH_2O$ | 35µl |
| Final volume | 50µl |

**Table 2.1: SDM reaction setup**

| Step | Temp (°C) | Time (min) | No. of Cycles |
|---|---|---|---|
| Initial denaturing | 92 | 1 | 1 |
| Denaturing | 92 | 1 | 12 |
| Annealing | 55 | 1 | |
| Extension | 68 | 2 / kb | |
| Final extension | 68 | 30 | 1 |

**Table 2.2: SDM PCR cycling parameters**

| Vpr Mutations | Primer sequence (5'-3') |
|---|---|
| A30S Fwd | GAACTGAAGAACGAGAGCGTGCGGCACTTCCCC |
| A30S Rev | GGGGAAGTGCCGCACGCTCTCGTTCTTCAGTTC |
| V31S Fwd | CTGAAGAACGAGGCCAGCCGGCACTTCCCCAGA |
| V31S Rev | TCTGGGGAAGTGCCGGCTGGCCTCGTTCTTCAG |
| F34I Fwd | GCCGTGCGGCACATCCCCAGACCTTGGCTGCATAGC |
| F34I Rev | GCTATGCAGCCAAGGTCTGGGGATGTGCCGCACGGC |
| P35N Fwd | GCCGTGCGGCACTTCAACAGACCTTGGCTGCATAGC |
| P35N Rev | GCTATGCAGCCAAGGTCTGTTGAAGTGCCGCACGGC |
| W54R Fwd | GAGACATACGGCGACACCCGGGCTGGCGTGGAAGCC |
| W54R Rev | GGCTTCCACGCCAGCCCGGGTGTCGCCGTATGTCTC |
| Q65R Fwd | GCCATCATCAGAATCCTGCGGCAGCTGCTGTTCATC |
| Q65R Rev | GATGAACAGCAGCTGCCGCAGGATTCTGATGATGGC |
| H71R Fwd | CAGCTGCTGTTCATCCGGTTCCGGATCGGCTGCCGG |
| H71R Rev | CCGGCAGCCGATCCGGAACCGGATGAACAGCAGCTG |
| R73S Fwd | CTGTTCATCCACTTCAGCATCGGCTGCCGGCAC |
| R73S Rev | GTGCCGGCAGCCGATGCTGAAGTGGATGAACAG |
| S79A Fwd | ATCGGCTGCCGGCACGCCAGAATCGGCATCACC |
| S79A Rev | GGTGATGCCGATTCTGGCGTGCCGGCAGCCGAT |
| R80A Fwd | GGCTGCCGGCACAGCGCCATCGGCATCACCCCT |
| R80A Rev | AGGGGTGATGCCGATGGCGCTGTGCCGGCAGCC |
| R90K Fwd | CCTCAGCGGAGAGCCAAGAACGGCGCCAGCAGA |
| R90K Rev | TCTGCTGGCGCCGTTCTTGGCTCTCCGCTGAGG |
| A30S V31S Fwd | GAACTGAAGAACGAGAGCAGCCGGCACTTCCCC |
| A30S V31S Rev | GGGGAAGTGCCGGCTGCTCTCGTTCTTCAGTTC |
| F34I P35N Fwd | GCCGTGCGGCACATCAACAGACCTTGGCTGCATAGC |
| F34I P35N Rev | GCTATGCAGCCAAGGTCTGTTGATGTGCCGCACGGC |

**Table 2.3:SDM primer sequences**

## 2.7 shRNA preparation

shRNA sequence targeting DCAF1 (GCGGACTGGAGGTGATCAT) was used. The oligos were annealed and then ligated into the digested HIV-1 SIREN vector as below. HB101 competent bacteria were transformed and colonies were screened for shRNA sequence by sequencing.

| Temperature (°C) | Duration |
|---|---|
| 95 | 30 sec |
| 72 | 2 min |
| 37 | 2 min |
| 25 | 2 min |

**Table 2.4: shRNA oligo annealing**

| Component | Amount per reaction |
|---|---|
| Digested HIV-1 SIREN vector | 50ng |
| Annealed oligo (0.5μM) | 1μl |
| 10X T4 ligase buffer | 1.5μl |
| BSA (10mg/ml) | 0.5μl |
| T4 DNA ligase | 1μl |
| Total Volume | Up to 15μl with water |

**Table 2.5: shRNA oligo ligation**

## 2.8 Reporter gene assays

For dual luciferase reporter gene assays in HEK293T cells, $2x10^5$ cells/ml were seeded in 48-well plates and transfected with 5ng IgK-luciferase reporter, 2.5ng thymidine kinase renilla luciferase reporter (Promega), 50ng empty or Vpr expressing pcDNA3.1, 1.5ng pcDNA3.1 flag-cGAS and STING using 0.75ul FuGENE 6 (Promega) and 20ul Opti-MEM (Promega). 48 hours later cells were lysed, and firefly and renilla luciferase activities were measured using a Glomax luminometer (Promega). For reporter gene assays in HEK293T cells containing an integrated NF-κB luciferase reporter $2x10^5$ cells/ml were seeded in 48-

well plates and transfected with pcDNA3.1 empty or Vpr. Cells were lysed in passive lysis buffer (Promega), and the firefly luciferase activity was measured using the Glomax luminometer (Promega). Firefly luciferase values were divided by renilla luciferase values and a fold induction of reporter activity was calculated by normalising each result to the luciferase activity of the unstimulated cells transfected with empty pcDNA3.1. For reporter gene assay in pIFIT1-Gluc THP-1 cells, $5x10^4$ cells/well were seeded in 96-well plates. Gaussia luciferase activity was measured in supernatants by using the Glomax luminometer (Promega). The fold induction of the reporter activity was calculated by normalising each result to the luciferase activity of the nonstimulated and untransduced cells. cGAMP (Invitrogen) was added into the culture media.

## 2.9 Cell culture

HEK293T cells were grown in Dulbecco's modified Eagle's medium (DMEM; Gibco) supplemented with 10% fetal calf serum (FCS; Gibco) and penicillin-streptomycin (50 µg/ml) (Gibco). HEK293T- cells with integrated NF-κB luciferase reporter were grown in DMEM supplemented with 15% fetal FCS, 50 µg/ml penicillin-streptomycin (Gibco) and 2µg/ml puromycin (Calbiochem). pIFIT1-Gluc THP-1 and *cGAS-/-* and *MAVS-/-* THP-1 cells were grown in Roswell Park Memorial Institute (RPMI 1640; Gibco) medium supplemented with 10% FCS and 50 µg/ml penicillin-streptomycin.

## 2.10 Nucleofection

5 x $10^6$ HEK293T cells were resuspended in 100ul of Nucleofector Solution T. The cell suspension was then combined with 1µg plasmid DNA. The cell/DNA suspension in a cuvette was inserted into the Nucleofector™ 2b Device (LONZA) and program T-016 was used. The sample was then incubated for 10 minutes at room temperature. The sample was mixed with appropriate media and 1x10^6 cells/well were plated in a 48-well plate. After 4-6 hours, the media was replaced with fresh media.

## 2.11 Flow Cytometry

Cells wer fixed in 4% paraformaldehyde for 20 min at room temperature and analysed by BD Accuri C6 (BDBiosciences). Live cells were gated by forward scatter height (FSC-H) and side scatter area (SSC-A). At least 5000 alive cells were measured for each sample. A gate for GFP-positive cells was made using an uninfected sample.

## 2.12 RNA extraction and cDNA synthesis

RNA was extracted from cells using the NORGEN RNA extraction kit according to the manufacturer's protocol. For reverse transcription to synthesise complementary DNA (cDNA), each reaction contained 1 µg RNA, 2.5 µM oligo dT, 500 µM dNTP, made up to 13 µl with nuclease-free water. These reactions were incubated at 65$^{o}$ C for 5 min and then transferred directly to ice for 1 min. To each reaction was then added 4 µl 5x First-strand buffer (Invitrogen), 5 mM DTT, 40 U RNase OUT (Invitrogen), 50 U Superscript III reverse transcriptase (Invitrogen), made up to a total of 20 µl with nuclease-free water. The reactions were incubated at 50$^{o}$ C for 1 hour, followed by 70$^{o}$ C for 15 min. cDNA was diluted 1:5 in nuclease-free water before quantitative reverse transcription-polymerase chain reaction (qRTPCR) analysis.

## 2.13 Real-time quantitative PCR (RT-qPCR)

Each qRT-PCR contained 2µl diluted cDNA, 10µl 2x SYBR® Green PCR master mix (Applied Biosystems), 1 µM of each primer, made up to 10 µl with water per well. A 7900HT Real-Time PCR machine (Applied Biosystems) was used to run the following programme.

| Temperature | Duration |
|---|---|
| 50° C | 2 min |
| 95° C | 10 min |
| 40 cycles:<br>95° C<br>60° C | <br>15 sec<br>1 min |

**Table 2.6: RT-qPCR reaction**

| Gene | Primer sequence (5'-3') |
|---|---|
| GAPDH Fwd | ACCCAGAAGACTGTGGATGG |
| GAPDH Rev | TTCTAGACGGCAGGTCAGGT |
| CXCL-10 Fwd | TGGCATTCAAGGAGTACCTC |
| CXCL-10 Rev | TTGTAGCAATGATCTCAACACG |
| IFIT2 Fwd | CAGCTGAGAATTGCACTGCAA |

| | |
|---|---|
| IFIT2 Rev | CGTAGGCTGCTCTCCAAGGA |
| MxA Fwd | ATCCTGGGATTTTGGGGCTT |
| MxARev | CCGCTTGTCGCTGGTGTCG |
| Viperin Fwd | CTGTCCGCTGGAAAGTG |
| Viperin Rev | GCTTCTTCTACACCAACATCC |

**Table 2.7: qPCR primer sequences**

## 2.14 Propidium iodide staining for cell cycle analysis

Cells were washed with PBS and then fixed in 1ml cold 70% ethanol on ice for 30 minutes. To ensure efficient fixing and minimise clumping, ethanol was added dropwise while vortexing. Ethanol was removed and cells were washed twice with PBS. To remove RNA from the samples RNase A (100 μg/ml) was added with propidium iodide (50ug/ml). Cells were incubated for 10 minutes at room temperature and analysed on a BD FACSCalibur cytometer (BD Biosciences). The data was analysed using the FlowJo software.

## 2.15 Preparation of cell lysates

Cells were lysed in passive lysis buffer (Promega) or cell lysis buffer (50 mM Tris pH 8, 150 mM NaCl, 1 mM EDTA, 10% (v/v) glycerol, 1 % (v/v) Triton X100, 0.05 % (v/v) NP40 supplemented with protease inhibitors (Roche), and phosphatase inhibitors (Roche) for immunoblotting with phospho-specific antibodies. The cells were collected in eppendorf tubes and the cell debris was collected by centrifugation at 14,000 x g for 10 min, 4$^{o}$ C. The cleared lysate was transferred to a clean eppendorf and stored at -20$^{o}$ C.

## 2.16 SDS-PAGE

For sodium dodecyl sulphate - polyacrylamide gel electrophoresis (SDS-PAGE) analysis cell lysates were heated at 100 $^{o}$C for 10 min in 6x protein loading buffer, containing 50 mM Tris-HCl (pH 6.8), 2 % (w/v) SDS, 10% (v/v) glycerol, 0.1% (w/v) bromophenol blue, 100 mM β-mercaptoethanol. The samples were loaded on an appropriate polyacrylamide gel and proteins were separated by electrophoresis at 120 V in SDS running buffer (25 mM Tris-HCl, 250 mM glycine, 0.1 % (w/v) SDS).

## 2.17 Immunoblotting

After PAGE, proteins were transferred to a Hybond nitrocellulose membrane (Amersham biosciences) in transfer buffer (25 mM Tris-HCl, 250 mM glycine, 20 % (v/v) methanol) using a semi-dry transfer system (Biorad) and blocked by incubation for 1 h at room temperature in 5 % (w/v) milk proteins + 0.01 % (v/v) Tween-20 in PBS (PBST). The membranes were then incubated overnight at 4 $^{o}$C with primary antibody (Ab) diluted in 5 % (w/v) milk proteins in PBST. Membranes were washed three times for 5 min in PBST and then were incubated with secondary Ab diluted in 5 % (w/v) milk proteins in PBST for 1 h at room temperature. The membranes were again washed three times for 5 min in PBST and once in PBS. Membranes were imaged using the Odyssey infrared imager (LI-COR Biosciences).

| **Antibody** | **Source** | **Dilution** |
|---|---|---|
| Rabbit-anti-VSV-G | Sigma | 1:20000 |
| Rabbit-anti-HIV-1 p24 | NIH AIDS reagent program | 1:1000 |
| Rabbit-anti-Vpr | NIH AIDS reagent program | 1:1000 |
| Rabbit-anti-STING | Cell signalling | 1:1000 |
| Rabbit-anti-pSTING | Cell signalling | 1:1000 |
| Rabbit-anti-TBK1 | Cell signalling | 1:1000 |
| Rabbit-anti-pTBK1 | Cell signalling | 1:1000 |
| Rabbit-anti-IRF3 | Cell signalling | 1:1000 |
| Rabbit-anti-pIRF3-386 | Sigma | 1:1000 |
| Mouse-anti-actin | Abcam | 1:20000 |
| Mouse-anti-TREX-1 | Sant Cruz Biotechnology | 1:250 |
| Rabbit-anti-DCAF1 | Bethyl | 1:1000 |
| Rabbit-anti-Nup358 | Abcam | 1:2000 |
| Mouse-anti-TNPO3 | Abcam | 1:100 |

| | | |
|---|---|---|
| Rabbit-anti-VCP | Santa Cruz Biotechnology | 1:1000 |
| Mouse-anti-flag | Sigma | 1:1000 |
| Mouse-anti-Tubulin | Millipore | 1:10000 |
| Rabbit-anti-GFP | Abcam | 1:20000 |
| anti-rabbit IRDye 800CW | LICOR Biosciences | 1:10000 |
| anti-mouse IRDye 800CW | LICOR Biosciences | 1:10000 |

**Table 2.8: Antibodies used for immunoblotting**

## 2.18 Immunofluorescence

For confocal microscopy, HeLa cells ($5x10^4$ cells/ml) were seeded into 24-well plates containing sterile glass coverslips. For nuclear translocation assays, THP-1 cells ($4x10^5$ cells/ml) were adhered in an optical 96-well plate with PMA (50ng/ml) for 72 hours. Cells were washed twice with ice-cold PBS and fixed in 4% (v/v) paraformaldehyde. Autofluorescence was then quenched in 150 mM ammonium chloride, the cells permeabilised in 0.1% (vol/vol) Triton X-100 in PBS, and blocked for 30 min in 5% (vol/vol) FCS in PBS. Cells were incubated with primary Ab for 1 hour followed by incubation with secondary Ab for 1 hour. Cells were washed with PBS three times between each step. The coverslips were placed on a slide prepared with a 30µl drop of mounting medium (Vectashield, containing 4',6-diamidino-2-phenylindole (DAPI)) and allowed to set before storing at $4^o$ C. Images were taken on a Leica TCS SPE confocal microscopes and analysed in ImageJ. For translocation assays DNA was visualised with DAPI. Images were taken on Hermes WiSan and analysed by Metamorph.

| Antibody | Source | Dilution |
|---|---|---|
| Mouse-anti-FXFG repeats containing nucleoporins (Mab414) | Abcam | 1:3000 |
| Rabbit-anti-flag | Sigma | 1:500 |
| Rabbit-anti-IRF3 | Sant Cruz Biotechnology | 1:400 |
| Mouse-anti-NF-kB p65 | Sant Cruz Biotechnology | 1:50 |
| Goat-anti-rabbit Alexa Fluor 488 IgG | Invitrogen | 1:500 |
| Goat-anti-mouse Alexa Fluor 546 IgG | Life Technologies | 1:500 |

**Table 2.9: Antibodies used for immunofluorescence**

## 2.19 CXCL-10 ELISA

PRO-BIND flat bottom 96-well assay plates (BD) were coated overnight at room temperature with 100 µl capture Ab (CXCL-10 ELISA Duosets, R&D Systems) per well diluted in PBS. The plates were washed 3 times in PBST (PBS + 0.1% Tween) and then were blocked for 1 h at room temperature with 300 µl 1 % (w/v) BSA in PBS (diluent) per well. The plates were washed 3 times in PBST. The standards were prepared in duplicate (CXCL-10: 2000 pg/ml-31.3 pg/ml) by preparing a two-fold dilution in diluent. One-hundred µl un-diluted cell culture supernatant was added per well and incubated for 2 h at room temperature. The plates were washed again 3 times in PBST. The detection Ab (CXCL-10 ELISA Duosets, R&D Systems) was prepared in diluent, 100 µl was added per well and the plate was incubated at room temperature for 2 h. The plates were washed 3 times in PBST. Streptavidin HRP (R&D systems) was diluted 1:200 in diluent, 100 µl was added per well and the plate was incubated at room temperature for 20 min. The plates were again washed 3 times in PBST and the ELISA substrate reagent (R&D systems) was prepared by mixing solutions A and B in a 1:1 ratio. One-hundred µl was added per well and the plate was incubated in the dark for 20 min. The reaction was stopped by the addition of 100µl 2N $H_2SO_4$ per well. The absorbance at 450 nm was measured.

## 2.20 Vector production

HEK293T cells were plated in T150 flasks and transfected with 2.5 µg p8.91, 2.5 µg pMDG and 3.75 µg lentiviral genome plasmid using 30ul FuGENE 6 (Promega) and 500ul Opti-MEM (Promega). Media was replaced 24 hours post-transfection. Supernatants were harvested 48 and 72 hours post-transfection and filtered through a 0.45 µm filter.

## 2.21 Vector concentration

Lentiviral vectors were concentrated by ultracentrifugation in a Sorvall Discovery (Hitachi) at 23000 rpm for 2 hours at 4$^{o}$C under vacuum conditions through a sucrose cushion (20% sucrose (w/v) in PBS). The pellet was then resuspended in RPMI + 10% FCS and stored at -80$^{o}$C.

## 2.22 Vector titration

THP-1 cells (2x10$^5$ cells/ml) were seeded in 48-well plates. Cells were transduced with a range of serially diluted (1:3) purified vector supernatant starting from 1:100 using 8ug/ml Polybrene. 48 hours later cells were fixed in 4% (v/v) paraformaldehyde in PBS and

analysed on an Accuri C6 Flow cytometer for GFP expression. The data was analysed in Microsoft Excel software.

## 2.23 SG-PERT

Activity of the HIV-1 reverse transcriptase was measured by the RT-qPCR assay known as SG-PERT to normalise input dose of VLPs. Virus was lysed and then the reaction was set up as below. Recombinant HIV RT (Applied Biosystems) was used to create standards for quantitation. A 7900HT Real-Time PCR machine (Applied Biosystems) was used to run the programme.

| Step | Temperature (°C) | Time | No. of cycles |
|---|---|---|---|
| Reverse transcription | 42 | 20 min | 1 |
| Taq initial heat activation | 95 | 15 min | |
| Denaturation | 95 | 10 sec | 40 |
| Annealing | 60 | 30 sec | |
| Extension | 72 | 15 sec | |

**Table 2.10: SG-PERT RT-qPCR cycling parameters**

## 2.24 Statistical tests

Data were analysed statistical tests as indicated in the figure legends. Stars (*) represent statistical significance: * ($p<0.05$), ** ($p<0.01$), *** ($p<0.001$), **** ($p<0.0001$).

# 3 Chapter 3: HIV-1 Vpr promotes viral replication by suppressing innate immune activation

## 3.1 Vpr is essential for HIV-1 replication in cGAMP stimulated MDMs

Numerous functions have been proposed for Vpr however its role in HIV-1 infection has remained poorly defined and its function is somewhat enigmatic. This is partly because under cell culture conditions Vpr is dispensable for replication in CD4+ T-cells and there are conflicting reports of Vpr-dependent HIV-1 replication in MDMs, suggesting that its function might only be apparent under certain conditions (464,474,496). To address the hypothesis that Vpr function might be required when innate immunity is activated, replication of an infectious molecular clone HIV-1 Yu2 (WT HIV-1) with or without the Vpr gene (HIV-1ΔVpr) was monitored in primary MDMs. In the absence of any innate immune stimulation WT HIV-1 and HIV-1ΔVpr replicated equally over the period of two weeks (Fig. 3.1A). However, in the presence of 1 µg/ml cGAMP HIV-1ΔVpr replicated significantly less compared to WT HIV-1 (Fig. 3.1B). Addition of 4 µg/ml cGAMP completely inhibited the replication of both viruses (Fig. 3.1C). These results demonstrated that in the absence of innate immune activation Vpr is not necessary for HIV-1 replication in MDMs. However, when innate immunity is activated with cGAMP Vpr is essential for HIV-1 replication.

## 3.2 Vpr inhibits cGAMP activation of ISGs in THP-1 cells

To characterise the role of Vpr in overcoming cGAMP-activated antiviral response in a more tractable system, the monocytic THP-1 cell line was used. THP-1 cells express endogenous cGAS and STING and have a functional DNA sensing pathway. THP-1 cells expressing the Gaussia luciferase gene under the control of the endogenous promoter for the *IFIT1* gene (pIFIT1-Gluc THP-1) were used to study the effect of Vpr on cGAMP activated gene expression. *IFIT1*, also known as *ISG56*, is a well-characterised ISG which is transcribed when transcription factors such as ISGF3 (STAT1, STAT2 and IRF9 complex) or IRFs bind to ISRE in the *IFIT1* promoter upon PRR stimulation (Fig. 3.2A).

To express Vpr in THP-1 cells a codon optimised Vpr gene from an HIV-1 founder clone, SUMA (515,516), was cloned downstream of the SFFV promoter in a lentiviral genome

plasmid that expressed GFP from an internal ribosome entry sequence (IRES) (Fig. 3.2B). Lentiviral vectors were produced in HEK293T cells and purified by ultracentrifugation at 72000g for 2 hours through a sucrose cushion (20% in PBS). Immunoblot of viral particles showed viral capsid protein (p24), vesicular stomatitis virus envelope glycoprotein (VSV-g) and Vpr (Fig. 3.2C).

Monocytic pIFIT1-Gluc THP-1 cells were transduced with an empty or a Vpr-expressing lentiviral vector at MOI 0.5 or 1 for 40 hours. Cells were then stimulated with 5 µg/ml cGAMP for 8 hours. Supernatants were collected from each sample and luciferase production was quantified by luminometry (Fig. 3.2D). cGAMP treatment activated the IFIT1 luciferase reporter in the untransduced or empty vector transduced cells. However, transduction with the Vpr-expressing vector significantly suppressed the IFIT1 luciferase reporter activation in a dose dependent manner (Fig. 3.2E). Analysis of the cells by flow cytometry for GFP expression showed a dose dependent increase in GFP expressing cells transduced with the Vpr-expressing vector, which was unaltered by cGAMP stimulation (Fig. 3.2F). These results showed that Vpr expression inhibits cGAMP activation of *IFIT1* gene expression.

To determine if Vpr inhibited expression of other ISGs, pIFIT1-Gluc THP-1 cells were transduced with empty or Vpr expressing lentiviral vectors for 40 hours and then stimulated with cGAMP for 8 hours. Analysis of GFP expression by flow cytometry showed equivalent transduction level by empty and Vpr vectors (Fig. 3.3B). Expression of endogenous *MxA, CXCL10, IFIT2* and *Viperin* genes was quantified by qRT-PCR and normalised to the housekeeping gene, GAPDH. cGAMP activated *MxA, CXCL10, IFIT2* and *Viperin* gene expression in untransduced and empty vector transduced cells however the expression of all of these ISGs was significantly reduced in Vpr vector transduced cells (Fig. 3.3A).

The effect of Vpr on cGAMP activity was also determined by quantification of cGAMP stimulated protein production. pIFIT1-Gluc THP-1 cells were transduced with empty or Vpr expressing lentiviral vectors for 40 hours and then stimulated with cGAMP for 8 hours. Supernatants were analysed by ELISA for CXCL10 protein production. cGAMP-stimulated CXCL10 protein production in untransduced and empty vector transduced cells and this was inhibited by Vpr in a dose dependent manner (Fig. 3.3C). Analysis of GFP expression by flow cytometry showed dose dependent increase in GFP expressing cells that were equivalent between empty or Vpr expressing vectors (Fig. 3.3D). These results indicated that Vpr overcomes cGAMP activated antiviral responses by suppressing cGAMP activation of ISGs RNA and protein production.

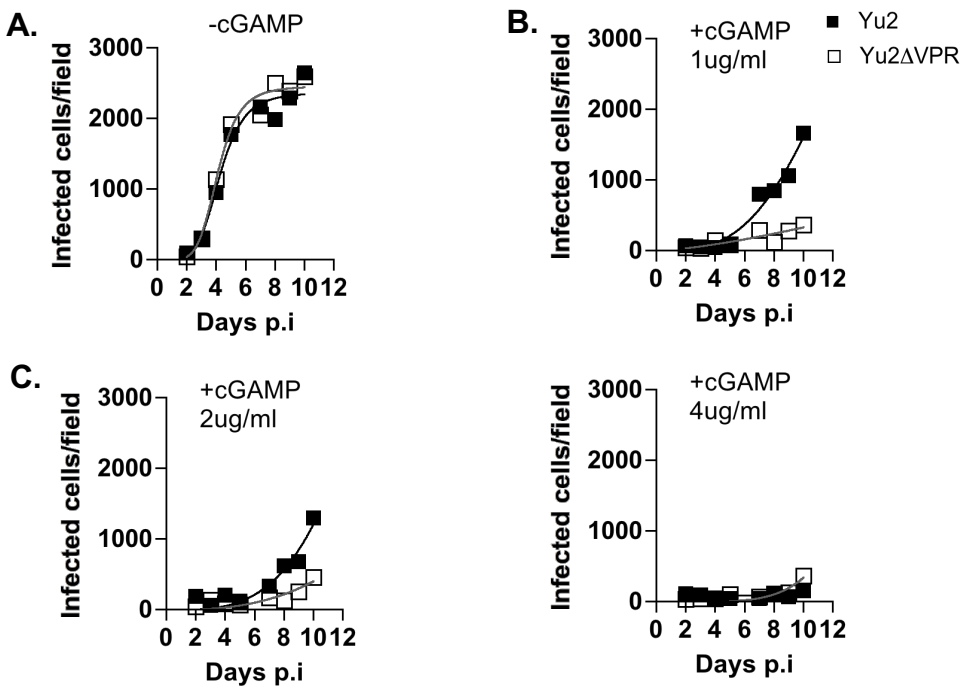


**Figure 3.1 Vpr is essential for HIV-1 replication in cGAMP stimulated MDMs**

Replication of WT Yu2 HIV-1 or Yu2 HIV-1ΔVpr in MDMs stimulated with 1 µg/ml cGAMP **(B)**, 2 µg/ml cGAMP **(C)**, 4 µg/ml cGAMP **(C)** or left unstimulated **(A)** measured by ELISpot. Experiment is representative of three independent experiments. Experiment done by Dr. Jane Rasaiyah.

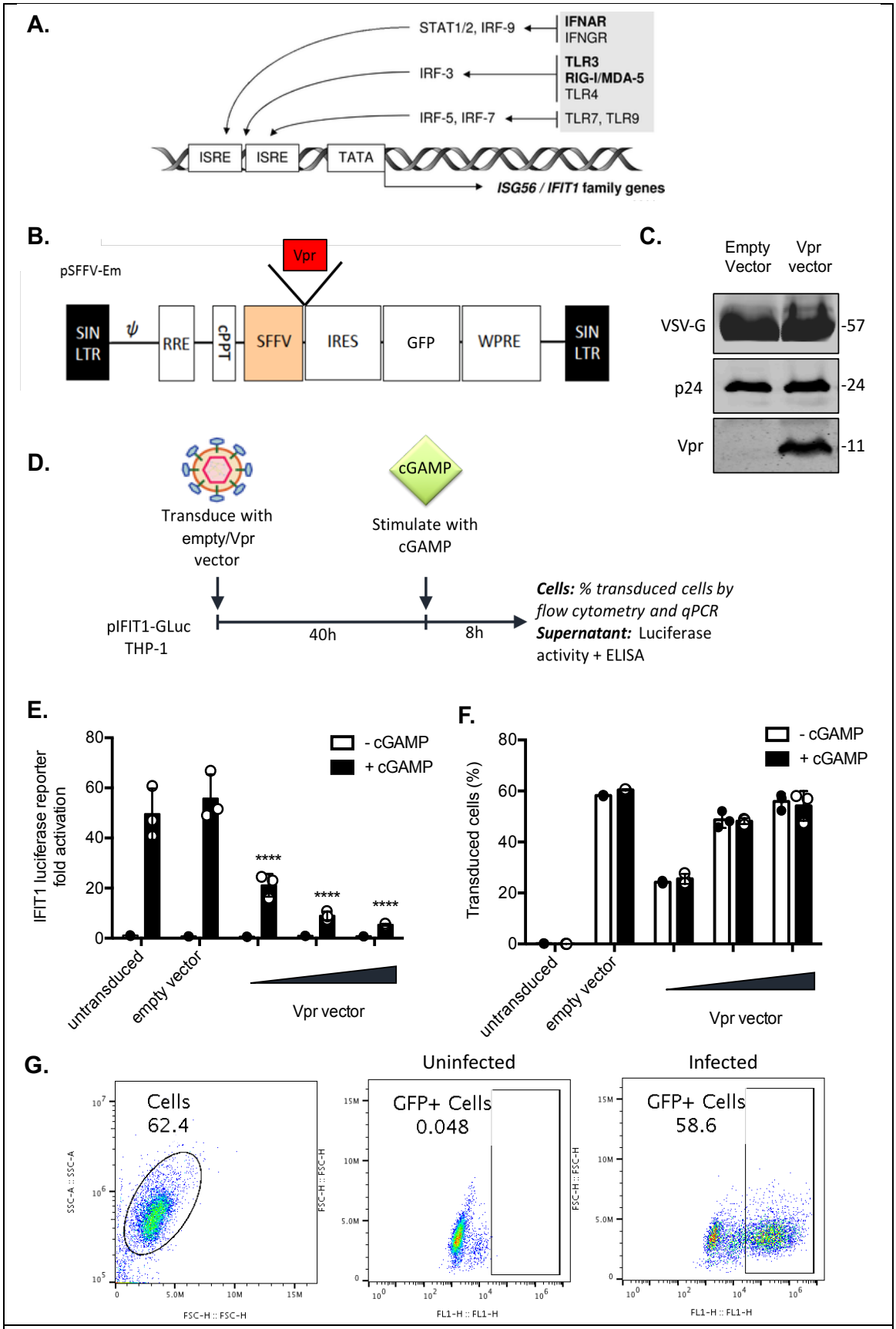


**Figure 3.2 Vpr inhibits cGAMP activation of IFIT1 luciferase reporter**

**(A)** Schematic of the *IFIT1* promoter. **(B)** Vpr encoding lentiviral expression construct contained self-inactivating Long terminal repeat (SIN LTR), Rev response element (RRE), Central polypurine tract (cPPT), Spleen focus-forming virus promoter (SFFV), internal ribosome entry site (IRES), green fluorescent protein (GFP) and Woodchuck hepatitis virus post-transcriptional regulatory element (WPRE). **(C)** Immunoblot detecting VSV-G, capsid

(p24) or Vpr in vector supernatants. Size markers (in kDa) are indicated on the right. **(D)** Schematic of THP-1 cells based Gaussia luciferase reporter gene assay to study the function of Vpr**. (E)** Fold induction of IFIT1-Luc after activation of STING by cGAMP (5 µg/ml) and expression of Vpr from a lentiviral vector, or empty vector or in untransduced IFIT1-Luc reporter THP-1 cells. **(F)** Percentage of THP-1 cells from (E) transduced by the vector encoding Vpr and GFP or GFP alone (empty vector) treated with cGAMP (5 µg/ml) or left untreated as a control. **(G)** Flow cytometry plots showing gating strategy for F. Error bars represent standard deviation of biological repeats (n=3). Experiments are representative of three independent experiments. Data were analysed using two-way ANOVA test. Stars (*) represent statistical significance: * ($p<0.05$), ** ($p<0.01$), *** ($p<0.001$), **** ($p<0.0001$) compared to empty vector.

## 3.3 Vpr inhibits IFIT1 luciferase reporter activation downstream of various innate immune agonists

There are numerous PRRs that can be activated by various stimuli to induce an ISG response (517). To determine whether Vpr has a broad activity against innate signalling pathways, activity of Vpr was tested against Herring Testis DNA (HT-DNA), Sendai virus (SeV) and Lipopolysaccharide (LPS) which activate three different PRRs. HT-DNA is a potent stimulator of the cytoplasmic DNA sensors (518). SeV is an RNA virus that induces ISG expression via RIG-I activation (519). LPS is an outer membrane component of Gram-negative bacteria and activates TLR4 (520).

Monocytic pIFIT1-Gluc THP-1 cells were transduced with an empty or a Vpr expressing lentiviral vector for 40 hours. Cells were then stimulated with HT-DNA (5 µg/ml) transfection, SeV (200HAunits/ml) infection or LPS (1 µg/ml) for 8 hours. Supernatants were collected from each sample and luciferase production was quantified by luminometry. HT-DNA, SeV or LPS stimulation activated the IFIT1 luciferase reporter in the untransduced and empty vector transduced cells however transduction with the Vpr expressing vector significantly suppressed the IFIT1 luciferase reporter activation in a dose dependent manner (Fig 3.4A, C, E). Analysis of GFP expression by flow cytometry showed a dose dependent increase in GFP expressing cells transduced with empty or Vpr expressing vectors (Fig. 3.4B, 4D, 4F). These results showed that Vpr has broad activity against innate immune agonists indicating that Vpr may target a step conserved between different PRR signalling pathways.

## 3.4 Vpr does not inhibit STING, TBK1 or IRF3-S386 phosphorylation

To identify the step inhibited by Vpr in the innate immune signalling pathways, activation of signalling molecules involved in the HT-DNA-induced signalling cascade was probed by immunoblotting. HT-DNA stimulation activates cytoplasmic DNA sensors including cGAS (518). Activated cGAS catalyses the synthesis of secondary messenger molecule cGAMP from ATP and GTP (175). cGAMP binds and activates STING in the endoplasmic reticulum (182,183). Activated STING translocates to the Golgi where it recruits TBK1 and IRF3 (192). TBK1 then phosphorylates IRF3 which then translocates to the nucleus and upregulates type I IFN genes (193,194). Monocytic pIFIT1-Gluc THP-1 cells were transduced with an empty or a Vpr expressing lentiviral vector at MOI of 1 for 40 hours to express Vpr. Cells were then stimulated with HT-DNA (5 µg/ml) transfection using Lipofectamine 2000 and harvested for immunoblotting after 3 hours. After 8 hours

supernatants were collected for luminometry and cells were fixed and analysed for GFP expression by flow cytometry. HT-DNA stimulation activated the IFIT1 luciferase reporter in the untransduced and empty vector transduced cells and transduction with the Vpr expressing vector inhibited this by 4-fold (Fig. 3.5B). Analysis of GFP expression by flow cytometry showed equivalent GFP expressing cells with empty or Vpr expressing vectors (Fig. 3.5C). Immunoblotting showed that HT-DNA stimulation resulted in phosphorylation of STING, TBK1 and IRF3-serine386 (IRF3-S386) in the untransduced or empty vector transduced cells. However, despite the reduction in IFIT1 reporter gene activation by Vpr vector transduction, there was no reduction in the levels of total or phosphorylated STING, TBK1 or IRF3-S386 (Fig. 3.5A). These results demonstrated that Vpr suppresses HT-DNA activation of ISGs without inhibiting the phosphorylation of STING and TBK1. Given that IRF3 phosphorylation at S386 has been shown to be necessary and sufficient for IRF3 activation (521–524) and that Vpr did not inhibit IRF3 phosphorylation at S386 suggests that Vpr may block the signalling pathway downstream of IRF3 activation.

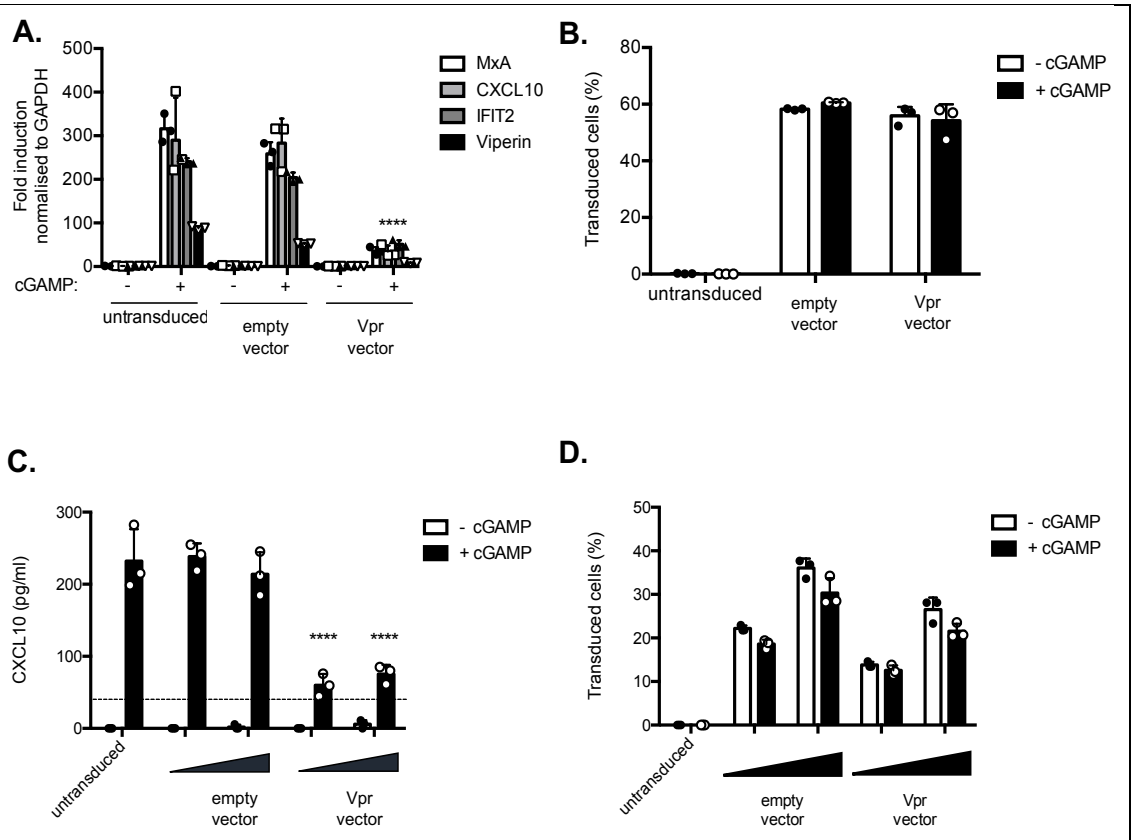


**Figure 3.3 Vpr inhibits cGAMP activation of ISG mRNA expression and protein production**

**(A)** Fold induction of ISGs MxA, CXCL10, IFIT2 and Viperin after activation of STING by cGAMP (5 µg/ml) and expression of Vpr from a lentiviral vector, or after transduction by empty vector or in untransduced THP-1 cells. **(B)** Percentage of THP-1 cells from (A) transduced by the vector encoding Vpr and GFP or GFP alone (empty vector), treated with cGAMP or left untreated as a control. **(C)** Secreted CXCL10 (ELISA) from THP-1 cells expressing Vpr from a lentiviral vector delivered at two doses or after transduction by empty vector at two doses or from untransduced THP-1 cells, stimulated with cGAMP (5µg/ml) or left untreated as a control. **(D)** Percentage of THP-1 cells from (C) transduced by the vector encoding Vpr and GFP or GFP alone (empty vector) at two doses, treated with cGAMP (5 µg/ml) or left untreated as a control. Error bars represent standard deviation of biological repeats (n=3). Data were analysed using two-way ANOVA test. Stars (*) represent statistical significance: * ($p<0.05$), ** ($p<0.01$), *** ($p<0.001$), **** ($p<0.0001$) compared to empty vector.

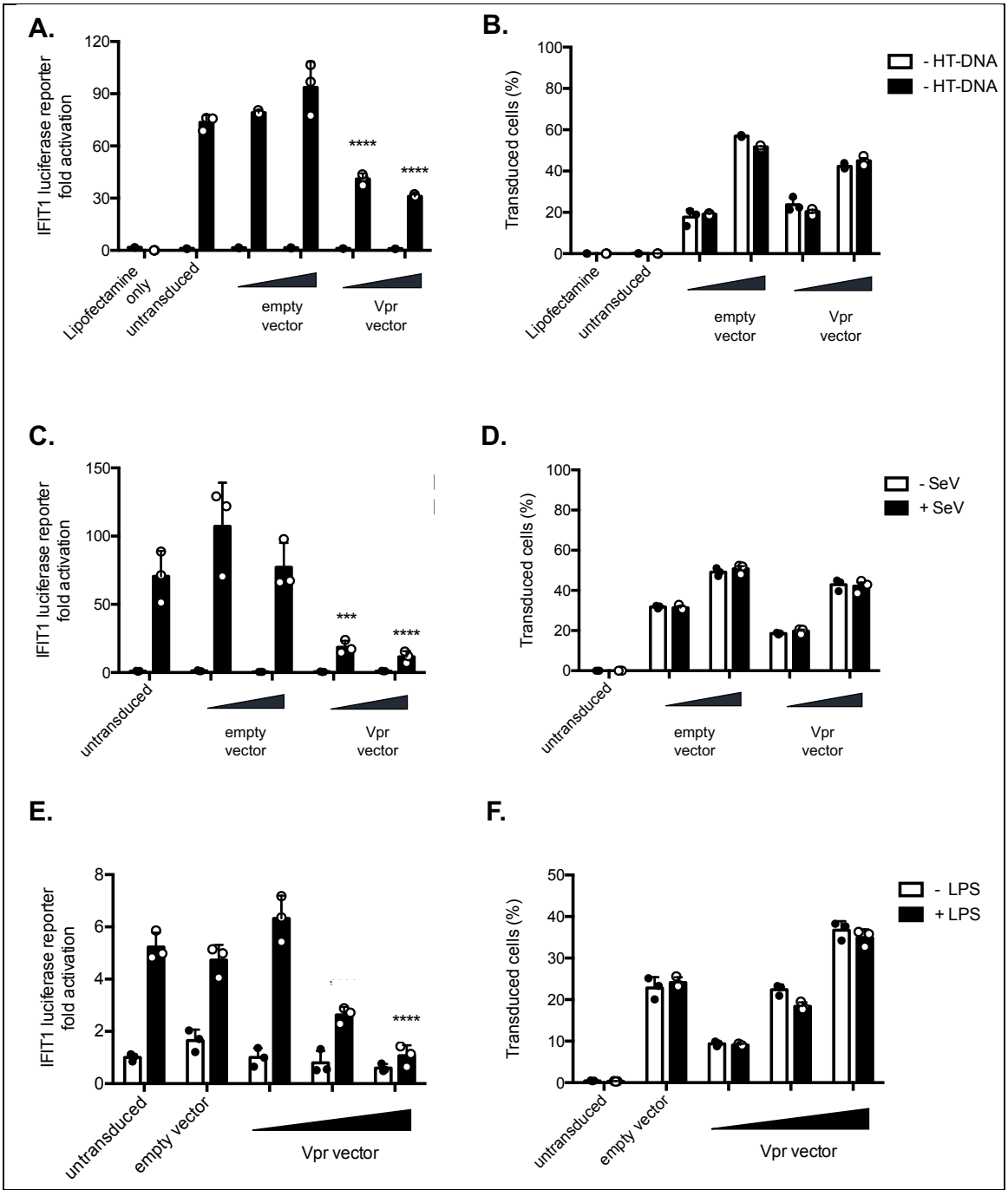


**Figure 3.4 Vpr inhibits IFIT1 luciferase activation downstream of various innate immune agonists**

**(A), (C), (E)** Fold induction of IFIT1-Luc after **(A)** HT-DNA transfection (5 µg/ml), **(C)** Sendai virus infection or **(E)** LPS (1 µg/ml) treatment and expression of Vpr from a lentiviral vector, or after transduction by empty vector or in untransduced IFIT1-Luc reporter THP-1 cells. **(B), (D), (F)** Percentage of THP-1 cells from (A, C and E) transduced by the vector encoding Vpr and GFP or GFP alone (empty vector) and stimulated with HT-DNA transfection (5 µg/ml) **(B),** Sendai virus infection **(D)** or LPS (1 µg/ml) treatment **(F)** or left untreated as a control in each case. Error bars represent standard deviation of biological repeats (n=3). Experiments are representative of three independent experiments. Data were analysed using two-way ANOVA test. Stars (*) represent statistical significance: * ($p<0.05$), ** ($p<0.01$), *** ($p<0.001$), **** ($p<0.0001$) compared to empty vector.

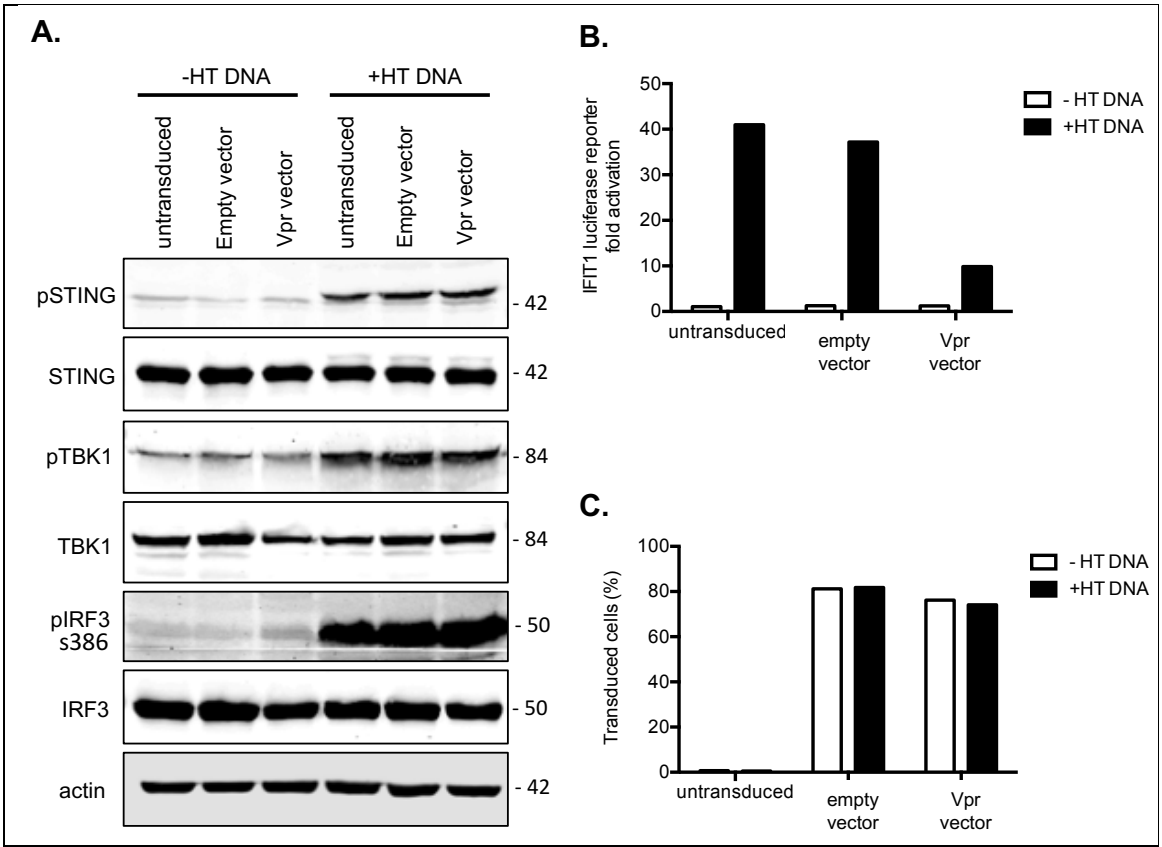


**Figure 3.5 Vpr suppresses ISG expression without inhibiting STING, TBK1 or IRF3 phosphorylation**

**(A)** Immunoblot detecting Phosho-STING (S366), total STING, phospho-TBK1 (S172), total TBK1, phosphor-IRF3 (S386), total IRF3, or actin as a loading control, from extracted THP-1 cells expressing Vpr, empty vector or left untransduced as a control and transfected with HT-DNA or left untransfected as a control. Size markers are shown (kDa). **(B)** Fold induction of IFIT1-Luc in cells from (A) expressing Vpr or not and transfected with HT-DNA or left untransfected as a control. **(C)** Percentage of THP-1 cells from (B) transduced by the vector encoding Vpr and GFP or GFP alone (empty vector) transfected with HT-DNA (5 µg/ml) or left untransfected as a control. Experiments are representative of two independent experiments.

## 3.5 IRF3 phosphorylation at S396 is affected by Vpr

The C-terminal of IRF3 spanning amino acids 385 to 405 contains a cluster of serine/threonine residues ($^{385}$SSLENTVDLHISNSHPLSLTS$^{405}$) that can be phosphorylated (525). Phosphorylation of IRF3 at S396 has also been shown to be induced by TBK1 during infection (194). Therefore, the effect of Vpr on IRF3 phosphorylation at S396 was investigated. Flow cytometry was used to detect IRF3 phosphorylation at S396 because this antibody did not work in immunoblotting. HIV-1 virus-like particles bearing Vpr protein were made in HEK293T cells with p8.91 packaging plasmid, VSV-glycoprotein envelope plasmid (pMDG) and a pcDNA3.1 plasmid expressing Vpr. Monocytic pIFIT1-Gluc THP-1 cells were stimulated with cGAMP (5 µg/ml) or HT-DNA (5 µg/ml) transfection and treated with empty or WT Vpr VLP (1URT/ml). After 3 hours cells were fixed in PFA, stained with phospho-IRF3-S396 specific antibody and analysed by flow cytometry. cGAMP or HT-DNA stimulation phosphorylated IRF3 at S396 in about 16% and 20% cells, respectively, when treated with empty VLP (Fig. 3.6A, B). On the other hand, Vpr VLP treatment inhibited HT-DNA or cGAMP stimulated IRF3 phosphorylation at S396 by almost 10- and 3-fold, respectively (Fig. 3.6A, B). These results showed that IRF3 phosphorylation at S396, which is dispensable for IRF3 activation (521–524), is inhibited in the presence of Vpr.

## 3.6 Vpr blocks IRF3 and NF-κB (p65) nuclear translocation

Given the differential effects of Vpr on IRF3 phosphorylation, immunofluorescence microscopy was used to quantify nuclear translocation of IRF3 and NF-κB (p65) as a consequence of activation. Firstly, translocation assays were optimised with cGAMP and LPS stimulations. THP-1 cells were differentiated into adherent macrophage-like cells with phorbol 12-myristate 13-acetate (PMA) (50ng/ml) stimulation for 72 hours. Cells were then stimulated with cGAMP (5 µg/ml) for 3 hours or LPS (1 µg/ml) for 2 hours. Cells were fixed with 4% PFA, permeabilised with triton and then stained for IRF3 or NF-κB (p65). DAPI was used to stain nuclei. Immunofluorescence images were taken using the Hermes WiScan Cell Imaging System. Nuclear:cytoplasmic ratios of IRF3 and NF-κB (p65) immunostain were measured at the single cell level by quantitation of IRF3 or NF-κB (p65) signal intensities overlapping the nucleus and represented as a translocation coefficient. An increase in the translocation coefficient is indicative of nuclear translocation and vice versa. Results with cGAMP or LPS stimulation showed a very similar increase in IRF3 nuclear translocation. However, the nuclear translocation for NF-κB (p65) was increased significantly by LPS treatment but not cGAMP under the conditions tested (Fig. 3.7A).

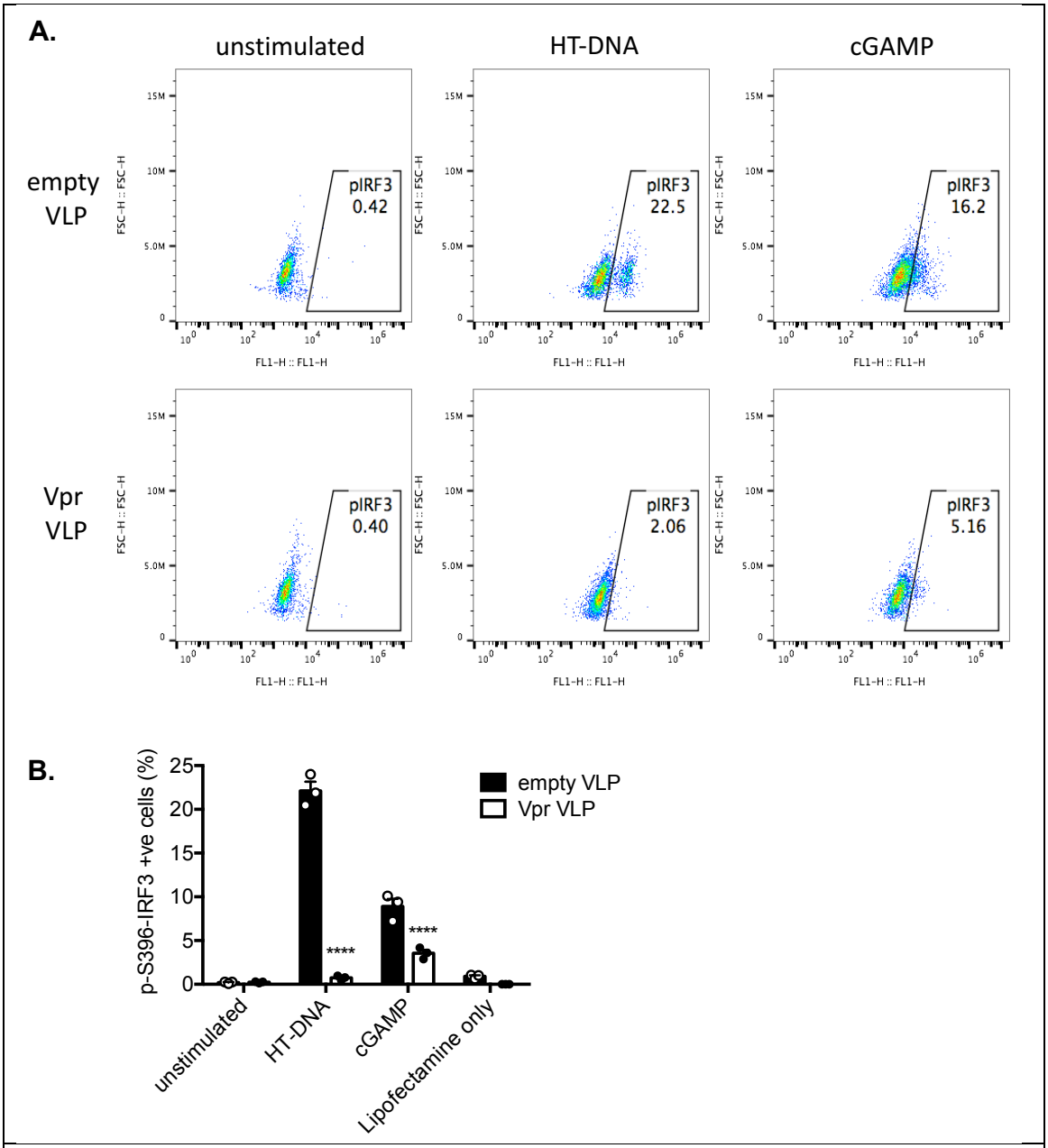


**Figure 3.6 IRF3 phosphorylation at Ser396 is affected by Vpr**

**(A)** Flow cytometry plot (forward scatter vs pIRF3-S396 fluorescence) of THP-1 cells infected with an empty or Vpr bearing virus-like particles and stimulated with cGAMP (5 µg/ml) or HT-DNA transfection (5 µg/ml). **(B)** Flow cytometry plot in (A) represented as a bar graph, plotting pIRF3-S396 positive cells in each case. Error bars represent standard deviation of biological repeats (n=3). Experiments are representative of three independent experiments. Data were analysed using two-way ANOVA test. Stars (*) represent statistical significance: * ($p<0.05$), ** ($p<0.01$), *** ($p<0.001$), **** ($p<0.0001$) compared to empty vector.

To further analyse this data an arbitrary threshold was set at 0.5 (red line) and the number of cells with a translocation coefficient greater than 0.5 were counted and the data was plotted as a bar graph. This analysis showed that cGAMP stimulation resulted in about 20% cells with nuclear IRF3 but did not increase NF-κB (p65) positive nuclei. On the other hand, LPS stimulation gave 20% IRF3 and 70% NF-κB (p65) positive nuclei (Fig. 3.7B).

To assess the activity of Vpr against IRF3 nuclear translocation THP-1 cells were differentiated into adherent macrophage like cells with PMA (50ng/ml) stimulation for 72 hours. Cells were then treated with empty or Vpr vector (4-fold serial dilution starting from 1 URT/ml) in the presence or absence of cGAMP (5 µg/ml) for 3 hours. Cells were fixed with 4% PFA and stained for IRF3 (red). DAPI was used to stain nuclei (blue). Figure 3.7C shows representative immunofluorescence images taken using the Hermes WiScan Cell Imaging System. Quantification of IRF3 nuclear translocation showed that cGAMP increased the IRF3 nuclear translocation in cells treated with or without the empty vector. However, Vpr vector treatment inhibited the cGAMP-stimulated increase in IRF3 nuclear translocation in a dose dependent manner (Fig. 3.7D). Further analysis by setting the translocation coefficient threshold at 0.5 (red line) showed that cGAMP stimulation resulted in IRF3 nuclear translocation in 30% cells treated with or without empty vector and Vpr vector treatment decreased IRF3 positive nuclei in a dose dependent manner to 5% (Fig. 3.7E).

To assess the activity of Vpr against NF-κB (p65) nuclear translocation THP-1 cells were infected as above and treated with LPS (1 µg/ml) for 2 hours or transfected with poly I:C (0.5 µg/ml) for 3 hours. Cells were fixed with 4% PFA and stained for NF-κB (p65) (red). DAPI was used to stain nuclei (blue). Quantification of NF-κB (p65) nuclear translocation showed that LPS and poly I:C increased NF-κB (p65) nuclear translocation in cells treated with or without the empty vector. However, Vpr vector treatment inhibited LPS or poly I:C stimulated increase in NF-κB (p65) nuclear translocation (Fig. 3.8A, C). Further analysis by setting the translocation coefficient threshold at 0.5 (red line) showed that LPS or poly I:C stimulation resulted in NF-κB (p65) nuclear translocation in 70% and 20% of the cells respectively. On the contrary, Vpr vector treatment decreased the number of NF-κB (p65) positive nuclei in both cases (Fig. 3.8B, D). Taken together, these results showed that Vpr blocks IRF3 and NF-κB (p65) nuclear translocation stimulated with diverse innate immune agonists, which may explain the ability of this protein to block ISG expression.

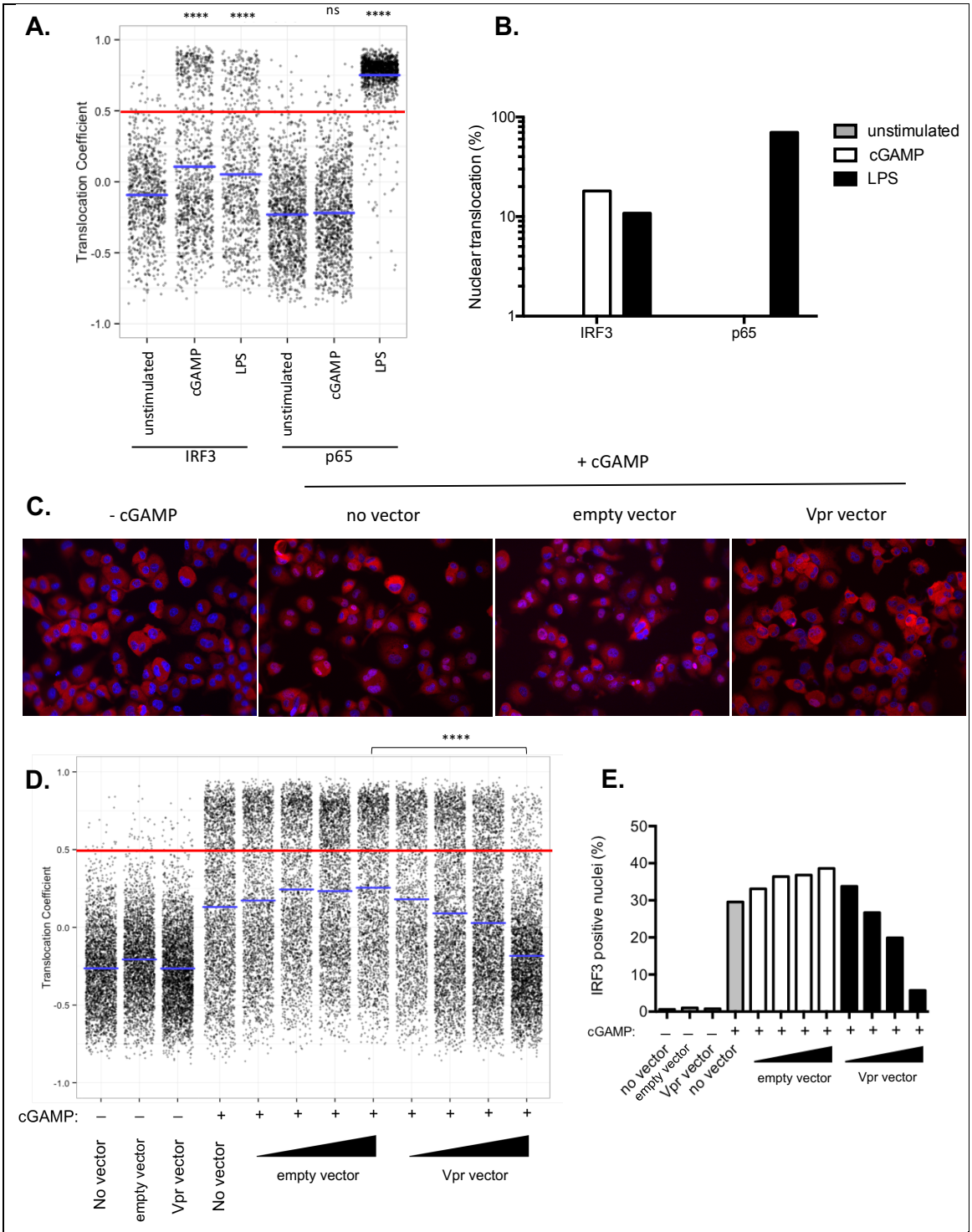


**Figure 3.7 Vpr blocks cGAMP activated nuclear translocation of IRF3**

**(A)** Single cell measurement of IRF3 and NF-kB(p65) nuclear translocation in PMA differentiated THP-1 cells treated with cGAMP (5 µg/ml), LPS (1 µg/ml) or left untreated. **(B)** Number of cells from (A) with translocation coefficient of greater than 0.5 (red line) were plotted as a percentage. **(C)** Immunofluorescence images showing IRF3 (red) in PMA differentiated THP-1 cells treated with cGAMP (5 µg/ml) or left untreated and infected with empty vector, Vpr vector or left uninfected. **(D)** Single cell measurement of IRF3 nuclear translocation in cells from (C). **(E)** Number of cells with translocation coefficient of greater than 0.5 plotted as a percentage from (C). Red line shows the translocation coefficient threshold. Blue lines represent mean translocation coefficient. Experiments are representative of three independent experiments. Data were analysed using Unpaired

Student's T tests. Stars (*) represent statistical significance: * ($p<0.05$), ** ($p<0.01$), *** ($p<0.001$), **** ($p<0.0001$).

## 3.7 Vpr deficient HIV-1 activates a genome dependent innate immune response

Given that Vpr is specifically packaged into budding virons and is present during early stages of the HIV-1 lifecycle when its DNA is prone to detection by DNA sensors, it was hypothesised that particle associated Vpr may suppress innate immune responses. To test this hypothesis HIV-1 vectors were produced by transfecting HEK293T cells with either p8.91 packaging plasmid that expresses Gag-Pol, tat and rev (HIV-GFP) or p8.2 packaging plasmid that expresses Gag-pol, tat, rev, vpr, vpu, vif and nef (HIV-GFP-Vpr). Vectors made with p8.2 packaging plasmid will incorporate only Vpr into virions but not express the accessory proteins in the infected cells, ruling out a role for the other accessory proteins in this assay.

THP-1 Lucia cells expressing Lucia, a secreted luciferase reporter gene, driven by an IFN-β minimal promoter fused to five copies of the NF-κB consensus transcriptional response element and three copies of the c-Rel binding site were infected with HIV-GFP or HIV-GFP-Vpr at MOI of 0.3, 1 or 3. After 24 hours supernatants were collected for luminometry and cells were harvested for qRT-PCR and flow cytometry. The results showed that at MOI of 0.3, which infected about 20% cells, there was no significant difference in NF-κB luciferase reporter activation or *CXCL10* gene induction by HIV-GFP or HIV-GFP-Vpr (Fig. 3.9A, B, C). However at high MOIs of 1 or 3, which infected almost 90% of cells, HIV-GFP triggered 5-fold more NF-κB luciferase reporter activation and CXCL10 gene induction when compared to HIV-GFP-Vpr (Fig. 3.9A, B, C). These results suggest that at high multiplicity of infection, HIV-1 triggers an innate immune response that is suppressed by the virion delivered Vpr.

To investigate whether the viral genome is responsible for innate immune activation in the absence of Vpr, HIV-1 VLPs were made with p8.91 packaging plasmid and VSV-g envelope but without the genome plasmid. To equalise the dose, RT activity of vector supernatants was determined by SG-PERT. THP-1 Lucia cells were infected with 3, 10 or 30 mURT/ml (MOI 0.3, 1 and 3, respectively) of HIV-GFP or HIV-VLP for 24 hours. Supernatants were collected for luminometry and cells were harvested for qRT-PCR and flow cytometry. The results showed that HIV-GFP activated NF-κB luciferase reporter and *CXCL10* gene expression in a dose dependent manner (Fig. 3.9D, E, F). In contrast, HIV-VLP did not induce any NF-κB luciferase reporter activation or *CXCL10* gene expression

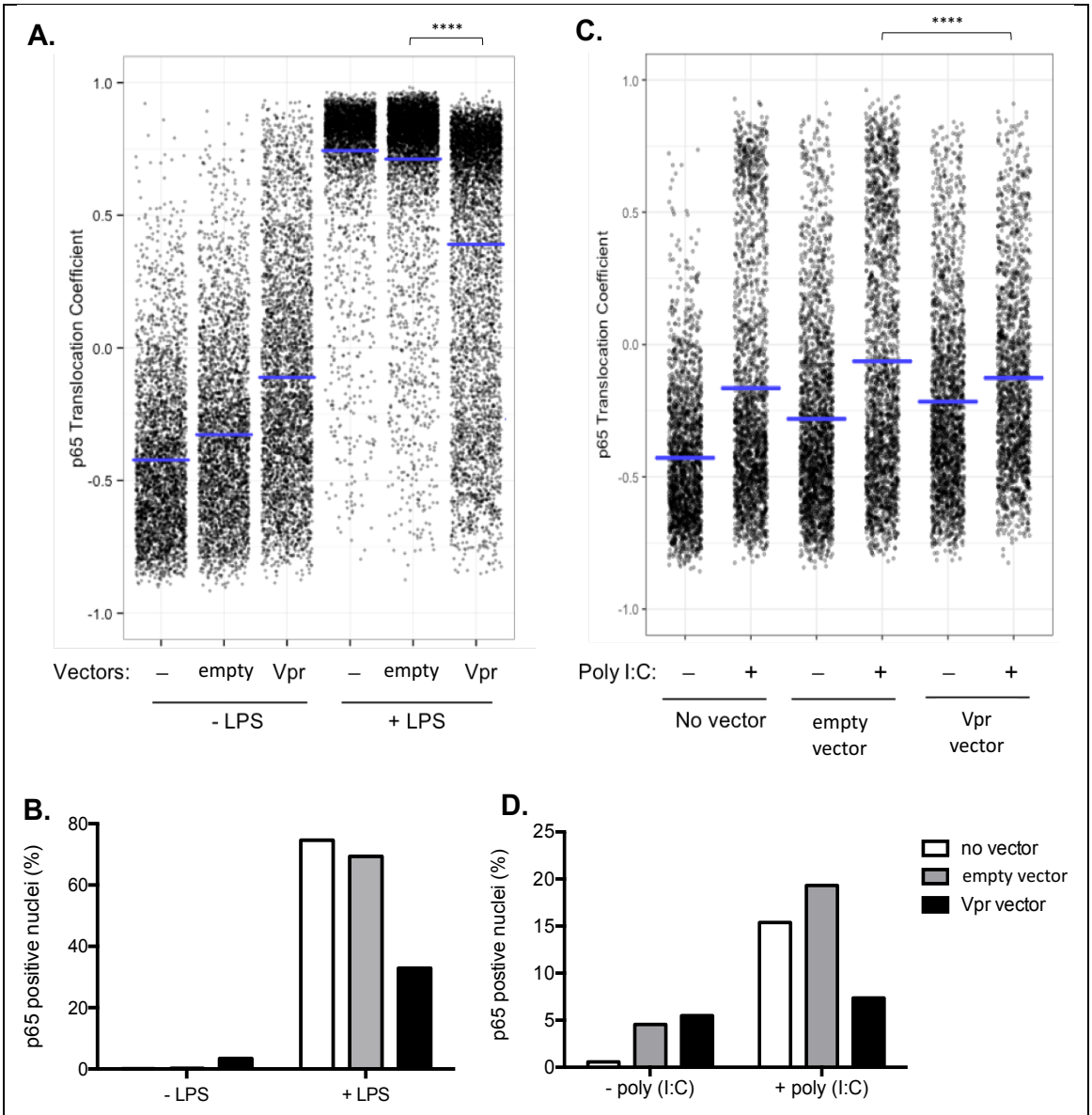


**Figure 3.8 Vpr blocks LPS and poly I:C activated p65 nuclear translocation**

**(A), (C)** Single cell measurement of NF-kB(p65) nuclear translocation in PMA differentiated THP-1 cells treated with LPS (5 µg/ml) (A), or transfected with poly I:C (0.5 µg/ml) (C) or left untreated and infected with empty vector, Vpr vector or left uninfected. (B and D) Number of cells with translocation coefficient of greater than 0.5 plotted as a percentage from (A) and (C). Red line shows the translocation coefficient threshold. Blue lines represent mean translocation coefficient. A and B are representative of three independent experiments. Data were analysed using Unpaired Student's T tests. Stars (*) represent statistical significance: * ($p<0.05$), ** ($p<0.01$), *** ($p<0.001$), **** ($p<0.0001$).

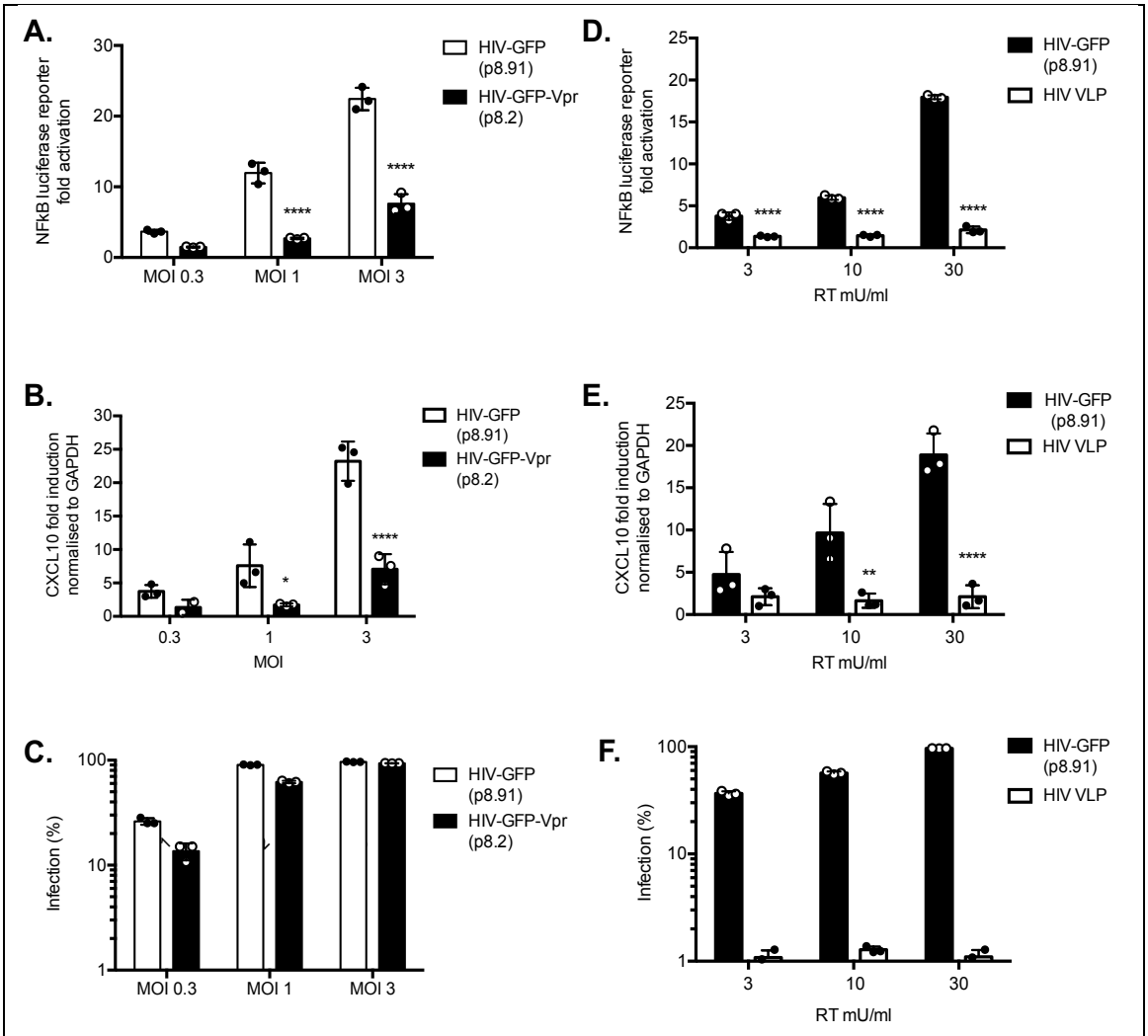


**Figure 3.9 Vpr deficient HIV-1 activates ISG expression in a viral genome dependent manner**

**(A), (D)** Fold induction of NF-κB-Luc after infection of THP-1 cells with HIV-GFP (p8.91), HIV-GFP-Vpr (p8.2) or HIV-VLP at three doses. **(B), (E)** Fold induction of *CXCL10* after infection of THP-1 cells with HIV-GFP (p8.91), HIV-GFP-Vpr (p8.2) or HIV-VLP at three doses. **(C), (F)** Percentage of THP-1 cells from (C) infected by HIV-GFP (p8.91), HIV-GFP-Vpr (p8.2) or HIV-VLP at three doses. Error bars represent standard deviation of biological repeats (n=3). Experiments are representative of three independent experiments. Data were analysed using two-way ANOVA test. Stars (*) represent statistical significance: * ($p<0.05$), ** ($p<0.01$), *** ($p<0.001$), **** ($p<0.0001$) compared to empty vector.

at any dose (Fig. 3.9D, E, F). This suggested that the viral nucleic acids are the PAMP for innate immune response in the absence of Vpr.

## 3.8 ISG expression by Vpr deficient HIV-1 depends on cGAS but not MAVS

HIV-1 reverse transcribed DNA has been shown to be the PAMP that under certain conditions is recognised by the DNA sensor, cGAS (268), (78). Given that Vpr deficient HIV-1 activated a genome dependent innate immune response, the role of the DNA sensor cGAS in this sensing event was investigated. THP-1 cells in which cGAS or MAVS was deleted by CRISPR/Cas-9 were obtained (Veit Hornung, LMU Munich). Loss of cGAS and MAVS expression was confirmed by immunoblotting (Fig. 3.10C). Cells were infected with Vpr deficient HIV-GFP and harvested for RT-qPCR 24 hours post infection. Flow cytometry was carried out 48 hours after infection. Vpr deficient HIV-GFP activated CXCL10 gene expression in control cells and MAVS-/- cells but not in cGAS -/- cells (Fig. 3.10A). Flow cytometry for GFP 48 hours post infection showed that infection by HIV-GFP was equivalent between different cell types (Fig. 3.10B). These data demonstrated that cGAS is responsible for detecting HIV-1 DNA and triggers an innate immune response in the absence of Vpr.

## 3.9 Summary

This section summarises the data presented in this chapter. Several recent studies have shown that HIV-1 reverse transcribed DNA is recognised by the DNA sensor, cGAS, resulting in innate immune activation and suppression of viral replication (268), (78). Given that Vpr is specifically packaged into HIV-1 virions and present during early stages of HIV-1 life cycle when its DNA is vulnerable to detection by cGAS, it was hypothesised that Vpr may suppress innate immune activation to allow HIV-1 replication. To this end, Vpr was found to be essential for HIV-1 replication in cGAMP-stimulated MDMs (Fig. 3.1B). However, in the absence of innate immune activation Vpr did not provide any advantage for viral replication (Fig. 3.1A). Expression of Vpr by lentiviral transduction in a myeloid cell line, THP-1, inhibited activation of ISG RNA and protein production downstream of cGAMP activation of STING in a concentration dependent manner (Fig 3.2, 3.3). Testing the activity of Vpr against different innate immune stimuli revealed that Vpr has broad activity against PRR signalling pathways indicating that Vpr likely targets a step conserved in innate immune activation (Fig. 3.4). To identify the step blocked by Vpr, activation of key signalling molecules in the DNA sensing pathway was tested by immunoblotting.

Intriguingly, Vpr expression did not affect phosphorylation of STING or TBK1 (Fig. 3.5A). Investigation of IRF3 phosphorylation showed that in the presence of Vpr IRF3 was phosphorylated at S386 (Fig. 3.5A) but not at S396 (Fig. 3.6) when stimulated with HT-DNA transfection. Quantification of IRF3 or NF-κB (p65) nuclear translocation at the single cell level by immunofluorescence microscopy showed that Vpr inhibited IRF3 and NF-κB (p65) nuclear translocation stimulated by various innate immune agonists (Fig. 3.7, 3.8). Given that IRF3 phosphorylation at s386 is necessary and sufficient for IRF3 nuclear translocation, these results indicate that Vpr may inhibit nuclear translocation of s386-phosphorylated IRF3 to prevent ISG expression.

To investigate whether virion-associated Vpr is sufficient to block innate immune activation, HIV-GFP vectors with or without incorporated Vpr were used. At high multiplicity of infection HIV-1 lacking virion associated Vpr triggered genome dependent *CXCL10* mRNA expression, however HIV-GFP vector bearing Vpr did not (Fig. 3.9). Finally, CRISPR/Cas9 mediated deletion of cGAS, but not MAVS, prevented induction of *CXCL10* mRNA by Vpr deficient HIV-1, confirming that at high multiplicity of infection HIV-1 triggers a DNA-dependent innate immune response which is dampened by Vpr (Fig. 3.10).

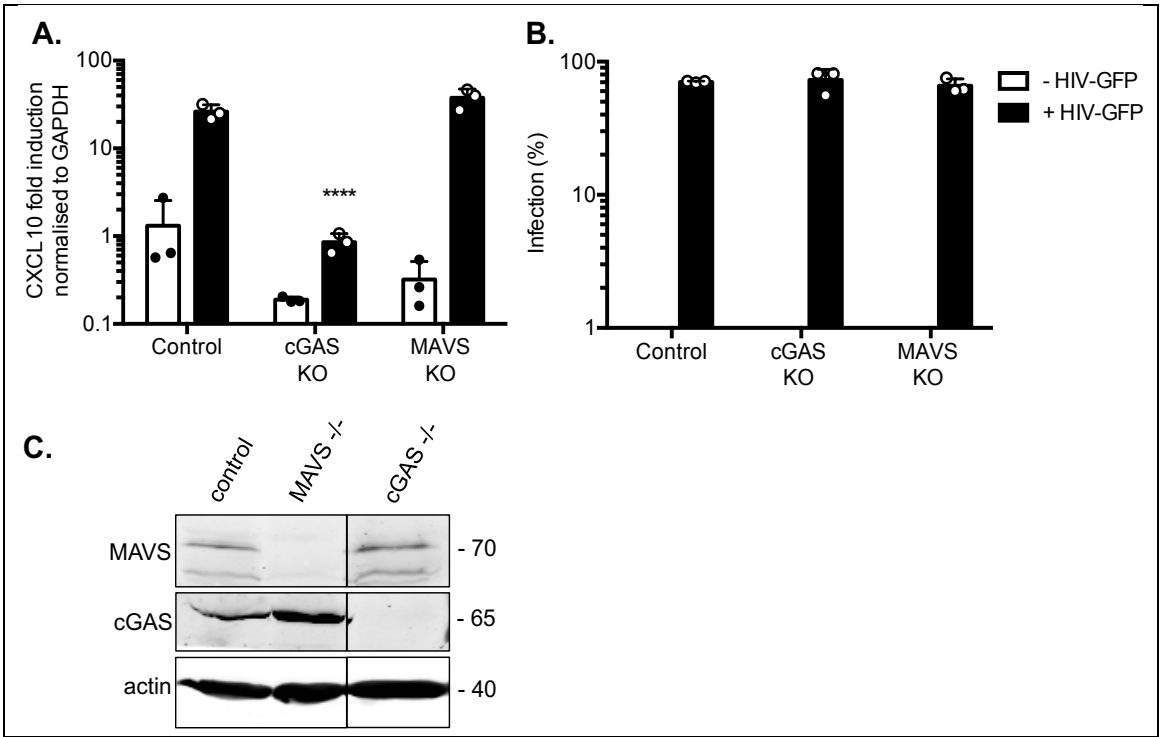


**Figure 3.10 ISG expression by Vpr deficient HIV-1 depends on cGAS but not MAVS**

**(A)** Fold induction of *CXCL10* after infection of control, cGAS-/- or MAVS-/- THP-1 cells with HIV-GFP (p8.91). **(B)** Percentage of control, *cGAS-/-* or *MAVS-/-* THP-1 cells from (A) infected by HIV-GFP (p8.91). **(C)** Immunoblot detecting cGAS, MAVS and actin as a loading control from extracted control, cGAS-/- or MAVS-/- THP-1 cells. Size markers are shown (kDa). Error bars represent standard deviation of biological repeats (n=3). Experiments are representative of three independent experiments. Immunoblot in (C) was kindly provided by Dr. Rebecca Sumner. Data were analysed using two-way ANOVA test. Stars (*) represent statistical significance: * ($p<0.05$), ** ($p<0.01$), *** ($p<0.001$), **** ($p<0.0001$) compared to empty vector.

# 4 Chapter 4: Characterisation of Vpr antagonism of innate immunity

## 4.1 Vpr suppresses ISG expression independently of cell cycle arrest

For further characterisation of Vpr antagonism of innate immune activation, mutations that have been described in the literature to prevent Vpr interaction with cellular target proteins were introduced into Vpr by site directed mutagenesis (Fig. 4.1 A, B, C). One of the best-characterised functions of Vpr is its ability to induce cell cycle arrest (468). Vpr recruits a DCAF1/DDB1/Cul4 E3 ligase complex to degrade a SLX4 endonuclease-containing complex and block cell cycle in the G2/M phase (468). To determine whether cell cycle arrest and suppression of innate immune signalling are independent functions of Vpr, three mutant Vpr proteins, VprF34I-P35N, VprQ65R and VprR80A, were constructed. VprQ65R is a DCAF1 binding mutant that cannot degrade Vpr cellular targets via the proteasome (526). VprR80A can recruit DCAF1 but is unable to interact with some members of the SLX4 complex and does not arrest cell cycle (468). Vpr has been shown to interact with importins and cyclophilin A through residues F34 and P35 respectively (476), (495). To abrogate these interactions a double mutant VprF34I-P35N was constructed.

The ability of Vpr mutants to cause cell cycle arrest was confirmed by cell cycle analysis using propidium iodide (PI) staining. PI is a fluorescent nucleic acid binding dye that allows DNA content quantification and classification of cells into three phases of the cell cycle. Cells in the G1/G0 phase are diploid with 2n DNA content, whereas cells in G2 and just prior to mitosis (G2/M) contain double the amount of DNA and are 4n. In S-phase, synthesis of DNA results in DNA content ranging between 2n and 4n. Monocytic THP-1 cells were transduced with an empty vector, WT Vpr or a mutant Vpr expressing lentiviral vector at MOI 1. After 48 hours, cells were fixed with ethanol, stained with PI in the presence of RNase A and analysed by flow cytometry. A histogram plot of DNA content against cell number was plotted (Fig. 4.1D). Untransduced or empty vector transduced cells showed a typical DNA profile of proliferating cells with 60% cells in G1/G0 phase, 10% in S phase and 30% in the G2/M phase (Fig. 4.1D). However, WT Vpr expression resulted in 60% of the cells being in the G2/M phase. Similarly, VprF34I+P35N increased the number of cells in the in the G2/M phase (Fig. 4.1D). These results were consistent with previous reports of Vpr function in cell cycle arrest and confirmed that mutations

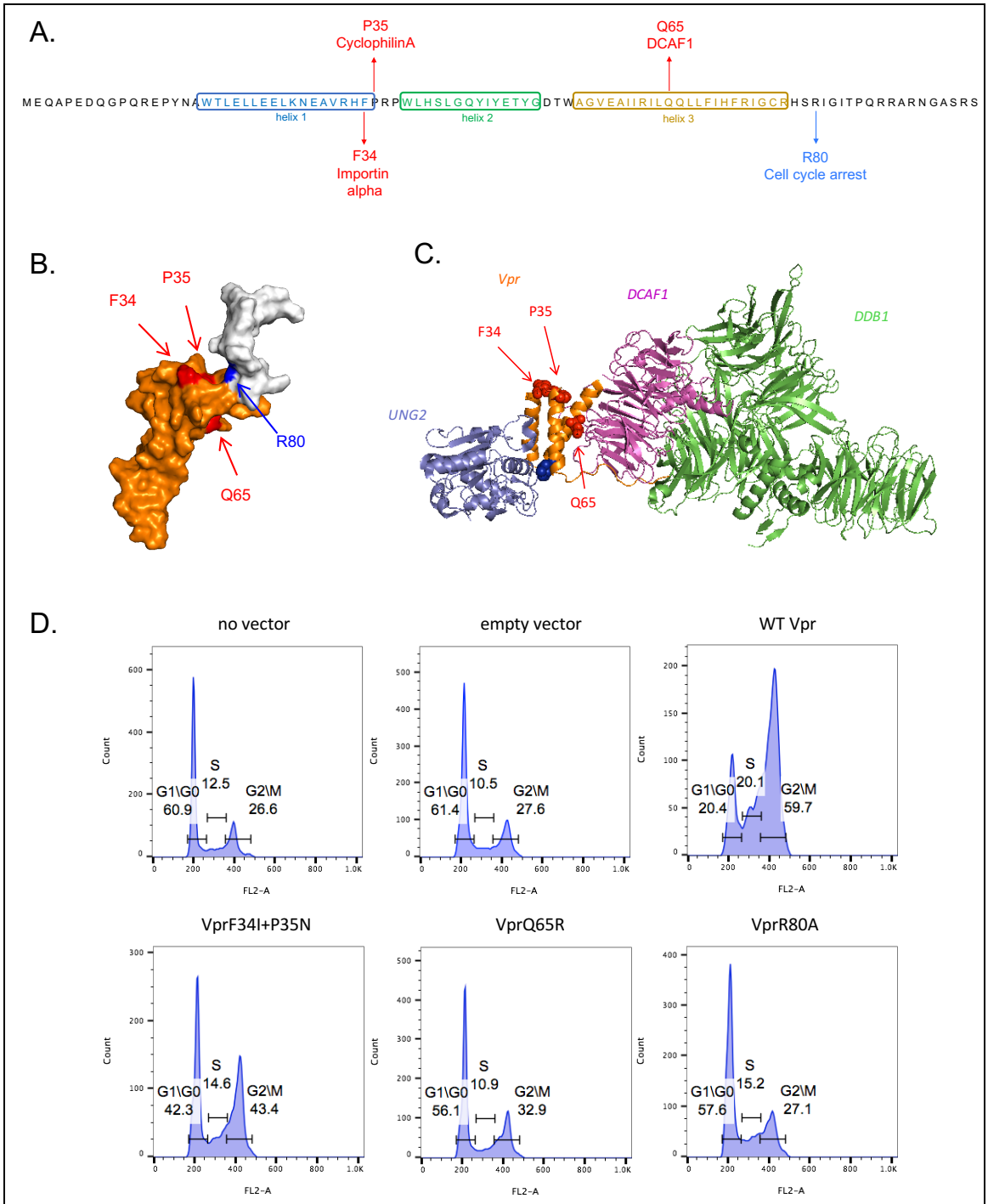


**Figure 4.1 Cell cycle analysis of Vpr proteins**

**(A)** Schematic showing position of Vpr mutants on a linear amino acid sequence of Vpr. **(B)** NMR structure of full length Vpr showing position of Vpr mutants (PDB 1M8L). (C) Crystal structure of Vpr with its target protein UNG2 and cofactors DCAF1 and DDB1 showing position of Vpr mutants (PDB 5JK7). White region of Vpr in (B) is unresolved in the crystal structure. **(D)** Flow cytometry plots showing cell cycle phases of THP-1 cells transduced with an empty vector, WT Vpr or mutant Vpr encoding vector or left untransduced as a control. Each experiment is representative of two independent experiments.

at residue 65 or 80 prevent cell cycle arrest by Vpr, whereas mutating residues 34 and 35 does not significantly impact cell cycle arrest function of Vpr.

To investigate whether Vpr mutant proteins were able to inhibit innate immune activation, pIFIT1-Gluc THP-1 cells were transduced with an empty, WT or a mutant Vpr expressing lentiviral vector at MOI 1 for 40 hours and then stimulated with 5 µg/ml cGAMP or Lipofectamine2000-transfected HT-DNA (5 µg/ml) for 8 hours. Culture supernatants were collected for luciferase quantification by luminometry. Cells were harvested for qRT-PCR analysis using primers specific for the endogenous MxA ISG and for flow cytometry for GFP expression. Transduction with the VprF34I-P35N or VprQ65R vector did not suppress cGAMP or HT-DNA stimulated IFIT1 reporter gene activation or MxA induction. Interestingly, VprR80A suppressed IFIT1 reporter activation, as well as *MxA* gene induction, to a similar extent as wild type Vpr (Fig. 4.2A, B, D). Flow cytometry showed equivalent levels of transduction with the empty vector or Vpr encoding vectors (Fig. 4.2C, E).

Next, the activity of Vpr proteins against IRF3 nuclear translocation was tested. THP-1 cells were differentiated into adherent macrophage-like cells with PMA (50ng/ml) for 72 hours. Cells were then treated with empty vector, WT Vpr vector or mutant Vpr vector (1 URT/ml) in the presence or absence of cGAMP (5 µg/ml), HT-DNA (1 µg/ml) or polyI:C (0.5 µg/ml) for 3 hours. Cells were fixed with PFA and stained for IRF3. DAPI was used to stain the nuclei. Immunofluorescence images were taken using the Hermes WiScan Cell Imaging System. Nuclear:cytoplasmic ratios of IRF3 immunostaining were represented as a translocation coefficient by quantitation of IRF3 signal intensities inside and outside the nucleus at the single cell level. cGAMP, HT-DNA or poly I:C stimulation increased the IRF3 nuclear translocation in cells treated with or without the empty vector (Fig. 4.3A, C, E). WT Vpr or VprR80A inhibited the cGAMP, HT-DNA or poly I:C activated increase in IRF3 nuclear translocation (Fig. 4.3A, C, E). In contrast, VprF34I+P35N or VprQ65R did not inhibit the increase in IRF3 nuclear translocation activated with cGAMP, HT-DNA or poly I:C (Fig. 4.3A, C, E). Further analysis by setting the translocation coefficient threshold at 0.5 (red line) showed that cGAMP, HT-DNA or poly I:C stimulation resulted in IRF3 nuclear translocation in approximately 15-20% cells treated with or without the empty vector and WT Vpr or VprR80A decreased IRF3 positive nuclei to $\leq$ 5% (Fig. 4.3B, D, F). In contrast, VprF34I+P35N or VprQ65R did not decrease the number of IRF3 positive nuclei (Fig. 4.3B, D, F). Taken together, these results demonstrated that cell cycle arrest and inhibition of innate immune activation are genetically separable functions of Vpr. Furthermore, it suggests that Vpr interaction with its cofactor DCAF1 and other proposed cellular targets

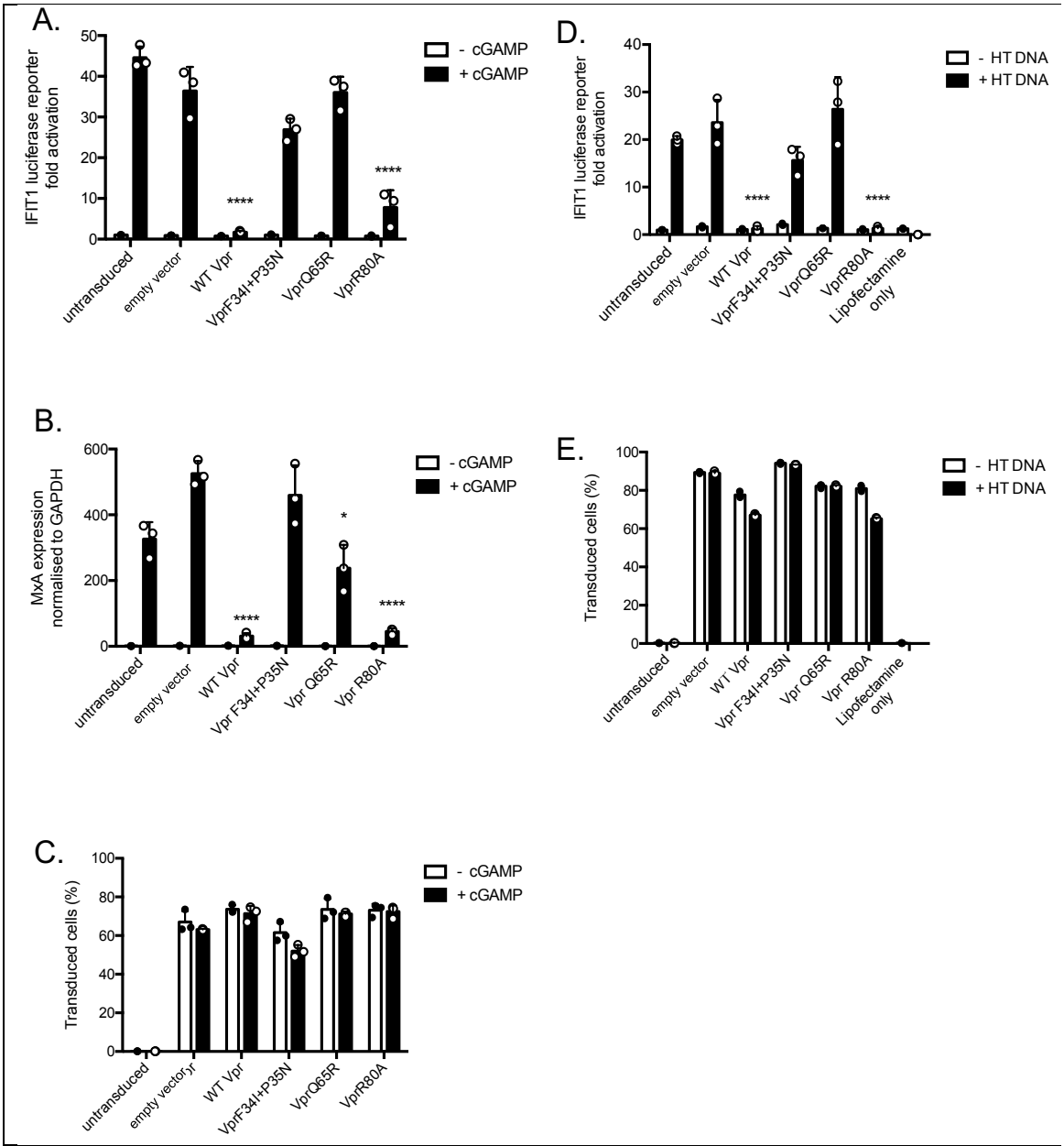


**Figure 4.2 Vpr suppresses ISG expression independently of cell cycle arrest**

**(A)** Fold induction of IFIT1-Luc after activation of STING by cGAMP (5 µg/ml) and expression of WT or mutant Vpr from a lentiviral vector, or empty vector or in untransduced IFIT1-Luc reporter THP-1 cells. **(B)** Fold induction of *MxA* after activation of STING by cGAMP (5 µg/ml) and expression of WT or mutant Vpr from a lentiviral vector, or after transduction by empty vector or in untransduced THP-1 cells. **(C)** Percentage of THP-1 cells from (A and B) transduced by the vector encoding WT or mutant Vpr and GFP or GFP alone (empty vector) treated with cGAMP (5 µg/ml) or left untreated as a control. **(D)** Fold induction of IFIT1-Luc after HT-DNA transfection (5 µg/ml) and expression of WT or mutant Vpr from a lentiviral vector, or empty vector or in untransduced IFIT1-Luc reporter THP-1 cells. **(E)** Percentage of THP-1 cells from (D) transduced by the vector encoding WT or mutant Vpr and GFP or GFP alone (empty vector) transfected with (5 µg/ml) or left untransfected as a control. Error bars represent standard deviation of biological repeats (n=3). Each experiment is representative of three independent experiments. Data were analysed using two-way ANOVA test. Stars (*) represent statistical significance: * ($p<0.05$), ** ($p<0.01$), *** ($p<0.001$), **** ($p<0.0001$) compared to empty vector.

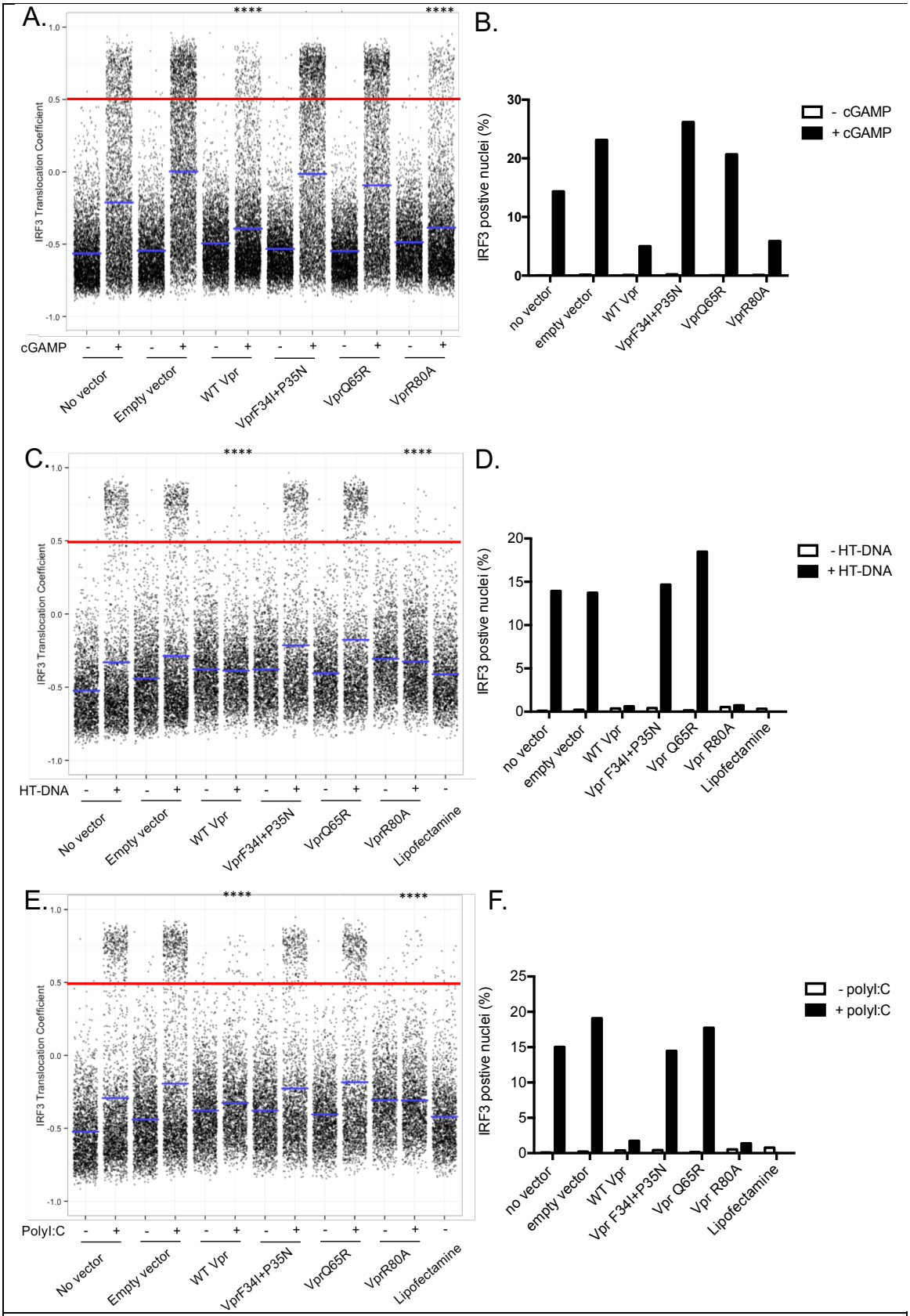


**Figure 4.3 Vpr blocks IRF3 nuclear translocation independently of the cell cycle arrest**

**(A), (C), (E)** Single cell measurement of IRF3 nuclear translocation in PMA differentiated THP-1 cells stimulated with **(A)** cGAMP (5 µg/ml), **(C)** HT-DNA transfection (5 µg/ml) or **(E)** poly I:C (0.5 µg/ml) transfection or left unstimulated and infected with empty vector, WT or mutant Vpr encoding vector or left uninfected. **(B), (D), (F)** Number of cells with translocation

coefficient of greater than 0.5 plotted as a percentage from (A), (C) and (E). Red line shows the translocation coefficient threshold. Blue lines represent mean translocation coefficient. Error bars represent standard deviation. Each experiment is representative of three independent experiments. Data were analysed using Unpaired Student's T tests. Stars (*) represent statistical significance: * ($p<0.05$), ** ($p<0.01$), *** ($p<0.001$), **** ($p<0.0001$).

such as cyclophilin A or importin-α may be essential for its function in innate immune antagonism.

To further confirm the requirement of DCAF1 for Vpr-mediated antagonism of innate signalling, activity of Vpr was investigated in DCAF1 depleted pIFIT1-Gluc THP-1 cells. A control or DCAF1-targeting short hairpin RNA (shRNA) was expressed in THP-1 cells by lentiviral transduction for 72 hours. Cells were then selected with 1 µg/ml Puromycin for 48 hours. After selection cells were transduced with an empty or a Vpr expressing lentiviral vector at MOI 0.25, 0.5 or 1 for 40 hours and then stimulated with 5 µg/ml cGAMP for 8 hours. Culture supernatants were collected for luciferase quantification by luminometry. The cells were fixed with PFA and analysed by flow cytometry for GFP expression. Transduction of cells expressing the control shRNA with Vpr expressing vector resulted in a dose dependent decrease in cGAMP activation of the IFIT1 luciferase reporter compared to the empty vector transduced cells (Fig 4.4A). In contrast, transduction of cells expressing the DCAF1 shRNA with Vpr expressing vector had no effect on cGAMP activation of the IFIT1 luciferase reporter compared to the empty vector transduced cells (Fig 4.4A). Importantly, flow cytometry results showed that both cell types were transduced to the same level by empty vector or Vpr expressing vector (Fig 4.4B). Immunoblotting was performed to confirm DCAF1 protein depletion (Fig 4.4C). This data further supports the mutational analysis of Vpr and confirms the requirement of DCAF1 for antagonism of innate immune signalling by Vpr, suggesting ubiquitination of a Vpr cellular target and its degradation via the proteasome.

## 4.2 Virion delivered Vpr is sufficient for suppression of cGAMP activated IFIT1 luciferase reporter

To investigate whether virion delivered Vpr can inhibit cGAMP activation of ISGs, HIV-1 virus-like particles (VLPs) which do not contain a genome were used. Empty VLPs were made in HEK293T cells by transfecting the p8.91 packaging plasmid and the VSV-glycoprotein envelope plasmid (pMDG). To produce Vpr VLPs (Vpr bearing HIV-1 particles) pcDNA3.1 plasmid expressing Vpr was used in addition to the p8.91 and pMDG. Monocytic pIFIT1-Gluc THP-1 cells were stimulated with cGAMP (5 µg/ml) and infected with empty or WT Vpr VLP (1URT/ml). After 6, 8 or 24 hours supernatants were collected

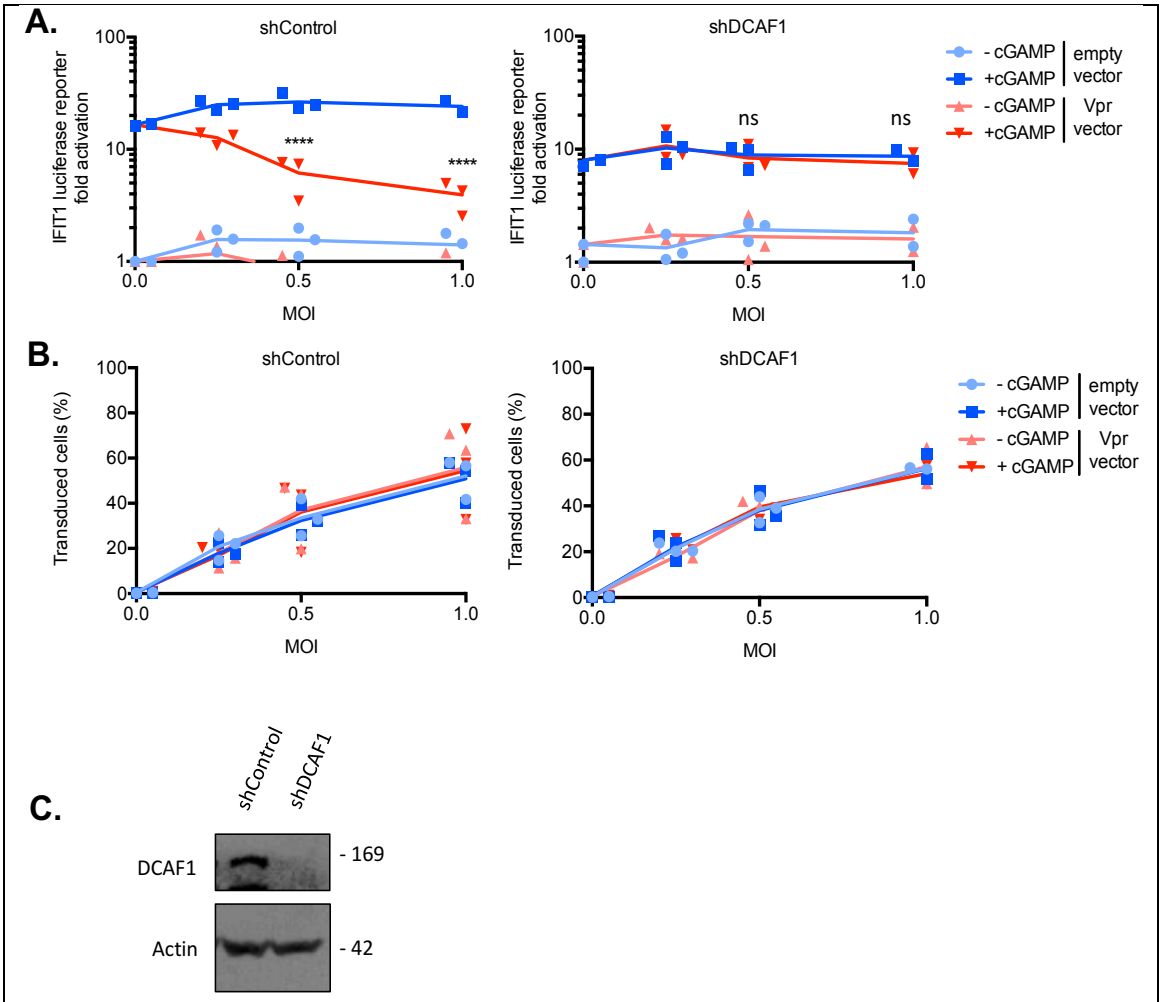


**Figure 4.4 Vpr suppresses ISG expression in a DCAF1 dependent manner**

**(A)** Fold induction of IFIT1-Luc after activation of STING by cGAMP (5 µg/ml) and expression of Vpr from a lentiviral vector, or empty vector, or in untransduced IFIT1-Luc reporter THP-1 cells expressing a control, or a DCAF1 targeting shRNA. **(B)** Percentage of THP-1 cells from (A) transduced by the vector encoding Vpr and GFP or GFP alone (empty vector) treated with cGAMP (5 µg/ml) or left untreated. **(C)** Immunoblot detecting DCAF1, and actin as a loading control, from extracted THP-1 cells expressing a control or DCAF1-targeting shRNA. Size markers are shown (kDa). Dots in the graphs represents biological repeats (n=3). Data were analysed using two-way ANOVA test. Stars (*) represent statistical significance: * ($p<0.05$), ** ($p<0.01$), *** ($p<0.001$), **** ($p<0.0001$) compared to empty vector.

and luciferase activity was quantified by luminometry (Fig. 4.5A). cGAMP stimulation resulted in 200-fold activation of the IFIT1 luciferase reporter after infection by the empty VLP. However, Vpr bearing VLP infection inhibited the IFIT1 luciferase reporter activation by 20-fold after 6 and 8 hours (Fig. 4.5A). Twenty four hours after Vpr bearing VLP infection the reporter activation recovers and only 5-fold difference is observed compared to empty VLP infection (Fig. 4.5A). This is likely due to degradation of incoming Vpr by the cellular degradation machinery.

Next the activity of Vpr mutants was tested in this assay. Consistent with previous results, VLP carrying the cell cycle arrest mutant, VprR80A, had the same effect as VLP bearing WT Vpr and inhibited IFIT1 luciferase reporter activation to the same degree (Fig. 4.5B). In contrast, VLPs containing VprF34I+P35N or VprQ65R did not inhibit the IFIT1 luciferase reporter activation as effectively (Fig. 4.5B). The incorporation of Vpr proteins into VLPs was confirmed by immunoblotting and all Vpr mutants showed similar levels suggesting that the differential effects of Vpr proteins were not due to varying incorporation (Fig. 4.5C). Overall, these results demonstrated that virion delivered Vpr is sufficient for suppression of cGAMP-activated IFIT1 luciferase reporter.

## 4.3 Localisation of Vpr to the nuclear envelope correlates with suppression of ISG expression

Given that the WT Vpr and various Vpr mutants suppressed innate signalling to different extents, the localisation of wild type Vpr was compared with the different Vpr mutants. HeLa cells were transfected with flag-tagged wild type or mutant Vprs. Cells were fixed after 24 hours and stained for immunofluorescence microscopy using antibodies against the flag-tag (green) and nuclear pore complex proteins (Mab414) (red). Nuclei were visualised by DAPI staining (blue). Wild type Vpr localised exclusively to the nucleus (Fig. 4.6A) and showed clear nuclear rim staining (Fig. 4.6B). Vpr mutants that lacked the ability to block immune signalling, VprF34I+P35N and VprQ65R, lost the nuclear rim localisation and showed diffuse cytoplasmic staining (Fig. 4.6A, B). The cell cycle arrest mutant, VprR80A, localised only to the nucleus and showed significant nuclear rim accumulation similar to the WT Vpr (Fig. 4.6A, B), further supporting the notion that the ability of Vpr to suppress innate signalling is independent of the cell cycle arrest function of Vpr. These observations showed a correlation between nuclear envelope localisation of Vpr and its function in inhibiting innate immune signalling, suggesting that Vpr may interact with proteins at the nuclear envelope to disable IRF3 and NF-κB (p65) activation or nuclear translocation thereby suppressing innate immune activation.

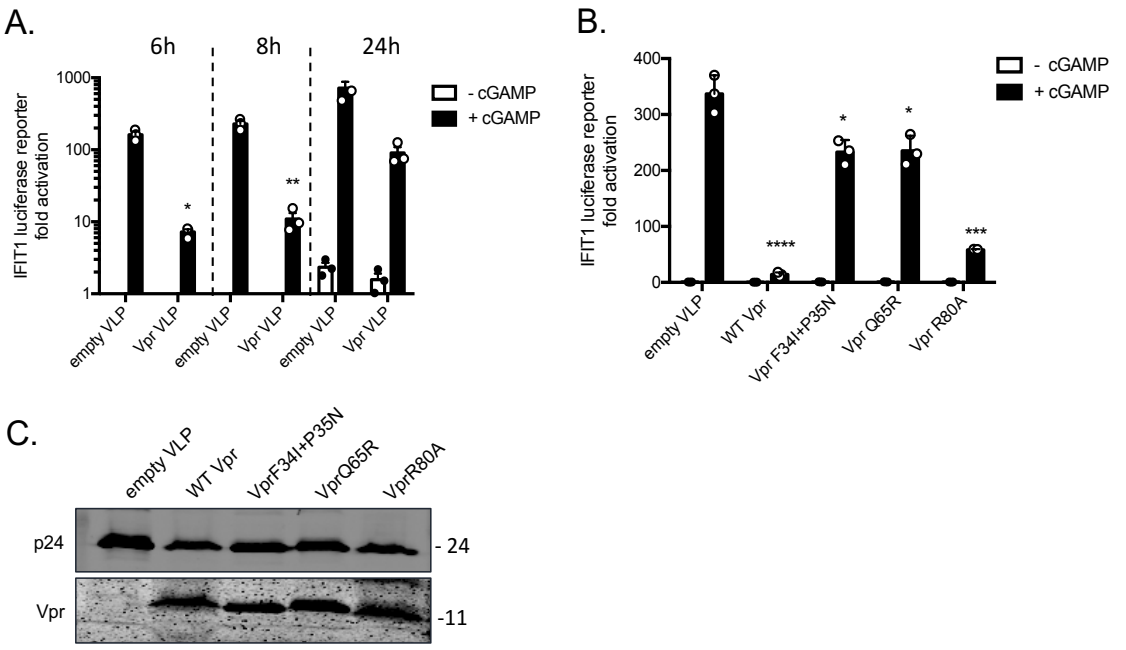


**Figure 4.5 Virion delivered Vpr is sufficient for suppression of ISG expression**

**(A)** Fold induction of IFIT1-Luc after activation of STING by cGAMP (5 µg/ml) and infection with WT Vpr bearing VLP or empty VLP in IFIT1-Luc reporter THP-1 cells. **(B)** Fold induction of IFIT1-Luc after activation of STING by cGAMP (5 µg/ml) and infection with WT or mutant Vpr bearing VLP, or empty VLP in IFIT1-Luc reporter THP-1 cells. **(C)** Immunoblot detecting p24 (capsid) and Vpr in VLPs. Size markers are shown (kDa). Error bars represent standard deviation of biological repeats (n=3). Each experiment is representative of two independent experiments. Data were analysed using two-way ANOVA test. Stars (*) represent statistical significance: * ($p<0.05$), ** ($p<0.01$), *** ($p<0.001$), **** ($p<0.0001$) compared to empty vector.

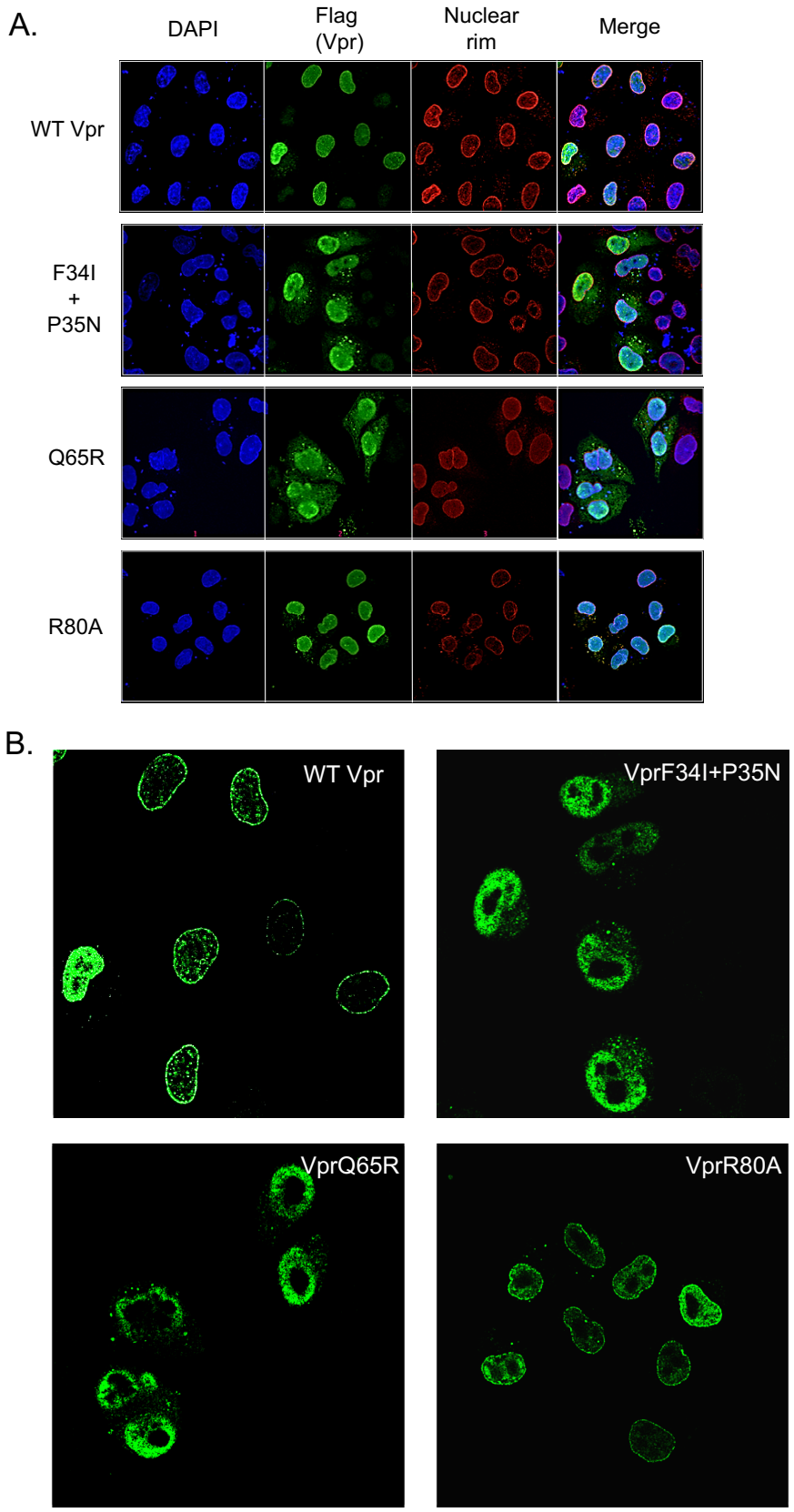


**Figure 4.6 Localisation of Vpr to the nuclear envelope correlates with suppression of ISG expression**

**(A)** Immunofluorescence images of HeLa cells transfected with 50ng of flag-tagged WT or a mutant Vpr expressing pcDNA3.1 plasmid using antibodies against the flag-tag (green) and nuclear pore complex (mab414) (red). **(B)** z-section of cells in (a) showing nuclear rim accumulation of Vpr.

## 4.4 Nup358 is not required for Vpr antagonism of innate immune activation

Given the localisation of Vpr to the nuclear rim and previous reports of Vpr being a cyclophilin A binding protein (476), it was hypothesised that Vpr may interact with cyclophilin A or cyclophilin-like domain containing proteins to block IRF3 and NF-κB (p65) activation. Unpublished data from the lab showed that cyclophilin A was not involved in innate immune signalling pathways and did not interact with Vpr. Nucleoporin 358 (Nup358) is a nuclear pore complex protein that has been implicated in HIV-1 infection (81) and contains a cyclophilin-like domain, therefore, the role of Nup358 as a Vpr target or cofactor was explored.

First the localisation of Vpr was investigated in Nup358 depleted cells by immunofluorescence microscopy. An empty vector or flag-tagged Vpr vector was transfected into HeLa cells previously stably transduced with a control shRNA or shRNA targeting Nup358. Cells were fixed after 24 hours and stained for immunofluorescence using antibodies against the flag-tag (green) and nuclear pore complex proteins (red). Nuclei were visualised by DAPI staining (blue). Depleting Nup358 did not alter the localisation of Vpr as Vpr localised to the nucleus (Fig. 4.7A) and showed significant nuclear rim accumulation (Fig. 4.7B) in cells treated with shRNA targeting Nup358. Nup358 depletion was confirmed by immunoblotting (Fig. 4.7C). This result demonstrated that Vpr did not use Nup358 to localise to the nucleus.

Next, the role of the Nup358 cyclophilin domain in various signalling pathways was probed. THP-1 cells in which the cyclophilin domain of Nup358 was deleted by insertion of a stop codon using CRISPR/Cas9 were obtained (Torsten Schaller – Heidelberg University). WT or two clones with deleted Nup358 cyclophilin domain (Nup358ΔCyp) were stimulated with LPS (1 µg/ml), TNFα (250 ng/ml) or cGAMP (5 µg/ml). After 24 hours RNA was extracted from the cells, cDNA was synthesised and used for qRT-PCR analysis using primers specific for *IL-8, IκBα and IFIT1*. Gene expression was normalised to the housekeeping gene *GAPDH*. The results showed that deletion of the Nup358 cyclophilin domain did not inhibit expression of *IFIT1* (Fig. 4.8A)*, IL-8* (Fig. 4.8B) *or IκBα* (Fig. 4.8C) when stimulated with LPS, TNFα or cGAMP, demonstrating that the Nup358 cyclophilin domain is not required for gene activation downstream of these stimuli.

Overall, the localisation of Vpr to the nuclear rim in Nup358 depleted cells and lack of a role for Nup358 cyclophilin domain in activating ISG or proinflammatory gene expression indicated that Nup358 was unlikely to be involved in Vpr-mediated suppression of ISGs.

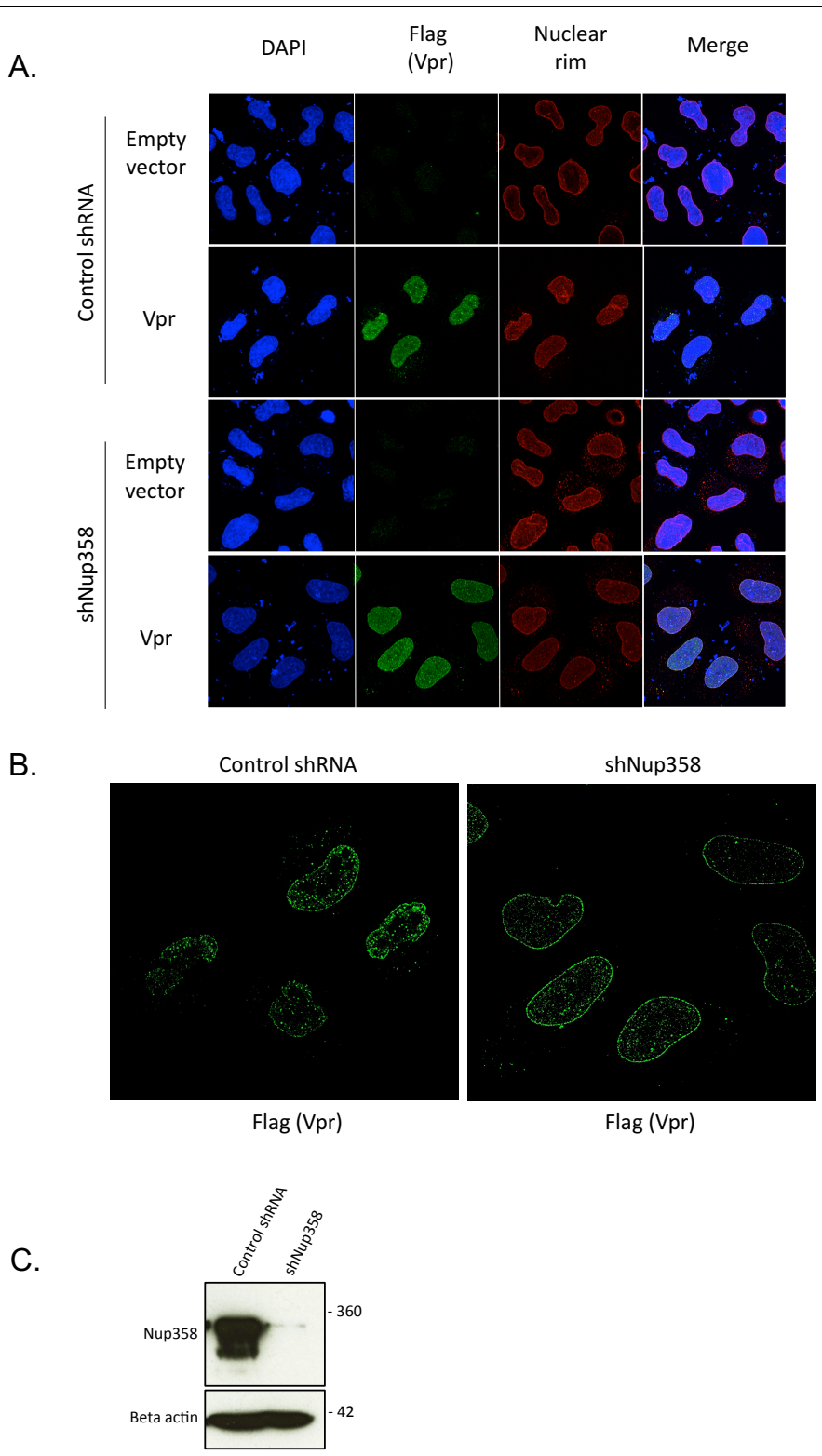


**Figure 4.7 Nup358 depletion does not affect localisation of Vpr**

**(A)** Immunofluorescence images of HeLa cells expressing a control or Nup358 targeting shRNA transfected with empty vector or flag-tagged Vpr expressing pcDNA3.1 plasmid using antibodies against the flag-tag (green) and the nuclear pore complex (mab414) (red). **(B)** z-section of cells from (A) showing nuclear rim accumulation of Vpr. **(C)** Immunoblot detecting Nup358 and actin as a loading control from extracted Hela cells expressing a control or Nup358 targeting shRNA (A). Expression of Nup358 in HeLa cells expressing a control or Nup358 targeting shRNA. Size markers are shown (kDa).

## 4.5 TNPO3 is required for PRR signalling activated with various stimuli

TNPO3 is an HIV-1 cofactor that belongs to the β-karyopherin family of proteins (527). It imports proteins such as CPSF6 that contain RS domains (Arg-Ser rich sequence) (90). Several studies have reported interaction of Vpr with importins (471,505,506). Given that the Vpr importin binding mutant did not localise to the nuclear rim (Fig.4.6) and did not inhibit innate immune activation (Fig. 4.2), it was hypothesised that TNPO3 may play a role in Vpr mediated suppression of innate signalling. To test this hypothesis, pIFIT1-GLuc THP-1 cells were transduced with a control or a TNPO3 targeting shRNA for 72 hours. After 48 hours of puromycin (1 µg/ml) selection TNPO3 knockdown was confirmed by immunoblotting (Fig. 4.9B). Cells were then stimulated with cGAMP (5 µg/ml), Sendai virus (200HAunits/ml) or LPS (1µg/ml). Supernatants were collected after 8 hours and luciferase activity was quantified by luminometry. cGAMP or Sendai virus stimulation of TNPO3 depleted cells resulted in about 4-fold less IFIT1 reporter activation compared to the control cells (Fig. 4.9A). Similarly, LPS stimulation gave 10-fold less IFIT1 luciferase reporter activation in TNPO3 depleted cells than in control cells (Fig. 4.9A). This suggested that TNPO3 may play a role in ISG induction downstream of various PRR stimuli.

To identify the step in the innate signalling cascade at which TNPO3 was required, activation of key signalling proteins, TBK1 and IRF3, was probed by immunoblotting. Wild type or TNPO3-depleted monocytic THP-1 cells were stimulated with 5, 2.5 or 1.25 µg/ml HT-DNA. After 3 hours cells were harvested in cell lysis buffer, the proteins were separated by SDS-PAGE and immunoblotted with antibodies against phospho-TBK1, TBK1, phospho-S386-IRF3 and IRF3. Luciferase was quantified by luminometry after 8 hours. Immunoblotting showed that TNPO3 depletion had no effect on total or phosphorylated TBK1 or IRF3 when stimulated with HT-DNA (Fig. 4.9C). This suggested that TNPO3 was acting downstream of IRF3 phosphorylation.

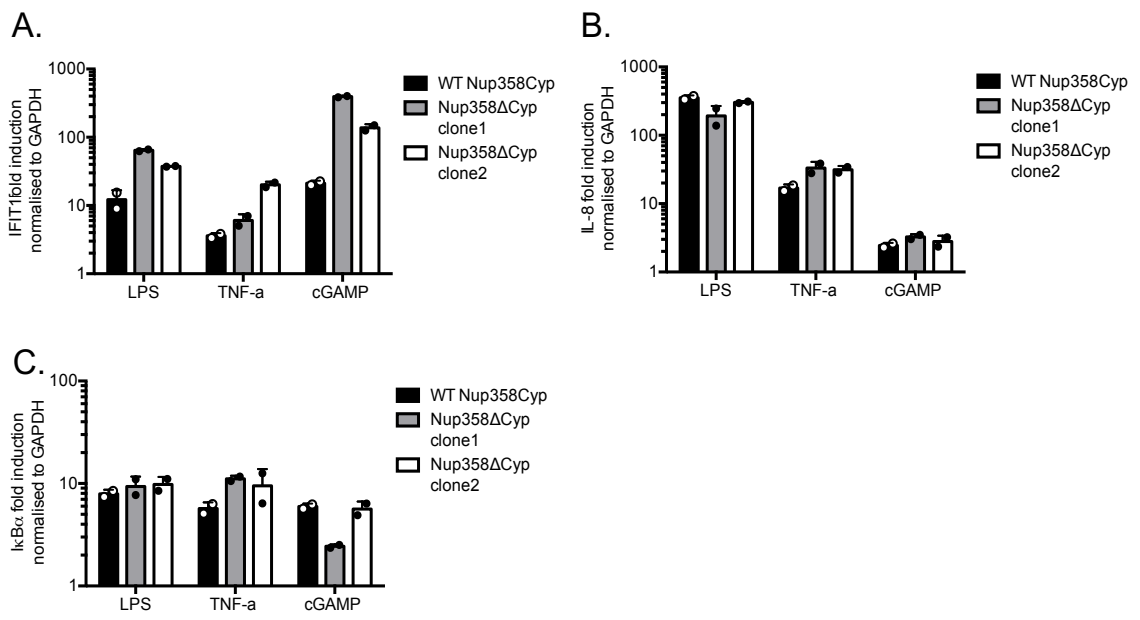


**Figure 4.8 Deleting the Cyp-like domain in Nup358 does not prevent ISG or proinflammatory gene expression**

**(A), (B), (C)** Fold induction of **(A)** *IFIT1*, **(B)** *IL-8*, and **(C)** *IκBα* genes after LPS (1µg/ml), TNFα (250ng/ml) or cGAMP (5µg/ml) treatment of WT or Nup358ΔCyp THP-1 cells. Error bars represent standard deviation of biological repeats (n=3).

To test whether TNPO3 was involved in nuclear import of IRF3 or NF-κB (p65) an immunofluorescence based assay was used to quantify nuclear translocation of these proteins at the single cell level. THP-1 cells stably expressing a control or TNPO3 targeting shRNA were differentiated into adherent macrophage-like cells with PMA (50 ng/ml) for 72 hours. Cells were then stimulated with a dose range of cGAMP, HT-DNA or Poly I:C for 3 hours. Cells were fixed with PFA and stained for IRF3 and NF-κB (p65). DAPI was used to stain the nuclei. Immunofluorescence images were taken using the Hermes WiScan Cell Imaging System. Nuclear:cytoplasmic ratios of immunostaining were measured at a single cell level by quantitation of IRF3 or NF-κB (p65) signal intensities inside and outside the nucleus and represented as translocation coefficient. cGAMP or HT-DNA stimulation resulted in IRF3 nuclear translocation in a dose dependent manner in control cells however TNPO3 depletion resulted in about a 2-fold decrease in IRF3 nuclear translocation (Fig. 4.10). Similarly, TNPO3 depletion decreased NF-κB (p65) nuclear translocation in response to HT-DNA or Poly I:C stimulation compared to the control cells (Fig. 4.11). This suggested that TNPO3 may be involved in innate signalling pathways at the level of IRF3 and NF-κB (p65) nuclear translocation.

## 4.6 Vpr does not degrade or alter TNPO3 function

Given that TNPO3 played a role in innate signalling pathways at the level of IRF3 and NF-κB (p65) nuclear translocation and Vpr blocked the nuclear translocation of IRF3 and NF-κB (p65), it was hypothesised that Vpr may target TNPO3 for degradation to block IRF3 and NF-κB (p65) nuclear translocation. To address this hypothesis, expression of endogenous TNPO3 protein was investigated in 293T cells transfected with a Vpr expressing pcDNA3.1 plasmid. After 24 hours of Vpr expression cells were lysed and subjected to SDS-PAGE and immunoblotted for TNPO3. Immunoblot analysis showed that Vpr expression did not reduce TNPO3 protein level (Fig. 4.12A) suggesting that Vpr did not target TNPO3 for degradation to block IRF3 or NF-κB (p65) nuclear translocation.

To explore the possibility that Vpr may modulate TNPO3 functions without targeting it for degradation, localisation of CPSF6 in the presence or absence of Vpr was quantified by immunofluorescence. CPSF6 is a SR-protein that contains a RS-domain (90). The RS-domain is thought to be phosphorylated and allows TNPO3 to transport CPSF6 from the cytoplasm to the nucleus (90). To address this, THP-1 cells were differentiated into adherent macrophage-like cells with PMA (50 ng/ml) for 72 hours. Cells were then stimulated with cGAMP (5 µg/ml) and treated with an empty or a Vpr bearing VLP (1URT/ml) for 3 hours. Cells were fixed with PFA and stained for IRF3 and CPSF6. DAPI

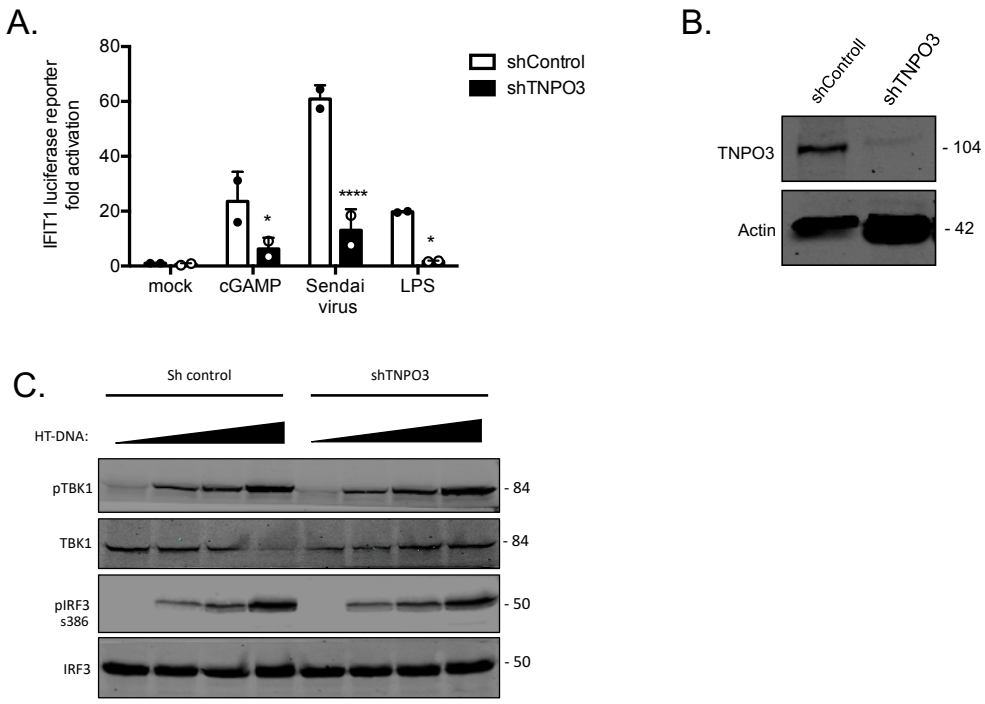


**Figure 4.9 TNPO3 depletion inhibits ISG expression downstream of various innate immune agonists**

**(A)** Fold induction of IFIT1-Luc after cGAMP (5 µg/ml), Sendai virus (200HAunits/ml) or LPS (1µg/ml) stimulation of IFIT1-Luc reporter THP-1 cells expressing a control or TNPO3 targeting shRNA. **(B)** Immunoblot detecting TNPO3 and actin as a loading control from extracted IFIT1-Luc reporter THP-1 cells expressing a control or TNPO3 targeting shRNA. **(C)** Immunoblot detecting phospho-TBK1 (Ser172), total TBK1, phosphor-IRF3 (Ser386) and total IRF3 from extracted THP-1 cells stimulated with HT-DNA transfection. Error bars represent standard deviation of biological repeats (n=2). Each experiment is representative of two independent experiments. Data were analysed using two-way ANOVA test. Stars (*) represent statistical significance: * ($p<0.05$), ** ($p<0.01$), *** ($p<0.001$), **** ($p<0.0001$) compared to empty vector.

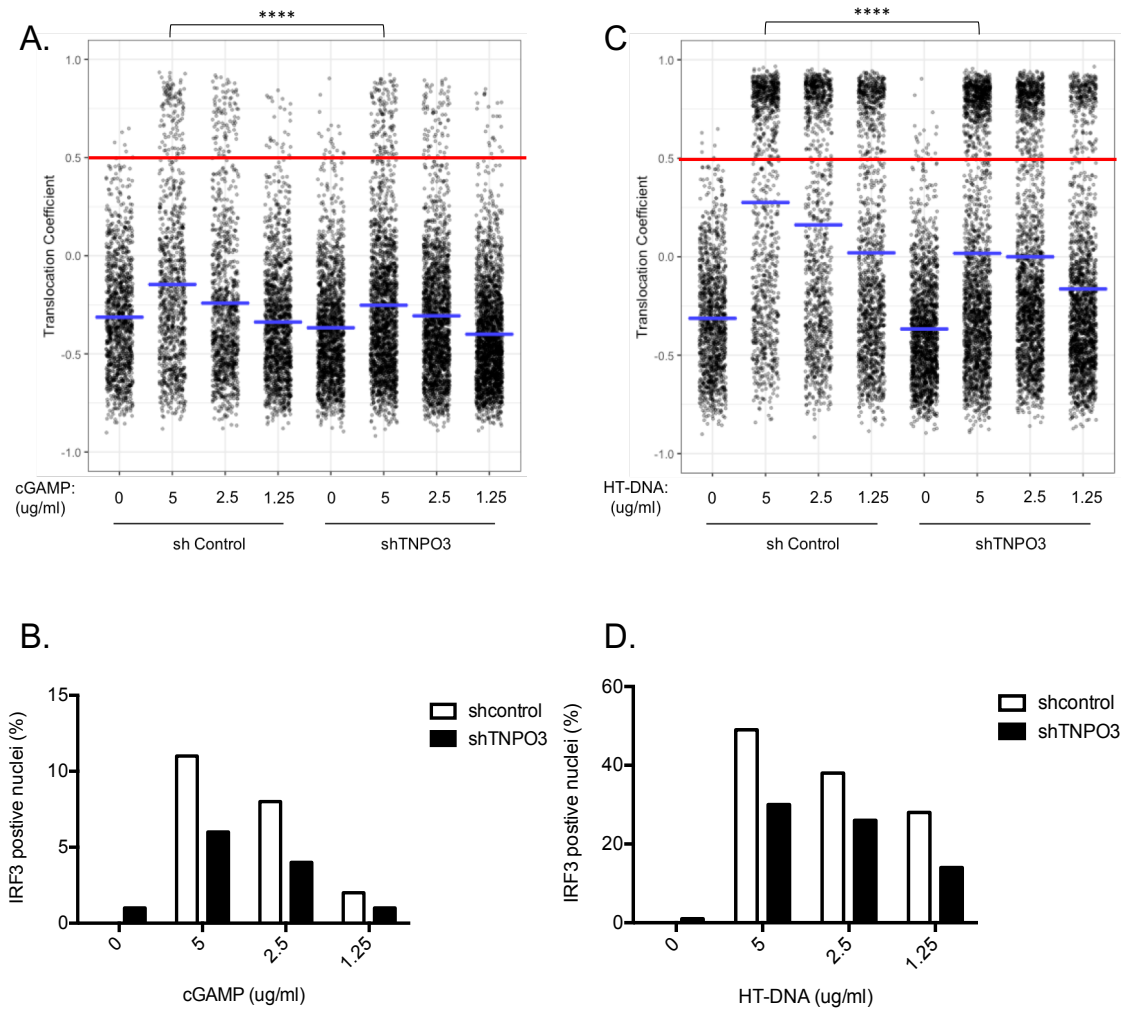


**Figure 4.10 TNPO3 depletion inhibits nuclear translocation of IRF3**

Single cell measurement of IRF3 nuclear translocation in PMA differentiated THP-1 cells expressing a control or TNPO3 targeting shRNA and treated with three doses of **(A)** cGAMP or **(C)** HT-DNA or left untreated. **(B), (D)** Number of cells from (A) and (C) with translocation coefficient of greater than 0.5 were plotted as a percentage. Red line shows the translocation coefficient threshold. Blue lines represent mean translocation coefficient. Data were analysed using Unpaired Student's T tests. Stars (*) represent statistical significance: * ($p<0.05$), ** ($p<0.01$), *** ($p<0.001$), **** ($p<0.0001$).

was used to stain the nuclei. Immunofluorescence images were taken using the Hermes WiScan Cell Imaging System.

Nuclear:cytoplasmic ratios of immunostaining were measured at a single cell level by quantitation of IRF3 or CPSF6 signal intensities inside and outside the nucleus and represented as a translocation coefficient. (Fig. 4.12B) shows representative images of CPSF6 staining. CPSF6 was found almost exclusively in the nucleus and this was not altered by Vpr, with or without cGAMP stimulation (Fig. 4.12C, D). However, Vpr was able to inhibit IRF3 nuclear translocation downstream of cGAMP stimulation (Fig. 4.12E, F). These results suggest that although TNPO3 has a role in nuclear import of IRF3 and NF-κB (p65) downstream of different innate immune stimuli, Vpr may not target TNPO3 to block IRF3 and NF-κB (p65) nuclear translocation.

## 4.7 Summary

This section summarises the data presented in this chapter. Figure 4.13 illustrates the data in a schematic diagram. A genetics approach was taken to further characterise Vpr-mediated suppression of innate immune activation. Mutations were introduced in WT Vpr to prevent its interactions with known cellular proteins. Vpr has been well characterised for its cell cycle arrest function. To determine whether Vpr suppressed innate immune activation and arrested cell cycle by the same mechanism, activity of the cell cycle arrest mutant VprR80A was tested against innate immune activation. VprR80A was found to be able to inhibit ISG expression (Fig 4.2 A) and block IRF3 nuclear translocation downstream of different innate immune stimuli just like the WT Vpr (Fig. 4.3). This demonstrated that the cell cycle arrest and suppression of innate immunity are two independent functions of Vpr. Vpr interacts with DCAF1 and hijacks the Cul4 E3 ligase complex to target cellular proteins for proteasomal degradation. The VprQ65R mutant was used to abrogate Vpr interaction with DCAF1. In contrast to VprR80A, VprQ65R was unable to inhibit ISG induction (Fig 4.2 A) or IRF3 nuclear translocation (Fig 4.3). Furthermore, DCAF1 depletion prevented Vpr inhibition of ISGs (Fig. 4.4). A double mutation was introduced at residues F34 and P35 to abrogate interaction with importin-$\alpha$ or cyclophilin A. Like VprQ65R, Vpr F34I+P35N was also defective for suppressing innate immune activation (Fig 4.2 A). Altogether, this suggests that Vpr targets a cellular protein, possibly cyclophilin A or importin-$\alpha$, for proteasomal degradation by recruitment of the Cul4 E3 ubiquitin ligase complex via DCAF1 interaction.

Vpr is present in viral particles and mutations in Vpr can reduce its packaging. Immunoblotting of viral particles showed similar levels of incorporation by Vpr mutants

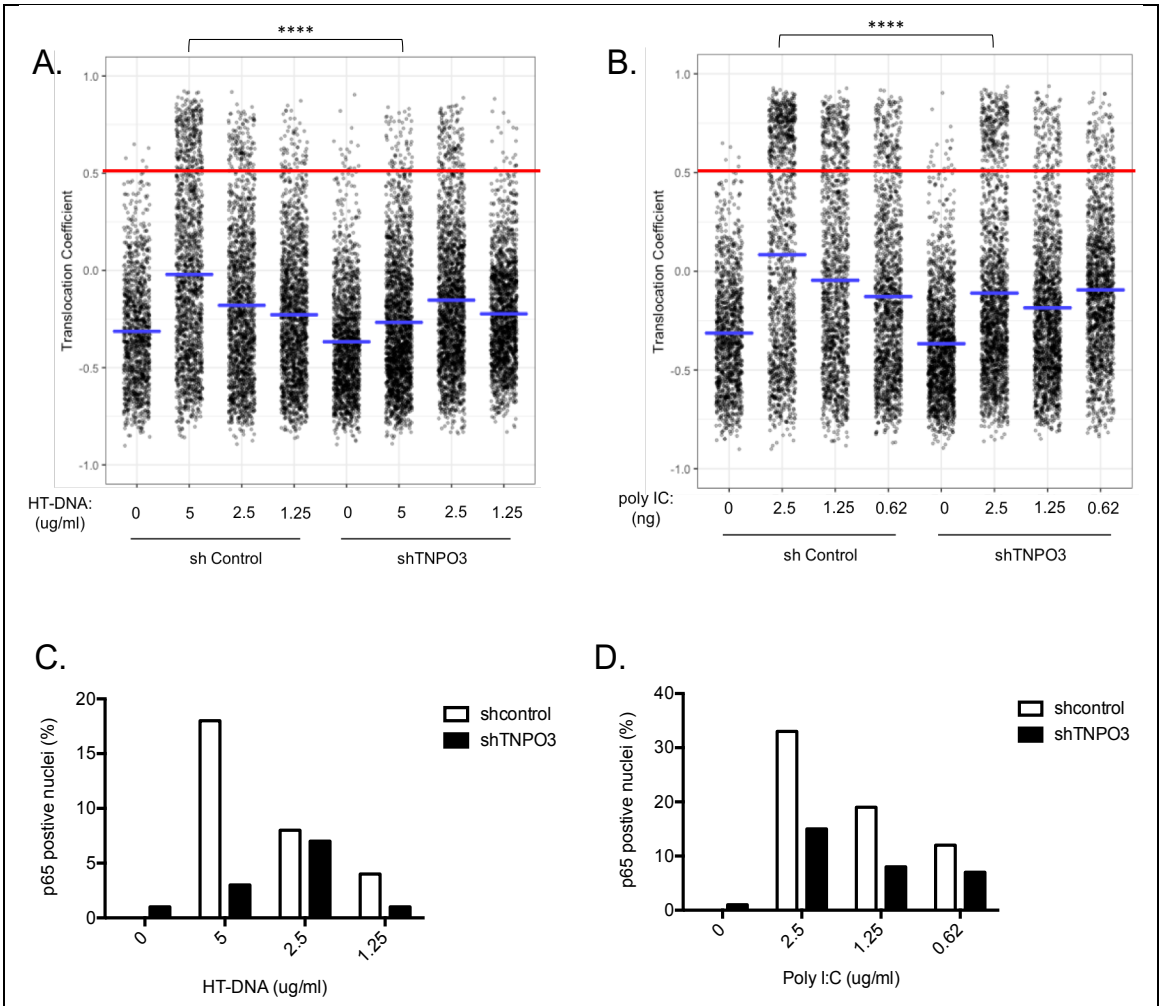


**Figure 4.11 TNPO3 depletion prevents nuclear translocation of p65**

Single cell measurement of NF-κB (p65) nuclear translocation in PMA differentiated THP-1 cells expressing a control or TNPO3 targeting shRNA and transfected with three doses of **(A)** HT-DNA, **(C)** poly I:C or left untransfected. **(B), (D)** Number of cells from (A) and (C) with NF-κB (p65) translocation coefficient of greater than 0.5 were plotted as a percentage. Red line shows the translocation coefficient threshold. Blue lines represent mean translocation coefficient. Data were analysed using Unpaired Student's T tests. Stars (*) represent statistical significance: * ($p<0.05$), ** ($p<0.01$), *** ($p<0.001$), **** ($p<0.0001$).

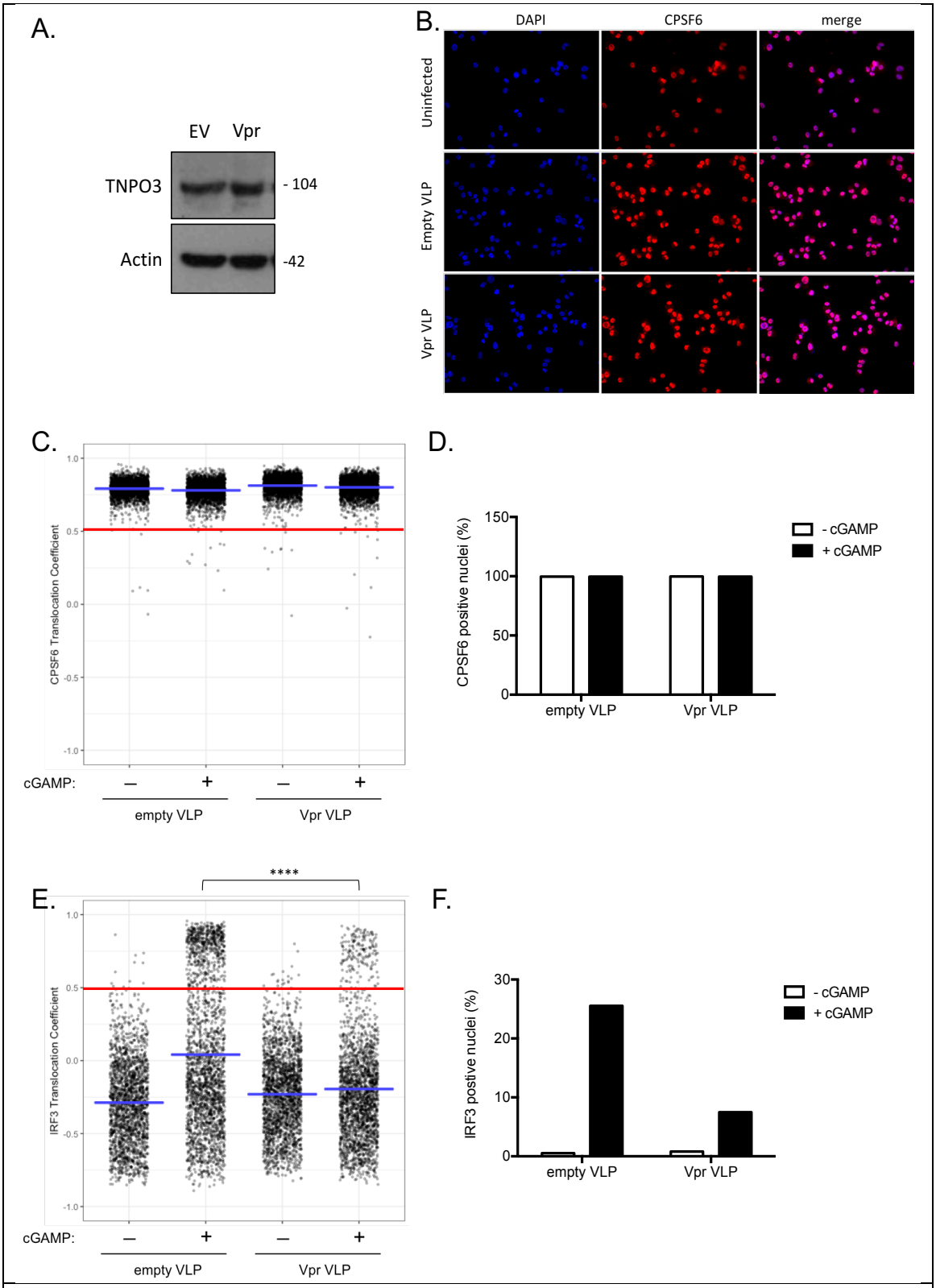


**Figure 4.12 Vpr does not degrade or alter TNPO3 function**

**(A)** Immunoblot detecting TNPO3 and actin as a loading control from extracted HEK293T cells transfected with empty vector or Vpr expressing pcDNA3.1 plasmid. Size markers are shown (kDa). **(B)** Immunofluorescence images showing CPSF6 localisation in PMA differentiated THP-1 cells infected with empty VLP, Vpr VLP or left uninfected. **(C)** Single cell measurement of CPSF6 nuclear translocation from cells in (B). **(D)** Number of cells in (B) with CPSF6 translocation coefficient of greater than 0.5 plotted as a percentage. **(E)** Single cell measurement of IRF3 nuclear translocation in PMA differentiated THP-1 cells stimulated with cGAMP (5 µg/ml) and infected with empty VLP or Vpr bearing VLP. **(F)**

Number of cells in (E) with IRF3 translocation coefficient of greater than 0.5 (red line) plotted as a percentage. Red line shows the translocation coefficient threshold. Blue lines represent mean translocation coefficient. Data were analysed using Unpaired Student's T tests. Stars (*) represent statistical significance: * ($p<0.05$), ** ($p<0.01$), *** ($p<0.001$), **** ($p<0.0001$).

(Fig. 4.5C). Consistent with Vpr expression data, virion delivered WT Vpr or VprR80A inhibited IFIT1 reporter activation whereas VprF34I+P35N or VprQ65R were unable to do so (Fig. 4.5B). Visualisation of Vpr by immunofluorescence microscopy revealed that Vpr proteins active against innate immune activation, WT and VprR80A, localised to the nucleus and showed significant nuclear rim accumulation (Fig. 4.6). On the other hand, VprF34I+P35N and VprQ65R which were defective for innate immune suppression lost nuclear rim accumulation and showed diffuse cytoplasmic and nuclear staining (Fig. 4.6). These results showed a correlation between nuclear rim accumulation of Vpr and inhibition of innate immune activation.

Given that localisation of Vpr to the nuclear rim correlates with its ability to inhibit innate immune activation and a Vpr-mediated block to nuclear translocation of transcription factors such as IRF3, the role of proteins involved in nuclear transport was investigated. Vpr has been shown to bind cyclophilin A and the cyclophilin A binding mutant Vpr was unable to localise to the nuclear rim or inhibit innate immune activation. Unpublished data from the lab showed that cyclophilin A was not involved in innate immune signalling pathways and did not interact with Vpr. A nuclear pore protein, Nup358, contains a cyclophilin-like domain. Nup358 is implicated in HIV-1 infection and present at the nuclear envelope like Vpr. Therefore, role of Nup358 in Vpr-mediated innate immune suppression was probed. Firstly, localisation of Vpr was investigated in Nup358-depleted cells by immunofluorescence microscopy which showed no impact on Vpr nuclear rim localisation (Fig. 4.7). Secondly, cells in which the Nup358 cyclophilin domain was deleted by CRISPR/Cas9 were tested for innate immune activation with various stimuli. Nup358ΔCyp cells were found to be competent for innate immune signalling (Fig. 4.8), suggesting that Vpr may not target Nup358 to suppress innate immune activation.

TNPO3 belongs to the β-karyopherin family of proteins and transport proteins that contain SR-domains such as CPSF6 (90). Depletion of TNPO3 inhibited activation of innate immunity downstream of various stimuli (Fig. 4.9A). Interestingly, TNPO3 depletion inhibited translocation of transcription factors such as IRF3 or NF-κB (p65) (Fig. 4.10, 4.11) without inhibiting IRF3 phosphorylation at S386 (Fig. 4.9C) suggesting that TNPO3 may play a role in nuclear import of IRF3 and NF-κB (p65). However, Vpr expression did not result in TNPO3 degradation (Fig. 4.12A) or a block to CPSF6 nuclear translocation (Fig. 4.12C, D) suggesting that although TNPO3 plays a role in IRF3 and NF-κB (p65) nuclear import, Vpr may not target TNPO3 to inhibit innate immune activation.

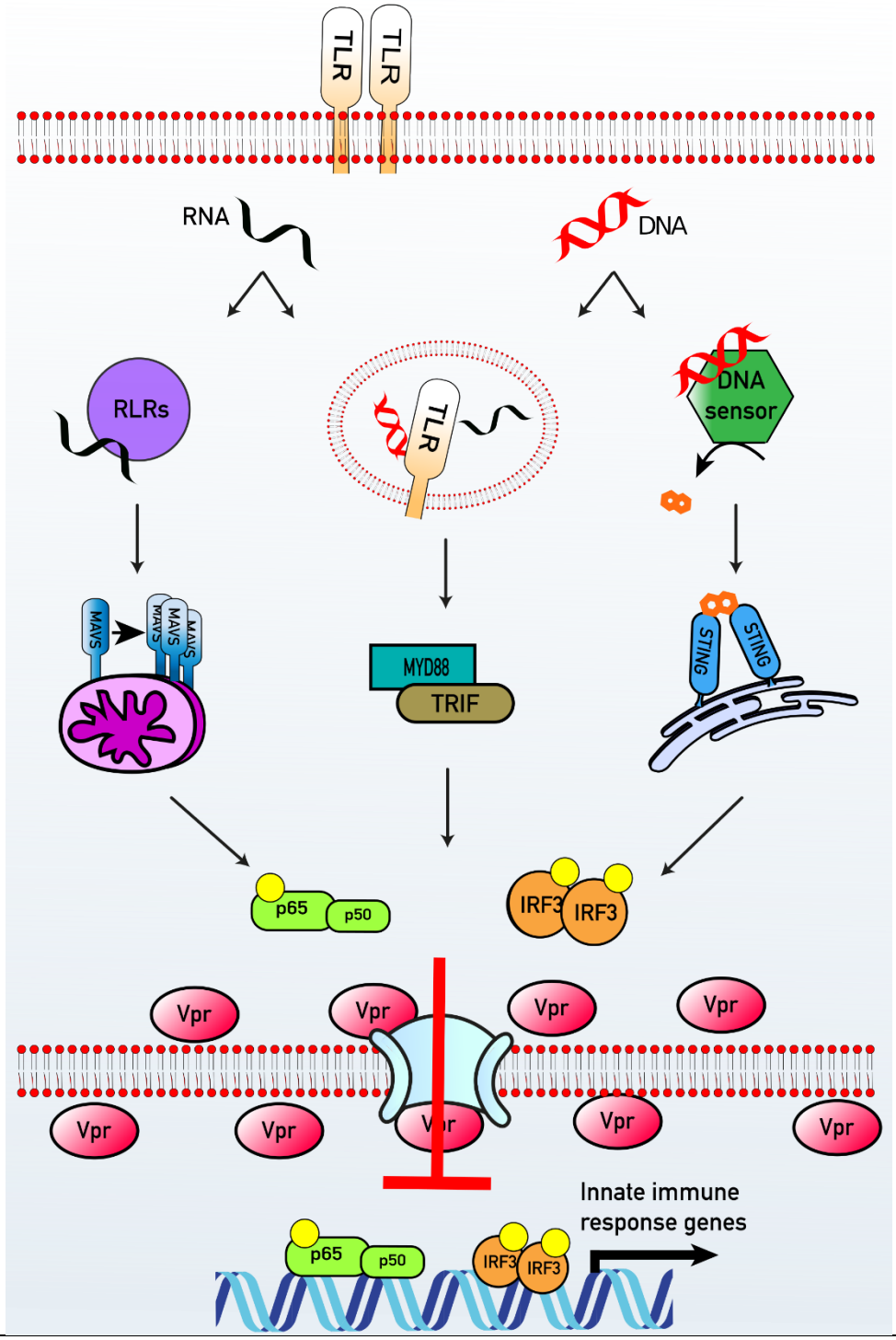


**Figure 4.13 A model for HIV-1 Vpr antagonism of innate immunity**

Activation of various pattern recognition receptors result in a signalling cascade that culminates in phosphorylation and activation of transcription factors such as IRF3 and NF-kB. Activated IRF3 and NF-κB translocate to the nucleus through the nuclear pore complex to activate ISGs and proinflammatory genes expression, respectively. HIV-1 Vpr localise to the nuclear pore complex and may recruit the DCAF1 E3 ubiquitin ligase to importin-α and target it for proteasomal degradation. This inhibits nuclear translocation of activated IRF3 and NF-κB and prevent activation of innate immune responses downstream of diverse pattern recognition receptors.

# 5 Chapter 5: HIV-1 Vpr suppresses expression from transfected plasmid DNA by blocking nuclear import of the plasmid

## 5.1 Vpr expression in 293T cells inhibits RNA expression from co-transfected cGAS and STING plasmids and subsequent suppression of the downstream signalling pathway

To further characterise the mechanism by which Vpr antagonises innate immune activation in a highly tractable and manipulatable system, dual luciferase assays were performed in HEK293T cells. (Fig. 5.1A). HEK293T cells do not express detectable levels of cGAS or STING proteins (Fig. 5.1B), therefore the cGAS and STING signalling pathway was reconstituted by exogenous transient expression of flag-cGAS and STING. To measure the activation of the pathway flag-cGAS alone or flag-cGAS with STING were co-transfected with IFNβ promoter driven firefly luciferase and constitutively expressed thymidine kinase (TK) renilla luciferase reporters. Cells were lysed in passive lysis buffer and the luminescence of each sample was measured after 48 hours. Expression of cGAS alone did not activate the IFNβ promoter driven firefly luciferase reporter, however, co-transfection of cGAS and STING activated the reporter by almost 100-fold (Fig. 5.1B). Antagonism of the cGAS and STING signalling pathway by Vpr was then determined by transfecting a codon optimised Vpr from an HIV-1 founder clone SUMA or empty vector with an NF-κB-sensitive immunoglobulin light chain kappa (Igκ) promoter firefly luciferase reporter and TK renilla luciferase reporter. At the same time cells were stimulated with empty vector or flag-cGAS and STING- transfection for 12, 24 or 48 hours. cGAS and STING expression activated the NF-κB-sensitive Igκ reporter and co-transfection of Vpr suppressed this activation. This was accompanied by the loss of co-transfected STING at 12, 24 and 48 hours (Fig. 5.1C). Testing Vpr proteins from other HIV-1 molecular clones, Yu2 and NL4-3, in this assay revealed that this was not a strain specific effect of Vpr as the Igκ luciferase reporter activation was also inhibited by Yu2 and NL4-3 Vpr expression (Fig. 5.1D). These data suggested that Vpr suppressed NF-κB activation downstream of cGAS and STING, potentially by inducing the loss of these signalling proteins.

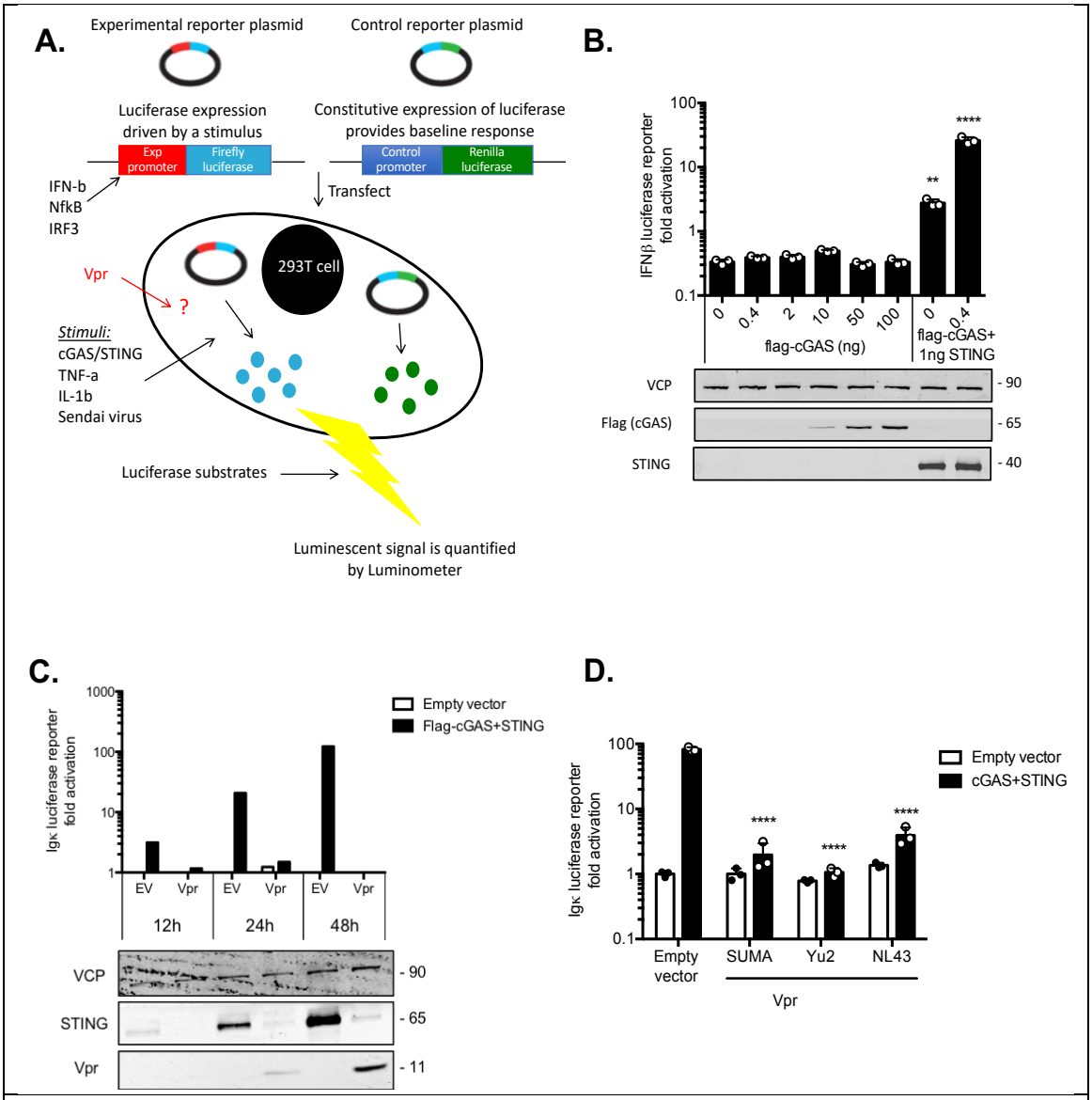


**Figure 5.1 NF-κB-sensitive luciferase reporter activation with co-transfected cGAS and STING is suppressed by Vpr in HEK293T cells**

**(A)** Schematic of HEK293T cell line based dual luciferase reporter gene assay. **(B)** Induction of IFNβ-Luc in HEK293T cells when Flag-cGAS alone or flag-cGAS and STING were co-transfected with IFNβ firefly luciferase and thymidine kinase luciferase reporters. Immunoblot detecting the flag-tag, STING and VCP as a loading control. Size markers are shown (kDa). **(C)** Induction of NF-κB sensitive Igκ-Luc in HEK293T cells expressing Vpr or empty vector after transfection of NF-κB sensitive Igκ firefly luciferase reporter and thymidine kinase luciferase reporter with empty vector or flag-cGAS and STING. Immunoblot detecting Vpr, STING and VCP as a loading control. Size markers are shown (kDa). **(D)** Induction of NF-κB sensitive Igκ-Luc in HEK293T cells expressing Vpr from different HIV-1 strains or empty vector after transfection of NF-κB sensitive Igκ firefly luciferase reporter and thymidine kinase luciferase reporter with empty vector or flag-cGAS and STING. Error bars represent standard deviation of biological repeats (n=3). Each experiment is representative of three independent experiments. Data were analysed using two-way ANOVA test. Stars (*) represent statistical significance: * ($p<0.05$), ** ($p<0.01$), *** ($p<0.001$), **** ($p<0.0001$) compared to empty vector.

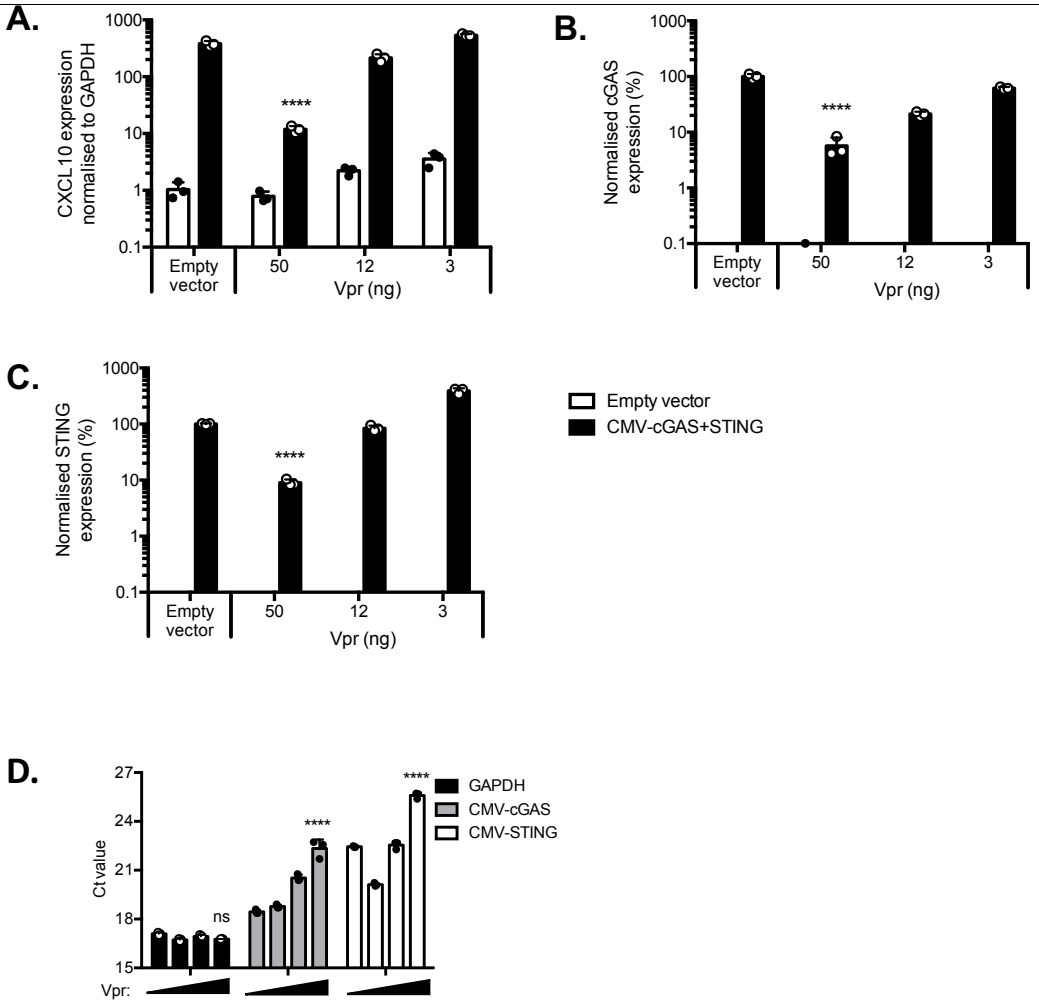


**Figure 5.2 Vpr blocks RNA expression from co-transfected cGAS and STING plasmids**

**(A)** Fold induction of CXCL10 in HEK293T cells transfected with 50, 12 or 3ng of Vpr expressing plasmid or empty vector and CMV promoter driven flag-cGAS and STING plasmids or empty vector. **(B)** Induction of cGAS from the transfected flag-tagged cGAS expressing plasmid in (A). **(C)** Induction of STING from the transfected STING expressing plasmid in (A). **(D)** Ct values of GAPDH, cGAS and STING transcripts from HEK293T cells co-transfected with a dose range of empty vector or Vpr vector and CMV promoter driven flag-cGAS and STING plasmids or empty vector. Error bars represent standard deviation of biological repeats (n=3). Each experiment is representative of two independent experiments. Data were analysed using two-way ANOVA test. Stars (*) represent statistical significance: * ($p<0.05$), ** ($p<0.01$), *** ($p<0.001$), **** ($p<0.0001$) compared to empty vector.

To determine whether Vpr was having an effect on protein levels or expression of cGAS and STING mRNA from the co-transfected plasmids, cGAS and STING mRNA was measured by qRT-PCR. Viral CMV immediate early (CMVie) promoter-driven flag-cGAS and STING plasmids were co-transfected with a dose range of Vpr into HEK293T cells. Forty eight hours later cells were lysed for RNA extraction. cDNA was synthesised after DNase treatment of the RNA and used for quantitative PCR analysis using primers specific for the *cGAS* and *STING gene*. CMVie promoter-driven cGAS and STING expression resulted in the induction of the ISG *CXCL10*, which was inhibited by Vpr in a dose-dependent manner (Fig. 5.2A). Critically, Vpr also inhibited *cGAS* and *STING* RNA expression from the co-transfected CMVie promoter driven plasmid, with the apparent reduction in RNA expression correlating with the inhibition of *CXCL10* gene induction (Fig. 5.2B, C). Furthermore, Vpr did not inhibit RNA expression of the endogenous *GAPDH* gene (Fig. 5.2D). This indicated that the inhibition of cGAS/STING signalling by Vpr may be due to reduced levels of *cGAS* and *STING* mRNA transcripts and not due to degradation of cGAS and STING proteins.

To further investigate the possibility of Vpr-mediated degradation of cGAS and STING proteins the proteasomal and autophagosomal degradation pathways were inhibited by chemical inhibition with MG132 or bafilomycin respectively. HEK293T cells were transfected with an empty- or a Vpr-expressing plasmid and stimulated with flag-cGAS and STING transfection. Cells were then treated with 20 μM MG132 or 400 nM bafilomycin for 2, 4, 8 or 10 hours. Cells were lysed in cell lysis buffer, proteins were separated by SDS-PAGE and immunoblotted with antibodies for VCP, flag-tag, STING and Vpr. MG132 or bafilomycin treatment of the cells did not rescue cGAS or STING protein expression (Fig. 5.3A, C). Quantification of luciferase activity by luminometry showed that MG132 treatment inhibited activation of the NF-κB luciferase reporter. This suggested effective inhibition of the proteasome by MG132 because NF-κB activation depends on ubiquitination of various signalling molecules and MG132 inhibits the proteasome which prevents ubiquitin recycling and NF-κB activation (Fig. 5.3B). Taken together, these results demonstrated that in transfection-based reporter gene assays Vpr inhibited the cGAS/STING-signalling pathway and this was accompanied by reduced transcript levels for these proteins.

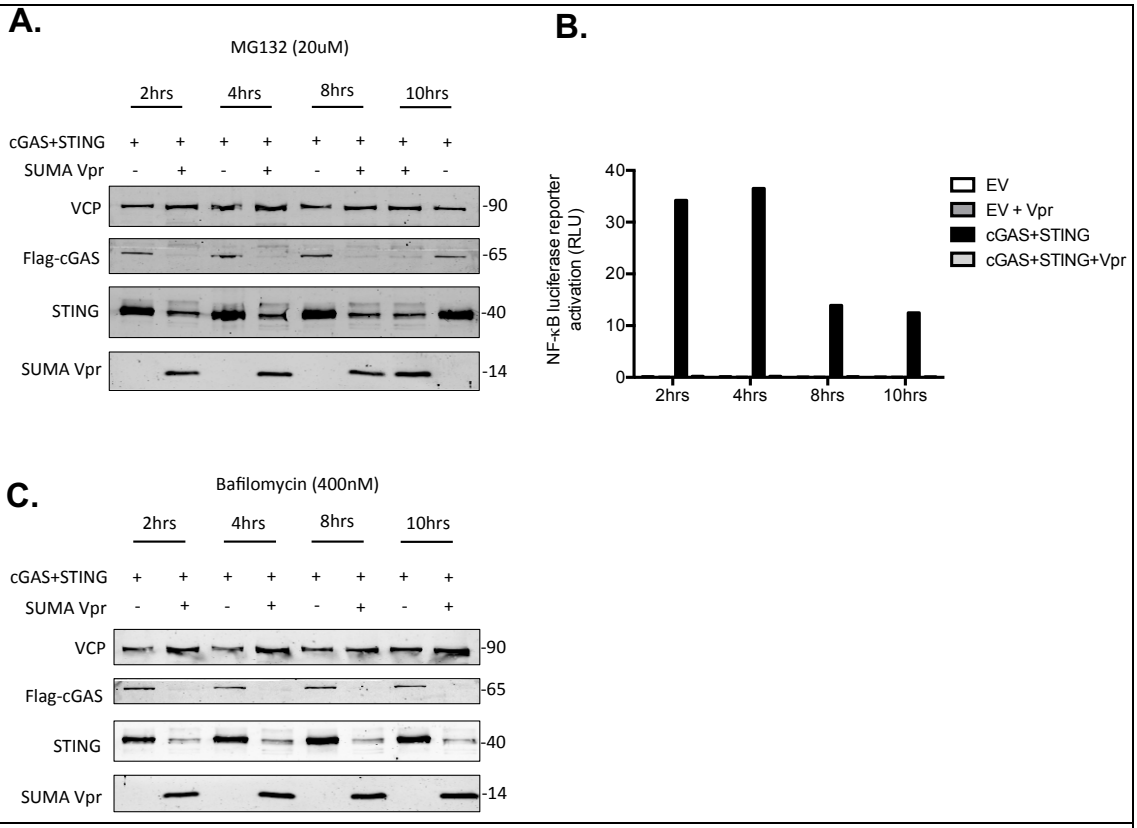


**Figure 5.3 Vpr mediated block to expression from co-transfected plasmids is not rescued by proteasome or autophagosome inhibition**

**(A)** Immunoblot detecting Vpr, STING, Flag-cGAS and VCP as a loading control from extracted HEK293T cells after STING and flag-cGAS co-transfection with Vpr or empty vector and MG132 treatment for 2, 4, 8 or 10 hours. **(B)** Induction of NF-κB-Luc in HEK293T cells from (A) after STING and flag-cGAS co-transfection with Vpr or empty vector and MG132 treatment for 2, 4, 8 or 10 hours. **(C)** Immunoblot detecting Vpr, STING, Flag-cGAS and VCP as a loading control from extracted HEK293T cells after STING and flag-cGAS co-transfection with Vpr or empty vector and Bafilomycin treatment for 2, 4, 8 or 10 hours.

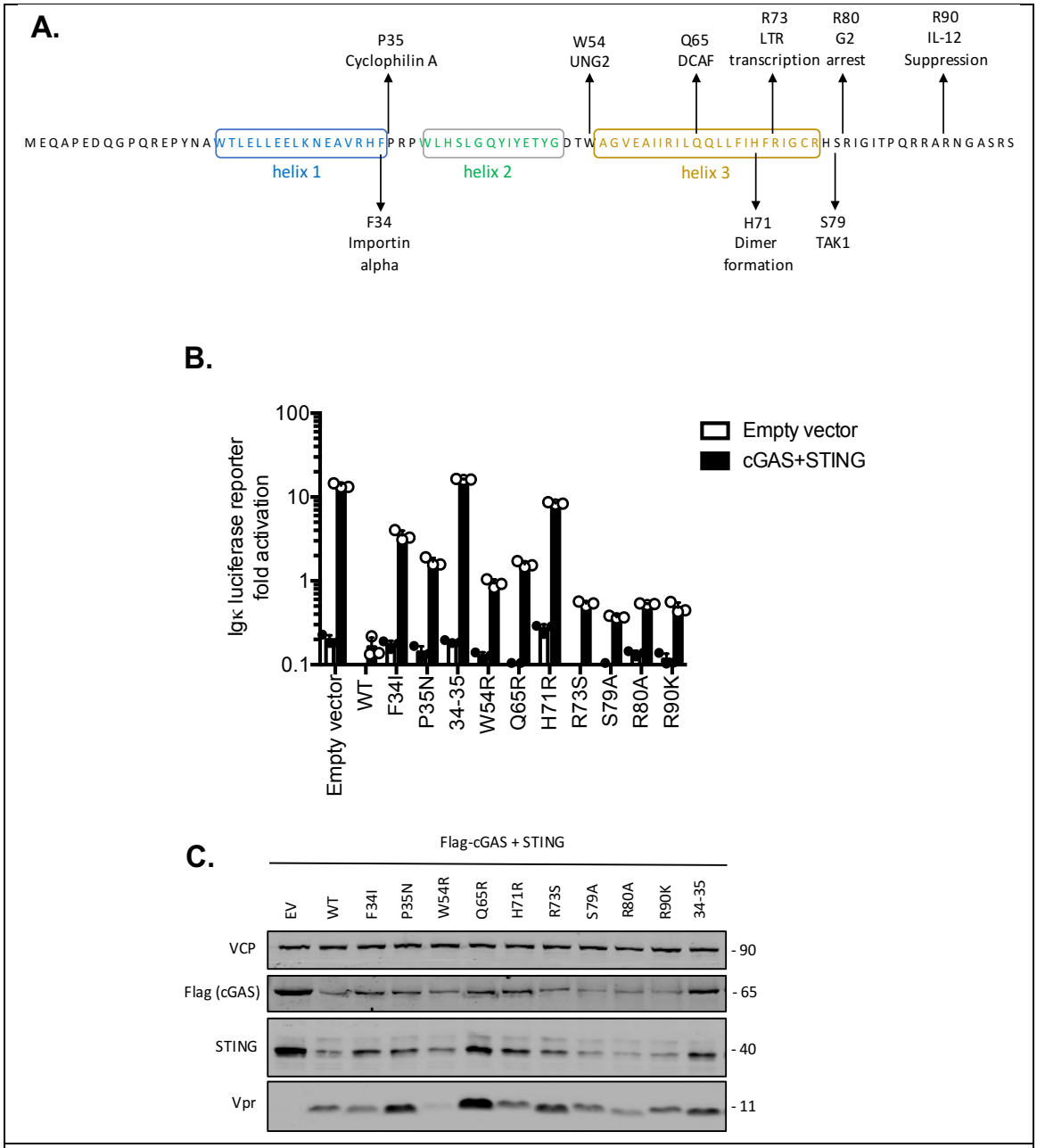


**Figure 5.4 Mutational analysis of Vpr**

**(A)** Schematic showing position of Vpr mutants on a linear amino acid sequence of Vpr. **(B)** Induction of NF-κB sensitive Igκ-Luc in HEK293T cells expressing Vpr or empty vector after transfection of NF-κB sensitive Igκ firefly luciferase reporter and thymidine kinase luciferase reporter with empty vector or flag-cGAS and STING. **(C)** Immunoblot detecting Vpr, STING flag-cGAS and VCP as a loading control from HEK293T cells in (A). Size markers are shown (kDa). Error bars represent standard deviation of biological repeats (n=3). Each experiment is representative of three independent experiments.

## 5.2 Mutational analysis of Vpr revealed a correlation between Vpr nuclear envelope accumulation and suppression of expression from co-transfected plasmids

For further characterisation of Vpr-mediated suppression of transcript levels from plasmid DNA, various mutants of Vpr that have previously been described in the literature were generated by site-directed mutagenesis (Fig. 5.4A) (Table 5.1). HIV-1 wild type or mutant Vpr were co-transfected with the IgK firefly luciferase reporter and TK renilla luciferase reporter. At the same time cells were stimulated by co-transfection with empty vector or flag-cGAS and STING. Forty eight hours later the cells were lysed in passive lysis buffer and luminescence of each sample was measured by luminometry. Expression of proteins expressed from transfected plasmids was probed by SDS-PAGE and immunoblotting with antibodies detecting the flag-tag, STING, Vpr and VCP as a loading control. Vpr mutants F34I, P35N, Q65R, H71R and F34I+P35N had reduced ability to suppress the NF-κB-sensitive Igκ firefly luciferase reporter activation (Fig. 5.4B) and this correlated with reduced inhibition of cGAS and STING expression from co-transfected plasmids compared to WT Vpr (Fig. 5.4C). In contrast to this, Vpr mutants R73S, S79A, R80A, R90A inhibited NF-κB-sensitive IgK firefly luciferase reporter activation (Fig. 5.4B) and cGAS and STING expression from the co-transfected plasmids (Fig. 5.4C).

To gain further insight into Vpr function, localisation of functional and non-functional Vpr mutants was compared. HeLa cells were transfected with flag-tagged wild type or mutant Vprs. Twenty four hours later cells were fixed and stained for immunofluorescence microscopy using antibodies against the flag-tag (green) and nuclear pore complex proteins (red). Nuclei were visualised by DAPI staining (blue). Wild type Vpr localised exclusively to the nucleus and showed significant nuclear rim staining, however Vpr mutants that lacked the ability to block expression from transfected plasmids (F34I, P35N, F34I+P35N, Q65R and H71R) lost nuclear rim localisation and showed diffuse cytoplasmic staining (Fig. 5.5A, B). On the other hand, Vpr mutants, R73S, S79A, R80A, and R90A which behaved like WT Vpr in the reporter gene assay showed localisation similar to the WT Vpr (Fig 5.5A, B).

| Vpr residue | Reported function |
|---|---|
| A30 | - |
| V31 | - |
| A30+V31 | Inhibition of CMV promoter activity (528) |
| F34 | Importin-α interaction (495) |
| P35 | Cyclophilin A interaction (476) |
| F34+P35 | - |
| W54 | UNG2 interaction (469) |
| Q65 | DCAF1 interaction (468) |
| H71 | Vpr dimer formation (529) |
| R73 | LTR transcription activation (530) |
| S79 | TAK1 interaction (513) |
| R80 | cell cycle arrest (468) |
| R90 | IL-12 suppression in DC (531) |

**Table 5.1 Reported function of Vpr residues.**

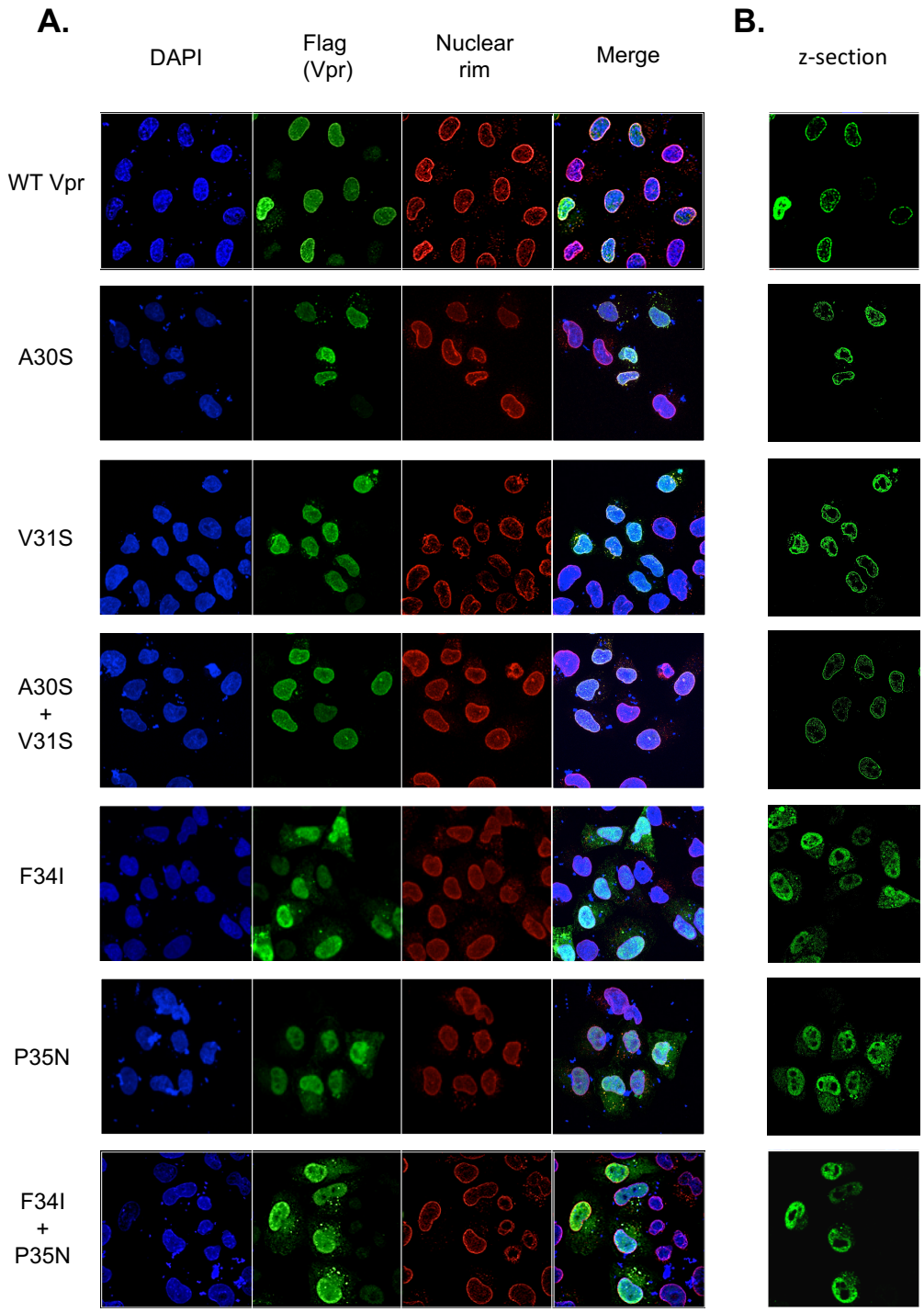


**Figure 5.5 Localisation of Vpr to the nuclear rim correlates with suppression of expression from co-transfected plasmids**

**(A)** Immunofluorescence images of HeLa cells transfected with 50ng of flag-tagged WT or a mutant Vpr expressing pcDNA3.1 plasmid using antibodies against the flag-tag (green) and nuclear pore complex (mab414) (red). **(B)** z-section of cells in (A) showing nuclear rim accumulation of Vpr.

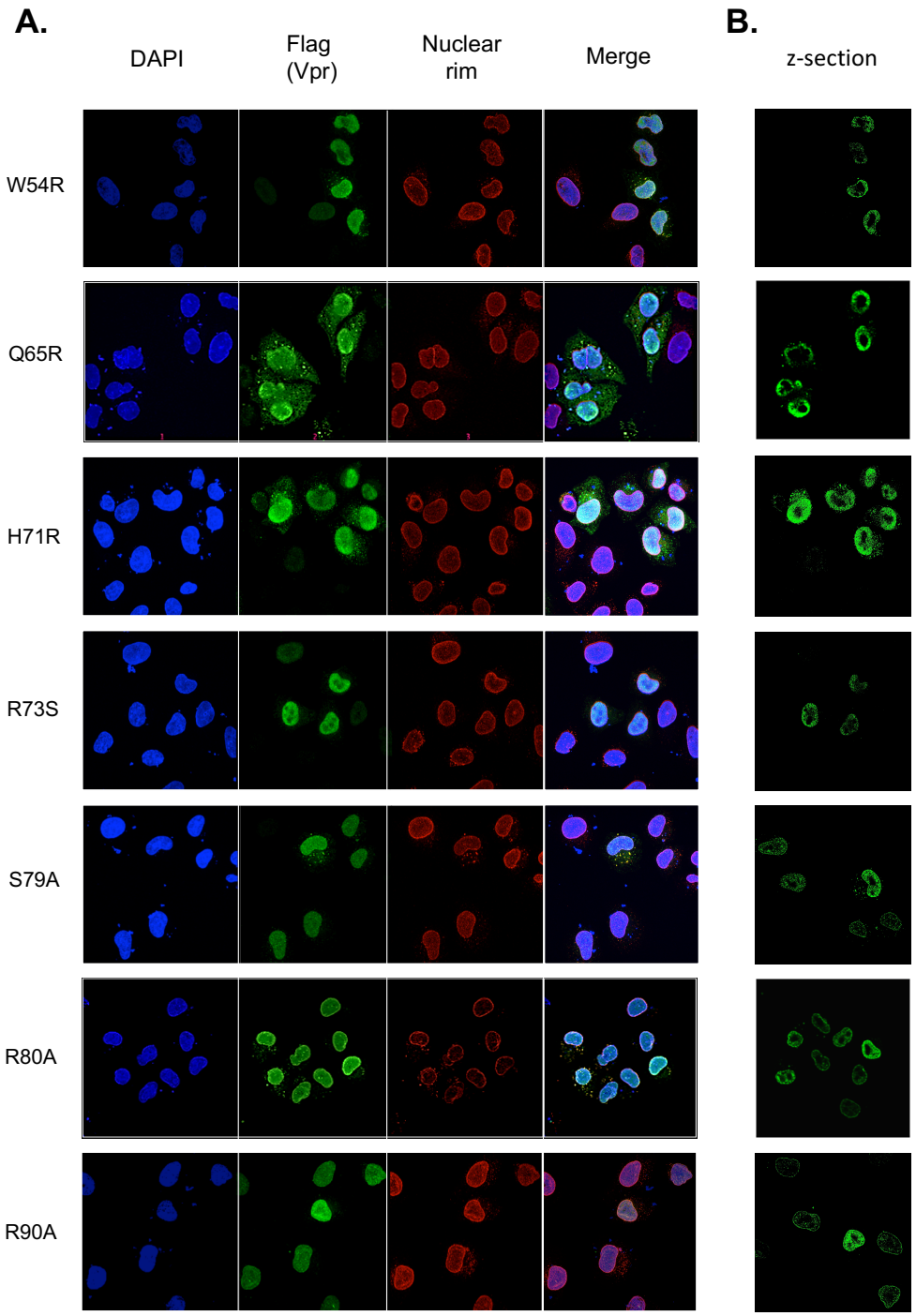


**Figure 5.5 continued: Localisation of Vpr to the nuclear rim correlates with suppression of expression from co-transfected plasmids**

**(A)** Immunofluorescence images of HeLa cells transfected with 50ng of flag-tagged WT or a mutant Vpr expressing pcDNA3.1 plasmid using antibodies against the flag-tag (green) and nuclear pore complex (mab414) (red). **(B)** z-section of cells in (A) showing nuclear rim accumulation of Vpr.

The mutational analysis of Vpr showed a correlation between Vpr localisation to the nuclear rim and suppression of expression from the co-transfected plasmids (Table 5.2). In addition, it revealed that this function of Vpr is genetically separable from the cell cycle arrest function of Vpr. Vpr mutants R73S, S79A, R80A, and R90A which are defective for the cell cycle arrest function were active for suppression of expression from the co-transfected plasmids. Conversely, Vpr mutants F34I, P35N and F34I+P35N which are able to arrest cell cycle did not suppress expression from the co-transfected plasmids.

## 5.3 Vpr mediated block to expression from co-transfected plasmids is not specific to cGAS or STING expressing plasmids

To investigate whether suppression of expression from co-transfected plasmids was specific for the *cGAS* or *STING* gene, activity of Vpr was tested against luciferase and GFP expression. To test the activity of Vpr against luciferase expression, a luciferase reporter gene assay was carried out. Luciferase reporters driven by different promoters were co-transfected with an increasing amount of Vpr into HEK293T cells. Cells were lysed with passive lysis buffer and luminescence was measured by luminometry after 24 hours. Vpr inhibited luciferase expression from all the plasmids tested in a dose-dependent manner (Fig. 5.6A, B). Next, the activity of Vpr was tested against an M5P promoter driven GFP expression. Empty vector, WT Vpr, VprF34I+P35N, VprQ65R, or VprR80A expressing plasmids were co-transfected with a GFP expressing plasmid into HEK293T cells. The cells were harvested 24 hours later in cell lysis buffer, proteins were separated by SDS-PAGE and immunoblotted for the flag-tag, Vpr and actin. WT Vpr or VprR80A inhibited GFP expression whereas VprF34I+P35N or VprQ65R were unable to inhibit GFP expression (Fig. 5.6C). These data suggested that Vpr suppression of expression from co-transfected plasmids is not specific to the cGAS or STING expressing plasmids.

## 5.4 Vpr expression does not inhibit HIV-1 gene expression or infectivity

Given that Vpr inhibited expression from co-transfected plasmids, the effect of Vpr on HIV-1 infection and gene expression was tested. HEK293T cells were transfected with an empty or a Vpr expressing plasmid. 24 hours later cells were infected with a VSV-g pseudotyped HIV-1 vector expressing GFP. After 48 hours cells were fixed with PFA and GFP expression was analysed by flow cytometry. In parallel, Vpr was co-transfected with

| Vpr | Nuclear rim localisation | Block plasmid expression | Cell cycle arrest |
|---|---|---|---|
| WT | Yes | Yes | Yes |
| A30S | Yes | Yes | ND |
| V31S | Yes | Yes | ND |
| A30S+V31S | Yes | Yes | ND |
| F34I | No | No | Yes |
| P35N | No | No | Yes |
| F34I+P35N | No | No | Yes |
| W54R | Yes | Yes | Yes |
| Q65R | No | No | No |
| H71R | No | No | No |
| R73S | Yes | Yes | No |
| S79A | Yes | Yes | No |
| R80A | Yes | Yes | No |
| R90K | Yes | Yes | No |

**Table 5.2 Summary of Vpr mutant localisation and function. ND (not determined)**

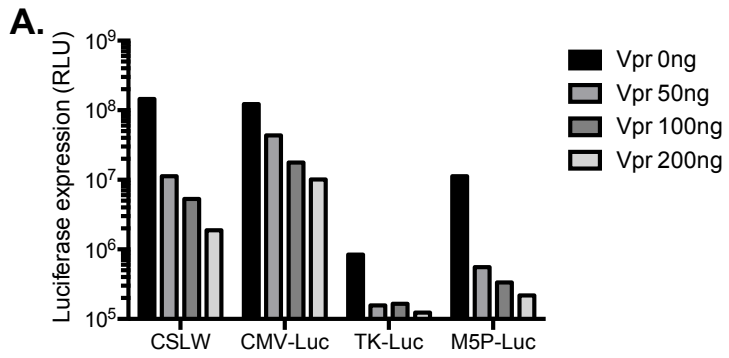


**B.**

| Plasmid | Promoter |
|---|---|
| CSLW | SFFV |
| CMV-Luc | CMV immediate early |
| TK-Luc | Thymidine kinase |
| M5P-Luc | MLV LTR |

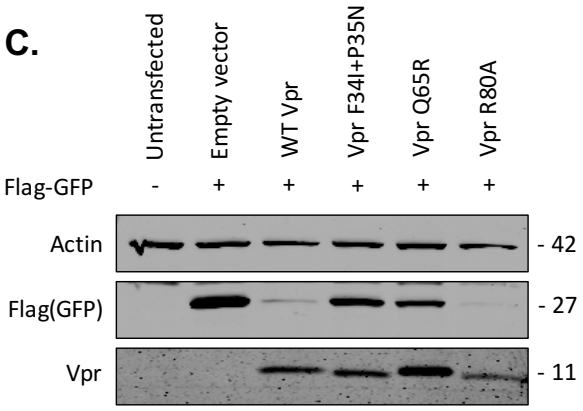


**Figure 5.6 Vpr block to expression from co-transfected plasmids is not specific to the cGAS or STING expressing plasmids**

**(A)** Induction of luciferase reporter in HEK293T cells transfected with CSLW, CMV-Luc, TK-Luc or M5P-Luc and empty vector or three doses of Vpr expressing plasmid. **(B)** Table showing the promoters driving the luciferase reporter plasmids used in (A). **(C)** Immunoblot detecting Vpr, STING, flag-GFP and actin as a loading control from HEK293T cells transfected with empty vector, WT Vpr or mutant Vpr and flag-GFP, or left untransfected. Size markers are shown (kDa).

a TK-renilla luciferase plasmid. After 72 hours cells were lysed in passive lysis buffer and luciferase activity was quantified by luminometry. Flow cytometry data showed that Vpr expression did not inhibit the number of cells expressing GFP when compared to the empty vector transfected cells (Fig. 5.7A). Similarly, there was no effect of Vpr on mean fluorescence intensity of GFP suggesting that Vpr did not inhibit GFP expression when the GFP is encoded by an HIV vector (Fig. 5.7B). On the other hand, luminometry data showed that Vpr was able to inhibit luciferase expression from the transfected plasmid (Fig. 5.7C).

Vpr is packaged into viral particles therefore the effect of packaged Vpr on HIV-1 infectivity was investigated. HIV-1 vectors were produced by transfecting HEK293T cells with the packaging plasmid (p8.91), VSV-g envelope plasmid and a Vpr expressing HIV-1 genome encoding plasmid that also expressed GFP from the same promoter via an IRES. Vectors were purified by ultracentrifugation through a sucrose cushion (20% in PBS). To quantify vector production RT activity of vector supernatants was measured by qPCR based RT assay (SG-PERT). Empty vector and vectors carrying VprF34I+P35N or VprQ65R gave an RT activity of about $2x10^{10}$ pURT/ul whereas vectors carrying WT Vpr or VprR80A gave 10-fold less RT activity (Fig. 5.8A). This reduction in RT activity was accompanied by an equal reduction in titres of WT or VprR80A carrying vectors in HeLa cells (Fig. 5.8B). To examine the infectivity of the vectors, infectious units per unit of RT (IU/URT) was calculated. All the vectors showed $1x10^{7}$ IU/URT which suggested that all the vectors were equally infectious (Fig. 5.8C). Cell lysates and normalised dose of purified vector ($1x10^{11}$pURT) were subjected to SDS-PAGE and immunoblotted for the capsid (p24) and Vpr proteins. WT Vpr or VprR80A expression led to a decrease in capsid (p24) expression in the producer HEK293T cells however by normalising the vector dose similar levels of the capsid (p24) could be detected in the vector supernatants (Fig. 5.8D).

These results demonstrated that Vpr expression or packaging into viral particles does not reduce HIV-1 infectivity. The low titre observed for the WT Vpr or VprR80A vectors was likely due to Vpr-mediated suppression of expression from the co-transfected packaging plasmid (p8.91), resulting in lower vector production.

## 5.5 Vpr does not block expression from integrated or nucleofected DNA

In addition to transfection, which delivers plasmid DNA into the cellular cytoplasm, plasmid DNA can be introduced directly into the nucleus by applying specific voltage and reagents in a process called nucleofection. To test the activity of Vpr against expression from

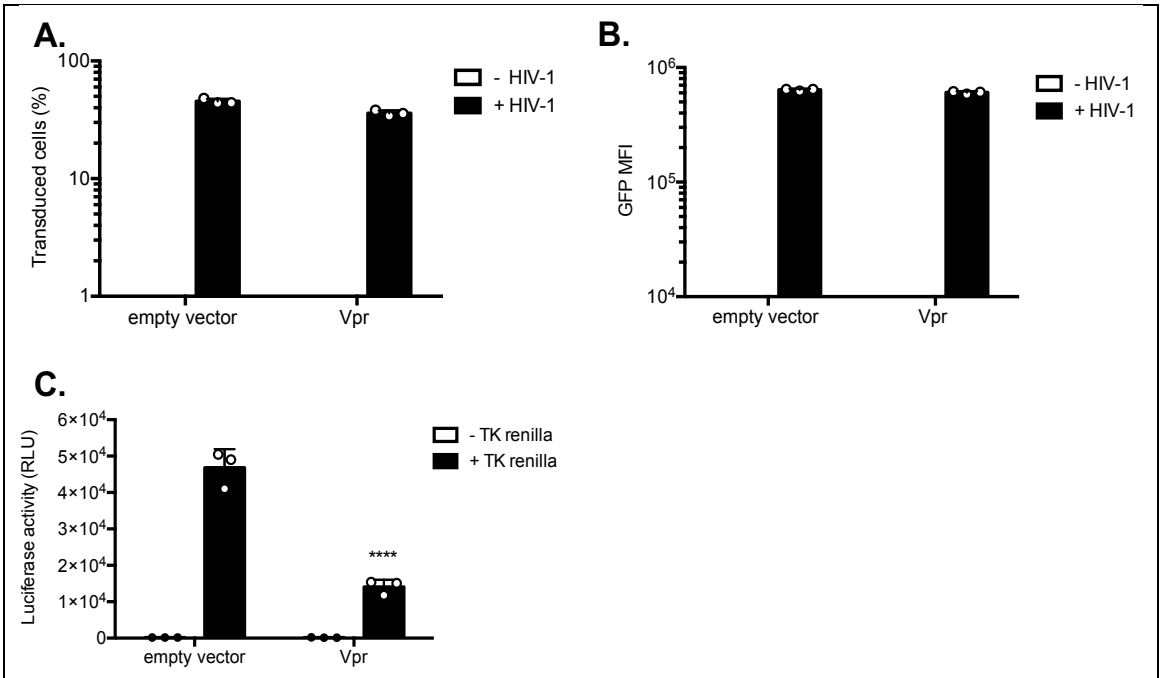


**Figure 5.7 Vpr does not inhibit HIV-1 gene expression**

**(A)** Percentage of HEK293T cells expressing Vpr or empty vector transduced by GFP encoding HIV-1 vector or left untransduced. **(B)** Mean fluorescence intensity of GFP expressed by HIV-1 vector in HEK293T cells from (A). **(C)** Induction of TK renilla luciferase reporter in HEK293T cells transfected with empty vector or Vpr expressing plasmid and TK renilla luciferase reporter, or left untransfected. Error bars represent standard deviation of biological repeats (n=3). Each experiment is representative of three independent experiments. Data were analysed using two-way ANOVA test. Stars (*) represent statistical significance: * ($p<0.05$), ** ($p<0.01$), *** ($p<0.001$), **** ($p<0.0001$) compared to empty vector.

nucleofected plasmid HEK293T cells were nucleofected with a GFP expressing plasmid with or without the Vpr expressing plasmid. The cells were lysed in cell lysis buffer 24 hours later and the lysates were subjected to SDS-PAGE and immunoblotting using antibodies against the flag-tag or tubulin. Surprisingly, Vpr did not inhibit expression from the nucleofected GFP expressing plasmid (Fig. 5.9A). As nucleofection bypasses nuclear import of the plasmid DNA and delivers it directly into the nucleus, this result indicated that Vpr might be inhibiting the specific pathway which imports plasmids into the nucleus of transfected cells.

To further investigate this finding, HEK293T cells were transduced with a lentiviral vector containing the *luciferase* gene under the control of a synthetic NF-κB-sensitive-promoter. Cells were selected with 2 μg/ml puromycin and a stable cell line was generated. Cells were then transfected with an empty vector or a Vpr expressing plasmid. In parallel, WT HEK293T cells were transfected with the synthetic NF-κB luciferase reporter and an empty vector or a Vpr expressing plasmid. After 24 hours cells were lysed in passive lysis buffer and luciferase activity was quantified by luminometry. Vpr inhibited basal luciferase activity when the NF-κB reporter was transfected, however Vpr was unable to inhibit luciferase activity from the integrated NF-κB reporter (Fig. 5.9B). Overall, these results are consistent with a model in which Vpr does not inhibit transcription directly, but instead may inhibit nuclear import of the co-transfected plasmids.

Since Vpr was unable to suppress expression from the integrated NF-κB reporter in HEK293T cells, these cells were used to test the activity of Vpr against NF-κB activation. Cells were transfected with an empty or a Vpr expressing plasmid. After 24 hours cells were stimulated with a dose range of TNF-α for 8 hours. Cells were lysed in passive lysis buffer and luciferase activity was quantified by luminometry. Vpr expression inhibited TNF-α activation of the NF-κB luciferase reporter (Fig. 5.10A). The experiment was repeated as above with a fixed concentration of TNF-α (10ng/ml) and a dose range of Vpr expressing plasmid, which showed a dose-dependent decrease in TNF-α activation of NF-κB luciferase reporter activation by Vpr (Fig. 5.10B).

Next, Vpr mutants were tested in this assay. 300ng of empty, WT Vpr, VprF34I+P35N, VprQ65R, VprR80A or GFP expressing plasmids were transfected into HEK293T cells containing an integrated *luciferase* gene under the control of the synthetic NF-κB promoter. After 24 hours the cells were stimulated with 40ng/ml TNF-α for 8 hours. WT Vpr or VprR80A inhibited TNF-α activation of the NF-κB luciferase reporter compared to the empty vector control (Fig. 5.10C). In contrast, VprF34I+P35N and Vpr Q65R were unable to significantly inhibit TNF-α activation of the NF-κB luciferase reporter (Fig. 5.10C). Similarly, GFP expression did not have any impact on TNF-α activation of the NF-κB

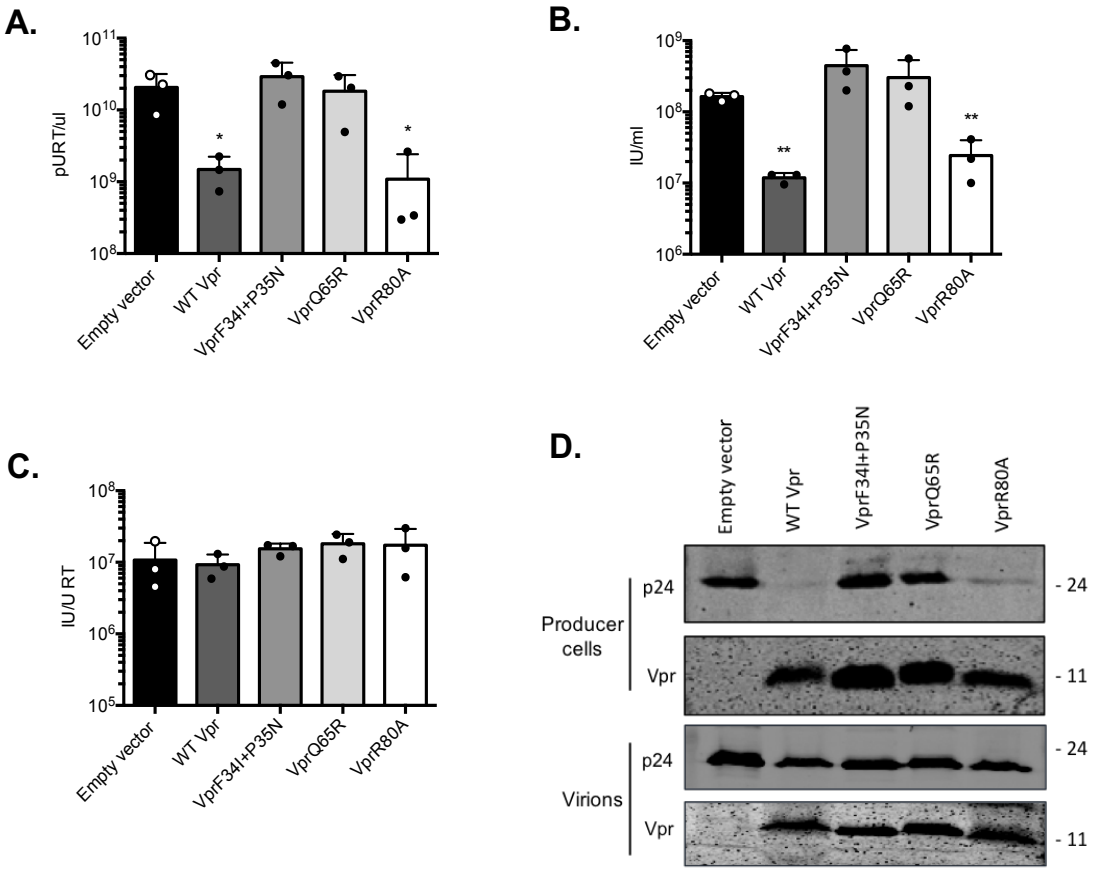


**Figure 5.8 Vpr expression *in trans* does not reduce infectivity of HIV-1 virions**

**(A)** Vector production determined by quantification of RT activity in the vector supernatants. **(B)** Vector titre determined by infecting HeLa cells with a titration of vector supernatants. **(C)** Infectivity of vectors calculated by dividing vector titres in (B) with RT activity in (A). **(D)** Immunoblot detecting Vpr and p24 (capsid) from extracted vector producer HEK293T cells or purified vector supernatants. Size markers are shown (kDa). Error bars represent standard deviation of biological repeats (n=3). Each experiment is representative of three independent experiments. Data were analysed using two-way ANOVA test. Stars (*) represent statistical significance: * ($p<0.05$), ** ($p<0.01$), *** ($p<0.001$), **** ($p<0.0001$) compared to empty vector.

luciferase reporter activation (Fig. 5.10C). These results demonstrated that in a reporter assay where no reporters or signalling proteins are transfected and the signalling is activated with soluble factors such as TNF-α, which activates the NF-κB pathway through binding and activation of the TNF-α receptor at the cell surface, Vpr is able to inhibit NF-κB reporter activation.

## 5.6 Vpr does not block expression from the EF1-α or ubiquitin promoter

Transfection typically relies on cytoplasmic delivered DNA to be transported to the nuclear envelope and then imported into the nucleus for successful transcription (532–534). Nuclear import is thought to occur through the nuclear pore complex. Transport is carried out by proteins known as importins karyopherins (535). Importins recognise nuclear localisation signals in cargos and transport the cargoes across the nuclear pore in an energy dependent process (535). Nucleic acids are not thought to contain any nuclear localisation signals so their nuclear import likely relies on proteins that contain nuclear localisation signals and binds nucleic acids (536). Previous results in the THP-1 cells based model showed that Vpr blocked nuclear import of transcription factors such as NF-κB and IRF3 (Fig. 3.7, 3.8). Transcription factors contain nuclear localisation signals and are capable of binding specific sequences known as response elements in promoters of responsive genes. Expression plasmids are designed to contain promoters that have response elements for various transcription factors to give transcription factor dependent gene expression. With this in mind, it was hypothesised that the block to expression from transfected plasmids by Vpr might be a consequence of a Vpr-mediated block to NF-κB or IRF3 nuclear translocation.

To test this hypothesis, activity of Vpr was tested against expression from plasmids containing the CMV, EF1-α or ubiquitin (Ub) promoter. The CMV promoter contains the NF-κB response element (GGGACTTTCC) which was not found in the EF1-α or Ub promoters (Fig. 5.11A). HEK293T cells were transfected with 50ng of CMV-GFP, EF1-α-GFP or Ub-GFP plasmids. Cells were co-transfected with 0, 50, 100 or 200ng of Vpr expressing plasmid. After 24 hours the cells were lysed in cell lysis buffer. Proteins were separated by SDS-PAGE and detected by immunoblot using antibodies specific for the flag-tag, GFP or actin as a loading control. Vpr expression resulted in a dose-dependent decrease in GFP expression from the co-transfected CMV-GFP plasmid (Fig. 5.11B). In contrast, expression from the EF1-α and particularly the Ub promoter was significantly less

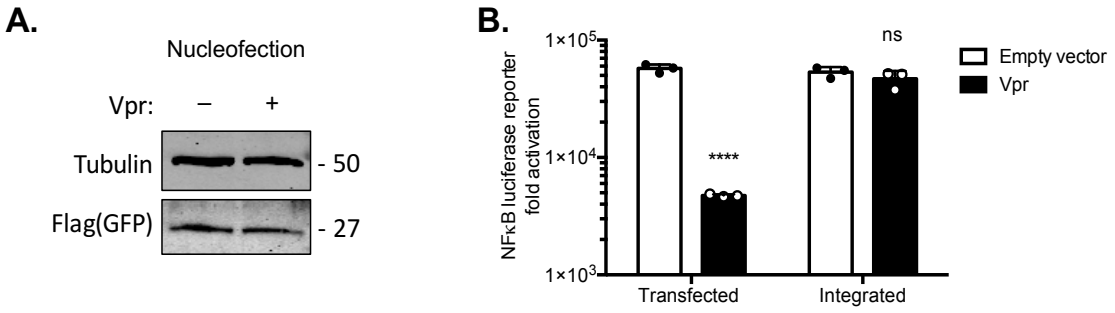


**Figure 5.9 Vpr does not inhibit expression from integrated or nucleofected plasmid DNA**

**(A)** Immunoblot detecting flag-GFP and tubulin as a loading control in extracted HEK293T cells nucleofected with empty vector or Vpr expressing plasmid and flag-GFP plasmid. **(B)** Induction of NF-κB-Luc in HEK293T cells containing an integrated NF-κB luciferase reporter or HEK293T cells transfected with NF-κB luciferase reporter. Both cell types were transfected with an empty vector or Vpr expressing plasmid. Error bars represent standard deviation of biological repeats (n=3). Data were analysed using two-way ANOVA test. Stars (*) represent statistical significance: * ($p<0.05$), ** ($p<0.01$), *** ($p<0.001$), **** ($p<0.0001$) compared to empty vector.

sensitive to Vpr mediated inhibition (Fig. 5.11B). To confirm this finding, another plasmid containing the ubiquitin promoter driving expression of the *cherry* gene (SFxUC) was tested. HEK293T cells were transfected with a dose range of SFxUC plasmid and co-transfected with 50ng of Vpr expressing plasmid. 24 hours later cells were lysed in cell lysis buffer. Proteins were separated by SDS-PAGE and immunoblotted with antibodies against Vpr, cherry and VCP. Consistent with the previous result, ubiquitin promoter-driven cherry expression from the co-transfected SFxUC plasmid was generally insensitive to Vpr expression (Fig. 5.11C).

These results link Vpr-mediated suppression of expression from co-transfected plasmids and the presence of the NF-κB response element in the promoter of the plasmids. This suggests that the block to expression from transfected plasmids by Vpr may be a consequence of Vpr inhibiting nuclear translocation of NF-κB, which not only inhibits NF-κB signalling, but also prevents nuclear import of the co-transfected plasmids.

## 5.7 Summary

To test the activity of Vpr against innate immune activation, plasmid transfection based reporter gene assays using HEK293T cells were set up. Since HEK293T do not have a functional DNA sensing pathway (537), cGAS and STING expressing plasmids were transfected to activate the DNA sensing signalling cascade. Co-transfection of Vpr resulted in the loss of cGAS and STING protein expression with the subsequent inhibition of the signalling pathway (Fig 5.1). Vpr is known to target proteins for degradation via the proteasome, however, inhibiting the proteasomal or the autophagosomal degradation pathway with chemical inhibitors did not rescue cGAS or STING protein expression in the presence of Vpr (Fig. 5.3). Quantification of cGAS and STING RNA expression by RT-qPCR revealed that Vpr reduced transcript levels of *cGAS* and *STING* from the co-transfected plasmids (Fig. 5.2). This effect of Vpr was not specific to the cGAS or STING plasmids because plasmids expressing luciferase or GFP from various viral promoters were also affected by Vpr (Fig. 5.6).

Mutational analysis of Vpr showed that residues at position F34, P35, Q65, or H71 were important for the Vpr-mediated block to expression from the co-transfected plasmids (Fig. 5.4). In addition, it demonstrated that this function is independent of the cell cycle arrest function of Vpr, as the Vpr mutants, which were defective for the cell cycle arrest, were able to block expression from the co-transfected plasmids. Further characterisation of mutant Vpr proteins by immunofluorescence staining correlated this function of Vpr to its nuclear rim accumulation (Fig. 5.5).

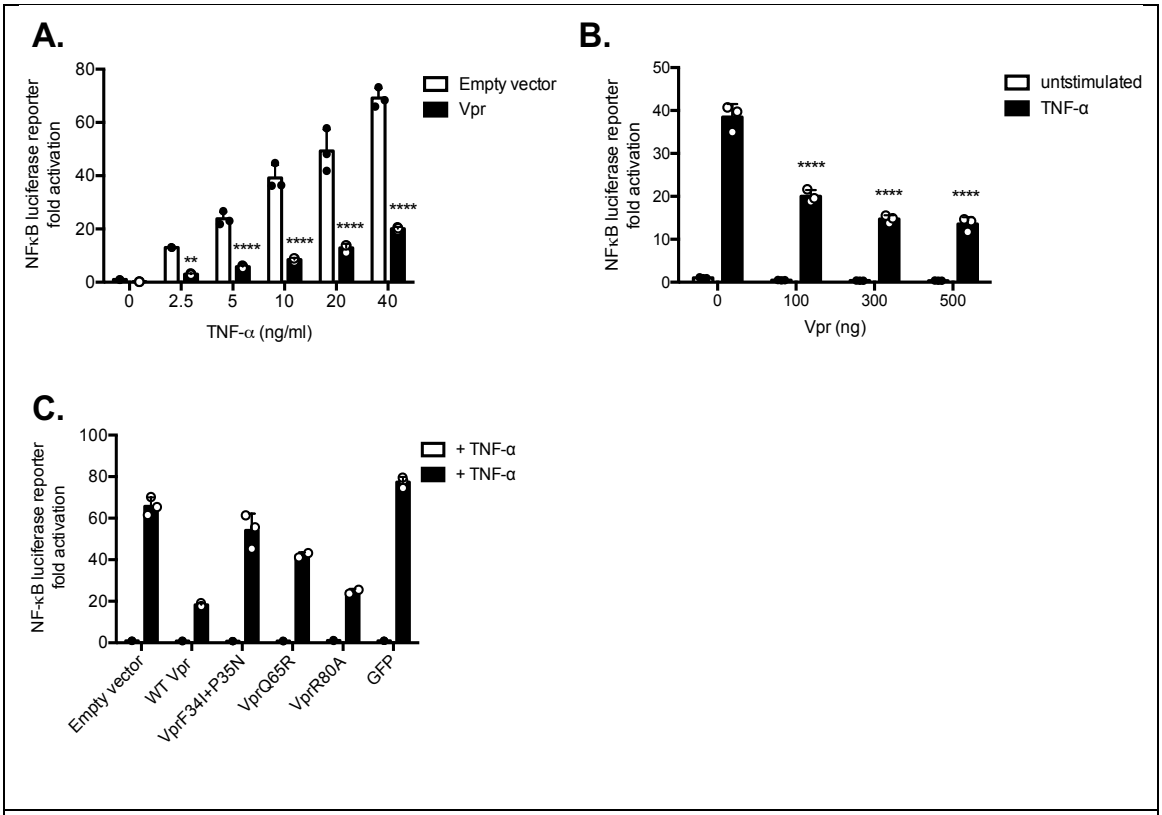


**Figure 5.10 Vpr inhibits TNF-α activation of the integrated NF-κB luciferase reporter**

**(A)** Induction of NF-κB-Luc in HEK293T cells containing an integrated NF-κB luciferase reporter stimulated with a dose range of TNF-α (0-40 ng/ml) and transfected with an empty vector or a Vpr expressing plasmid (300ng). **(B)** Induction of NF-κB-Luc in HEK293T cells containing an integrated NF-κB luciferase reporter stimulated with TNF-α (10 ng/ml) and transfected with 100, 300 or 500 ng of empty vector or Vpr expressing plasmid. **(C)** Induction of NF-κB-Luc in HEK293T cells containing an integrated NF-κB luciferase reporter stimulated with TNF-α (10 ng/ml) and transfected with 300ng of empty vector, WT Vpr or mutant Vpr expressing plasmid. Error bars represent standard deviation of biological repeats (n=3). Each experiment is representative of two independent experiments. Data were analysed using two-way ANOVA test. Stars (*) represent statistical significance: * ($p<0.05$), ** ($p<0.01$), *** ($p<0.001$), **** ($p<0.0001$) compared to empty vector.

To gain further insight into this function of Vpr, activity of Vpr was tested against other methods of gene delivery. Transfection with Fugene6 is a liposome based method that delivers DNA into the target cell cytoplasm. In contrast, nucleofection and lentiviral gene transduction deliver DNA directly into the nucleus. Surprisingly, Vpr was unable to inhibit expression from nucleofected plasmid DNA (Fig. 5.9A). Challenging control or Vpr expressing HEK293T cells with HIV-1 vector gave equivalent levels of infection and gene expression (Fig. 5.7A, B). Furthermore, Vpr packaging into an HIV-1 vector did not reduce infectivity of the viral particles as measured by vector-encoded GFP expression in infected cells (Fig. 5.8). Given that Vpr did not inhibit lentiviral gene transduction, an NF-κB luciferase reporter was stably integrated into HEK293T cells by lentiviral transduction. Activity of Vpr was tested against TNF-α activation of this reporter. Consistent with Vpr inhibition of NF-κB nuclear translocation (Fig. 3.8), Vpr inhibited TNF-α activation of NF-κB signalling (Fig. 5.10).

Correlation of Vpr localisation to the nuclear rim with suppression of expression from co-transfected plasmids, and insensitivity of nucleofected or lentiviral vector delivered DNA to Vpr suppression suggested that Vpr might be affecting DNA nuclear import rather than gene expression. Gene expression from transfected plasmid DNA requires trafficking of the plasmid to the nucleus and nuclear import. Nuclear import of the plasmid DNA is thought to be carried out by DNA binding proteins that contain nuclear localisation signals (532). Given that Vpr blocked nuclear import of transcription factors such as NF-κB (Fig. 3.8), it was hypothesised that Vpr blocked NF-κB assisted nuclear import of plasmid DNA that resulted in reduced expression from the co-transfected plasmids. Indeed, Vpr was found to inhibit expression from the CMV promoter that contains NF-κB response element (Fig. 5.11A) whereas expression from the EF1-α or ubiquitin promoters that do not contain the NF-κB response element was unaffected (fig. 5.11A, B, C). Overall, the results suggested that Vpr inhibited nuclear import of co-transfected plasmids containing NF-κB response element which resulted in reduced expression.

**A.**

NF-κB response element = gggactttcc

| Promoter | Sequence |
|---|---|
| CMV | atgaccttat**gggactttcc**tacttggcagtac |
| EF1-α | aaaggaaaa**ggg**c**ctttcc**gtcctcagccgtc |
| Ubiquitin | cacccgaata**a**g**agctttcc**cgcattagcga |

**B.**

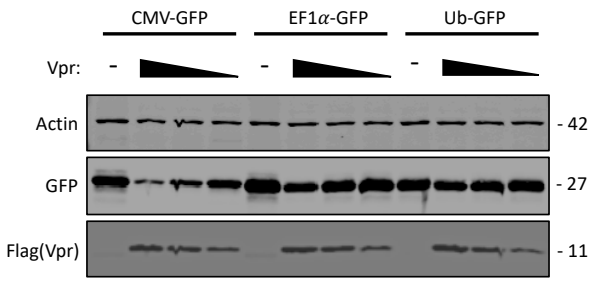


**C.**

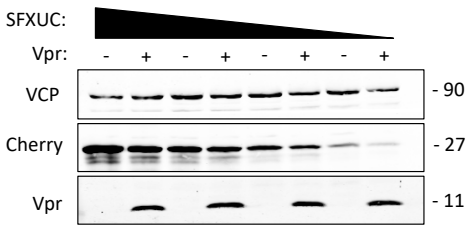


**Figure 5.11 Vpr does not block expression from elongation factor 1 alpha or ubiquitin promoter**

**(A)** Alignment of NF-κB response element with CMV, EF1α and ubiquitin promoters. **(B)** Immunoblot detecting flag-Vpr, GFP and actin as a loading control from HEK293T cells transfected with empty vector or Vpr expressing plasmid (50ng, 100ng, 200ng) and CMV-GFP, EF1α-GFP or Ub-GFP plasmids (50ng). Size markers are shown (kDa). **(C)** Immunoblot detecting Vpr, cherry and VCP as a loading control from HEK293T cells transfected with empty vector or Vpr expressing plasmid and a dose range of SFXUC plasmid. Size markers are shown (kDa). Each experiment is representative of two independent experiments. Immunoblot in (C) was kindly provided by Dr Rebecca Sumner.

# 6 Chapter 6: Discussion

## 6.1 Vpr promotes HIV-1 replication in cGAMP stimulated MDMs

All viruses must overcome intracellular innate immunity to replicate successfully. The ability to antagonise or evade this response is one of the most important determinants of viral replication in a host. Three out of four accessory proteins encoded by HIV-1 antagonise innate restriction factors to enhance viral replication. Vpu antagonises tetherin, Vif antagonises APOBEC3s and Nef antagonises SERINCs. Despite numerous reported functions of the accessory protein Vpr, its role in HIV-1 infection has remained poorly defined and its function has been somewhat enigmatic. This is partly because *in vitro* Vpr is dispensable for replication in CD4+ T-cells and there are conflicting reports of Vpr-dependent HIV-1 replication in MDMs, suggesting that its function might only be apparent under certain conditions (464,474,496). To address this hypothesis, previous work in the lab demonstrated that when the DNA sensing pathway was activated in MDMs by treatment of cells with cGAMP, Vpr is essential for viral replication. The Vpr-deleted virus replicated less well compared to wild type HIV-1 in cGAMP stimulated MDMs (Fig. 3.1). Since these experiments utilised sucrose purified HIV-1, previous inconsistent observations of inefficient replication of HIV-1ΔVpr, under unstimulated conditions, might be the result of inadvertent stimulation of MDMs with plasmid DNA, cytokines or cell debris present in the unpurified viral supernatants collected from the 293T virus producer cells (538). Furthermore, the immunological status of the MDM donor, as well as the activation level of the cultured MDMs at the time of infection, may impact the outcome of HIV-1 replication. For example, Vpr may provide a replication advantage in MDMs with activated innate immune responses. *In vivo,* early stages of HIV-1 infection have been associated with the activation of a dramatic cytokine cascade likely initiated by dendritic cells (539). Analysis of cytokine and chemokine profiles of plasma samples obtained from HIV-1 infected individuals revealed that during acute-phase of HIV-1 replication, chemokines and cytokines such as IFN-α, CXCL10 and IL-8 are upregulated as the viral titres increase (539). Given the ability of Vpr to suppress inflammatory signalling (Fig. 3.3, 5.10), it is possible that Vpr provides an advantage to HIV-1 replication by dampening some of these immune responses during the acute-phase of HIV-1 replication *in vivo*. Furthermore, in humans, infection with a Vpr-defective HIV-1 has been reported to result in markedly delayed seroconversion, suppressed viremia and normal T-cell levels without treatment (466).

## 6.2 Vpr suppresses ISG expression by inhibiting IRF3 nuclear translocation

To characterise the function of Vpr, a tractable THP-1 cell line based model was established. Unlike many other cancer cell lines THP-1 cells express endogenous cGAS and STING and have a functional DNA sensing pathway. Consistent with previous reports of HIV-1 detection of reverse transcribed DNA by cGAS (268), infection of THP-1 cells with VSV-g pseudotyped HIV-1 GFP lacking packaged Vpr activated a cGAS dependent ISG response whereas the HIV-1 GFP bearing Vpr activated significantly less ISG expression (Fig. 3.9, 3.10). Exogenous expression of Vpr by lentiviral transduction inhibited ISG mRNA (Fig. 3.3A) and protein expression (Fig. 3.3C) downstream of various innate immune stimuli suggesting that Vpr targeted a step in innate immune activation that is conserved between different signalling pathways (Fig. 3.4). Immunofluorescence analysis of IRF3 and NF-κB nuclear translocation at a single cell level showed decreased IRF3 and NF-κB nuclear translocation downstream of various innate immune stimuli in the presence of Vpr (Fig. 3.7, 3.8). However, Vpr inhibition of STING or TBK1 phosphorylation downstream of HT-DNA stimulation could not be detected (Fig. 3.5A).

C-terminal IRF3 contains a cluster of serine/threonine residues ($^{385}$SSLENTVDLHISNSHPLSLTS$^{405}$) that can be phosphorylated (540). Phosphorylated IRF3 dimerises and translocates to the nucleus. In the nucleus, dimeric IRF3 interacts with the coactivator cAMP-response element-binding protein-binding protein (CBP/p300) which facilitates IRF3 binding to distinct positive regulatory domains (PRD) in the type I IFN promoters and ISRE sites found in various other genes that encode chemokines, cytokines and ISGs (193,194). It was surprising that Vpr affected IRF3 phosphorylation at S396 (Fig. 3.6) but not at S386 (Fig. 3.5A) and this prevented IRF3 nuclear translocation (Fig. 3.7) Previous studies have assessed the role of specific IRF3 phosphorylation at S386 and S396 as follows.

Phosphorylation of S386 and S396 has been observed during viral infection and TBK1 has been shown to be the kinase responsible for this phosphorylation and induced gene expression (194,521,540). Lin et al. (1998) carried out immunoblot of Sendai virus infected HEK293T cells detecting IRF3 and detected a slow migrating band which disappeared following phosphatase treatment, but was maintained when the phosphatase and its inhibitor were added to the reaction (194). Immunoblot of HEK293 cells after transfection of WT or mutant IRF3 in which serine residues in the C-terminus were mutated to alanine showed that Sendai virus infection was unable to induce IRF3 phosphorylation when S386 or S396 was mutated to alanine. Furthermore, immunofluorescence microscopy showed

that GFP-tagged IRF3 in which five C-terminal serine residues were mutated to alanine did not translocate to the nucleus after Sendai virus infection of COS-7 cells. Finally, the authors showed that over-expression of WT IRF3 activated an IFN-β reporter in HEK293 cells. However, mutation of various serine residues in the C-terminus of IRF3 to alanine inhibited activation of IFN-β reporter activation. In this assay activity of IRF3 mutants after Sendai virus infection was not determined. The role of IRF3-S386A or IRF3-S396A was also not determined in the IFN-β reporter gene assay. Fitzgerald et al. (2003) used a reporter gene assay involving the luciferase reporter gene containing the Gal4 upstream activation sequence and IRF3 lacking its own DNA-binding domain fused with Gal4 DNA-binding domain (540). Luciferase reporter gene expression from the Gal4 upstream activation sequence in this assay requires activation of IRF3. The authors showed that the Gal4 reporter gene was activated by viral infection or TBK1 expression in the presence of a Gal4 fusion protein of wild-type IRF3, but not in the presence of a fusion protein in which the serine or threonine residues 385, 386, 396, 398, 402, 404 and 405 had been replaced by alanine.

Phosphorylation at S386 seems to be necessary and sufficient for IRF3 activation. Yoneyama et al. (1998) used Newcastle Disease Virus (NDV), an RNA virus known to trigger RIG-I activation, to interrogate IRF3 activation (541). Immunoblot showed that a single point mutation at S386 to alanine in IRF3 inhibits NDV stimulated IRF3 phosphorylation (521). Consistently, immunofluorescence microscopy revealed that IRF3 S386A does not translocate to the nucleus after NDV infection. In contrast, IRF3-5A mutant in which residues at position 396, 398, 402, 404, and 405 were replaced with alanine did not abrogate IRF3 activity in a reporter gene assay (522). This suggests that in the absence of S396 phosphorylation, S386 phosphorylation may be sufficient for IRF3 activation. IRF3-5D mutant in which residues at position 396, 398, 402, 404, and 405 are replaced with phosphomimetic aspartic acid residue has been shown to be constitutively active (523). However, immunoblot of HEK293T cells overexpressing IRF3-5D with antibody specific for IRF3 phosphorylation at S386 revealed that this phosphomimetic IRF3 mutant is postranslationally phosphorylated at S386 in the absence of any stimulation (524).

Additionally, the phosphomimetic IRF3-5D mutant has been shown to be more active in human 293T cells than in murine L929 cells (522,542). In 293T cells over-expression of IRF3-5D resulted in spontaneous expression of the RANTES promoter driven reporter gene (522). However, over-expression of IRF3-5D mutant did not activate expression of an IRF3 positive regulatory domains containing reporter gene in L929 cells (542). The difference between these two studies might be due to the difference between the promoters used. It is possible that RANTES promoter is more sensitive to phosphorylated

IRF3 than the promoter containing IRF3 positive regulatory domains. Furthermore, the difference in transfection efficiency of 293T cells compared to L929 cells may result in different expression of IRF3-5D mutant i.e. 293T cells which are very transfectable may express more IRF3-5D than L929 cells.

Unlike S386 phosphorylation, IRF3 phosphorylation at S396 seems to be stimulus and cell type dependent (523,524). Immunoblot detection of IRF3 phosphorylation at S386 with S386phosphorylation specific antibody in U373/CD14 astrocytes after NDV infection or LPS stimulation of TLR4 resulted in S386 phosphorylation (524). In contrast, immunoblot detection of IRF3 phosphorylation at S396 with S396 phosphorylation specific antibody in U373/CD14 astrocytes or U937 monocytic cells after RIG-I activation by Sendai virus infection resulted in IRF3 phosphorylation at S396 but not in response to LPS activation of TLR4 (523).

Taken together, these observations suggest that phosphorylation of IRF3 at S386 might be sufficient to activate IRF3. Observation of IRF3 S386 phosphorylation in the presence of Vpr (Fig. 3.6) suggests that Vpr may act to block nuclear translocation of S386 phosphorylated IRF3 to inhibit ISG expression. It is possible that the lack of IRF3 phosphorylation at S396 observed in the presence of Vpr (Fig. 3.6) is a consequence of Vpr-mediated block to IRF3 nuclear import and phosphorylation of IRF3 at S396 may have a shorter half-life than phosphorylation at S386. The consequence of block to nuclear import of phosphorylated IRF3 on IRF3 phosphorylation at various sites in the C-terminus requires further investigations.

There are conflicting reports of Vpr modulation of innate immunity. These studies lack mechanistic insight and fail to show relevance during viral replication. Consistent with the data presented in this thesis, Vpr was found to inhibit sensing of HIV-1 in Tzmbl cells reconstituted with STING which correlated with reduced nuclear translocation of IRF3 (543). Infection of Tzmbl-STING cells with HIV-1ΔVpr resulted in 8-fold more ISG56 induction compared to WT HIV-1. Single cell analysis of Tzmbl-STING cells for IRF3 nuclear translocation by immunofluorescence showed that HIV-1ΔVpr infection increased the number of cells with nuclear IRF3 by 3-fold compared to WT HIV-1 infection. Phosphorylation of IRF3 was not investigated in this study. On the other hand, in PM1 cells, Vpr was found to degrade IRF3 (512). Immunoblot of HIV-1 infected PM1 cells showed reduced IRF3 protein detection compared to uninfected cells. Although immunoblot of HEK293T cells overexpressing Vpr showed reduced IRF3 expression compared to cells not expressing Vpr, this did not occur during HIV-1 infection of Jurkat cells. My investigation of IRF3 level by immunoblot, in Vpr expressing monocytic THP-1

cells, did not show Vpr-mediated reduction in IRF3 levels (Fig. 3.5A). The differences between different cell types might be a reason for this discrepancy.

In contrast to the effects of Vpr on IRF3, NF-κB has been described to be activated and inhibited by Vpr in various cell types (513,544). Liu et al. 2014 showed that in HEK293T cells, Vpr over-expression activated NF-κB sensitive reporter gene expression. Immunoblot showed that Vpr over-expression resulted in phosphorylation of TAK1, a kinase involved in NF-κB activation (513). Co-immunoprecipitation suggested that Vpr interacted with TAK1. Immunoblot of Jurkat, THP-1 and PBMCs showed that infection with WT HIV-1 induced TAK1 phosphorylation which was not the case when these cells were infected with HIV-1ΔVpr. This is in contrast to my data that shows inhibition of NF-κB(p65) nuclear translocation (Fig. 3.8) and NF-κB reporter gene activation (Fig. 5.10A) by Vpr. Similarly, Kogan et al. (2013) showed that in primary macrophages, transduction with Vpr encoding adenovirus, inhibited NF-κB reporter gene activation downstream of LPS and TNF-α stimulation (544).

## 6.3 Vpr suppresses expression from co-transfected plasmids by inhibiting plasmid nuclear import

Vpr has been shown to inhibit expression from co-transfected CMV promoter-driven plasmids (528). My data confirms this report and extends this effect of Vpr to various other promoters such as the spleen focus-forming virus promoter and provide mechanistic insight into this activity. qPCR analysis showed that Vpr blocked mRNA expression from the transfected plasmids but did not shut down transcription globally as the expression of housekeeping gene, GAPDH, was unaffected (Fig. 5.2D) In addition, Vpr did not impact protein expression of the loading control used for immunoblotting (Fig. 5.4C), suggesting no global impact on RNA nuclear export or RNA translation. In contrast to transfection, nucleofection, which delivers plasmid DNA directly into the nucleus, was found to be insensitive to Vpr. Furthermore, a synthetic NF-κB promoter driven luciferase expression was inhibited by Vpr, when the plasmid was transfected, and not when it was integrated into the cellular genome by lentiviral mediated transduction. Assuming that the mechanism of transcription from a promoter is the same, when present in a plasmid or cellular genome, this suggests that Vpr may not directly affect transcription from co-transfected plasmids. Altogether, these data suggest that Vpr may block expression from co-transfected plasmids by inhibiting their nuclear import which has been shown to be essential for expression from transfected plasmid DNA (545,546).

## 6.4 Vpr antagonism of innate immunity and expression from co-transfected plasmids is independent of Vpr cell cycle arrest function

Laguette et al. (2014) showed that HIV-1 Vpr promotes premature activation of the SLX4 endonuclease complex to arrest cells in G2/M phase and inhibit innate immune activation (468). Taking a biochemical approach, the authors showed that Vpr manipulates an endonuclease complex to arrest cell cycle (468). They proposed this prevents innate immune sensing of the viral DNA (11). The data suggested that Vpr interacts directly with SLX4, which is implicated in DNA damage repair pathways. SLX4 recruits structure-specific endonucleases (SSE) MUS81-EME1, ERCC1-ERCC4 and SLX1 to form a complex (SLX4com) that repairs DNA damage. The activity of SSEs is kept under tight control during cell cycle. They are only activated at the G2/M transition, for example, by kinases such as polo-like kinase 1 (PLK1) leading to resolution of stalled replication forks and maintenance of genomic integrity. Vpr recruits PLK1 to the SLX4 complex prior to the G2/M transition. PLK1 then prematurely activates the SLX4 complex by phosphorylating EME1, resulting in abnormal processing of replication forks that eventually leads to replication stress and cell cycle arrest at the G2/M transition. This activity of Vpr is dependent on Cul4-DCAF1 ubiquitin E3 ligase complex as the DCAF1 binding mutant, VprQ65R, is unable to interact with the Cul4-DCAF1 ubiquitin E3 ligase complex to cause cell cycle arrest. Furthermore, SLX4 was found to bind HIV-1 reverse transcripts, only in the presence of Vpr, suggesting that Vpr may recruit SLX4 to process HIV-1 reverse transcripts and prevent innate sensing. My data shows that Vpr antagonises innate signalling and expression from co-transfected plasmids independently of the cell cycle arrest function. VprR80A which is defective for cell cycle arrest function is active for antagonism of innate signalling (Fig. 4.2A) and inhibition of expression from co-transfected plasmids containing NF-κB sensitive promoters (Fig. 5.6C). Conversely, Vpr mutant VprF34I+P35N showed activity for cell cycle arrest function (Fig. 4.1D) but did not antagonise innate signalling (Fig. 4.2A), or inhibit expression from co-transfected plasmids containing NF-κB sensitive promoters (Fig. 5.6C). Altogether, these data suggest that Vpr antagonism of innate immune activation and expression from plasmid DNA is independent of Vpr interaction with the SLX4 complex and suggests another as yet unidentified cellular target of Vpr.

## 6.5 Vpr localisation correlates with its function

The two Vpr phenotypes described here correlate with accumulation of Vpr to the nuclear envelope. Wild type Vpr localises to the nucleus and shows significant nuclear rim

localisation. Mutational analysis of Vpr shows that the mutants which do not localise to the nuclear rim are unable to block innate signalling pathways or expression from co-transfected plasmids containing NF-κB sensitive promoters (Table 6.1). Interestingly, VprQ65R, which has been shown to be unable to bind DCAF1, did not localise to the nuclear rim suggesting that perhaps interaction of Vpr with DCAF1 allows nuclear envelope localisation. However, Vpr has been shown to localise to the nuclear envelope in DCAF1 depleted cells (486). This suggests that Vpr mutation Q65R may have a dual affect. It not only prevents DCAF1 interaction with Vpr, but also abrogates Vpr localisation to the nuclear envelope. Mapping the residues of Vpr that are important for blocking innate signalling pathways and expression from transfected plasmids containing NF-κB sensitive promoters onto its structure resolved by NMR or crystallography reveals a potentially novel interface, distinct from the known interfaces for binding target proteins UNG2 or SLX4. This points towards a role of Vpr in targeting protein/s at the nuclear envelope to suppress nuclear import of transcription factors and plasmid DNA. Localisation of Vpr to the nuclear envelope has been associated with herniations in the nuclear envelope (547). These herniations were found to be devoid of nuclear pore complexes but coincided with Vpr induced disruption of the nuclear lamina (547). The nuclear envelope herniations ruptured intermittently which resulted in mixing of nuclear and cytoplasmic components (547). Finally, Vpr cell cycle arrest mutants were shown to be defective for induction of nuclear envelope herniations (547).

## 6.6 A unifying mechanism for Vpr functions

Correlation of Vpr localisation to the nuclear envelope (Fig. 4.6) with a block to nuclear import of transcription factors (Fig. 4.3) and plasmid DNA (Fig. 5.9) suggests that Vpr may orchestrate these functions by a single mechanism. Nuclear import of proteins and nucleic acids is carried out by proteins known as karyopherins or importins (535). Different groups of karyopherins recognise different classes of nuclear localisation signals (NLS) in target proteins. The classical nuclear import pathway is regulated by karyopherin-α (KPNA) and –β (KPNB). KPNA contains an NLS binding site that recognises a canonical basic NLS in protein cargoes. Upon binding the NLS, KPNA recruits KPNB which carries the complex through the nuclear pore via interactions with nucleoporins in a Ran GTPase dependent manner. KPNA 1-7 have been shown to mediate transport of various NF-κB complexes (548–550). Immunoblot and immunofluorescence microscopy showed that endogenous KPNA 1-7 bound endogenous NF-κB complexes when stimulated with TNF-α or Sendai virus infection (548–550). The specificity of NF-κB complexes for KPNA molecules was different and changed upon the composition of the imported NF-κB dimer (548–550). IRF3 nuclear import has been shown to be dependent on KPNA3 and 4 (551). *In vitro* translated

KPNA3 and 4 immunoprecipitated with GST-tagged IRF3 (551). In contrast to proteins, nucleic acids do not contain NLSs and therefore rely on nuclear import of NLS containing proteins, particularly the transcription factors which shuttle continuously between the cytoplasm and the nucleus (533,536). Labelling of plasmid DNA by site-specific hybridization to rhodamine-conjugated PNA clamps showed that the presence of NF-κB binding sites in the plasmid DNA increases its nuclear localisation (533,536).

Transcription factors such as NF-κB, SRF and HIF-1α are thought to bind the promoter of plasmids containing DNA binding sites of these transcription factors and allow nuclear import of the plasmid (532,552). For example, Vacik et al. (1999) used the promoter from the smooth muscle gamma actin (SMGA) gene whose expression is limited to smooth muscle cells which express the transcription factor SRF, required for SMGA gene activation (532). Plasmids containing portions of the SMGA promoter were shown to localise to the nucleus of smooth muscle cells, but remained cytoplasmic in fibroblasts and CV1 cells which did not express SRF. Nuclear import of the SMGA promoter-containing plasmid was achieved when the smooth muscle specific transcription factor SRF was expressed in CV1 cells. Badding et al. (2013) took a proteomics approach to identify the proteins that are involved in plasmid trafficking to the nucleus and subsequent nuclear import (534). They developed a live cell DNA-protein pull-down assay to isolate DNA-protein complexes at certain time points post-transfection for analysis by mass spectrometry (MS). Plasmids containing promoter sequences bound hundreds of unique proteins including importin-α and importin-β, whereas a plasmid lacking any eukaryotic sequences failed to bind many of the proteins. siRNA mediated depletion of importin-α and importin-β inhibited nuclear import of plasmid DNA whereas importin 7 depletion did not affect plasmid nuclear import (534).

Considering these observations, one possibility is that Vpr localises to the nuclear envelope and modulates activity of importins to block nuclear import of IRF3 and NF-κB, which in the context of plasmid transfection, will also prevent nuclear import of the transfected plasmid DNA that contains NF-κB or IRF3 binding sites (Fig. 6.1). This mechanism is supported by several reports of Vpr interaction with KPNA/s (471,506) and my observation that one of the inactive mutant Vprs has been described as a KPNA binding mutant (495). Furthermore, lack of inhibition of expression from EF1-α or ubiquitin promoters, which lack NF-κB binding sites, suggests that Vpr targeting of NF-κB nuclear import may also prevent nuclear import of plasmids containing NF-κB binding sites resulting in inhibition of expression from these plasmids. Consistent with this, nuclear import of HIV-1 vector, which is dependent on nuclear pore proteins such as Nup153 and Nup358, was unaffected by Vpr (Fig. 5.7) (63,68).

Based on Vpr localisation to the nuclear envelope and its ability to interact with importins, the role of Nup358, a nuclear pore protein, and TNPO3, a β-karyopherin, was investigated. Localisation of Vpr to the nuclear envelope in Nup358 depleted cells suggests that Vpr may not interact with Nup358 to localise to the nuclear envelope (Fig. 4.7). Although, TNPO3 was found to be involved in IRF3 and NF-κB nuclear translocation (Fig. 4.10, 4.11), but not degraded by Vpr (Fig. 4.12A), or modulated by Vpr in such a way which inhibits CPSF6 nuclear import (Fig. 4.12C, D) suggests that TNPO3 may not be the Vpr target protein. However, it is possible that TNPO3 mediates nuclear transport of NF-κB and IRF3 independently of CPSF6 nuclear import and Vpr is able to inhibit TNPO3 mediated IRF3 and NF-κB nuclear import without affecting CPSF6 nuclear import function of TNPO3. Another possibility is that Vpr recruits DCAF1 E3 ubiquitin ligase complex to TNPO3 resulting in TNPO3 ubiquitination which does not lead to proteasomal degradation or affect CPSF6 nuclear transport but prevents IRF3 and NF-κB nuclear import by TNPO3.

Several viruses have been shown to target importins to dysregulate innate signalling. Japanese encephalitis virus NS5 targets KPNA2, 3 and 4 to prevent IRF3 and NF-κB nuclear translocation (553). Co-IP experiments showed that NS5 interaction with KPNA2, 3 and 4 inhibited recruitment of IRF3 and NF-κB (p65) to KPNA2, 3 and 4. A block to IRF3 and NF-κB (p65) nuclear import, in the presence of NS5, was demonstrated by immunoblot after cell fractionation. IRF3 phosphorylation was not affected by NS5 expression, however, the IRF3 phosphorylation site detected by the antibody used is not specified in the published manuscript. Hantaan virus nucleocapsid protein inhibits p65 translocation by targeting KPNA1, -2, and -4 (554). Immunofluorescence showed that the nucleocapsid protein over-expression inhibited nuclear translocation of GFP tagged-p65 in HEK293T cells. Co-IP and immunoblot showed that the nucleocapsid protein interacted with overexpressed flag tagged KPNA1, 2 and 4 in HEK293T cells. Crystal structure of Ebola Virus VP24 protein with KPNA5 revealed that Vp24 targets a unique NLS binding site on KPNA5 to compete with nuclear import of phosphorylated STAT1 (555). Recently, vaccinia virus A55 protein was shown to interact with KPNA2 to disturb the interaction between NF-κB and KPNA2 in HEK293T cells overexpressing flag tagged KPNAs. Co-IP and immunoblot showed reduced interaction of HA-p65 with KPNA2 in A55 expressing cells (556). Similar to the effect of Vpr on IRF3 phosphorylation, A55 expression inhibited NF-κB (p65) nuclear translocation and phosphorylation at S276 but did not affect S536 phosphorylation suggesting that blocking nuclear import of NF-κB (p65) may impact phosphorylation of NF-κB at S276. In contrast to targeting importin-α, Hepatitis C virus NS3/4A protein restricts IRF3 and NF-κB translocation by cleaving KPNB1 (importin-β) (557). Immunoblot of HEK293T cells overexpressing NS3/4A protein showed cleavage of KPNB1 and immunofluorescence microscopy of NS3/4A expressing A549 cells showed inhibition of IRF3 and NF-κB nuclear translocation. Effect of NS3/4A on upstream

activation events such as IRF3 phosphorylation was not determined. Except for Hepatitis C virus NS3/4A, all other reports show that viral proteins bind importins and prevent recruitment of NF-κB and IRF3. The C-terminal tail of Vpr has been shown to bind both the major and minor NLS binding sites in KPNA2 (507). This suggests that similar to other viral proteins, Vpr might prevent recruitment of cellular NLS containing cargoes such as NF-κB by KPNA2 which would inhibit innate immune activation and expression from co-transfected plasmids. Furthermore, my data demonstrate that DCAF1 is essential for the function of Vpr. Vpr interacts with DCAF1 to hijack the CLR4 E3 ubiquitin ligase complex to target proteins for proteasomal degradation (469). This suggests that unlike other viral proteins, Vpr binding to the KPNA/s may lead to their ubiquitination, which may alter their function or target them to the proteasome.

Based on the data presented herein, the localisation of Vpr to the nuclear envelope seems to be essential for its function. However, the mechanism of nuclear envelope localisation is unclear. Vpr has been shown to interact with the nuclear pore proteins Pom121 and hCG1 (496,498). It is possible that the novel binding interface identified in the mutational analysis is actually the nuclear pore protein binding interface which allows Vpr localisation to the nuclear rim and another region of Vpr is involved in binding the cryptic target protein. The C-terminal tail of Vpr is unresolved in the full length Vpr crystal structure suggesting that it is flexible and could adopt different conformations (478). Indeed, the C-terminal tail was shown to adopt different conformations to bind the major and minor NLS binding sites in KPNA2 (507). Taken together, it is possible that the interface identified by the mutational analysis of Vpr is involved in an interaction with nuclear pore proteins that allow nuclear envelope localisation whereas the C-terminal tail of Vpr binds KPNA/s to block nuclear import of NF-κB and IRF3.

A recent study by Hotter et al. (2017) analysed 32 Vpr proteins from a large panel of divergent primate lentiviruses. Consistent with the data presented in this thesis HIV-1 Vprs were found to inhibit NF-κB (558). SIVcol and SIVolc infecting *Colobinae* monkeys were found to be be most potent at suppressing NF-κB activation. SIVcol and SIVolc differ from all other primate lentiviruses investigated by the lack of both, a *vpu* gene and efficient Nef-mediated downmodulation of CD3. In contrast to my data, analyses of SIVolc and SIVcol Vprs showed that the inhibitory activity of Vprs is independent of DCAF1 (Fig. 4.4). On the other hand, independence of the cell cycle arrest function and the inhibition of NF-κB activation by SIVolc and SIVcol is consistent with my data (Fig. 4.2). While both Vprs, SIVcol and SIVolc, target the IKK complex or a factor further downstream in the NF-κB signaling cascade, only SIVolc Vpr stabilised IκBα and inhibited p65 phosphorylation (558). Furthermore, unlike my data showing NF-κB inhibition by virion associated (Fig. 4.5)

and de novo synthesised HIV-1 Vpr (Fig. 3.2) this study found that only *de-novo* synthesised but not virion-associated Vpr suppressed the activation of NF-κB (558).

## 6.7 Current model of Vpr action during HIV-1 infection

Current data suggest that Vpr plays a role during very early stages of the viral life cycle in myeloid cells such as macrophages. After fusion, virion associated Vpr traffics to the nucleus and may associate with the nuclear envelope (492). The viral capsid stays intact as it traverses the hostile cytoplasm of the cell (68). The capsid protects the RNA genome and the reverse transcribed DNA from cytoplasmic nucleases and innate sensors (78,266). Although *in vitro* HIV-1 infection of macrophages does not activate innate immunity, acute-phase replication of HIV-1 *in vivo* is thought to activate dendritic cells which produce cytokines and chemokines (559). Under these conditions Vpr may provide an advantage in viral replication. Vpr present at the nuclear envelope may inhibit nuclear translocation of activated transcription factors such as IRF3 and NF-κB to suppress ISGs and proinflammatory genes activation, possibly by targeting KPNAs for proteasomal degradation via recruitment of CRL4 E3 ubiquitin ligase. NF-κB is one of the transcription factors which enhance HIV-1 promoter activity (560,561). It is possible that Vpr-mediated inhibition of NF-κB nuclear translocation may inhibit HIV-1 promoter activity. However, it is envisaged that this function of Vpr will be transient and active only during very early stages after viral entry. Once the integrated provirus expresses Gag, Vpr will bind the p6 domain of Gag which will localise it to the plasma membrane for incorporation into budding virions (25,486).

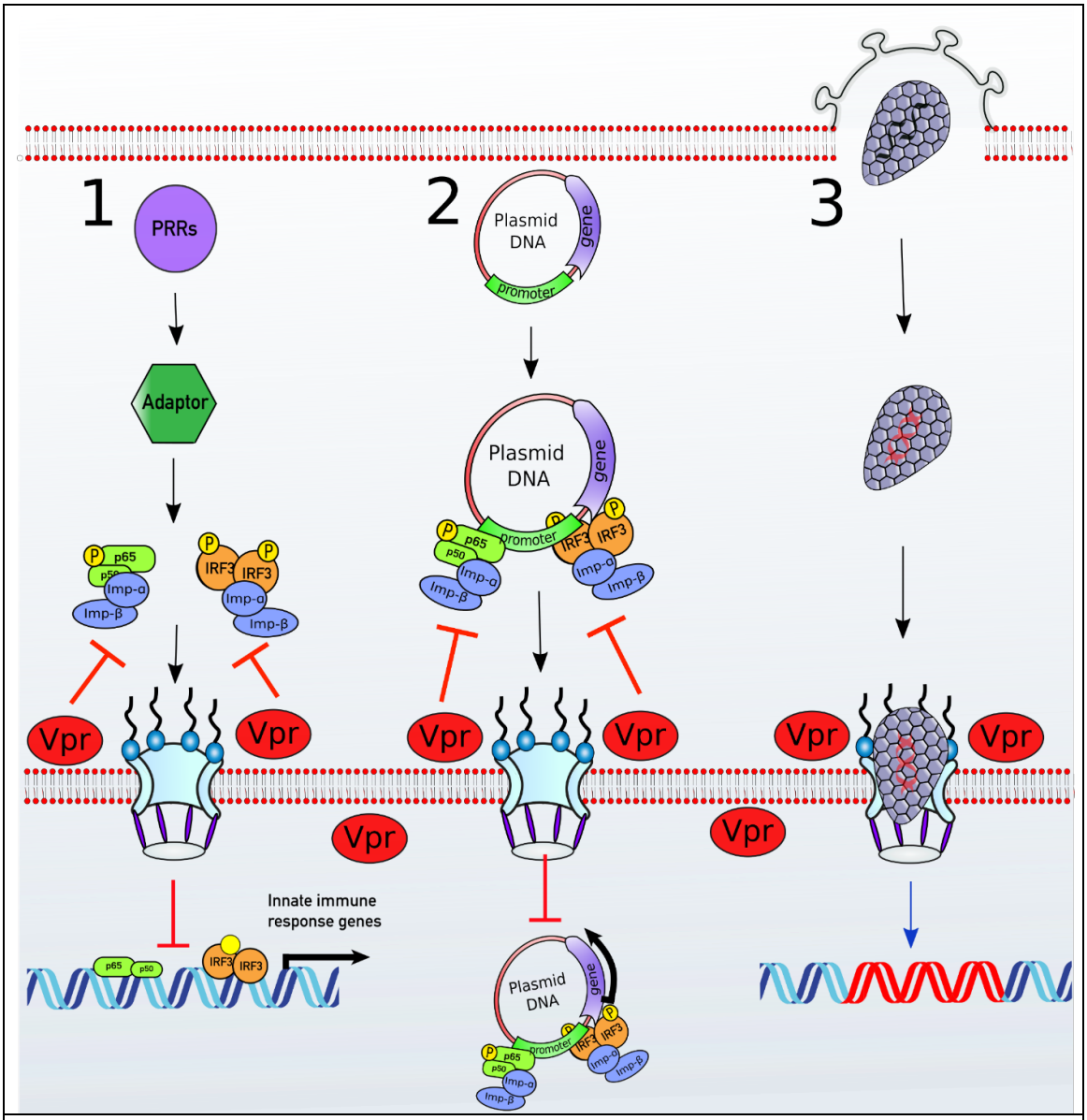


**Figure 6.1 A unifying model of Vpr function**

**(1)** Stimulation of various innate pattern PRRs result in activation of transcription factors such as IRF3 and NF-κB. To activate ISGs or proinflammatory genes expression, NF-κB and IRF3 translocate to the nucleus via the classical Imp-α/β dependent nuclear import pathway. **(2)** Nuclear import of a plasmid transfected into cellular cytoplasm is essential for gene expression. Transcription factors such as IRF3 and NF-κB bind to their cognate response elements present in the promoter of the plasmid and allow nuclear import via the classical Imp-α/β dependent pathway. **(3)** HIV-1 based vectors deliver genes to the nucleus in an Imp-α/β independent manner. Vpr localises to the nuclear pores and targets Imp-α/β dependent nuclear import. Vpr may recruit DCAF1 E3 ubiquitin ligase to Imp-α and target it for proteasomal degradation. This inhibits nuclear translocation of transcription factors such as IRF3 and NF-κB which in turn inhibits IRF3 and NF-κB mediated plasmid nuclear import but does not impact lentiviral gene delivery.

# 7 Future work

Observation that exogenously expressed Vpr inhibits various innate immune pathways such as the TLR4 or the RNA sensing pathway in THP-1 cells warrants further investigations in MDMs during HIV-1 infection. Like cGAMP, stimulation of MDMs with the TLR4 agonist, LPS, or the RNA sensing agonist, poly I:C, may inhibit replication of HIV-1ΔVpr but not WT HIV-1. Furthermore, the activity of Vpr mutants such as VprQ65R, VprP35N+F34I and VprR80A could be verified in MDMs during HIV-1 infection. To further support the inhibition of NF-kB (p65) nuclear translocation by Vpr, phosphorylation of NF-κB (p65) at S276 and S536 in the presence of Vpr should be investigated. It is possible that like vaccinia virus A55 protein, Vpr may inhibit NF-kB phosphorylation at S276 without inhibiting S536 phosphorylation.

To confirm the Vpr-mediated block to plasmid nuclear import and rule out the possibility of Vpr affecting plasmid stability, localisation of transfected DNA in the presence or absence of Vpr could be analysed by staining the plasmid DNA with fluorescent dyes or by fluorescence in situ hybridisation (FISH). The effect of Vpr on nuclear import of plasmid DNA could be measured by comparing the localisation of the plasmid stain with the DAPI or the nuclear envelope stain. The effect of Vpr on plasmid stability can be measured by comparing the intensity of the plasmid DNA stain in the presence or absence of Vpr.

The role of the C-terminal tail in Vpr should be investigated in the functional assays. Mutations can be introduced in the C-terminal tail and activity of Vpr can be tested against innate immune activation and nuclear envelope localisation. Localisation and function of Vpr should also be tested in Pom121 and hCG1 depleted cells. Super resolution microscopy can be used to precisely define Vpr interactions at the nuclear envelope.

Given that Vpr blocks nuclear import of transcription factors and plasmid DNA, the role of karyopherins should be explored. Vpr has been shown to interact with KPNA1, KPNA2 and KPNA4 (471,506). Similarly, NF-κB nuclear translocation has been shown to require KPNA1-7 (548–550) whereas IRF3 nuclear translocation involves KPNA3 and KPNA4 (551). Depletion of the KPNA/s targeted by Vpr will inhibit innate immune activation downstream of various stimuli. Furthermore, it should inhibit expression from Vpr sensitive plasmids such as the CMV promoter-driven plasmid, however, expression from Vpr insensitive plasmids such as the EF-1α or the ubiquitin promoter-driven plasmids should be unaffected. Given the redundancy in KPNAs function in nuclear transport and reports of Vpr interaction with various KPNAs, it is likely that depletion of one KPNA may not be sufficient to see the effect and depletion of multiple KPNAs in different combinations might

be required. For further validation of KPNA/s as the Vpr target, an interaction between Vpr and KPNA/s could be investigated by co-immunoprecipitation (Co-IP). Since Vpr inhibits expression from co-transfected plasmids, Co-IP with overexpressed proteins might be problematic and therefore Vpr interaction with endogenous KPNA/s should be pursued.

Recent study by Greenwood et al. (2019) showed Vpr driven global cellular proteome remodeling. Comparison of total proteomes of uninfected CEM-T4 T-cell line with cells infected with either WT HIV-1 or an HIV-1 Vpr deletion mutant (HIV-1 ΔVpr) showed that 1,940 proteins changed significantly in wild-type HIV-1 infected cells whereas only 45 significant changes occurred in cells infected with HIV-1 ΔVpr (562). Vpr-dependent proteomic remodeling was found to be dependent on the interaction of Vpr with DCAF1/DDB/Cul4 ligase complex. Critically, depletion of DCAF1 alone did not phenocopy Vpr-mediated proteome remodeling, and the widespread effects of Vpr were therefore unlikely the result of DCAF1 depletion. Comparison of the proteomic profiles showed depletion of at least 302 proteins and upregulation of 413 proteins by Vpr. By combining data acquired from cell proteomics, MS co-IP with epitope-tagged Vpr, and pulsed SILAC, the authors proposed at least 38 direct targets for Vpr-dependent degradation, some of which were validated by immunoblotting. The role of these 38 Vpr target proteins can be investigated in various assays described in this thesis. Depletion of the protein responsible for the function of Vpr described herein would prevent activation of various innate signalling pathways and expression from a CMV promoter-driven plasmid but not from EF1α or ubiquitin promoter-driven plasmid. Furthermore, depletion of the Vpr target protein may prevent localisation of Vpr to the nuclear envelope.

The observations made by Greenwood et al. (2019) are limited to the CEM-T4 T cell line model. Some functions of Vpr might be exclusive to myeloid cells and may not be explained by protein targets identified in this study. An unbiased SILAC based approach could also be utilised for the discovery of novel Vpr binding partners in THP-1 cells and HEK293T cells used for characterisation of Vpr function described herein. Stable Isotope Labelling with Amino Acids in Cell Culture (SILAC) is a metabolic labelling technique for mass spectrometric (MS)-based quantitative proteomics. In a SILAC experiment, three cell populations are generated in media with light, medium and heavy isotope amino acids which are combined and analysed together by LC-MS/MS. In the MS spectra, each isotope labelled peptide appears as a doublet with a distinct difference in mass. The abundance of proteins between two samples is calculated by comparing the peak intensities (563). To carry out SILAC for Vpr interactions, THP-1 or 293T cells expressing WT Vpr or mutant VprF34I+P35N can be compared with untreated cells. VprF34I+P35N is active for cell cycle arrest function but defective for antagonism of innate immune signalling or expression from co-transfected plasmids, allowing differentiation of Vpr interactors that are

involved in cell cycle arrest from those involved in antagonism of innate immunity or expression from transfected plasmids by Vpr. The interaction of the top SILAC hits would then need to be validated by Co-IP and then tested in functional assays. Depletion of these proteins would be expected to prevent activation of various innate signalling pathways and expression from a CMV promoter-driven plasmid but not from EF1α or ubiquitin promoter-driven plasmid. Furthermore, depletion of the Vpr target protein may prevent localisation of Vpr to the nuclear envelope. It is possible that Vpr interacts with its target protein only when the inflammatory signalling pathways are activated. To explore this possibility, SILAC can be carried out with cGAMP treated or untreated THP-1 cells expressing Vpr.

# 8 References


1. Barré-Sinoussi F, Chermann JC, Rey F, Nugeyre MT, Chamaret S, Gruest J, Dauguet C, Axler-Blin C, Vézinet-Brun F, Rouzioux C, Rozenbaum W, Montagnier L. Isolation of a T-lymphotropic retrovirus from a patient at risk for acquired immune deficiency syndrome (AIDS). Rev Investig Clin. 2004;56(2):126–9.
2. Gallo RC, Salahuddin SZ, Popovic M, Shearer GM, Kaplan M, Haynes BF, Palker TJ, Redfield R, Oleske J, Safai B, White G, Foster P, Markham PD. Frequent detection and isolation of cytopathic retroviruses (HTLV-III) from patients with AIDS and at risk for AIDS. Science (80- ). 1984;4(224(4648)):500–3.
3. International Committee on Taxonomy of Viruses. Virus Taxonomy: Classification and Nomenclature of Viruses. Virus Taxonomy. 2012.
4. Yamashita M, Emerman M. Retroviral infection of non-dividing cells: Old and new perspectives. Virology. 2006. p. 88-93.
5. Alkhatib G, Combadiere C, Broder CC, Feng Y, Kennedy PE, Murphy PM, Berger EA. CC CKR5: A RANTES, MIP-1α, MIP-1β receptor as a fusion cofactor for macrophage-tropic HIV-1. Science (80- ). 1996;272(5270):1955–8.
6. Maddon PJ, Dalgleish AG, McDougal JS, Clapham PR, Weiss RA, Axel R. The T4 gene encodes the AIDS virus receptor and is expressed in the immune system and the brain. Cell. 1986;47(3):333–48.
7. Feng Y, Broder CC, Kennedy PE, Berger EA. HIV-1 entry cofactor: Functional cDNA cloning of a seven-transmembrane, G protein-coupled receptor. Science (80- ). 1996;272(5263):872–7.
8. Connor RI, Sheridan KE, Ceradini D, Choe S, Landau NR. Change in coreceptor use correlates with disease progression in HIV-1- infected individuals. J Exp Med. 1997;185(4):621–8.
9. UNAIDS. 2017 Global HIV Statistics. Fact sheet. 2018.
10. Moir S, Chun T-W, Fauci AS. Pathogenic Mechanisms of HIV Disease. Annu Rev Pathol Mech Dis. 2011;6:223–48.
11. Haase AT. Perils at mucosal front lines for HIV and SIV and their hosts. Nature Reviews Immunology. 2005. p. 783–92.
12. McCune JM. The dynamics of CD4+ T-cell depletion in HIV disease. Nature. 2001. p. 410(6831):974-9.
13. Sharp PM, Hahn BH. Origins of HIV and the AIDS pandemic. Cold Spring Harb Perspect Med. 2011;1(1).
14. Simon F, Mauclère P, Roques P, Loussert-Ajaka I, Müller-Trutwin MC, Saragosti S, Georges-Courbot MC, Barré-Sinoussi F, Brun-VÉZINET F. Identification of a new human immunodeficiency virus type 1 distinct from group M and group O. Nat Med.

1998;4(9):1032–7.

15. Plantier J-C, Leoz M, Dickerson JE, De Oliveira F, Cordonnier F, Lemée V, Damond F, Robertson DL, Simon F. A new human immunodeficiency virus derived from gorillas. Nat Med. 2009;15(8):871–2.
16. Vallari A, Holzmayer V, Harris B, Yamaguchi J, Ngansop C, Makamche F, Mbanya D, Kaptué L, Ndembi N, Gürtler L, Devare S, Brennan CA. Confirmation of putative HIV-1 group P in Cameroon. J Virol. 2011;85(3):1403–7.
17. Mourez T, Simon F, Plantiera JC. Non-M variants of human immunodeficiency virus type. Clin Microbiol Rev. 2013;26(3):448–61.
18. Geretti AM. HIV-1 subtypes: Epidemiology and significance for HIV management. Current Opinion in Infectious Diseases. 2006. p. 19(1):1-7.
19. Foster GM, Ambrose JC, Hué S, Delpech VC, Fearnhill E, Abecasis AB, Leigh Brown AJ, Geretti AM. Novel HIV-1 recombinants spreading across multiple risk groups in the United Kingdom: The identification and phylogeography of circulating recombinant form (CRF) 50-A1D. PLoS One. 2014;15;9(1):e8.
20. Pereira LA, Bentley K, Peeters A, Churchill MJ, Deacon NJ. A compilation of cellular transcription factor interactions with the HIV-1 LTR promoter. Nucleic Acids Res. 2000;28(3):663–8.
21. Jacks T, Power MD, Masiarz FR, Luciw PA, Barr PJ, Varmus HE. Characterization of ribosomal frameshifting in HIV-1 gag-pol expression. Nature. 1988;331(6153):280–3.
22. Hallenberger S, Bosch V, Angliker H, Shaw E, Klenk HD, Garten W. Inhibition of furin-mediated cleavage activation of HIV-1 glycoprotein gpl60. Nature. 1992;360(6402):358–61.
23. Briggs JAG, Wilk T, Welker R, Kräusslich HG, Fuller SD. Structural organization of authentic, mature HIV-1 virions and cores. EMBO J. 2003;22(7):1707–15.
24. Zhu P, Liu J, Bess Jr. J, Chertova E, Lifson JD, Grisé H, Ofek GA, Taylor KA, Roux KH. Distribution and three-dimensional structure of AIDS virus envelope spikes. Nature. 2006;441(7095):847–52.
25. Bachand F, Yao X-J, Hrimech M, Rougeau N, Cohen ÉA. Incorporation of Vpr into human immunodeficiency virus type 1 requires a direct interaction with the p6 domain of the p55 Gag precursor. J Biol Chem. 1999;274(13):9083–91.
26. Ward AB, Wilson IA. The HIV-1 envelope glycoprotein structure: nailing down a moving target. Immunol Rev. 2017;275(1):21–32.
27. Hartley O, Klasse PJ, Sattentau QJ, Moore JP. V3: HIV's switch-hitter. AIDS Res Hum Retroviruses. 2005;21(2):171–89.
28. Sabin C, Corti D, Buzon V, Seaman MS, Hulsik DL, Hinz A, Vanzetta F, Agatic G, Silacci C, Mainetti L, Scarlatti G, Sallusto F, Weiss R, Lanzavecchia A, Weissenhorn W. Crystal structure and size-dependent neutralization properties of

HK20, a human monoclonal antibody binding to the highly conserved heptad repeat 1 of gp41. PLoS Pathog. 2010;6(11).

29. Geijtenbeek TBH, Kwon DS, Torensma R, Van Vliet SJ, Van Duijnhoven GCF, Middel J, Cornelissen ILMH., Nottet HSL., KewalRamani VN, Littman DR, Figdor CG, Van Kooyk Y. DC-SIGN, a dendritic cell-specific HIV-1-binding protein that enhances trans-infection of T cells. Cell. 2000;100(5):587–97.
30. Saphire ACS, Bobardt MD, Zhang Z, David G, Gallay PA. Syndecans serve as attachment receptors for human immunodeficiency virus type 1 on macrophages. J Virol. 2001;75(19):9187–200.
31. Orloff GM, Orloff SL, Kennedy MS, Maddon PJ, McDougal JS. Penetration of CD4 T cells by HIV-1: The CD4 receptor does not internalize with HIV, and CD4-related signal transduction events are not required for entry. J Immunol. 1991;146(8):2578–87.
32. Kwong PD, Wyatt R, Robinson J, Sweet RW, Sodroski J, Hendrickson WA. Structure of an HIV gp 120 envelope glycoprotein in complex with the CD4 receptor and a neutralizing human antibody. Nature. 1998;393(6686):648–59.
33. Berger EA, Doms RW, Fenyo E-M, Korber BTM, Littman DR, Moore JP, Sattentau QJ, Schuitemaker H, Sodroski J, Weiss RA. A new classification for HIV-1 [6]. Nature. 1998;391(6664):240.
34. Chan DC, Fass D, Berger JM, Kim PS. Core structure of gp41 from the HIV envelope glycoprotein. Cell. 1997;89(2):263–73.
35. Weissenhorn W, Dessen A, Harrison SC, Skehel JJ, Wiley DC. Atomic structure of the ectodomain from HIV-1 gp41. Nature. 1997;387(6631):426–30.
36. Melikyan GB. Common principles and intermediates of viral protein-mediated fusion: The HIV-1 paradigm. Retrovirology. 2008;5(111):123–9.
37. McClure MO, Marsh M, Weiss RA. Human immunodeficiency virus infection of CD4-bearing cells occurs by a pH-independent mechanism. EMBO J. 1988;7(2):513–8.
38. Herold N, Anders-Ößwein M, Glass B, Eckhardt M, Müller B, Kräusslich H-G. HIV-1 entry in SupT1-R5, CEM-ss, and primary CD4+ T cells occurs at the plasma membrane and does not require endocytosis. J Virol. 2014;88(24):13956–70.
39. Kirchhausen T, Macia E, Pelish HE. Use of Dynasore, the Small Molecule Inhibitor of Dynamin, in the Regulation of Endocytosis. Methods in Enzymology. 2008. p. 438:77-93.
40. Miyauchi K, Kim Y, Latinovic O, Morozov V, Melikyan GB. HIV Enters Cells via Endocytosis and Dynamin-Dependent Fusion with Endosomes. Cell. 2009;137(3):433–44.
41. Jones DM, Alvarez LA, Nolan R, Ferriz M, Sainz Urruela R, Massana-Muñoz X, Novak-Kotzer H, Dustin ML, Padilla-Parra S. Dynamin-2 Stabilizes the HIV-1 Fusion Pore with a Low Oligomeric State. Cell Rep. 2017;18(2):443–53.

42. Mellman I. ENDOCYTOSIS AND MOLECULAR SORTING. Annu Rev Cell Dev Biol. 2002;12:575–625.
43. Russell RA, Chojnacki J, Jones DM, Johnson E, Do T, Eggeling C, Padilla-Parra S, Sattentau QJ. Astrocytes Resist HIV-1 Fusion but Engulf Infected Macrophage Material. Cell Rep. 2017;18(6):1473–83.
44. Dragic T, Trkola A, Thompson DAD, Cormier EG, Kajumo FA, Maxwell E, Lin SW, Ying W, Smith SO, Sakmar TP, Moore JP. A binding pocket for a small molecule inhibitor of HIV-1 entry within the transmembrane helices of CCR5. Proc Natl Acad Sci. 2000;97(10):5639–44.
45. Westby M, Smith-Burchnell C, Mori J, Lewis M, Mosley M, Stockdale M, Dorr P, Ciaramella G, Perros M. Reduced Maximal Inhibition in Phenotypic Susceptibility Assays Indicates that Viral Strains Resistant to the CCR5 Antagonist Maraviroc Utilize Inhibitor-Bound Receptor for Entry. J Virol. 2007;81(5):2359–71.
46. Zhao G, Perilla JR, Yufenyuy EL, Meng X, Chen B, Ning J, Ahn J, Gronenborn AM, Schulten K, Aiken C, Zhang P. Mature HIV-1 capsid structure by cryo-electron microscopy and all-atom molecular dynamics. Nature. 2013;497(7451):643–6.
47. Mattei S, Glass B, Hagen WJH, Kräusslich H-G, Briggs JAG. The structure and flexibility of conical HIV-1 capsids determined within intact virions. Science (80- ). 2016;354(6318):1434–7.
48. Rankovic S, Ramalho R, Aiken C, Rousso I. PF74 Reinforces the HIV-1 Capsid To Impair Reverse Transcription-Induced Uncoating. J Virol. 2018;92(20):845–18.
49. Du S, Betts L, Yang R, Shi H, Concel J, Ahn J, Aiken C, Zhang P, Yeh JI. Structure of the HIV-1 full-length capsid protein in a conformationally trapped unassembled state induced by small-molecule binding. J Mol Biol. 2011;406(3):371–86.
50. Cosnefroy O, Murray PJ, Bishop KN. HIV-1 capsid uncoating initiates after the first strand transfer of reverse transcription. Retrovirology. 2016;13(1):58.
51. Arhel NJ, Souquere-Besse S, Munier S, Souque P, Guadagnini S, Rutherford S, Prévost M-C, Allen TD, Charneau P. HIV-1 DNA Flap formation promotes uncoating of the pre-integration complex at the nuclear pore. EMBO J. 2007;26(12):3025–37.
52. Yang Y, Fricke T, Diaz-Griffero F. Inhibition of Reverse Transcriptase Activity Increases Stability of the HIV-1 Core. J Virol. 2013;87(1):683–7.
53. Hulme AE, Perez O, Hope TJ. Complementary assays reveal a relationship between HIV-1 uncoating and reverse transcription. Proc Natl Acad Sci. 2011;108(24):9975–80.
54. Rankovic S, Varadarajan J, Ramalho R, Aiken C, Rousso I. Reverse transcription mechanically initiates HIV-1 capsid disassembly. J Virol. 2017;91(12).
55. Jacques DA, McEwan WA, Hilditch L, Price AJ, Towers GJ, James LC. HIV-1 uses dynamic capsid pores to import nucleotides and fuel encapsidated DNA synthesis. Nature. 2016;536(7616):349–53.

56. Lightfoote MM, Coligan JE, Folks TM, Fauci AS, Martin MA, Venkatesan S. Structural characterization of reverse transcriptase and endonuclease polypeptides of the acquired immunodeficiency syndrome retrovirus. J Virol. 1986;60(2):771–5.
57. Kohlstaedt LA, Wang J, Friedman JM, Rice PA, Steitz TA. Crystal structure at 3.5 Å resolution of HIV-1 reverse transcriptase complexed with an inhibitor. Science (80- ). 1992;256(5065):1783–90.
58. Isel C, Lanchy J-M, Le Grice SFJ, Ehresmann C, Ehresmann B, Marquet R. Specific initiation and switch to elongation of human immunodeficiency virus type 1 reverse transcription require the post-transcriptional modifications of primer tRNALys. EMBO J. 1996;15(4):917–24.
59. Purohit V, Roques BP, Kim B, Bambara RA. Mechanisms that prevent template inactivation by HIV-1 reverse transcriptase RNase H cleavages. J Biol Chem. 2007;282(17):12598–609.
60. Panganiban AT, Fiore D. Ordered interstrand and intrastrand DNA transfer during reverse transcription. Science. 1988;241(4869):1064–9.
61. Charneau P, Alizon M, Clavel F. A second origin of DNA plus-strand synthesis is required for optimal human immunodeficiency virus replication. J Virol. 1992;66(5):2814–20.
62. Smith JS, Roth MJ. Specificity of human immunodeficiency virus-1 reverse transcriptase- associated ribonuclease H in removal of the minus-strand primer, tRNA(Lys3). J Biol Chem. 1992;267(21):15071–9.
63. Schaller T, Ocwieja KE, Rasaiyaah J, Price AJ, Brady TL, Roth SL, Hué S, Fletcher AJ, Lee K, KewalRamani VN, Noursadeghi M, Jenner RG, James LC, Bushman FD, Towers GJ. HIV-1 capsid-cyclophilin interactions determine nuclear import pathway, integration targeting and replication efficiency. PLoS Pathog. 2011;7(12).
64. Lee K, Ambrose Z, Martin TD, Oztop I, Mulky A, Julias JG, Vandegraaff N, Baumann JG, Wang R, Yuen W, Takemura T, Shelton K, Taniuchi I, Li Y, Sodroski J, Littman DR, Coffin JM, Hughes SH, Unutmaz D, et al. Flexible Use of Nuclear Import Pathways by HIV-1. Cell Host Microbe. 2010;7(3):221–33.
65. Yamashita M, Emerman M. Capsid is a dominant determinant of retrovirus infectivity in nondividing cells. J Virol. 2004;78(11):5670–8.
66. Yamashita M, Perez O, Hope TJ, Emerman M. Evidence for direct involvement of the capsid protein in HIV infection of nondividing cells. PLoS Pathog. 2007;3(10):1502–10.
67. Peng K, Muranyi W, Glass B, Laketa V, Yant SR, Tsai L, Cihlar T, Müller B, Kräusslich H-G. Quantitative microscopy of functional HIV post-entry complexes reveals association of replication with the viral capsid. Elife. 2014;3:e04114.
68. Bejarano DA, Peng K, Laketa V, Börner K, Jost KL, Lucic B, Glass B, Lusic M, Müller B, Kräusslich H-G. HIV-1 nuclear import in macrophages is regulated by

CPSF6-capsid interactions at the nuclear pore complex. Elife. 2019;8:e41800.

69. Koh Y, Wu X, Ferris AL, Matreyek KA, Smith SJ, Lee K, Kewalramani VN, Hughes SH, Engelman A. Differential effects of human immunodeficiency virus type 1 capsid and cellular factors nucleoporin 153 and LEDGF/p75 on the efficiency and specificity of viral DNA integration. J Virol. 2013;87(1):648–58.
70. Luban J, Bossolt KL, Franke EK, Kalpana G V, Goff SP. Human immunodeficiency virus type 1 Gag protein binds to cyclophilins A and B. Cell. 1993;73(6):1067–78.
71. Braaten D, Franke EK, Luban J. Cyclophilin A is required for an early step in the life cycle of human immunodeficiency virus type 1 before the initiation of reverse transcription. J Virol. 1996;70(6):3551–60.
72. Sokolskaja E, Sayah DM, Luban J. Target cell cyclophilin A modulates human immunodeficiency virus type 1 infectivity. J Virol. 2004;78(23):12800–8.
73. Bosco DA, Eisenmesser EZ, Pochapsky S, Sundquist WI, Kern D. Catalysis of cis/trans isomerization in native HIV-1 capsid by human cyclophilin A. Proc Natl Acad Sci U S A. 2002;99(8):5247–52.
74. Gamble TR, Vajdos FF, Yoo S, Worthylake DK, Houseweart M, Sundquist WI, Hill CP. Crystal structure of human cyclophilin A bound to the amino-terminal domain of HIV-1 capsid. Cell. 1996;87(7):1285–94.
75. Hatziioannou T, Perez-Caballero D, Cowan S, Bieniasz PD. Cyclophilin interactions with incoming human immunodeficiency virus type 1 capsids with opposing effects on infectivity in human cells. J Virol. 2005;79(1):176–83.
76. Liu C, Perilla JR, Ning J, Lu M, Hou G, Ramalho R, Himes BA, Zhao G, Bedwell GJ, Byeon I-J, Ahn J, Gronenborn AM, Prevelige PE, Rousso I, Aiken C, Polenova T, Schulten K, Zhang P. Cyclophilin A stabilizes the HIV-1 capsid through a novel non-canonical binding site. Nat Commun. 2016;7(10714):234–78.
77. Fricke T, Brandariz-Nunez A, Wang X, Smith AB, Diaz-Griffero F. Human Cytosolic Extracts Stabilize the HIV-1 Core. J Virol. 2013;87(19):10587–97.
78. Rasaiyaah J, Tan CP, Fletcher AJ, Price AJ, Blondeau C, Hilditch L, Jacques DA, Selwood DL, James LC, Noursadeghi M, Towers GJ. HIV-1 evades innate immune recognition through specific cofactor recruitment. Nature. 2013;503(7476):402–5.
79. Wu J, Matunis MJ, Kraemer D, Blobel G, Coutavas E. Nup358, a cytoplasmically exposed nucleoporin with peptide repeats, Ran- GTP binding sites, zinc fingers, a cyclophilin A homologous domain, and a leucine-rich region. J Biol Chem. 1995;270(23):14209–13.
80. Brass AL, Dykxhoorn DM, Benita Y, Yan N, Engelman A, Xavier RJ, Lieberman J, Elledge SJ. Identification of host proteins required for HIV infection through a functional genomic screen. Science (80- ). 2008;319(5865):921–6.
81. Bichel K, Price AJ, Schaller T, Towers GJ, Freund SM V, James LC. HIV-1 capsid undergoes coupled binding and isomerization by the nuclear pore protein NUP358.

Retrovirology. 2013;10(1).

82. Meehan AM, Saenz DT, Guevera R, Morrison JH, Peretz M, Fadel HJ, Hamada M, van Deursen J, Poeschla EM. A Cyclophilin Homology Domain-Independent Role for Nup358 in HIV-1 Infection. PLoS Pathog. 2014;10(2).
83. Strambio-De-Castillia C, Niepel M, Rout MP. The nuclear pore complex: Bridging nuclear transport and gene regulation. Nat Rev Mol Cell Biol. 2010;11(7):490–501.
84. König R, Zhou Y, Elleder D, Diamond TL, Bonamy GMC, Irelan JT, Chiang C -y., Tu BP, De Jesus PD, Lilley CE, Seidel S, Opaluch AM, Caldwell JS, Weitzman MD, Kuhen KL, Bandyopadhyay S, Ideker T, Orth AP, Miraglia LJ, et al. Global Analysis of Host-Pathogen Interactions that Regulate Early-Stage HIV-1 Replication. Cell. 2008;135(1):49–60.
85. Matreyek KA, Engelman A. The requirement for nucleoporin NUP153 during human immunodeficiency virus type 1 infection is determined by the viral capsid. J Virol. 2011;85(15):7818–27.
86. Zwerger M, Eibauer M, Medalia O. Insights into the gate of the nuclear pore complex. Nucleus. 2016;7(1):1–7.
87. Matreyek KA, Yücel SS, Li X, Engelman A. Nucleoporin NUP153 Phenylalanine-Glycine Motifs Engage a Common Binding Pocket within the HIV-1 Capsid Protein to Mediate Lentiviral Infectivity. PLoS Pathog. 2013;9(10).
88. Price AJ, Jacques DA, McEwan WA, Fletcher AJ, Essig S, Chin JW, Halambage UD, Aiken C, James LC. Host Cofactors and Pharmacologic Ligands Share an Essential Interface in HIV-1 Capsid That Is Lost upon Disassembly. PLoS Pathog. 2014;10(10).
89. Long JC, Caceres JF. The SR protein family of splicing factors: master regulators of gene expression. Biochem J. 2008;417(1):15–27.
90. Maertens GN, Cook NJ, Wang W, Hare S, Gupta SS, Oztop I, Lee K, Pye VE, Cosnefroy O, Snijders AP, KewalRamani VN, Fassati A, Engelman A, Cherepanov P. Structural basis for nuclear import of splicing factors by human Transportin 3. Proc Natl Acad Sci. 2014;111(7):2728–33.
91. Hori T, Takeuchi H, Saito H, Sakuma R, Inagaki Y, Yamaoka S. A carboxy-terminally truncated human CPSF6 lacking residues encoded by exon 6 inhibits HIV-1 cDNA synthesis and promotes capsid disassembly. J Virol. 2013;87(13):7726–36.
92. Lee KE, Mulky A, Yuen W, Martin TD, Meyerson NR, Choi L, Yu H, Sawyer SL, KewalRamani VN. HIV-1 capsid-targeting domain of cleavage and polyadenylation specificity factor 6. J Virol. 2012;86(7):3851–60.
93. Achuthan V, Perreira JM, Sowd GA, Puray-Chavez M, McDougall WM, Paulucci-Holthauzen A, Wu X, Fadel HJ, Poeschla EM, Multani AS, Hughes SH, Sarafianos SG, Brass AL, Engelman AN. Capsid-CPSF6 Interaction Licenses Nuclear HIV-1

Trafficking to Sites of Viral DNA Integration. Cell Host Microbe. 2018;24(3):392–404.

94. Craigie R, Bushman FD. HIV DNA integration. Cold Spring Harb Perspect Med. 2012;2(7).

95. Engelman A, Bushman FD, Craigie R. Identification of discrete functional domains of HIV-1 integrase and their organization within an active multimeric complex. EMBO J. 1993;12(8):3269–75.

96. Carayon K, leh H, Henry E, Simon F, Mouscadet J-F, Deprez E. A cooperative and specific DNA-binding mode of HIV-1 integrase depends on the nature of the metallic cofactor and involves the zinc-containing N-terminal domain. Nucleic Acids Res. 2010;38(11):3692–708.

97. Craigie R. HIV Integrase, a Brief Overview from Chemistry to Therapeutics. J Biol Chem. 2001;276(26):23213–6.

98. Manganaro L, Lusic M, Gutierrez MI, Cereseto A, Del Sal G, Giacca M. Concerted action of cellular JNK and Pin1 restricts HIV-1 genome integration to activated CD4+ T lymphocytes. Nat Med. 2010;16(3):329–33.

99. Dyda F, Hickman AB, Jenkins TM, Engelman A, Craigie R, Davies DR. Crystal structure of the catalytic domain of HIV-1 integrase: Similarity to other polynucleotidyl transferases. Science (80- ). 1994;266(5193):1981–6.

100. Eijkelenboom APAM, Van Den Ent FMI, Vos A, Doreleijers JF, Hård K, Tullius TD, Plasterk RHA, Kaptein R, Boelens R. The solution structure of the amino-terminal HHCC domain of HIV-2 integrase: A three-helix bundle stabilized by zinc. Curr Biol. 1997;7(10):739–46.

101. Cereseto A, Manganaro L, Gutierrez MI, Terreni M, Fittipaldi A, Lusic M, Marcello A, Giacca M. Acetylation of HIV-1 integrase by p300 regulates viral integration. EMBO J. 2005;24(17):3070–81.

102. Hare S, Gupta SS, Valkov E, Engelman A, Cherepanov P. Retroviral intasome assembly and inhibition of DNA strand transfer. Nature. 2010;464(7286):232–6.

103. Li L, Olvera JM, Yoder KE, Mitchell RS, Butler SL, Lieber M, Martin SL, Bushman FD. Role of the non-homologous DNA end joining pathway in the early steps of retroviral infection. EMBO J. 2001;20(12):3272–81.

104. Kilzer JM, Stracker T, Beitzel B, Meek K, Weitzman M, Bushman FD. Roles of host cell factors in circularization of retroviral DNA. Virology. 2003;314(1):460–7.

105. Cullen BR, Lomedico PT, Ju G. Transcriptional interference in avian retroviruses - implications for the promoter insertion model of leukaemogenesis. Nature. 1984;307(5948):241–5.

106. Klaver B, Berkhout B. Comparison of 5' and 3' long terminal repeat promoter function in human immunodeficiency virus. J Virol. 1994;68(6):3830–40.

107. Brady J, Kashanchi F. Tat gets the "Green" light on transcription initiation.

Retrovirology. 2005. p. 2:69.

108. Berkhout B, Silverman RH, Jeang KT. Tat trans-activates the human immunodeficiency virus through a nascent RNA target. Cell. 1989;59(2):273–82.
109. Raha T, Cheng SWG, Green MR. HIV-1 Tat stimulates transcription complex assembly through recruitment of TBP in the absence of TAFs. PLoS Biol. 2005;3(2):e44.
110. Wei P, Garber ME, Fang SM, Fischer WH, Jones KA. A novel CDK9-associated C-type cyclin interacts directly with HIV-1 Tat and mediates its high-affinity, loop-specific binding to TAR RNA. Cell. 1998;92(4):451–62.
111. Yamaguchi Y, Takagi T, Wada T, Yano K, Furuya A, Sugimoto S, Hasegawa J, Handa H. NELF, a multisubunit complex containing RD, cooperates with DSIF to repress RNA polymerase II elongation. Cell. 1999;97(1):41–51.
112. Wada T, Takagi T, Yamaguchi Y, Watanabe D, Handa H. Evidence that P-TEFb alleviates the negative effect of DSIF on RNA polymerase II-dependent transcription in vitro. EMBO J. 1998;
113. Komarnitsky P, Cho EJ, Buratowski S. Different phosphorylated forms of RNA polymerase II and associated mRNA processing factors during transcription. Genes Dev. 2000;
114. Zhou M, Halanski MA, Radonovich MF, Kashanchi F, Peng J, Price DH, Brady JN. Tat modifies the activity of CDK9 to phosphorylate serine 5 of the RNA polymerase II carboxyl-terminal domain during human immunodeficiency virus type 1 transcription. Mol Cell Biol. 2000;
115. Chiu YL, Ho CK, Saha N, Schwer B, Shuman S, Rana TM. Tat stimulates cotranscriptional capping of HIV mRNA. Mol Cell. 2002;
116. Zhou M, Deng L, Kashanchi F, Brady JN, Shatkin AJ, Kumar A. The Tat/TAR-dependent phosphorylation of RNA polymerase II C-terminal domain stimulates cotranscriptional capping of HIV-1 mRNA. Proc Natl Acad Sci. 2003;
117. Ho CK, Shuman S. Distinct roles for CTD Ser-2 and Ser-5 phosphorylation in the recruitment and allosteric activation of mammalian mRNA capping enzyme. Mol Cell. 1999;
118. Cherrington J, Ganem D. Regulation of polyadenylation in human immunodeficiency virus (HIV): contributions of promoter proximity and upstream sequences. EMBO J. 1992;
119. Ashe MP, Pearson LH, Proudfoot NJ. The HIV-1 5' LTR poly (A) site is inactivated by U1 snRNP interaction with the downstream major splice donor site. EMBO J. 1997;
120. Gilmartin GM, Fleming ES, Oetjen J, Graveley BR. CPSF recognition of an HIV-1 mRNA 3′-processing enhancer: Multiple sequence contacts involved in poly(A) site definition. Genes Dev. 1995;

121. Blencowe BJ. Exonic splicing enhancers: Mechanism of action, diversity and role in human genetic diseases. Trends in Biochemical Sciences. 2000.
122. GRAVELEY BR. Sorting out the complexity of SR protein functions. RNA. 2000;
123. Purcell DF, Martin MA. Alternative splicing of human immunodeficiency virus type 1 mRNA modulates viral protein expression, replication, and infectivity. J Virol. 1993;
124. Nasioulas G, Zolotukhin AS, Tabernero C, Solomin L, Cunningham CP, Pavlakis GN, Felber BK. Elements distinct from human immunodeficiency virus type 1 splice sites are responsible for the Rev dependence of env mRNA. J Virol. 1994;
125. Cullen BR. Nuclear RNA export. J Cell Sci. 2003;116(4):587–97.
126. Cullen BR. Nuclear mRNA export: Insights from virology. Trends in Biochemical Sciences. 2003.
127. Suhasini M, Reddy T. Cellular Proteins and HIV-1 Rev Function. Curr HIV Res. 2009;
128. Bolinger C, Boris-Lawrie K. Mechanisms employed by retroviruses to exploit host factors for translational control of a complicated proteome. Retrovirology. 2009.
129. De Breyne S, Chamond N, Décimo D, Trabaud MA, André P, Sargueil B, Ohlmann T. In vitro studies reveal that different modes of initiation on HIV-1 mRNA have different levels of requirement for eukaryotic initiation factor 4F. FEBS J. 2012;
130. Jacks T, Power MD, Masiarz FR, Luciw PA, Barr PJ, Varmus HE. Characterization of ribosomal frameshifting in HIV-1 gag-pol expression. Nature. 1988;331(6153):280–3.
131. Anderson JL, Johnson AT, Howard JL, Purcell DFJ. Both Linear and Discontinuous Ribosome Scanning Are Used for Translation Initiation from Bicistronic Human Immunodeficiency Virus Type 1 env mRNAs. J Virol. 2007;
132. Vallejos M, Carvajal F, Pino K, Navarrete C, Ferres M, Huidobro-Toro JP, Sargueil B, López-Lastra M. Functional and structural analysis of the internal ribosome entry site present in the mrna of natural variants of the hiv-1. PLoS One. 2012;
133. Gendron K, Ferbeyre G, Heveker N, Brakier-Gingras L. The activity of the HIV-1 IRES is stimulated by oxidative stress and controlled by a negative regulatory element. Nucleic Acids Res. 2011;
134. Amorim R, Costa SM, Cavaleiro NP, Da Silva EE, Da Costa LJ. HIV-1 transcripts use ires-initiation under conditions where cap-dependent translation is restricted by poliovirus 2A protease. PLoS One. 2014;
135. Buck CB, Shen X, Egan MA, Pierson TC, Walker CM, Siliciano RF. The Human Immunodeficiency Virus Type 1 gag Gene Encodes an Internal Ribosome Entry Site. J Virol. 2002;
136. Ono A, Freed EO. Cell-Type-Dependent Targeting of Human Immunodeficiency Virus Type 1 Assembly to the Plasma Membrane and the Multivesicular Body. J

Virol. 2004;78(3):1552–63.

137. Ono A, Ablan SD, Lockett SJ, Nagashima K, Freed EO. Phosphatidylinositol (4,5) bisphosphate regulates HIV-1 Gag targeting to the plasma membrane. Proc Natl Acad Sci U S A. 2004;101(41):14889–94.
138. Saad JS, Miller J, Tai J, Kim A, Ghanam RH, Summers MF. Structural basis for targeting HIV-1 Gag proteins to the plasma membrane for virus assembly. Proc Natl Acad Sci U S A. 2006;103(30):11364–9.
139. Hogue IB, Grover JR, Soheilian F, Nagashima K, Ono A. Gag induces the coalescence of clustered lipid rafts and tetraspanin-enriched microdomains at HIV-1 assembly sites on the plasma membrane. J Virol. 2011;85(19):9749–66.
140. Chen J, Nikolaitchik O, Singh J, Wright A, Bencsics CE, Coffin JM, Ni N, Lockett S, Pathak VK, Hu W-S. High efficiency of HIV-1 genomic RNA packaging and heterozygote formation revealed by single virion analysis. Proc Natl Acad Sci U S A. 2009;106(32):13535–40.
141. Nikolaitchik OA, Dilley KA, Fu W, Gorelick RJ, Tai S-HS, Soheilian F, Ptak RG, Nagashima K, Pathak VK, Hu W-S. Dimeric RNA Recognition Regulates HIV-1 Genome Packaging. PLoS Pathog. 2013;9(3).
142. Moore MD, Nikolaitchik OA, Chen J, Hammarskjöld M-L, Rekosh D, Hu W-S. Probing the HIV-1 genomic RNA trafficking pathway and dimerization by genetic recombination and single virion analyses. PLoS Pathog. 2009;5(10).
143. Levin JG, Guo J, Rouzina I, Musier-Forsyth K. Nucleic Acid Chaperone Activity of HIV-1 Nucleocapsid Protein: Critical Role in Reverse Transcription and Molecular Mechanism [Internet]. Vol. 80, Progress in Nucleic Acid Research and Molecular Biology. 2005. p. 217–86.
144. Lu K, Heng X, Summers MF. Structural determinants and mechanism of HIV-1 genome packaging. J Mol Biol. 2011;410(4):609–33.
145. Checkley MA, Luttge BG, Freed EO. HIV-1 envelope glycoprotein biosynthesis, trafficking, and incorporation. J Mol Biol. 2011;410(4):582–608.
146. Hanson PI, Shim S, Merrill SA. Cell biology of the ESCRT machinery. Curr Opin Cell Biol. 2009;21(4):568–74.
147. Hurley JH, Emr SD. The ESCRT complexes: Structure and mechanism of a membrane-trafficking network [Internet]. Vol. 35, Annual Review of Biophysics and Biomolecular Structure. 2006. p. 277–98.
148. Wollert T, Hurley JH. Molecular mechanism of multivesicular body biogenesis by ESCRT complexes. Nature. 2010;464(7290):864–9.
149. Hurley JH, Hanson PI. Membrane budding and scission by the ESCRT machinery: It's all in the neck. Nat Rev Mol Cell Biol. 2010;11(8):556–66.
150. Martin-Serrano J, Zang T, Bieniasz PD. HIV-1 and Ebola virus encode small peptide motifs that recruit Tsg101 to sites of particle assembly to facilitate egress. Nat Med.

2001;7(12):1313–9.

151. Fujii K, Munshi UM, Ablan SD, Demirov DG, Soheilian F, Nagashima K, Stephen AG, Fisher RJ, Freed EO. Functional role of Alix in HIV-1 replication. Virology. 2009;391(2):284–92.
152. Hanson PI, Roth R, Lin Y, Heuser JE. Plasma membrane deformation by circular arrays of ESCRT-III protein filaments. J Cell Biol. 2008;180(2):389–402.
153. Raiborg C, Stenmark H. The ESCRT machinery in endosomal sorting of ubiquitylated membrane proteins. Nature. 2009;458(7237):445–52.
154. Gottwein E, Kräusslich H-G. Analysis of human immunodeficiency virus type 1 Gag ubiquitination. J Virol. 2005;79(14):9134–44.
155. Wlodawer A, Erickson JW. Structure-based inhibitors of HIV-1 protease [Internet]. Vol. 62, Annual Review of Biochemistry. 1993. p. 543–85.
156. Kaplan AH, Zack JA, Knigge M, Paul DA, Kempf DJ, Norbeck DW, Swanstrom R. Partial inhibition of the human immunodeficiency virus type 1 protease results in aberrant virus assembly and the formation of noninfectious particles. J Virol. 1993;67(7):4050–5.
157. Wagner JM, Zadrozny KK, Chrustowicz J, Purdy MD, Yeager M, Ganser-Pornillos BK, Pornillos O. Crystal structure of an HIV assembly and maturation switch. Elife. 2016;5(2016JULY).
158. Mallery DL, Márquez CL, McEwan WA, Dickson CF, Jacques DA, Anandapadamanaban M, Bichel K, Towers GJ, Saiardi A, Böcking T, James LC. IP6 is an HIV pocket factor that prevents capsid collapse and promotes DNA synthesis. Elife. 2018;31(7):e35335.
159. Dick RA, Zadrozny KK, Xu C, Schur FKM, Lyddon TD, Ricana CL, Wagner JM, Perilla JR, Ganser-Pornillos BK, Johnson MC, Pornillos O, Vogt VM. Inositol phosphates are assembly co-factors for HIV-1. Nature. 2018. p. 560(7719):509-512.
160. Brubaker SW, Bonham KS, Zanoni I, Kagan JC. Innate Immune Pattern Recognition: A Cell Biological Perspective. Annu Rev Immunol. 2015;33:257–90.
161. Chow J, Franz KM, Kagan JC. PRRs are watching you: Localization of innate sensing and signaling regulators. Virology. 2015;479–480:104–9.
162. Akira S, Uematsu S, Takeuchi O. Pathogen recognition and innate immunity. Cell. 2006;
163. Gentili M, Lahaye X, Nadalin F, Nader GPF, Puig Lombardi E, Herve S, De Silva NS, Rookhuizen DC, Zueva E, Goudot C, Maurin M, Bochnakian A, Amigorena S, Piel M, Fachinetti D, Londono-Vallejo A, Manel N. The N-Terminal Domain of cGAS Determines Preferential Association with Centromeric DNA and Innate Immune Activation in the Nucleus. Cell Rep. 2019 Feb;26(9):2377-2393.e13.
164. Barnett KC, Coronas-Serna JM, Zhou W, Ernandes MJ, Cao A, Kranzusch PJ,

Kagan JC. Phosphoinositide Interactions Position cGAS at the Plasma Membrane to Ensure Efficient Distinction between Self- and Viral DNA. Cell. 2019 Mar;176(6):1432-1446.e11.

165. Rustagi A, Gale Jr. M. Innate antiviral immune signaling, viral evasion and modulation by HIV-1. J Mol Biol. 2014;426(6):1161–77.
166. Jain A, Pasare C. Innate Control of Adaptive Immunity: Beyond the Three-Signal Paradigm. J Immunol. 2017;
167. Sun L, Wu J, Du F, Chen X, Chen ZJ. Cyclic GMP-AMP synthase is a cytosolic DNA sensor that activates the type I interferon pathway. Science (80- ). 2013;339(6121):786–91.
168. Civril F, Deimling T, De Oliveira Mann CC, Ablasser A, Moldt M, Witte G, Hornung V, Hopfner K-P. Structural mechanism of cytosolic DNA sensing by cGAS. Nature. 2013;498(7454):332–7.
169. Li X-D, Wu J, Gao D, Wang H, Sun L, Chen ZJ. Pivotal roles of cGAS-cGAMP signaling in antiviral defense and immune adjuvant effects. Science (80- ). 2013;341(6152):1390–4.
170. Liu H, Zhang H, Wu X, Ma D, Wu J, Wang L, Jiang Y, Fei Y, Zhu C, Tan R, Jungblut P, Pei G, Dorhoi A, Yan Q, Zhang F, Zheng R, Liu S, Liang H, Liu Z, et al. Nuclear cGAS suppresses DNA repair and promotes tumorigenesis. Nature. 2018 Nov;563(7729):131–6.
171. Kranzusch P, Lee A-Y, Berger J, Doudna J. Structure of Human cGAS Reveals a Conserved Family of Second-Messenger Enzymes in Innate Immunity. Cell Rep. 2013;3(5):1362–8.
172. Li X, Shu C, Yi G, Chaton CT, Shelton CL, Diao J, Zuo X, Kao C, Herr AB, Li P. Cyclic GMP-AMP Synthase Is Activated by Double-Stranded DNA-Induced Oligomerization. Immunity. 2013;39(6):1019–31.
173. Zhang X, Wu J, Du F, Xu H, Sun L, Chen Z, Brautigam CA, Zhang X, Chen ZJ. The cytosolic DNA sensor cGAS forms an oligomeric complex with DNA and undergoes switch-like conformational changes in the activation loop. Cell Rep. 2014;6(3):421–30.
174. Du M, Chen ZJ. DNA-induced liquid phase condensation of cGAS activates innate immune signaling. Science. 2018 Aug;361(6403):704–9.
175. Wu J, Sun L, Chen X, Du F, Shi H, Chen C, Chen ZJ. Cyclic GMP-AMP is an endogenous second messenger in innate immune signaling by cytosolic DNA. Science (80- ). 2013;339(6121):826–30.
176. Gao P, Ascano M, Wu Y, Barchet W, Gaffney BL, Zillinger T, Serganov AA, Liu Y, Jones RA, Hartmann G, Tuschl T, Patel DJ. Cyclic [G(2′,5′)pA(3′,5′)p] is the metazoan second messenger produced by DNA-activated cyclic GMP-AMP synthase. Cell. 2013;153(5):1094–107.

177. Ablasser A, Goldeck M, Cavlar T, Deimling T, Witte G, Röhl I, Hopfner K-P, Ludwig J, Hornung V. CGAS produces a 2′-5′-linked cyclic dinucleotide second messenger that activates STING. Nature. 2013;498(7454):380–4.
178. Ablasser A, Schmid-Burgk JL, Hemmerling I, Horvath GL, Schmidt T, Latz E, Hornung V. Cell intrinsic immunity spreads to bystander cells via the intercellular transfer of cGAMP. Nature. 2013;503(7477):530–4.
179. Xu S, Ducroux A, Ponnurangam A, Vieyres G, Franz S, Müsken M, Zillinger T, Malassa A, Ewald E, Hornung V, Barchet W, Häussler S, Pietschmann T, Goffinet C. cGAS-Mediated Innate Immunity Spreads Intercellularly through HIV-1 Env-Induced Membrane Fusion Sites. Cell Host Microbe. 2016;20(4):443–57.
180. Bridgeman A, Maelfait J, Davenne T, Partridge T, Peng Y, Mayer A, Dong T, Kaever V, Borrow P, Rehwinkel J. Viruses transfer the antiviral second messenger cGAMP between cells. Science (80- ). 2015;349(6253):1228–32.
181. Gentili M, Kowal J, Tkach M, Satoh T, Lahaye X, Conrad C, Boyron M, Lombard B, Durand S, Kroemer G, Loew D, Dalod M, Théry C, Manel N. Transmission of innate immune signaling by packaging of cGAMP in viral particles. Science (80- ). 2015;349(6253):1232–6.
182. Zhang X, Shi H, Wu J, Zhang X, Sun L, Chen C, Chen Z. Cyclic GMP-AMP containing mixed Phosphodiester linkages is an endogenous high-affinity ligand for STING. Mol Cell. 2013;51(2):226–35.
183. Ishikawa H, Barber GN. STING is an endoplasmic reticulum adaptor that facilitates innate immune signalling. Nature. 2008;455(7213):674–8.
184. Huang Y-H, Liu X-Y, Du X-X, Jiang Z-F, Su X-D. The structural basis for the sensing and binding of cyclic di-GMP by STING. Nat Struct Mol Biol. 2012;19(7):728–30.
185. Shang G, Zhang C, Chen ZJ, Bai X chen, Zhang X. Cryo-EM structures of STING reveal its mechanism of activation by cyclic GMP–AMP. Nature. 2019.
186. Ouyang S, Song X, Wang Y, Ru H, Shaw N, Jiang Y, Niu F, Zhu Y, Qiu W, Parvatiyar K, Li Y, Zhang R, Cheng G, Liu Z-J. Structural Analysis of the STING Adaptor Protein Reveals a Hydrophobic Dimer Interface and Mode of Cyclic di-GMP Binding. Immunity. 2012;36(6):1073–86.
187. Dobbs N, Burnaevskiy N, Chen D, Gonugunta VK, Alto NM, Yan N. STING Activation by Translocation from the ER Is Associated with Infection and Autoinflammatory Disease. Cell Host Microbe. 2015 Aug;18(2):157–68.
188. Mukai K, Konno H, Akiba T, Uemura T, Waguri S, Kobayashi T, Barber GN, Arai H, Taguchi T. Activation of STING requires palmitoylation at the Golgi. Nat Commun. 2016;21(7):11932.
189. Ishikawa H, Ma Z, Barber GN. STING regulates intracellular DNA-mediated, type i interferon-dependent innate immunity. Nature. 2009;461(7265):788–92.
190. Konno H, Konno K, Barber GN. Cyclic dinucleotides trigger ULK1 (ATG1)

phosphorylation of STING to prevent sustained innate immune signaling. Cell. 2013 Oct;155(3):688–98.

191. Zhang C, Shang G, Gui X, Zhang X, Bai X chen, Chen ZJ. Structural basis of STING binding with and phosphorylation by TBK1. Nature. 2019. p. 567(7748):394-398.
192. Liu S, Cai X, Wu J, Cong Q, Chen X, Li T, Du F, Ren J, Wu YT, Grishin N V., Chen ZJ. Phosphorylation of innate immune adaptor proteins MAVS, STING, and TRIF induces IRF3 activation. Science (80- ). 2015;13(347):2630.
193. Weaver BK, Kumar KP, Reich NC. Interferon regulatory factor 3 and CREB-binding protein/p300 are subunits of double-stranded RNA-activated transcription factor DRAF1. Mol Cell Biol. 1998;
194. Lin R, Heylbroeck C, Pitha PM, Hiscott J. Virus-dependent phosphorylation of the IRF-3 transcription factor regulates nuclear translocation, transactivation potential, and proteasome-mediated degradation. Mol Cell Biol. 1998;
195. Ni G, Konno H, Barber GN. Ubiquitination of STING at lysine 224 controls IRF3 activation. Sci Immunol. 2017;
196. Stempel M, Chan B, Juranić Lisnić V, Krmpotić A, Hartung J, Paludan SR, Füllbrunn N, Lemmermann NA, Brinkmann MM. The herpesviral antagonist m152 reveals differential activation of STING-dependent IRF and NF-κB signaling and STING's dual role during MCMV infection. EMBO J. 2019;38(5):e100983.
197. Yoneyama M, Kikuchi M, Matsumoto K, Imaizumi T, Miyagishi M, Taira K, Foy E, Loo Y-M, Gale Jr. M, Akira S, Yonehara S, Kato A, Fujita T. Shared and unique functions of the DExD/H-box helicases RIG-I, MDA5, and LGP2 in antiviral innate immunity. J Immunol. 2005;175(5):2851–8.
198. Satoh T, Kato H, Kumagai Y, Yoneyama M, Sato S, Matsushita K, Tsujimura T, Fujita T, Akira S, Takeuchi O. LGP2 is a positive regulator of RIG-I- and MDA5-mediated antiviral responses. Proc Natl Acad Sci. 2010;
199. Bruns AM, Horvath CM. LGP2 synergy with MDA5 in RLR-mediated RNA recognition and antiviral signaling. Cytokine. 2015.
200. Hornung V, Ellegast J, Kim S, Brzózka K, Jung A, Kato H, Poeck H, Akira S, Conzelmann K-K, Schlee M, Endres S, Hartmann G. 5′-Triphosphate RNA is the ligand for RIG-I. Science (80- ). 2006;314(5801):994–7.
201. Peisley A, Jo MH, Lin C, Wu B, Orme-Johnson M, Walz T, Hohng S, Hur S. Kinetic mechanism for viral dsRNA length discrimination by MDA5 filaments. Proc Natl Acad Sci U S A. 2012;
202. Xu L-G, Wang Y-Y, Han K-J, Li L-Y, Zhai Z, Shu H-B. VISA is an adapter protein required for virus-triggered IFN-β signaling. Mol Cell. 2005;19(6):727–40.
203. Oshiumi H, Matsumoto M, Hatakeyama S, Seya T. Riplet/RNF135, a RING finger protein, ubiquitinates RIG-I to promote interferon-β induction during the early phase

of viral infection. J Biol Chem. 2009;284(2):807–17.

204. Gack MU, Shin YC, Joo C-H, Urano T, Liang C, Sun L, Takeuchi O, Akira S, Chen Z, Inoue S, Jung JU. TRIM25 RING-finger E3 ubiquitin ligase is essential for RIG-I-mediated antiviral activity. Nature. 2007;446(7138):916–20.
205. Liu HM, Loo Y-M, Horner SM, Zornetzer GA, Katze MG, Gale Jr. M. The mitochondrial targeting chaperone 14-3-3ε regulates a RIG-I translocon that mediates membrane association and innate antiviral immunity. Cell Host Microbe. 2012;11(5):528–37.
206. Seth RB, Sun L, Ea C-K, Chen ZJ. Identification and characterization of MAVS, a mitochondrial antiviral signaling protein that activates NF-κB and IRF3. Cell. 2005;122(5):669–82.
207. Hou F, Sun L, Zheng H, Skaug B, Jiang Q-X, Chen ZJ. MAVS forms functional prion-like aggregates to activate and propagate antiviral innate immune response. Cell. 2011;146(3):448–61.
208. Liu S, Chen J, Cai X, Wu J, Chen X, Wu Y-T, Sun L, Chen ZJ. MAVS recruits multiple ubiquitin E3 ligases to activate antiviral signaling cascades. Elife. 2013;2013(2).
209. Dixit E, Boulant S, Zhang Y, Lee ASY, Odendall C, Shum B, Hacohen N, Chen ZJ, Whelan SP, Fransen M, Nibert ML, Superti-Furga G, Kagan JC. Peroxisomes Are Signaling Platforms for Antiviral Innate Immunity. Cell. 2010;141(4):668–81.
210. Odendall C, Dixit E, Stavru F, Bierne H, Franz KM, Durbin AF, Boulant S, Gehrke L, Cossart P, Kagan JC. Diverse intracellular pathogens activate type III interferon expression from peroxisomes. Nat Immunol. 2014;15(8):717–26.
211. Bender S, Reuter A, Eberle F, Einhorn E, Binder M, Bartenschlager R. Activation of Type I and III Interferon Response by Mitochondrial and Peroxisomal MAVS and Inhibition by Hepatitis C Virus. PLoS Pathog. 2015 Nov;11(11):e1005264.
212. Morrone SR, Wang T, Constantoulakis LM, Hooy RM, Delannoy MJ, Sohn J. Cooperative assembly of IFI16 filaments on dsDNA provides insights into host defense strategy. Proc Natl Acad Sci. 2014;
213. Unterholzner L, Keating SE, Baran M, Horan KA, Jensen SB, Sharma S, Sirois CM, Jin T, Latz E, Xiao TS, Fitzgerald KA, Paludan SR, Bowie AG. IFI16 is an innate immune sensor for intracellular DNA. Nat Immunol. 2010;11(11):997–1004.
214. Jin T, Perry A, Jiang J, Smith P, Curry JA, Unterholzner L, Jiang Z, Horvath G, Rathinam VA, Johnstone RW, Hornung V, Latz E, Bowie AG, Fitzgerald KA, Xiao TS. Structures of the HIN domain:DNA complexes reveal ligand binding and activation mechanisms of the AIM2 inflammasome and IFI16 receptor. Immunity. 2012;
215. Hornung V, Ablasser A, Charrel-Dennis M, Bauernfeind F, Horvath G, Caffrey DR, Latz E, Fitzgerald KA. AIM2 recognizes cytosolic dsDNA and forms a caspase-1-

activating inflammasome with ASC. Nature. 2009;458(7237):514–8.
216. Kerur N, Veettil M V, Sharma-Walia N, Bottero V, Sadagopan S, Otageri P, Chandran B. IFI16 acts as a nuclear pathogen sensor to induce the inflammasome in response to Kaposi Sarcoma-associated herpesvirus infection. Cell Host Microbe. 2011;9(5):363–75.
217. Lamkanfi M, Dixit VM. Mechanisms and functions of inflammasomes. Cell. 2014;157(5):1013–22.
218. Guo H, Callaway JB, Ting JP-Y. Inflammasomes: mechanism of action, role in disease, and therapeutics. Nat Med. 2015 Jun 29;21:677.
219. Liu X, Zhang Z, Ruan J, Pan Y, Magupalli VG, Wu H, Lieberman J. Inflammasome-activated gasdermin D causes pyroptosis by forming membrane pores. Nature. 2016 Jul 6;535:153.
220. Gariano GR, Dell'Oste V, Bronzini M, Gatti D, Luganini A, de Andrea M, Gribaudo G, Gariglio M, Landolfo S. The intracellular DNA sensor IFI16 gene acts as restriction factor for human Cytomegalovirus replication. PLoS Pathog. 2012;8(1).
221. Jakobsen MR, Bak RO, Andersen A, Berg RK, Jensen SB, Jin T, Laustsen A, Hansen K, Østergaard L, Fitzgerald KA, Xiao TS, Mikkelsen JG, Mogensen TH, Paludan SR. IFI16 senses DNA forms of the lentiviral replication cycle and controls HIV-1 replication. Proc Natl Acad Sci U S A. 2013;110(48):E4571–80.
222. Veeranki S, Choubey D. Interferon-inducible p200-family protein IFI16, an innate immune sensor for cytosolic and nuclear double-stranded DNA: Regulation of subcellular localization. Mol Immunol. 2012;49(4):567–71.
223. Li T, Diner BA, Chen J, Cristea IM. Acetylation modulates cellular distribution and DNA sensing ability of interferon-inducible protein IFI16. Proc Natl Acad Sci U S A. 2012;109(26):10558–63.
224. Almine JF, O'Hare CAJ, Dunphy G, Haga IR, Naik RJ, Atrih A, Connolly DJ, Taylor J, Kelsall IR, Bowie AG, Beard PM, Unterholzner L. IFI16 and cGAS cooperate in the activation of STING during DNA sensing in human keratinocytes. Nat Commun. 2017;8:14392.
225. Dunphy G, Flannery SM, Almine JF, Connolly DJ, Paulus C, Jonsson KL, Jakobsen MR, Nevels MM, Bowie AG, Unterholzner L. Non-canonical Activation of the DNA Sensing Adaptor STING by ATM and IFI16 Mediates NF-kappaB Signaling after Nuclear DNA Damage. Mol Cell. 2018 Sep;71(5):745-760.e5.
226. Xu Y, Tao X, Shen B, Horng T, Medzhitov R, Manley JL, Tong L. Structural basis for signal transduction by the Toll/interleukin-1 receptor domains. Nature. 2000 Nov;408(6808):111–5.
227. Botos I, Segal DM, Davies DR. The structural biology of Toll-like receptors. Structure. 2011. p. 19(4):447-59.
228. Alexopoulou L, Holt AC, Medzhitov R, Flavell RA. Recognition of double-stranded

RNA and activation of NF-κB by Toll-like receptor 3. Nature. 2001;

229. Ahmad-Nejad P, Häcker H, Rutz M, Bauer S, Vabulas RM, Wagner H. Bacterial CpG-DNA and lipopolysaccharides activate toll-like receptors at distinct cellular compartments. Eur J Immunol. 2002;
230. Heil F, Ahmad-Nejad P, Hemmi H, Hochrein H, Ampenberger F, Gellert T, Dietrich H, Lipford G, Takeda K, Akira S, Wagner H, Bauer S. The Toll-like receptor 7 (TLR7)-specific stimulus loxoribine uncovers a strong relationship within the TLR7, 8 and 9 subfamily. Eur J Immunol. 2003 Nov;33(11):2987–97.
231. Matsumoto M, Funami K, Tanabe M, Oshiumi H, Shingai M, Seto Y, Yamamoto A, Seya T. Subcellular Localization of Toll-Like Receptor 3 in Human Dendritic Cells. J Immunol. 2003;
232. Godfroy JI, Roostan M, Moroz YS, Korendovych I V., Yin H. Isolated Toll-like Receptor Transmembrane Domains Are Capable of Oligomerization. PLoS One. 2012;
233. Slack JL, Schooley K, Bonnert TP, Mitcham JL, Qwarnstrom EE, Sims JE, Dower SK. Identification of two major sites in the type I interleukin-1 receptor cytoplasmic region responsible for coupling to pro-inflammatory signaling pathways. J Biol Chem. 2000;
234. O'Neill LAJ, Golenbock D, Bowie AG. The history of Toll-like receptors-redefining innate immunity. Nature Reviews Immunology. 2013.
235. Lin S-C, Lo Y-C, Wu H. Helical assembly in the MyD88-IRAK4-IRAK2 complex in TLR/IL-1R signalling. Nature. 2010 Jun;465(7300):885–90.
236. Kagan JC, Su T, Horng T, Chow A, Akira S, Medzhitov R. TRAM couples endocytosis of Toll-like receptor 4 to the induction of interferon-β. Nat Immunol. 2008;
237. Kagan JC, Medzhitov R. Phosphoinositide-Mediated Adaptor Recruitment Controls Toll-like Receptor Signaling. Cell. 2006;
238. Zelensky AN, Gready JE. The C-type lectin-like domain superfamily. FEBS Journal. 2005.
239. Taylor PR, Tsoni SV, Willment JA, Dennehy KM, Rosas M, Findon H, Haynes K, Steele C, Botto M, Gordon S, Brown GD. Dectin-1 is required for β-glucan recognition and control of fungal infection. Nat Immunol. 2007;
240. Rogers NC, Slack EC, Edwards AD, Nolte MA, Schulz O, Schweighoffer E, Williams DL, Gordon S, Tybulewicz VL, Brown GD, Reis E Sousa C. Syk-dependent cytokine induction by dectin-1 reveals a novel pattern recognition pathway for C type lectins. Immunity. 2005;
241. Fuller GLJ, Williams JAE, Tomlinson MG, Eble JA, Hanna SL, Pöhlmann S, Suzuki-Inoue K, Ozaki Y, Watson SP, Pearce AC. The C-type lectin receptors CLEC-2 and Dectin-1, but not DC-SIGN, signal via a novel YXXL-dependent signaling cascade.

J Biol Chem. 2007;

242. Gorjestani S, Darnay BG, Lin X. TRAF6 and TAK1 play essential roles in C-type lectin receptor signaling in response to Candida albicans infection. J Biol Chem. 2012;
243. Gringhuis SI, den Dunnen J, Litjens M, van der Vlist M, Wevers B, Bruijns SCM, Geijtenbeek TBH. Dectin-1 directs T helper cell differentiation by controlling noncanonical NF-κB activation through Raf-1 and Syk. Nat Immunol. 2009;
244. Saijo S, Ikeda S, Yamabe K, Kakuta S, Ishigame H, Akitsu A, Fujikado N, Kusaka T, Kubo S, Chung S hyun, Komatsu R, Miura N, Adachi Y, Ohno N, Shibuya K, Yamamoto N, Kawakami K, Yamasaki S, Saito T, et al. Dectin-2 recognition of α-mannans and induction of Th17 cell differentiation is essential for host defense against candida albicans. Immunity. 2010;
245. Hoving JC, Wilson GJ, Brown GD. Signalling C-type lectin receptors, microbial recognition and immunity. Cellular Microbiology. 2014. p. 16(2):185-94.
246. Zhu L Le, Zhao XQ, Jiang C, You Y, Chen XP, Jiang YY, Jia XM, Lin X. C-type lectin receptors dectin-3 and dectin-2 form a heterodimeric pattern-recognition receptor for host defense against fungal infection. Immunity. 2013;39(2):324–34.
247. Platnich JM, Muruve DA. NOD-like receptors and inflammasomes: A review of their canonical and non-canonical signaling pathways. Arch Biochem Biophys. 2019 Jul;670:4–14.
248. Girardin SE, Boneca IG, Carneiro LAM, Antignac A, Jéhanno M, Viala J, Tedin K, Taha MK, Labigne A, Zähringer U, Coyle AJ, DiStefano PS, Bertin J, Sansonetti PJ, Philpott DJ. Nod1 detects a unique muropeptide from gram-negative bacterial peptidoglycan. Science (80- ). 2003;300(5625):1584–7.
249. Girardin SE, Boneca IG, Viala J, Chamaillard M, Labigne A, Thomas G, Philpott DJ, Sansonetti PJ. Nod2 is a general sensor of peptidoglycan through muramyl dipeptide (MDP) detection. J Biol Chem. 2003;278(11):8869–72.
250. Kim JG, Lee SJ, Kagnoff MF. Nod1 Is An Essential Signal Transducer in Intestinal Epithelial Cells Infected with Bacteria That Avoid Recognition by Toll-Like Receptors. Infect Immun. 2004;72(3):1487–95.
251. Hisamatsu T, Suzuki M, Reinecker H-C, Nadeau WJ, McCormick BA, Podolsky DK. CARD15/NOD2 functions as an antibacterial factor in human intestinal epithelial cells. Gastroenterology. 2003 Apr;124(4):993–1000.
252. Girardin SE, Tournebize R, Mavris M, Page AL, Li X, Stark GR, Bertin J, DiStefano PS, Yaniv M, Sansonetti PJ, Philpott DJ. CARD4/Nod1 mediates NF-kappaB and JNK activation by invasive Shigella flexneri. EMBO Rep. 2001 Aug;2(8):736–42.
253. Inohara N, Koseki T, Lin J, del Peso L, Lucas PC, Chen FF, Ogura Y, Nunez G. An induced proximity model for NF-kappa B activation in the Nod1/RICK and RIP signaling pathways. J Biol Chem. 2000 Sep;275(36):27823–31.

254. Park J-H, Kim Y-G, McDonald C, Kanneganti T-D, Hasegawa M, Body-Malapel M, Inohara N, Nunez G. RICK/RIP2 mediates innate immune responses induced through Nod1 and Nod2 but not TLRs. J Immunol. 2007 Feb;178(4):2380–6.
255. Hasegawa M, Fujimoto Y, Lucas PC, Nakano H, Fukase K, Nunez G, Inohara N. A critical role of RICK/RIP2 polyubiquitination in Nod-induced NF-kappaB activation. EMBO J. 2008 Jan;27(2):373–83.
256. Barnich N, Aguirre JE, Reinecker HC, Xavier R, Podolsky DK. Membrane recruitment of NOD2 in intestinal epithelial cells is essential for nuclear factor-KB activation in muramyl dipeptide recognition. J Cell Biol. 2005;
257. Irving AT, Mimuro H, Kufer TA, Lo C, Wheeler R, Turner LJ, Thomas BJ, Malosse C, Gantier MP, Casillas LN, Votta BJ, Bertin J, Boneca IG, Sasakawa C, Philpott DJ, Ferrero RL, Kaparakis-Liaskos M. The immune receptor NOD1 and kinase RIP2 interact with bacterial peptidoglycan on early endosomes to promote autophagy and inflammatory signaling. Cell Host Microbe. 2014;15(5):623–35.
258. Windheim M, Lang C, Peggie M, Plater LA, Cohen P. Molecular mechanisms involved in the regulation of cytokine production by muramyl dipeptide: Biochem J. 2015;404(2):179–90.
259. Heil F, Hemmi H, Hochrein H, Ampenberger F, Kirschning C, Akira S, Lipford G, Wagner H, Bauer S. Species-Specific Recognition of Single-Stranded RNA via Toll-like Receptor 7 and 8. Science (80- ). 2004;303(5663):1526–9.
260. Beignon A-S, McKenna K, Skoberne M, Manches O, DaSilva I, Kavanagh DG, Larsson M, Gorelick RJ, Lifson JD, Bhardwaj N. Endocytosis of HIV-1 activates plasmacytoid dendritic cells via Toll-like receptor-viral RNA interactions. J Clin Invest. 2005;115(11):3265–75.
261. Berg RK, Melchjorsen J, Rintahaka J, Diget E, Søby S, Horan KA, Gorelick RJ, Matikainen S, Larsen CS, Ostergaard L, Paludan SR, Mogensen TH. Genomic HIV RNA induces innate immune responses through RIG-I-dependent sensing of secondary-structured RNA. PLoS One. 2012;7(1).
262. Solis M, Nakhaei P, Jalalirad M, Lacoste J, Douville R, Arguello M, Zhao T, Laughrea M, Wainberg MA, Hiscott J. RIG-I-mediated antiviral signaling is inhibited in HIV-1 infection by a protease-mediated sequestration of RIG-I. J Virol. 2011;85(3):1224–36.
263. Akiyama H, Miller CM, Ettinger CR, Belkina AC, Snyder-Cappione JE, Gummuluru S. HIV-1 intron-containing RNA expression induces innate immune activation and T cell dysfunction. Nat Commun. 2018;
264. Gringhuis SI, Hertoghs N, Kaptein TM, Zijlstra-Willems EM, Sarrami-Fooroshani R, Sprokholt JK, Van Teijlingen NH, Kootstra NA, Booiman T, Van Dort KA, Ribeiro CMS, Drewniak A, Geijtenbeek TBH. HIV-1 blocks the signaling adaptor MAVS to evade antiviral host defense after sensing of abortive HIV-1 RNA by the host

helicase DDX3. Nat Immunol. 2017;18(2):225–35.

265. Ringeard M, Marchand V, Decroly E, Motorin Y, Bennasser Y. FTSJ3 is an RNA 2′-O-methyltransferase recruited by HIV to avoid innate immune sensing. Nature. 2019;565(7740):500–4.
266. Yan N, Regalado-Magdos AD, Stiggelbout B, Lee-Kirsch MA, Lieberman J. The cytosolic exonuclease TREX1 inhibits the innate immune response to human immunodeficiency virus type 1. Nat Immunol. 2010;11(11):1005–13.
267. Gao D, Wu J, Wu Y-T, Du F, Aroh C, Yan N, Sun L, Chen ZJ. Cyclic GMP-AMP synthase is an innate immune sensor of HIV and other retroviruses. Science (80- ). 2013;341(6148):903–6.
268. Lahaye X, Satoh T, Gentili M, Cerboni S, Conrad C, Hurbain I, ElMarjou A, Lacabaratz C, Lelièvre J-D, Manel N. The Capsids of HIV-1 and HIV-2 Determine Immune Detection of the Viral cDNA by the Innate Sensor cGAS in Dendritic Cells. Immunity. 2013;39(6):1132–42.
269. Jønsson KL, Laustsen A, Krapp C, Skipper KA, Thavachelvam K, Hotter D, Egedal JH, Kjolby M, Mohammadi P, Prabakaran T, Sørensen LK, Sun C, Jensen SB, Holm CK, Lebbink RJ, Johannsen M, Nyegaard M, Mikkelsen JG, Kirchhoff F, et al. IFI16 is required for DNA sensing in human macrophages by promoting production and function of cGAMP. Nat Commun. 2017;8:14391.
270. Yoh SM, Schneider M, Seifried J, Soonthornvacharin S, Akleh RE, Olivieri KC, De Jesus PD, Ruan C, De Castro E, Ruiz PA, Germanaud D, Des Portes V, García-Sastre A, König R, Chanda SK. PQBP1 is a proximal sensor of the cGAS-dependent innate response to HIV-1. Cell. 2015;161(6):1293–305.
271. Doitsh G, Cavrois M, Lassen KG, Zepeda O, Yang Z, Santiago ML, Hebbeler AM, Greene WC. Abortive HIV infection mediates CD4 T cell depletion and inflammation in human lymphoid tissue. Cell. 2010;143(5):789–801.
272. Monroe KM, Yang Z, Johnson JR, Geng X, Doitsh G, Krogan NJ, Greene WC. IFI16 DNA sensor is required for death of lymphoid CD4 T cells abortively infected with HIV. Science (80- ). 2014;343(6169):428–32.
273. Doitsh G, Galloway NLK, Geng X, Yang Z, Monroe KM, Zepeda O, Hunt PW, Hatano H, Sowinski S, Muñoz-Arias I, Greene WC. Cell death by pyroptosis drives CD4 T-cell depletion in HIV-1 infection. Nature. 2014;505(7484):509–14.
274. Muñoz-Arias I, Doitsh G, Yang Z, Sowinski S, Ruelas D, Greene WC. Blood-Derived CD4 T Cells Naturally Resist Pyroptosis during Abortive HIV-1 Infection. Cell Host Microbe. 2015;18(4):463–70.
275. Cooper A, García M, Petrovas C, Yamamoto T, Koup RA, Nabel GJ. HIV-1 causes CD4 cell death through DNA-dependent protein kinase during viral integration. Nature. 2013;498(7454):376–9.
276. Vermeire J, Roesch F, Sauter D, Rua R, Hotter D, Van Nuffel A, Vanderstraeten H,

Naessens E, Iannucci V, Landi A, Witkowski W, Baeyens A, Kirchhoff F, Verhasselt B. HIV Triggers a cGAS-Dependent, Vpu- and Vpr-Regulated Type I Interferon Response in CD4+ T Cells. Cell Rep. 2016;17(2):413–24.

277. Lahaye X, Gentili M, Silvin A, Conrad C, Picard L, Jouve M, Zueva E, Maurin M, Nadalin F, Knott GJ, Zhao B, Du F, Rio M, Amiel J, Fox AH, Li P, Etienne L, Bond CS, Colleaux L, et al. NONO Detects the Nuclear HIV Capsid to Promote cGAS-Mediated Innate Immune Activation. Cell. 2018;175(2):488–501.
278. Jarmuz A, Chester A, Bayliss J, Gisbourne J, Dunham I, Scott J, Navaratnam N. An anthropoid-specific locus of orphan C to U RNA-editing enzymes on chromosome 22. Genomics. 2002;79(3):285–96.
279. LaRue RS, Andrésdóttir V, Blanchard Y, Conticello SG, Derse D, Emerman M, Greene WC, Jónsson SR, Landau NR, Löchelt M, Malik HS, Malim MH, Münk C, O'Brien SJ, Pathak VK, Strebel K, Wain-Hobson S, Yu X-F, Yuhki N, et al. Guidelines for naming nonprimate APOBEC3 genes and proteins. J Virol. 2009;83(2):494–7.
280. Chen K-M, Harjes E, Gross PJ, Fahmy A, Lu Y, Shindo K, Harris RS, Matsuo H. Structure of the DNA deaminase domain of the HIV-1 restriction factor APOBEC3G. Nature. 2008;452(7183):116–9.
281. MacGinnitie AJ, Anant S, Davidson NO. Mutagenesis of apobec-1, the catalytic subunit of the mammalian apolipoprotein B mRNA editing enzyme, reveals distinct domains that mediate cytosine nucleoside deaminase, RNA binding, and RNA editing activity. J Biol Chem. 1995;270(24):14768–75.
282. Bogerd HP, Cullen BR. Single-stranded RNA facilitates nucleocapsid: APOBEC3G complex formation. RNA. 2008;14(6):1228–36.
283. Huthoff H, Autore F, Gallois-Montbrun S, Fraternali F, Malim MH. RNA-dependent oligomerization of APOBEC3G Is required for restriction of HIV-1. PLoS Pathog. 2009;5(3).
284. Harris RS, Bishop KN, Sheehy AM, Craig HM, Petersen-Mahrt SK, Watt IN, Neuberger MS, Malim MH. DNA deamination mediates innate immunity to retroviral infection. Cell. 2003;113(6):803–9.
285. Bishop KN, Holmes RK, Sheehy AM, Davidson NO, Cho S-J, Malim MH. Cytidine deamination of retroviral DNA by diverse APOBEC proteins. Curr Biol. 2004;14(15):1392–6.
286. Yang B, Chen K, Zhang C, Huang S, Zhang H. Virion-associated uracil DNA glycosylase-2 and apurinic/apyrimidinic endonuclease are involved in the degradation of APOBEC3G-edited nascent HIV-1 DNA. J Biol Chem. 2007;282(16):11667–75.
287. Langlois M-A, Neuberger MS. Human APOBEC3G can restrict retroviral infection in avian cells and acts independently of both UNG and SMUG1. J Virol.

2008;82(9):4660–4.

288. Iwatani Y, Chan DSB, Wang F, Maynard KS, Sugiura W, Gronenborn AM, Rouzina I, Williams MC, Musier-Forsyth K, Levin JG. Deaminase-independent inhibition of HIV-1 reverse transcription by APOBEC3G. Nucleic Acids Res. 2007;35(21):7096–108.
289. Guo F, Cen S, Niu M, Yang Y, Gorelick RJ, Kleiman L. The interaction of APOBEC3G with human immunodeficiency virus type 1 nucleocapsid inhibits tRNA3Lys annealing to viral RNA. J Virol. 2007;81(20):11322–31.
290. Li X-Y, Guo F, Zhang L, Kleiman L, Cen S. APOBEC3G inhibits DNA strand transfer during HIV-1 reverse transcription. J Biol Chem. 2007;282(44):32065–74.
291. Nowarski R, Prabhu P, Kenig E, Smith Y, Britan-Rosich E, Kotler M. APOBEC3G inhibits HIV-1 RNA elongation by inactivating the viral trans-activation response element. J Mol Biol. 2014;426(15):2840–53.
292. Bishop KN, Verma M, Kim E-Y, Wolinsky SM, Malim MH. APOBEC3G inhibits elongation of HIV-1 reverse transcripts. PLoS Pathog. 2008;4(12).
293. Pollpeter D, Parsons M, Sobala AE, Coxhead S, Lang RD, Bruns AM, Papaioannou S, McDonnell JM, Apolonia L, Chowdhury JA, Horvath CM, Malim MH. Deep sequencing of HIV-1 reverse transcripts reveals the multifaceted antiviral functions of APOBEC3G. Nat Microbiol. 2018 Feb;3(2):220–33.
294. Koning FA, Newman ENC, Kim E-Y, Kunstman KJ, Wolinsky SM, Malim MH. Defining APOBEC3 expression patterns in human tissues and hematopoietic cell subsets. J Virol. 2009;83(18):9474–85.
295. Gillick K, Pollpeter D, Phalora P, Kim E-Y, Wolinsky SM, Malim MH. Suppression of HIV-1 infection by APOBEC3 proteins in primary human CD4+ T cells is associated with inhibition of processive reverse transcription as well as excessive cytidine deamination. J Virol. 2013;87(3):1508–17.
296. Chaipan C, Smith JL, Hu W-S, Pathak VK. APOBEC3G restricts HIV-1 to a greater extent than APOBEC3F and APOBEC3DE in human primary CD4+ T cells and macrophages. J Virol. 2013;87(1):444–53.
297. Land AM, Ball TB, Luo M, Pilon R, Sandstrom P, Embree JE, Wachihi C, Kimani J, Plummer FA. Human immunodeficiency virus (HIV) type 1 proviral hypermutation correlates with CD4 count in HIV-infected women from Kenya. J Virol. 2008;82(16):8172–82.
298. Koning FA, Goujon C, Bauby H, Malim MH. Target Cell-Mediated editing of HIV-1 cDNA by APOBEC3 proteins in human macrophages. J Virol. 2011;85(24):13448–52.
299. Mohanram V, Sköld AE, Bächle SM, Kumar Pathak S, Spetz A-L. IFN-α induces APOBEC3G, F, and A in immature dendritic cells and limits HIV-1 spread to CD4+ T cells. J Immunol. 2013;190(7):3346–53.

300. Stavrou S, Blouch K, Kotla S, Bass A, Ross SR. Nucleic acid recognition orchestrates the anti-viral response to retroviruses. Cell Host Microbe. 2015;17(4):478–88.
301. Kim E-Y, Bhattacharya T, Kunstman K, Swantek P, Koning FA, Malim MH, Wolinsky SM. Human APOBEC3G-mediated editing can promote HIV-1 sequence diversification and accelerate adaptation to selective pressure. J Virol. 2010;84(19):10402–5.
302. Sato K, Takeuchi JS, Misawa N, Izumi T, Kobayashi T, Kimura Y, Iwami S, Takaori-Kondo A, Hu W-S, Aihara K, Ito M, An DS, Pathak VK, Koyanagi Y. APOBEC3D and APOBEC3F Potently Promote HIV-1 Diversification and Evolution in Humanized Mouse Model. PLoS Pathog. 2014;10(10).
303. Kim E-Y, Lorenzo-Redondo R, Little SJ, Chung Y-S, Phalora PK, Maljkovic Berry I, Archer J, Penugonda S, Fischer W, Richman DD, Bhattacharya T, Malim MH, Wolinsky SM. Human APOBEC3 Induced Mutation of Human Immunodeficiency Virus Type-1 Contributes to Adaptation and Evolution in Natural Infection. PLoS Pathog. 2014;10(7).
304. Casartelli N, Guivel-Benhassine F, Bouziat R, Brandler S, Schwartz O, Moris A. The antiviral factor APOBEC3G improves CTL recognition of cultured HIV-infected T cells. J Exp Med. 2010;207(1):39–49.
305. Norman JM, Mashiba M, McNamara LA, Onafuwa-Nuga A, Chiari-Fort E, Shen W, Collins KL. The antiviral factor APOBEC3G enhances the recognition of HIV-infected primary T cells by natural killer cells. Nat Immunol. 2011;12(10):975–83.
306. Brass AL, Huang I-C, Benita Y, John SP, Krishnan MN, Feeley EM, Ryan BJ, Weyer JL, van der Weyden L, Fikrig E, Adams DJ, Xavier RJ, Farzan M, Elledge SJ. The IFITM Proteins Mediate Cellular Resistance to Influenza A H1N1 Virus, West Nile Virus, and Dengue Virus. Cell. 2009;139(7):1243–54.
307. Huang I-C, Bailey CC, Weyer JL, Radoshitzky SR, Becker MM, Chiang JJ, Brass AL, Ahmed AA, Chi X, Dong L, Longobardi LE, Boltz D, Kuhn JH, Elledge SJ, Bavari S, Denison MR, Choe H, Farzan M. Distinct patterns of IFITM-mediated restriction of filoviruses, SARS coronavirus, and influenza A virus. PLoS Pathog. 2011;7(1).
308. Lu J, Pan Q, Rong L, Liu S-L, Liang C. The IFITM proteins inhibit HIV-1 infection. J Virol. 2011;85(5):2126–37.
309. Bailey CC, Zhong G, Huang I-C, Farzan M. IFITM-family proteins: The cell's first line of antiviral defense. Annu Rev Virol. 2014;1(1):261–83.
310. Weston S, Czieso S, White IJ, Smith SE, Kellam P, Marsh M. A membrane topology model for human interferon inducible transmembrane protein 1. PLoS One. 2014;9(8).
311. Jia R, Pan Q, Ding S, Rong L, Liu S-L, Geng Y, Qiao W, Liang C. The N-terminal region of IFITM3 modulates its antiviral activity by regulating IFITM3 cellular

localization. J Virol. 2012;86(24):13697–707.

312. Jia R, Xu F, Qian J, Yao Y, Miao C, Zheng Y-M, Liu S-L, Guo F, Geng Y, Qiao W, Liang C. Identification of an endocytic signal essential for the antiviral action of IFITM3. Cell Microbiol. 2014;16(7):1080–93.
313. Foster TL, Wilson H, Iyer SS, Coss K, Doores K, Smith S, Kellam P, Finzi A, Borrow P, Hahn BH, Neil SJD. Resistance of Transmitted Founder HIV-1 to IFITM-Mediated Restriction. Cell Host Microbe. 2016;20(4):429–42.
314. Anafu AA, Bowen CH, Chin CR, Brass AL, Holm GH. Interferon-inducible transmembrane protein 3 (IFITM3) restricts reovirus cell entry. J Biol Chem. 2013;288(24):17261–71.
315. Sällman Almén M, Bringeland N, Fredriksson R, Schiöth HB. The Dispanins: A novel gene family of ancient origin that contains 14 human members. PLoS One. 2012;7(2).
316. Bailey CC, Kondur HR, Huang I-C, Farzan M. Interferon-induced transmembrane protein 3 is a type II transmembrane protein. J Biol Chem. 2013;288(45):32184–93.
317. Yount JS, Moltedo B, Yang Y-Y, Charron G, Moran TM, López CB, Hang HC. Palmitoylome profiling reveals S-palmitoylation-dependent antiviral activity of IFITM3. Nat Chem Biol. 2010;6(8):610–4.
318. Ling S, Zhang C, Wang W, Cai X, Yu L, Wu F, Zhang L, Tian C. Combined approaches of EPR and NMR illustrate only one transmembrane helix in the human IFITM3. Sci Rep. 2016;6.
319. John SP, Chin CR, Perreira JM, Feeley EM, Aker AM, Savidis G, Smith SE, Elia AEH, Everitt AR, Vora M, Pertel T, Elledge SJ, Kellam P, Brassa AL. The CD225 domain of IFITM3 is required for both IFITM protein association and inhibition of influenza a virus and dengue virus replication. J Virol. 2013;87(14):7837–52.
320. Amini-Bavil-Olyaee S, Choi YJ, Lee JH, Shi M, Huang I-C, Farzan M, Jung JU. The antiviral effector IFITM3 disrupts intracellular cholesterol homeostasis to block viral entry. Cell Host Microbe. 2013;13(4):452–64.
321. Desai TM, Marin M, Chin CR, Savidis G, Brass AL, Melikyan GB. IFITM3 Restricts Influenza A Virus Entry by Blocking the Formation of Fusion Pores following Virus-Endosome Hemifusion. PLoS Pathog. 2014;10(4).
322. Foster TL, Pickering S, Neil SJD. Inhibiting the Ins and Outs of HIV Replication: Cell-Intrinsic Antiretroviral Restrictions at the Plasma Membrane. Front Immunol. 2017;8:1853.
323. Fu B, Wang L, Li S, Dorf ME. ZMP STE24 defends against influenza and other pathogenic viruses. J Exp Med. 2017;214(4):919–29.
324. Compton AA, Bruel T, Porrot F, Mallet A, Sachse M, Euvrard M, Liang C, Casartelli N, Schwartz O. IFITM proteins incorporated into HIV-1 virions impair viral fusion and spread. Cell Host Microbe. 2014;16(6):736–47.

325. Tartour K, Appourchaux R, Gaillard J, Nguyen X-N, Durand S, Turpin J, Beaumont E, Roch E, Berger G, Mahieux R, Brand D, Roingeard P, Cimarelli A. IFITM proteins are incorporated onto HIV-1 virion particles and negatively imprint their infectivity. Retrovirology. 2014;11(1).
326. Yu J, Li M, Wilkins J, Ding S, Swartz TH, Esposito AM, Zheng Y-M, Freed EO, Liang C, Chen BK, Liu S-L. IFITM Proteins Restrict HIV-1 Infection by Antagonizing the Envelope Glycoprotein. Cell Rep. 2015;13(1):145–56.
327. Haller O, Kochs G. Human MxA protein: An interferon-induced dynamin-like GTPase with broad antiviral activity. J Interf Cytokine Res. 2011;31(1):79–87.
328. Staeheli P, Haller O, Boll W, Lindenmann J, Weissmann C. Mx protein: Constitutive expression in 3T3 cells transformed with cloned Mx cDNA confers selective resistance to influenza virus. Cell. 1986;44(1):147–58.
329. Pavlovic J, Zurcher T, Haller O, Staeheli P. Resistance to influenza virus and vesicular stomatitis virus conferred by expression of human MxA protein. J Virol. 1990;64(7):3370–5.
330. Schoggins JW, Wilson SJ, Panis M, Murphy MY, Jones CT, Bieniasz P, Rice CM. A diverse range of gene products are effectors of the type i interferon antiviral response. Nature. 2011;472(7344):481–5.
331. Liu S-Y, Sanchez DJ, Aliyari R, Lu S, Cheng G. Systematic identification of type I and type II interferon-induced antiviral factors. Proc Natl Acad Sci U S A. 2012;109(11):4239–44.
332. Haller O, Staeheli P, Schwemmle M, Kochs G. Mx GTPases: Dynamin-like antiviral machines of innate immunity. Trends in Microbiology. 2015. p. 23(3):154-63.
333. Goujon C, Moncorge O, Bauby H, Doyle T, Barclay WS, Malim MH. Transfer of the Amino-Terminal Nuclear Envelope Targeting Domain of Human MX2 Converts MX1 into an HIV-1 Resistance Factor. J Virol. 2014;88(16):9017–26.
334. Kane M, Yadav SS, Bitzegeio J, Kutluay SB, Zang T, Wilson SJ, Schoggins JW, Rice CM, Yamashita M, Hatziioannou T, Bieniasz PD. MX2 is an interferon-induced inhibitor of HIV-1 infection. Nature. 2013;502(7472):563–6.
335. Goujon C, Moncorgé O, Bauby H, Doyle T, Ward CC, Schaller T, Hué S, Barclay WS, Schulz R, Malim MH. Human MX2 is an interferon-induced post-entry inhibitor of HIV-1 infection. Nature. 2013;502(7472):559–62.
336. Busnadiego I, Kane M, Rihn SJ, Preugschas HF, Hughes J, Blanco-Melo D, Strouvelle VP, Zang TM, Willett BJ, Boutell C, Bieniasz PD, Wilson SJ. Host and viral determinants of Mx2 antiretroviral activity. J Virol. 2014;88(14):7738–52.
337. Alvarez FJD, He S, Perilla JR, Jang S, Schulten K, Engelman AN, Scheres SHW, Zhang P. CryoEM structure of MxB reveals a novel oligomerization interface critical for HIV restriction. Sci Adv. 2017;
338. Dicks MDJ, Goujon C, Pollpeter D, Betancor G, Apolonia L, Bergeron JRC, Malim

MH. Oligomerization requirements for MX2-mediated suppression of HIV-1 infection. J Virol. 2016;90(1):22–32.

339. Goujon C, Greenbury RA, Papaioannou S, Doyle T, Malim MH. A triple-arginine motif in the amino-terminal domain and oligomerization are required for HIV-1 inhibition by human MX2. J Virol. 2015;89(8):4676–80.
340. Schulte B, Buffone C, Opp S, Di Nunzio F, De Souza Aranha Vieira DA, Brandariz-Nuñez A, Diaz-Griffero F. Restriction of HIV-1 requires the N-terminal region of MxB as a capsid-binding motif but not as a nuclear localization signal. J Virol. 2015;89(16):8599–610.
341. Fricke T, White TE, Schulte B, de Souza Aranha Vieira DA, Dharan A, Campbell EM, Brandariz-Nuñez A, Diaz-Griffero F. MxB binds to the HIV-1 core and prevents the uncoating process of HIV-1. Retrovirology. 2014;11(1).
342. Fribourgh JL, Nguyen HC, Matreyek KA, Alvarez FJD, Summers BJ, Dewdney TG, Aiken C, Zhang P, Engelman A, Xiong Y. Structural insight into HIV-1 restriction by MxB. Cell Host Microbe. 2014;16(5):627–38.
343. Liu Z, Pan Q, Ding S, Qian J, Xu F, Zhou J, Cen S, Guo F, Liang C. The interferon-inducible MxB protein inhibits HIV-1 infection. Cell Host Microbe. 2013;14(4):398–410.
344. Dicks MDJ, Betancor G, Jimenez-Guardeno JM, Pessel-Vivares L, Apolonia L, Goujon C, Malim MH. Multiple components of the nuclear pore complex interact with the amino-terminus of MX2 to facilitate HIV-1 restriction. PLoS Pathog. 2018 Nov;14(11):e1007408.
345. Kane M, Rebensburg S V, Takata MA, Zang TM, Yamashita M, Kvaratskhelia M, Bieniasz PD. Nuclear pore heterogeneity influences HIV-1 infection and the antiviral activity of MX2. Elife. 2018;7:e35738.
346. Laguette N, Sobhian B, Casartelli N, Ringeard M, Chable-Bessia C, Ségéral E, Yatim A, Emiliani S, Schwartz O, Benkirane M. SAMHD1 is the dendritic- and myeloid-cell-specific HIV-1 restriction factor counteracted by Vpx. Nature. 2011;474(7353):654–7.
347. Descours B, Cribier A, Chable-Bessia C, Ayinde D, Rice G, Crow Y, Yatim A, Schwartz O, Laguette N, Benkirane M. SAMHD1 restricts HIV-1 reverse transcription in quiescent CD4 + T-cells. Retrovirology. 2012;9:87.
348. Hrecka K, Hao C, Gierszewska M, Swanson SK, Kesik-Brodacka M, Srivastava S, Florens L, Washburn MP, Skowronski J. Vpx relieves inhibition of HIV-1 infection of macrophages mediated by the SAMHD1 protein. Nature. 2011;474(7353):658–61.
349. Goldstone DC, Ennis-Adeniran V, Hedden JJ, Groom HCT, Rice GI, Christodoulou E, Walker PA, Kelly G, Haire LF, Yap MW, De Carvalho LPS, Stoye JP, Crow YJ, Taylor IA, Webb M. HIV-1 restriction factor SAMHD1 is a deoxynucleoside triphosphate triphosphohydrolase. Nature. 2011;480(7377):379–82.

350. Amie SM, Bambara RA, Kim B. GTP is the primary activator of the anti-HIV restriction factor SAMHD1. J Biol Chem. 2013;288(35):25001–6.
351. Ji X, Tang C, Zhao Q, Wang W, Xiong Y, Goff SP. Structural basis of cellular dNTP regulation by SAMHD1. Proc Natl Acad Sci U S A. 2014;111(41):E4305–14.
352. Li Y, Kong J, Peng X, Hou W, Qin X, Yu X-F. Structural insights into the high-efficiency catalytic mechanism of the sterileα-motif/histidine-aspartate domain-containing protein. J Biol Chem. 2015;290(49):29428–37.
353. Miazzi C, Ferraro P, Pontarin G, Rampazzo C, Reichard P, Bianchi V. Allosteric regulation of the human and mouse deoxyribonucleotide triphosphohydrolase sterile α-motif/histidine-aspartate domain-containing protein 1 (SAMHD1). J Biol Chem. 2014;289(26):18339–46.
354. Cribier A, Descours B, Valadão A, Laguette N, Benkirane M. Phosphorylation of SAMHD1 by Cyclin A2/CDK1 Regulates Its Restriction Activity toward HIV-1. Cell Rep. 2013;3(4):1036–43.
355. Pauls E, Ruiz A, Badia R, Permanyer M, Gubern A, Riveira-Muñoz E, Torres-Torronteras J, Álvarez M, Mothe B, Brander C, Crespo M, Menéndez-Arias L, Clotet B, Keppler OT, Martí R, Posas F, Ballana E, Esté JA. Cell cycle control and HIV-1 susceptibility are linked by CDK6-Dependent CDK2 phosphorylation of SAMHD1 in myeloid and lymphoid cells. J Immunol. 2014;193(4):1988–97.
356. Mauney CH, Rogers LC, Harris RS, Daniel LW, Devarie-Baez NO, Wu H, Furdui CM, Poole LB, Perrino FW, Hollis T. The SAMHD1 dNTP Triphosphohydrolase Is Controlled by a Redox Switch. Antioxidants Redox Signal. 2017;27(16):1317–31.
357. Seamon KJ, Bumpus NN, Stivers JT. Single-Stranded Nucleic Acids Bind to the Tetramer Interface of SAMHD1 and Prevent Formation of the Catalytic Homotetramer. Biochemistry. 2016;55(44):6087–99.
358. Mlcochova P, Sutherland KA, Watters SA, Bertoli C, de Bruin RAM, Rehwinkel J, Neil SJ, Lenzi GM, Kim B, Khwaja A, Gage MC, Georgiou C, Chittka A, Yona S, Noursadeghi M, Towers GJ, Gupta RK. A G1-like state allows HIV-1 to bypass SAMHD1 restriction in macrophages. EMBO J. 2017;36(5):604–16.
359. Beloglazova N, Flick R, Tchigvintsev A, Brown G, Popovic A, Nocek B, Yakunin AF. Nuclease activity of the human SAMHD1 protein implicated in the aicardi-goutières syndrome and HIV-1 restriction. J Biol Chem. 2013;288(12):8101–10.
360. White TE, Brandariz-Nuñez A, Valle-Casuso JC, Amie S, Nguyen LA, Kim B, Tuzova M, Diaz-Griffero F. The retroviral restriction ability of SAMHD1, but not its deoxynucleotide triphosphohydrolase activity, is regulated by phosphorylation. Cell Host Microbe. 2013;13(4):441–51.
361. Ryoo J, Choi J, Oh C, Kim S, Seo M, Kim S-Y, Seo D, Kim J, White TE, Brandariz-Nuñez A, Diaz-Griffero F, Yun C-H, Hollenbaugh JA, Kim B, Baek D, Ahn K. The ribonuclease activity of SAMHD1 is required for HIV-1 restriction. Nat Med.

2014;20(8):936–41.

362. Rice GI, Bond J, Asipu A, Brunette RL, Manfield IW, Carr IM, Fuller JC, Jackson RM, Lamb T, Briggs TA, Ali M, Gornall H, Couthard LR, Aeby A, Attard-Montalto SP, Bertini E, Bodemer C, Brockmann K, Brueton LA, et al. Mutations involved in Aicardi-Goutières syndrome implicate SAMHD1 as regulator of the innate immune response. Nat Genet. 2009;41(7):829–32.
363. Crow YJ, Chase DS, Lowenstein Schmidt J, Szynkiewicz M, Forte GMA, Gornall HL, Oojageer A, Anderson B, Pizzino A, Helman G, Abdel-Hamid MS, Abdel-Salam GM, Ackroyd S, Aeby A, Agosta G, Albin C, Allon-Shalev S, Arellano M, Ariaudo G, et al. Characterization of human disease phenotypes associated with mutations in TREX1, RNASEH2A, RNASEH2B, RNASEH2C, SAMHD1, ADAR, and IFIH1. Am J Med Genet Part A. 2015;167(2):296–312.
364. Martinez-Lopez A, Martin-Fernandez M, Buta S, Kim B, Bogunovic D, Diaz-Griffero F. SAMHD1 deficient human monocytes autonomously trigger type I interferon. Mol Immunol. 2018 Sep;101:450–60.
365. Mathias SL, Scott AF, Kazazian Jr. HH, Boeke JD, Gabriel A. Reverse transcriptase encoded by a human transposable element. Science (80- ). 1991;254(5039):1808–10.
366. Zhao K, Du J, Han X, Goodier JL, Li P, Zhou X, Wei W, Evans SL, Li L, Zhang W, Cheung LE, Wang G, Kazazian HH, Yu X-F. Modulation of LINE-1 and Alu/SVA Retrotransposition by Aicardi-Goutières Syndrome-Related SAMHD1. Cell Rep. 2013;4(6):1108–15.
367. Hu S, Li J, Xu F, Mei S, Le Duff Y, Yin L, Pang X, Cen S, Jin Q, Liang C, Guo F. SAMHD1 Inhibits LINE-1 Retrotransposition by Promoting Stress Granule Formation. PLoS Genet. 2015;11(7).
368. Chen S, Bonifati S, Qin Z, St. Gelais C, Kodigepalli KM, Barrett BS, Kim SH, Antonucci JM, Ladner KJ, Buzovetsky O, Knecht KM, Xiong Y, Yount JS, Guttridge DC, Santiago ML, Wu L. SAMHD1 suppresses innate immune responses to viral infections and inflammatory stimuli by inhibiting the NF-κB and interferon pathways. Proc Natl Acad Sci. 2018;115(16):E3798–807.
369. Maelfait J, Bridgeman A, Benlahrech A, Cursi C, Rehwinkel J. Restriction by SAMHD1 Limits cGAS/STING-Dependent Innate and Adaptive Immune Responses to HIV-1. Cell Rep. 2016;16(6):1492–501.
370. Inuzuka M, Hayakawa M, Ingi T. Serine, an activity-regulated protein family, incorporates serine into membrane lipid synthesis. J Biol Chem. 2005;280(42):35776–83.
371. Trautz B, Wiedemann H, Lüchtenborg C, Pierini V, Kranich J, Glass B, Kräusslich H-G, Brocker T, Pizzato M, Ruggieri A, Brügger B, Fackler OT. The host-cell restriction factor SERINC5 restricts HIV-1 infectivity without altering the lipid

composition and organization of viral particles. J Biol Chem. 2017;292(33):13702–13.

372. Schulte B, Selyutina A, Opp S, Herschhorn A, Sodroski JG, Pizzato M, Diaz-Griffero F. Localization to detergent-resistant membranes and HIV-1 core entry inhibition correlate with HIV-1 restriction by SERINC5. Virology. 2018;515:52–65.
373. Firrito C, Bertelli C, Vanzo T, Chande A, Pizzato M. SERINC5 as a New Restriction Factor for Human Immunodeficiency Virus and Murine Leukemia Virus. Annu Rev Virol. 2018;
374. Rosa A, Chande A, Ziglio S, De Sanctis V, Bertorelli R, Goh SL, McCauley SM, Nowosielska A, Antonarakis SE, Luban J, Santoni FA, Pizzato M. HIV-1 Nef promotes infection by excluding SERINC5 from virion incorporation. Nature. 2015;526(7572):212–7.
375. Usami Y, Wu Y, Göttlinger HG. SERINC3 and SERINC5 restrict HIV-1 infectivity and are counteracted by Nef. Nature. 2015;526(7576):218–23.
376. Sood C, Marin M, Chande A, Pizzato M, Melikyan GB. SERINC5 protein inhibits HIV-1 fusion pore formation by promoting functional inactivation of envelope glycoproteins. J Biol Chem. 2017;292(14):6014–26.
377. Beitari S, Ding S, Pan Q, Finzi A, Liang C. Effect of HIV-1 env on SERINC5 antagonism. J Virol. 2017;91(4).
378. Neil SJD, Zang T, Bieniasz PD. Tetherin inhibits retrovirus release and is antagonized by HIV-1 Vpu. Nature. 2008;451(7177):425–30.
379. Sakuma T, Noda T, Urata S, Kawaoka Y, Yasuda J. Inhibition of lassa and marburg virus production by tetherin. J Virol. 2009;83(5):2382–5.
380. Kong W-S, Irie T, Yoshida A, Kawabata R, Kadoi T, Sakaguchi T. Inhibition of virus-like particle release of Sendai virus and Nipah virus, but not that of Mumps virus, by Tetherin/CD317/BST-2. Hiroshima J Med Sci. 2012;61(3):59–67.
381. Schubert HL, Zhai Q, Sandrin V, Eckert DM, Garcia-Maya M, Saul L, Sundquist WI, Steiner RA, Hill CP. Structural and functional studies on the extracellular domain of BST2/tetherin in reduced and oxidized conformations. Proc Natl Acad Sci U S A. 2010;107(42):17951–6.
382. Yang H, Wang J, Jia X, McNatt MW, Zang T, Pan B, Meng W, Wang H-W, Bieniasz PD, Xiong Y. Structural insight into the mechanisms of enveloped virus tethering by tetherin. Proc Natl Acad Sci U S A. 2010;107(43):18428–32.
383. Rollason R, Korolchuk V, Hamilton C, Schu P, Banting G. Clathrin-mediated endocytosis of a lipid-raft-associated protein is mediated through a dual tyrosine motif. J Cell Sci. 2007;120(21):3850–8.
384. Ohtomo T, Sugamata Y, Ozaki Y, Ono K, Yoshimura Y, Kawai S, Koishihara Y, Ozaki S, Kosaka M, Hirano T, Tsuchiya M. Molecular cloning and characterization of a surface antigen preferentially overexpressed on multiple myeloma cells.

Biochem Biophys Res Commun. 1999;258(3):583–91.

385. Kupzig S, Korolchuk V, Rollason R, Sugden A, Wilde A, Banting G. Bst-2/HM1.24 is a raft-associated apical membrane protein with an unusual topology. Traffic. 2003;4(10):694–709.
386. Cole G, Simonetti K, Ademi I, Sharpe S. Dimerization of the transmembrane domain of human tetherin in membrane mimetic environments. Biochemistry. 2012;51(25):5033–40.
387. Hammonds J, Wang J-J, Yi H, Spearman P. Immunoelectron microscopic evidence for tetherin/BST2 as the physical bridge between HIV-1 virions and the plasma membrane. PLoS Pathog. 2010;6(2).
388. Bego MG, Mercier J, Cohen ÉA. Virus-activated interferon regulatory factor 7 upregulates expression of the interferon-regulated BST2 gene independently of interferon signaling. J Virol. 2012;86(7):3513–27.
389. Blasius AL, Giurisato E, Cella M, Schreiber RD, Shaw AS, Colonna M. Bone marrow stromal cell antigen 2 is a specific marker of type I IFN-producing cells in the naive mouse, but a promiscuous cell surface antigen following IFN stimulation. J Immunol. 2006;177(5):3260–5.
390. Amet T, Byrd D, Hu N, Sun Q, Li F, Zhao Y, Hu S, Grantham A, Yu Q. BST-2 expression in human hepatocytes is inducible by all three types of interferons and restricts production of hepatitis C virus. Curr Mol Med. 2014;14(3):349–60.
391. Jiménez VC, Booiman T, De Taeye SW, Van Dort KA, Rits MAN, Hamann J, Kootstra NA. Differential expression of HIV-1 interfering factors in monocyte-derived macrophages stimulated with polarizing cytokines or interferons. Sci Rep. 2012;2.
392. Homann S, Smith D, Little S, Richman D, Guatelli J. Upregulation of BST-2/Tetherin by HIV infection in vivo. J Virol. 2011;85(20):10659–68.
393. Guzzo C, Jung M, Graveline A, Banfield BW, Gee K. IL-27 increases BST-2 expression in human monocytes and T cells independently of type i IFN. Sci Rep. 2012;2.
394. Sayeed A, Luciani-Torres G, Meng Z, Bennington JL, Moore DH, Dairkee SH. Aberrant Regulation of the BST2 (Tetherin) Promoter Enhances Cell Proliferation and Apoptosis Evasion in High Grade Breast Cancer Cells. PLoS One. 2013;8(6).
395. Cocka LJ, Bates P. Identification of Alternatively Translated Tetherin Isoforms with Differing Antiviral and Signaling Activities. PLoS Pathog. 2012;8(9).
396. Matsuda A, Suzuki Y, Honda G, Muramatsu S, Matsuzaki O, Nagano Y, Doi T, Shimotohno K, Harada T, Nishida E, Hayashi H, Sugano S. Large-scale identification and characterization of human genes that activate NF-κB and MAPK signaling pathways. Oncogene. 2003;22(21):3307–18.
397. Galão RP, Le Tortorec A, Pickering S, Kueck T, Neil SJD. Innate sensing of HIV-1 assembly by tetherin induces NFκB-dependent proinflammatory responses. Cell

Host Microbe. 2012;12(5):633–44.
398. Tokarev A, Suarez M, Kwan W, Fitzpatrick K, Singh R, Guatelli J. Stimulation of NF-kB Activity by the HIV Restriction Factor BST2. J Virol. 2013;87(4):2046–57.
399. Galão RP, Pickering S, Curnock R, Neil SJD. Retroviral retention activates a Syk-dependent HemITAM in Human tetherin. Cell Host Microbe. 2014;16(3):291–303.
400. Rollason R, Korolchuk V, Hamilton C, Jepson M, Banting G. A CD317/tetherin - RICH2 complex plays a critical role in the organization of the subapical actin cytoskeleton in polarized epithelial cells. J Cell Biol. 2009;184(5):721–36.
401. Alvarez RA, Hamlin RE, Monroe A, Moldt B, Hotta MT, Caprio GR, Fierer DS, Simon V, Chen BK. HIV-1 Vpu antagonism of tetherin inhibits antibody-dependent cellular cytotoxic responses by natural killer cells. J Virol. 2014;88(11):6031–46.
402. Pham TNQ, Lukhele S, Hajjar F, Routy J-P, Cohen TA. HIV Nef and Vpu protect HIV-infected CD4+ T cells from antibody-mediated cell lysis through down-modulation of CD4 and BST2. Retrovirology. 2014;11(1).
403. Cao W, Bover L, Cho M, Wen X, Hanabuchi S, Bao M, Rosen DB, Wang Y-H, Shaw JL, Du Q, Li C, Arai N, Yao Z, Lanier LL, Liu Y-J. Regulation of TLR7/9 responses in plasmacytoid dendritic cells by BST2 and ILT7 receptor interaction. J Exp Med. 2009;206(7):1603–14.
404. Stremlau M, Owens CM, Perron MJ, Kiessling M, Autissier P, Sodroski J. The cytoplasmic body component TRIM5α restricts HIV-1 infection in Old World monkeys. Nature. 2004;427(6977):848–53.
405. Han K, Lou DI, Sawyer SL. Identification of a genomic reservoir for new trim genes in primate genomes. PLoS Genet. 2011;7(12).
406. James LC, Keeble AH, Khan Z, Rhodes DA, Trowsdale J. Structural basis for PRYSPRY-mediated tripartite motif (TRIM) protein function. Proc Natl Acad Sci U S A. 2007;104(15):6200–5.
407. Sawyer SL, Wu LI, Emerman M, Malik HS. Positive selection of primate TRIM5α identifies a critical species-specific retroviral restriction domain. Proc Natl Acad Sci U S A. 2005;102(8):2832–7.
408. Stremlau M, Perron M, Lee M, Li Y, Song B, Javanbakht H, Diaz-Griffero F, Anderson DJ, Sundquist WI, Sodroski J. Specific recognition and accelerated uncoating of retroviral capsids by the TRIM5α restriction factor. Proc Natl Acad Sci U S A. 2006;103(14):5514–9.
409. Sebastian S, Luban J. TRIM5α selectively binds a restriction-sensitive retroviral capsid. Retrovirology. 2005;2.
410. Ganser-Pornillos BK, Chandrasekaran V, Pornillos O, Sodroski JG, Sundquist WI, Yeager M. Hexagonal assembly of a restricting TRIM5α protein. Proc Natl Acad Sci U S A. 2011;108(2):546–50.
411. Wu X, Anderson JL, Campbell EM, Joseph AM, Hope TJ. Proteasome inhibitors

uncouple rhesus TRIM5α restriction of HIV-1 reverse transcription and infection. Proc Natl Acad Sci U S A. 2006;103(19):7465–70.

412. Reymond A, Meroni G, Fantozzi A, Merla G, Cairo S, Luzi L, Riganelli D, Zanaria E, Messali S, Cainarca S, Guffanti A, Minucci S, Pelicci PG, Ballabio A. The tripartite motif family identifies cell compartments. EMBO J. 2001;20(9):2140–51.
413. Campbell EM, Dodding MP, Yap MW, Wu X, Gallois-Montbrun S, Malim MH, Stoye JP, Hope TJ. TRIM5α cytoplasmic bodies are highly dynamic structures. Mol Biol Cell. 2007;18(6):2102–11.
414. Li X, Sodroski J. The TRIM5α B-box 2 domain promotes cooperative binding to the retroviral capsid by mediating higher-order self-association. J Virol. 2008;82(23):11495–502.
415. Diaz-Griffero F, Kar A, Perron M, Xiang S-H, Javanbakht H, Li X, Sodroski J. Modulation of retroviral restriction and proteasome inhibitor-resistant turnover by changes in the TRIM5α B-box 2 domain. J Virol. 2007;81(19):10362–78.
416. Pertel T, Hausmann S, Morger D, Züger S, Guerra J, Lascano J, Reinhard C, Santoni FA, Uchil PD, Chatel L, Bisiaux A, Albert ML, Strambio-De-Castillia C, Mothes W, Pizzato M, Grütter MG, Luban J. TRIM5 is an innate immune sensor for the retrovirus capsid lattice. Nature. 2011;472(7343):361–5.
417. Diaz-Griffero F, Li X, Javanbakht H, Song B, Welikala S, Stremlau M, Sodroski J. Rapid turnover and polyubiquitylation of the retroviral restriction factor TRIM5. Virology. 2006;349(2):300–15.
418. Javanbakht H, Diaz-Griffero F, Stremlau M, Si Z, Sodroski J. The contribution of RING and B-box 2 domains to retroviral restriction mediated by monkey TRIM5α. J Biol Chem. 2005;280(29):26933–40.
419. Fletcher AJ, Christensen DE, Nelson C, Tan CP, Schaller T, Lehner PJ, Sundquist WI, Towers GJ. TRIM5α requires Ube2W to anchor Lys63-linked ubiquitin chains and restrict reverse transcription. EMBO J. 2015;34(15):2078–95.
420. Roa A, Hayashi F, Yang Y, Lienlaf M, Zhou J, Shi J, Watanabe S, Kigawa T, Yokoyama S, Aiken C, Diaz-Griffero F. RING domain mutations uncouple TRIM5α restriction of HIV-1 from inhibition of reverse transcription and acceleration of uncoating. J Virol. 2012;86(3):1717–27.
421. Jimenez-Moyano E, Ruiz A, Kløverpris HN, Rodriguez-Plata MT, Peña R, Blondeau C, Selwood DL, Izquierdo-Useros N, Moris A, Clotet B, Goulder P, Towers GJ, Prado JG. Nonhuman TRIM5 variants enhance recognition of HIV-1-infected cells by CD8+ T cells. J Virol. 2016;90(19):8552–62.
422. Battivelli E, Migraine J, Lecossier D, Yeni P, Clavel F, Hance AJ. Gag cytotoxic T lymphocyte escape mutations can increase sensitivity of HIV-1 to human TRIM5α, linking intrinsic and acquired immunity. J Virol. 2011;85(22):11846–54.
423. Jimenez-Guardeño JM, Apolonia L, Betancor G, Malim MH. Immunoproteasome

activation enables human TRIM5α restriction of HIV-1. Nat Microbiol. 2019;4(6):933–40.

424. Ribeiro CMS, Sarrami-Forooshani R, Setiawan LC, Zijlstra-Willems EM, Van Hamme JL, Tigchelaar W, Van Der Wel NN, Kootstra NA, Gringhuis SI, Geijtenbeek TBH. Receptor usage dictates HIV-1 restriction by human TRIM5α in dendritic cell subsets. Nature. 2016;540(7633):448–52.
425. Klimkait T, Strebel K, Hoggan MD, Martin MA, Orenstein JM. The human immunodeficiency virus type 1-specific protein vpu is required for efficient virus maturation and release. J Virol. 1990;64(2):621–9.
426. Sakai H, Tokunaga K, Kawamura M, Adachi A. Function of human immunodeficiency virus type 1 Vpu protein in various cell types. J Gen Virol. 1995;76(11):2717–22.
427. Neil SJD, Sandrin V, Sundquist WI, Bieniasz PD. An Interferon-α-Induced Tethering Mechanism Inhibits HIV-1 and Ebola Virus Particle Release but Is Counteracted by the HIV-1 Vpu Protein. Cell Host Microbe. 2007;2(3):193–203.
428. Skasko M, Wang Y, Tian Y, Tokarev A, Munguia J, Ruiz A, Stephens EB, Opella SJ, Guatelli O. HIV-1 Vpu protein antagonizes innate restriction factor BST-2 via lipid-embedded helix-helix interactions. J Biol Chem. 2012;287(1):58–67.
429. Kueck T, Foster TL, Weinelt J, Sumner JC, Pickering S, Neil SJD. Serine Phosphorylation of HIV-1 Vpu and Its Binding to Tetherin Regulates Interaction with Clathrin Adaptors. PLoS Pathog. 2015;11(8).
430. Mitchell RS, Katsura C, Skasko MA, Fitzpatrick K, Lau D, Ruiz A, Stephens EB, Margottin-Goguet F, Benarous R, Guatelli JC. Vpu antagonizes BST-2-mediated restriction of HIV-1 release via β-TrCP and endo-lysosomal trafficking. PLoS Pathog. 2009;5(5).
431. Weinelt J, Neil SJD. Differential sensitivities of tetherin isoforms to counteraction by primate lentiviruses. J Virol. 2014;88(10):5845–58.
432. Bour S, Perrin C, Akari H, Strebel K. The Human Immunodeficiency Virus Type 1 Vpu Protein Inhibits NF-κB Activation by Interfering with βTrCP-mediated Degradation of IκB. J Biol Chem. 2001;
433. Sauter D, Hotter D, Van Driessche B, Stürzel CM, Kluge SF, Wildum S, Yu H, Baumann B, Wirth T, Plantier J-C, Leoz M, Hahn BH, Van Lint C, Kirchhoff F. Differential regulation of NF-κB-mediated proviral and antiviral host gene expression by primate lentiviral nef and vpu proteins. Cell Rep. 2015;10(4):586–99.
434. Klotman ME, Kim SY, Buchbinder A, DeRossi A, Baltimore D, Wong-Staal F. Kinetics of expression of multiply spliced RNA in early human immunodeficiency virus type 1 infection of lymphocytes and monocytes. Proc Natl Acad Sci. 2006;
435. Guy B, Kieny MP, Riviere Y, Le Peuch C, Dott K, Girard M, Montagnier L, Lecocq JP. HIV F/3' orf encodes a phosphorylated GTP-binding protein resembling an

oncogene product. Nature. 1987 Nov;330(6145):266–9.

436. Schwartz O, Maréchal V, Le Gall S, Lemonnier F, Heard JM. Endocytosis of major histocompatibility complex class I molecules is induced by the HIV-1 Nef protein. Nat Med. 1996;2(3):338–42.

437. Aiken C, Konner J, Landau NR, Lenburg ME, Trono D. Nef induces CD4 endocytosis: Requirement for a critical dileucine motif in the membrane-proximal CD4 cytoplasmic domain. Cell. 1994;76(5):853–64.

438. Chaudhuri R, Lindwasser OW, Smith WJ, Hurley JH, Bonifacino JS. Downregulation of CD4 by human immunodeficiency virus type 1 Nef is dependent on clathrin and involves direct interaction of Nef with the AP2 clathrin adaptor. J Virol. 2007;

439. daSilva LLP, Sougrat R, Burgos P V., Janvier K, Mattera R, Bonifacino JS. Human Immunodeficiency Virus Type 1 Nef Protein Targets CD4 to the Multivesicular Body Pathway. J Virol. 2009;

440. Chowers MY, Spina CA, Kwoh TJ, Fitch NJS, Richman DD, Guatelli JC. Optimal infectivity in vitro of human immunodeficiency virus type 1 requires an intact nef gene. J Virol. 1994;68(5):2906–14.

441. Carl S, Greenough TC, Krumbiegel M, Greenberg M, Skowronski J, Sullivan JL, Kirchhoff F. Modulation of Different Human Immunodeficiency Virus Type 1 Nef Functions during Progression to AIDS. J Virol. 2002;

442. Pizzato M, Helander A, Popova E, Calistri A, Zamborlini A, Palù G, Göttlinger HG. Dynamin 2 is required for the enhancement of HIV-1 infectivity by Nef. Proc Natl Acad Sci U S A. 2007;104(16):6812–7.

443. Craig HM, Pandori MW, Guatelli JC. Interaction of HIV-1 Nef with the cellular dileucine-based sorting pathway is required for CD4 down-regulation and optimal viral infectivity. Proc Natl Acad Sci U S A. 1998;95(19):11229–34.

444. Usami Y, Wu Y, Göttlinger HG. SERINC3 and SERINC5 restrict HIV-1 infectivity and are counteracted by Nef. Nature. 2015;526(7572):218–23.

445. Rosa A, Chande A, Ziglio S, De Sanctis V, Bertorelli R, Goh SL, McCauley SM, Nowosielska A, Antonarakis SE, Luban J, Santoni FA, Pizzato M. HIV-1 Nef promotes infection by excluding SERINC5 from virion incorporation. Nature. 2015;

446. Shi J, Xiong R, Zhou T, Su P, Zhang X, Qiu X, Li H, Li S, Yu C, Wang B, Ding C, Smithgall TE, Zheng Y-H. HIV-1 Nef antagonizes SERINC5 restriction by downregulation of SERINC5 via the endosome/lysosome system. J Virol. 2018;92(11).

447. Trautz B, Pierini V, Wombacher R, Stolp B, Chase AJ, Pizzato M, Fackler OT. The antagonism of HIV Nef to SERINC5 particle infectivity restriction involves the counteraction of virion-associated pools of the restriction factor. J Virol. 2016;90(23):10915–27.

448. Gabuzda DH, Lawrence K, Langhoff E, Terwilliger E, Dorfman T, Haseltine WA, Sodroski J. Role of vif in replication of human immunodeficiency virus type 1 in CD4+ T lymphocytes. J Virol. 1992;66(11):6489–95.
449. Sheehy AM, Gaddis NC, Malim MH. The antiretroviral enzyme APOBEC3G is degraded by the proteasome in response to HIV-1 Vif. Nat Med. 2003;9(11):1404–7.
450. Bergeron JRC, Huthoff H, Veselkov DA, Beavil RL, Simpson PJ, Matthews SJ, Malim MH, Sanderson MR. The SOCS-Box of HIV-1 vif interacts with elonginBC by induced-folding to recruit its Cul5-containing ubiquitin ligase complex. PLoS Pathog. 2010;6(6).
451. Guo Y, Dong L, Qiu X, Wang Y, Zhang B, Liu H, Yu Y, Zang Y, Yang M, Huang Z. Structural basis for hijacking CBF-β and CUL5 E3 ligase complex by HIV-1 Vif. Nature. 2014;505(7482):229–33.
452. Mehle A, Wilson H, Zhang C, Brazier AJ, McPike M, Pery E, Gabuzda D. Identification of an APOBEC3G binding site in human immunodeficiency virus type 1 Vif and inhibitors of Vif-APOBEC3G binding. J Virol. 2007;81(23):13235–41.
453. Russell RA, Pathak VK. Identification of two distinct human immunodeficiency virus type 1 vif determinants critical for interactions with human APOBEC3G and APOBEC3F. J Virol. 2007;81(15):8201–10.
454. Pery E, Rajendran KS, Brazier AJ, Gabuzda D. Regulation of APOBEC3 proteins by a Novel YXXL motif in human immunodeficiency virus type 1 vif and simian immunodeficiency virus SIVagm vif. J Virol. 2009;83(5):2374–81.
455. Binka M, Ooms M, Steward M, Simon V. The activity spectrum of Vif from multiple HIV-1 subtypes against APOBEC3G, APOBEC3F, and APOBEC3H. J Virol. 2012;86(1):49–59.
456. Kim DY, Kwon E, Hartley PD, Crosby DC, Mann S, Krogan NJ, Gross JD. CBFβ Stabilizes HIV Vif to Counteract APOBEC3 at the Expense of RUNX1 Target Gene Expression. Mol Cell. 2013;49(4):632–44.
457. Schröfelbauer B, Chen D, Landau NR. A single amino acid of APOBEC3G controls its species-specific interaction with virion infectivity factor (Vif). Proc Natl Acad Sci U S A. 2004;101(11):3927–32.
458. Mercenne G, Bernacchi S, Richer D, Bec G, Henriet S, Paillart J-C, Marquet R. HIV-1 Vif binds to APOBEC3G mRNA and inhibits its translation. Nucleic Acids Res. 2009;38(2):633–46.
459. Goila-Gaur R, Khan MA, Miyagi E, Kao S, Opi S, Takeuchi H, Strebel K. HIV-1 Vif promotes the formation of high molecular mass APOBEC3G complexes. Virology. 2008;372(1):136–46.
460. Feng Y, Love RP, Chelico L. HIV-1 viral infectivity factor (Vif) alters processive single-stranded DNA scanning of the retroviral restriction factor APOBEC3G. J Biol

Chem. 2013;288(9):6083–94.

461. Hyde JL, Diamond MS. Innate immune restriction and antagonism of viral RNA lacking 2'-O methylation. Virology. 2015. p. 479-480:66-74.

462. Daffis S, Szretter KJ, Schriewer J, Li J, Youn S, Errett J, Lin TY, Schneller S, Zust R, Dong H, Thiel V, Sen GC, Fensterl V, Klimstra WB, Pierson TC, Buller RM, Gale Jr M, Shi PY, Diamond MS. 2′-O methylation of the viral mRNA cap evades host restriction by IFIT family members. Nature. 2010;468(7322):452–6.

463. Cohen EA, Terwilliger EF, Jalinoos Y, Proulx J, Sodroski JG, Haseltine WA. Identification of HIV-1 vpr product and function. J Acquir Immune Defic Syndr. 1990;3(1):11–8.

464. Douglas Dedera, Wen Hu, Nancy Vander, Heyden LR. Viral Protein R of Human Immunodeficiency Virus Types 1 and 2 Is Despensable for Replication and Cytopathogenicity in Lymphoid Cells. J Virol. 1989;63(7):3205–8.

465. Lang SM, Weeger M, Stahl-Hennig C, Coulibaly C, Hunsmann G, Müller J, Müller-Hermelink H, Fuchs D, Wachter H, Daniel MM. Importance of vpr for infection of rhesus monkeys with simian immunodeficiency virus. J Virol [Internet]. 1993;67(2):902–12.

466. Ali A, Ng HL, Blankson JN, Burton DR, Buckheit RW 3rd, Moldt B, Fulcher JA, Ibarrondo FJ, Anton PA, Yang OO. Highly Attenuated Infection With a Vpr-Deleted Molecular Clone of Human Immunodeficiency Virus-1. J Infect Dis. 2018 Sep;218(9):1447–52.

467. Schrofelbauer B, Hakata Y, Landau NR. HIV-1 Vpr function is mediated by interaction with the damage-specific DNA-binding protein DDB1. Proc Natl Acad Sci. 2007;104(10):4130–5.

468. Laguette N, Brégnard C, Hue P, Basbous J, Yatim A, Larroque M, Kirchhoff F, Constantinou A, Sobhian B, Benkirane M. Premature activation of the slx4 complex by vpr promotes g2/m arrest and escape from innate immune sensing. Cell. 2014;156(1–2):134–45.

469. Ahn J, Vu T, Novince Z, Guerrero-Santoro J, Rapic-Otrin V, Gronenborn AM. HIV-1 Vpr loads uracil DNA glycosylase-2 onto DCAF1, a substrate recognition subunit of a cullin 4A-RING E3 ubiquitin ligase for proteasome-dependent degradation. J Biol Chem. 2010;258(48):37333–41.

470. Lahouassa H, Blondot M-L, Chauveau L, Chougui G, Morel M, Leduc M, Guillonneau F, Ramirez BC, Schwartz O, Margottin-Goguet F. HIV-1 Vpr degrades the HLTF DNA translocase in T cells and macrophages. Proc Natl Acad Sci U S A. 2016;113(19):5311–6.

471. Nitahara-Kasahara Y, Kamata M, Yamamoto T, Zhang X, Miyamoto Y, Muneta K, Iijima S, Yoneda Y, Tsunetsugu-Yokota Y, Aida Y. Novel Nuclear Import of Vpr Promoted by Importin Is Crucial for Human Immunodeficiency Virus Type 1

Replication in Macrophages. J Virol. 2007;81(10):5284–93.

472. Andersen JL, DeHart JL, Zimmerman ES, Ardon O, Kim B, Jacquot G, Benichou S, Planelles V. HIV-1 Vpr-induced apoptosis is cell cycle dependent and requires Bax but not ANT. PLoS Pathog. 2006;2(12):1106–19.
473. Vanitharani R, Mahalingam S, Rafaeli Y, Singh SP, Srinivasan A, Weiner DB, Ayyavoo V. HIV-1 Vpr transactivates LTR-directed expression through sequences present within -278 to -176 and increases virus replication in vitro. Virology. 2001;289(2):334–42.
474. Hattori N, Michaels F, Fargnoli K, Marcon L, Gallo RC, Franchini G. The human immunodeficiency virus type 2 vpr gene is essential for productive infection of human macrophages. Proc Natl Acad Sci. 1990;87(20):8080–4.
475. Morellet N, Bouaziz S, Petitjean P, Roques BP. NMR structure of the HIV-1 regulatory protein VPR. J Mol Biol. 2003;285(5):2105–17.
476. Zander K, Sherman MP, Tessmer U, Bruns K, Wray V, Prechtel AT, Schubert E, Henklein P, Luban J, Neidleman J, Greene WC, Schubert U. Cyclophilin A Interacts with HIV-1 Vpr and Is Required for Its Functional Expression. J Biol Chem. 2003;278(44):43202–13.
477. Fritz J V., Dujardin D, Godet J, Didier P, De Mey J, Darlix J-L, Mely Y, de Rocquigny H. HIV-1 Vpr Oligomerization but Not That of Gag Directs the Interaction between Vpr and Gag. J Virol. 2010;84(3):1585–96.
478. Wu Y, Zhou X, Barnes CO, DeLucia M, Cohen AE, Gronenborn AM, Ahn J, Calero G. The DDB1-DCAF1-Vpr-UNG2 crystal structure reveals how HIV-1 Vpr steers human UNG2 toward destruction. Nat Struct Mol Biol. 2016;23(10):933–9.
479. Welker R, Hohenberg H, Tessmer U, Huckhagel C, Kräusslich HG. Biochemical and structural analysis of isolated mature cores of human immunodeficiency virus type 1. J Virol. 2000;74(3):1168–77.
480. Kudoh A, Takahama S, Sawasaki T, Ode H, Yokoyama M, Okayama A, Ishikawa A, Miyakawa K, Matsunaga S, Kimura H, Sugiura W, Sato H, Hirano H, Ohno S, Yamamoto N, Ryo A. The phosphorylation of HIV-1 Gag by atypical protein kinase C facilitates viral infectivity by promoting Vpr incorporation into virions. Retrovirology. 2014;11(9):129–76.
481. Kondo E, Göttlinger HG. A conserved LXXLF sequence is the major determinant in p6gag required for the incorporation of human immunodeficiency virus type 1 Vpr. J Virol. 1996;70(1):159–64.
482. Zhu H, Jian H, Zhao LJ. Identification of the 15FRFG domain in HIV-1 Gag p6 essential for Vpr packaging into the virion. Retrovirology. 2004;1(26):343–98.
483. Jenkins Y, Pornillos O, Rich RL, Myszka DG, Sundquist WI, Malim MH. Biochemical analyses of the interactions between human immunodeficiency virus type 1 Vpr and p6Gag. J Virol. 2001;75(21):10537–42.

484. Selig L, Pages J-C, Tanchou V, Prévéral S, Berlioz-Torrent C, Liu LX, Erdtmann L, Darlix J-L, Benarous R, Benichou S. Interaction with the p6 domain of the Gag precursor mediates incorporation into virions of Vpr and Vpx proteins from primate lentiviruses. J Virol. 1999;73(1):592–600.
485. Accola MA, Öhagen A, Göttlinger HG. Isolation of human immunodeficiency virus type 1 cores: Retention of Vpr in the absence of p6(gag). J Virol. 2000;74(13):6198–202.
486. Belzile JP, Abrahamyan LG, Gérard FCA, Rougeau N, Cohen ÉA. Formation of mobile chromatin-associated nuclear foci containing HIV-1 Vpr and VPRBP is critical for the induction of G2 cell cycle arrest. PLoS Pathog. 2010;6(9):e1001080.
487. Cavrois M, De Noronha C, Greene WC. A sensitive and specific enzyme-based assay detecting HIV-1 virion fusion in primary T lymphocytes. Nat Biotechnol. 2002;20(11):1151–4.
488. Liu H, Wu X, Xiao H, Kappes JC. Targeting human immunodeficiency virus (HIV) type 2 integrase protein into HIV type 1. J Virol. 1999;73(10):8831–6.
489. Wu X, Liu H, Xiao H, Kim J, Seshaiah P, Natsoulis G, Boeke JD, Hahn BH, Kappes JC. Targeting foreign proteins to human immunodeficiency virus particles via fusion with Vpr and Vpx. J Virol. 1995;69(6):3389–98.
490. Loeb JE, Weitzman MD, Hope TJ. Enhancement of green fluorescent protein expression in adeno-associated virus with the woodchuck hepatitis virus post-transcriptional regulatory element. Methods Mol Biol. 2002;183:331–40.
491. Fritz J V, Didier P, Clamme J-P, Schaub E, Muriaux D, Cabanne C, Morellet N, Bouaziz S, Darlix J-L, Mély Y, de Rocquigny H. Direct Vpr-Vpr Interaction in Cells monitored by two photon fluorescence correlation spectroscopy and fluorescence lifetime imaging. Retrovirology. 2008;5.
492. Desai TM, Marin M, Sood C, Shi J, Nawaz F, Aiken C, Melikyan GB. Fluorescent protein-tagged Vpr dissociates from HIV-1 core after viral fusion and rapidly enters the cell nucleus. Retrovirology. 2015;12(88):653–98.
493. Campbell EM, Perez O, Melar M, Hope TJ. Labeling HIV-1 virions with two fluorescent proteins allows identification of virions that have productively entered the target cell. Virology. 2007;360(2):286–93.
494. Jacquot G, Le Rouzic E, David A, Mazzolini J, Bouchet J, Bouaziz S, Niedergang F, Pancino G, Benichou S. Localization of HIV-1 Vpr to the nuclear envelope: Impact on Vpr functions and virus replication in macrophages. Retrovirology. 2007;4(84):123–76.
495. Vodicka MA, Koepp DM, Silver PA, Emerman M. HIV-1 Vpr interacts with the nuclear transport pathway to promote macrophage infection. Genes Dev. 1998;12(2):175–85.
496. Fouchier RAM, Meyer BE, Simon JHM, Fischer U, Albright A V, González-Scarano

F, Malim MH. Interaction of the human immunodeficiency virus type 1 Vpr protein with the nuclear pore complex. J Virol. 1998;72(7):6004–13.

497. Popov S, Rexach M, Ratner L, Blobel G, Bukrinsky M. Viral protein R regulates docking of the HIV-1 preintegration complex to the nuclear pore complex. J Biol Chem. 1998;273(21):13347–52.

498. Le Rouzic E, Mousnier A, Rustum C, Stutz F, Hallberg E, Dargemont C, Benichou S. Docking of HIV-1 vpr to the nuclear envelope is mediated by the interaction with the nucleoporin hCG1. J Biol Chem. 2002;277(47):45091–8.

499. McDonald D, Vodicka MA, Lucero G, Svitkina TM, Borisy GG, Emerman M, Hope TJ. Visualization of the intracellular behavior of HIV in living cells. J Cell Biol. 2002;159(3):441–52.

500. Stewart M, Baker RP, Bayliss R, Clayton L, Grant RP, Littlewood T, Matsuura Y. Molecular mechanism of translocation through nuclear pore complexes during nuclear protein import. FEBS Letters. 2001. p. 498(2-3):145-9.

501. Gallay P, Stitt V, Mundy C, Oettinger M, Trono D. Role of the karyopherin pathway in human immunodeficiency virus type 1 nuclear import. J Virol. 1996;70(2):1027–32.

502. Jenkins Y, McEntee M, Weis K, Greene WC. Characterization of HIV-1 Vpr nuclear import: Analysis of signals and pathways. J Cell Biol. 1998;143(4):875–85.

503. Depienne C, Roques P, Créminon C, Fritsch L, Casseron R, Dormont D, Dargemont C, Benichou S. Cellular distribution and karyophilic properties of matrix, integrase, and Vpr proteins from the human and simian immunodeficiency viruses. Exp Cell Res. 2000;260(2):387–95.

504. Kamata M, Nitahara-Kasahara Y, Miyamoto Y, Yoneda Y, Aida Y. Importin- Promotes Passage through the Nuclear Pore Complex of Human Immunodeficiency Virus Type 1 Vpr. J Virol. 2005;79(6):3557–64.

505. Nitahara-Kasahara Y, Kamata M, Yamamoto T, Zhang X, Miyamoto Y, Muneta K, Iijima S, Yoneda Y, Tsunetsugu-Yokota Y, Aida Y. Novel nuclear import of Vpr promoted by importin a is crucial for human immunodeficiency virus type 1 replication in macrophages. J Virol. 2007;81(10):5284–93.

506. Takeda E, Murakami T, Matsuda G, Murakami H, Zako T, Maeda M, Aida Y. Nuclear exportin receptor cas regulates the NPI-1-mediated nuclear import of HIV-1 vpr. PLoS One. 2011;

507. Miyatake H, Sanjoh A, Murakami T, Murakami H, Matsuda G, Hagiwara K, Yokoyama M, Sato H, Miyamoto Y, Dohmae N, Aida Y. Molecular Mechanism of HIV-1 Vpr for Binding to Importin-α. J Mol Biol. 2016;428(13):2744–57.

508. Le Rouzic E, Belaïdouni N, Estrabaud E, Morel M, Rain J-C, Transy C, Margottin-Goguet F. HIV1 Vpr arrests the cell cycle by recruiting DCAF1/VprBP, a receptor of the Cul4-DDB1 ubiquitin ligase. Cell Cycle. 2007;6(2):182–8.

509. Fregoso OI, Emerman M. Activation of the DNA damage response is a conserved function of HIV-1 and HIV-2 Vpr that is independent of SLX4 recruitment. MBio. 2016;7(5).
510. Berger G, Lawrence M, Hué S, Neil SJD. G2/M cell cycle arrest correlates with primate lentiviral Vpr interaction with the SLX4 complex. J Virol. 2015;89(1):230–40.
511. Trotard M, Tsopoulidis N, Tibroni N, Willemsen J, Binder M, Ruggieri A, Fackler OT. Sensing of HIV-1 Infection in Tzm-bl Cells with Reconstituted Expression of STING. J Virol. 2016;
512. Okumura A, Alce T, Lubyova B, Ezelle H, Strebel K, Pitha PM. HIV-1 accessory proteins VPR and Vif modulate antiviral response by targeting IRF-3 for degradation. Virology. 2008;373(1):85–97.
513. Liu R, Lin Y, Jia R, Geng Y, Liang C, Tan J, Qiao W. HIV-1 Vpr stimulates NF-κB and AP-1 signaling by activating TAK1. Retrovirology. 2014;11(1).
514. Greenwood EJD, Williamson JC, Sienkiewicz A, Naamati A, Matheson NJ, Lehner PJ. Promiscuous Targeting of Cellular Proteins by Vpr Drives Systems-Level Proteomic Remodeling in HIV-1 Infection. Cell Rep. 2019 Apr;27(5):1579-1596.e7.
515. Fischer W, Ganusov V V, Giorgi EE, Hraber PT, Keele BF, Leitner T, Han CS, Gleasner CD, Green L, Lo C-C, Nag A, Wallstrom TC, Wang S, McMichael AJ, Haynes BF, Hahn BH, Perelson AS, Borrow P, Shaw GM, et al. Transmission of single HIV-1 genomes and dynamics of early immune escape revealed by ultra-deep sequencing. PLoS One. 2010 Aug 20;5(8):e12303–e12303.
516. Ochsenbauer C, Edmonds TG, Ding H, Keele BF, Decker J, Salazar MG, Salazar-Gonzalez JF, Shattock R, Haynes BF, Shaw GM, Hahn BH, Kappes JC. Generation of transmitted/founder HIV-1 infectious molecular clones and characterization of their replication capacity in CD4 T lymphocytes and monocyte-derived macrophages. J Virol. 2012;86(5):2715–28.
517. Ozinsky A, Underhill DM, Fontenot JD, Hajjar AM, Smith KD, Wilson CB, Schroeder L, Aderem A. The repertoire for pattern recognition of pathogens by the innate immune system is defined by cooperation between Toll-like receptors. Proc Natl Acad Sci U S A. 2000;97(25):13766–71.
518. O'Neill LAJ. Sensing the dark side of DNA. Science (80- ). 2013;339(6121):763–4.
519. Rehwinkel J, Tan CP, Goubau D, Schulz O, Pichlmair A, Bier K, Robb N, Vreede F, Barclay W, Fodor E, Reis e Sousa C. RIG-I Detects Viral Genomic RNA during Negative-Strand RNA Virus Infection. Cell. 2010;140(3):397–408.
520. Tanimura N, Saitoh S, Matsumoto F, Akashi-Takamura S, Miyake K. Roles for LPS-dependent interaction and relocation of TLR4 and TRAM in TRIF-signaling. Biochem Biophys Res Commun. 2008;368(1):94–9.
521. Yoneyama M, Suhara W, Fukuhara Y, Fukuda M, Nishida E, Fujita T. Direct

triggering of the type I interferon system by virus infection: Activation of a transcription factor complex containing IRF-3 and CBP/p300. EMBO J. 1998;17(4):1087–95.

522. Suhara W, Yoneyama M, Iwamura T, Yoshimura S, Tamura K, Namiki H, Aimoto S, Fujita T. Analyses of virus-induced homomeric and heteromeric protein associations between IRF-3 and coactivator CBP/p300. J Biochem. 2000;128(2):301–7.
523. Servant MJ, Grandvaux N, TenOever BR, Duguay D, Lin R, Hiscott J. Identification of the minimal phosphoacceptor site required for in vivo activation of interferon regulatory factor 3 in response to virus and double-stranded RNA. J Biol Chem. 2003;278(11):9441–7.
524. Mori M, Yoneyama M, Ito T, Takahashi K, Inagaki F, Fujita T. Identification of Ser-386 of Interferon Regulatory Factor 3 as Critical Target for Inducible Phosphorylation That Determines Activation. J Biol Chem. 2004;279(11):9698–702.
525. Fitzgerald KA, McWhirter SM, Faia KL, Rowe DC, Latz E, Golenbock DT, Coyle AJ, Liao S-M, Maniatis T. IKKE and TBKI are essential components of the IRF3 signalling pathway. Nat Immunol. 2003;4(5):491–6.
526. Wen X, Duus KM, Friedrich TD, De Noronha CMC. The HIV1 protein Vpr acts to promote G2 cell cycle arrest by engaging a DDB1 and cullin4A-containing ubiquitin ligase complex using VprBP/DCAF1 as an adaptor. J Biol Chem. 2007;282(37):27046–51.
527. De Iaco A, Luban J. Inhibition of HIV-1 infection by TNPO3 depletion is determined by capsid and detectable after viral cDNA enters the nucleus. Retrovirology. 2011;8:98.
528. Liu X, Guo H, Wang H, Markham R, Wei W, Yu XF. HIV-1 Vpr suppresses the cytomegalovirus promoter in a CRL4(DCAF1) E3 ligase independent manner. Biochem Biophys Res Commun. 2015;459(2):214–9.
529. Venkatachari NJ, Walker LA, Tastan O, Le T, Dempsey TM, Li Y, Yanamala N, Srinivasan A, Klein-Seetharaman J, Montelaro RC, Ayyavoo V. Human immunodeficiency virus type 1 Vpr: Oligomerization is an essential feature for its incorporation into virus particles. Virol J. 2010;7.
530. Sawaya BE, Khalili K, Gordon J, Srinivasan A, Richardson M, Rappaport J, Amini S. Transdominant Activity of Human Immunodeficiency Virus Type 1 Vpr with a Mutation at Residue R73. J Virol. 2002;74(10):4877–4881.
531. Tcherepanova I, Starr A, Lackford B, Adams MD, Routy J-P, Boulassel MR, Calderhead D, Healey D, Nicolette C. The immunosuppressive properties of the HIV Vpr protein are linked to a single highly conserved residue, R90. PLoS One. 2009 Jun;4(6):e5853.
532. Vacik J, Dean BS, Zimmer WE, Dean DA. Cell-specific nuclear import of plasmid

DNA. Gene Ther. 1999;6(6):1006–14.

533. Mesika A, Grigoreva I, Zohar M, Reich Z. A regulated, NFκB-assisted import of plasmid DNA into mammalian cell nuclei. Mol Ther. 2001;3(5Pt1):653–7.
534. Badding MA, Lapek JD, Friedman AE, Dean DA. Proteomic and functional analyses of protein-DNA complexes during gene transfer. Mol Ther. 2013;21(4):775–85.
535. Stewart M. Molecular mechanism of the nuclear protein import cycle. Nature Reviews Molecular Cell Biology. 2007. p. 8(3):195-208.
536. Gonçalves C, Ardourel MY, Decoville M, Breuzard G, Midoux P, Hartmann B, Pichon C. An optimized extended DNA kappa B site that enhances plasmid DNA nuclear import and gene expression. J Gene Med. 2009;11(5):401–11.
537. Lau A, Gray EE, Brunette RL, Stetson DB. DNA tumor virus oncogenes antagonize the cGAS-STING DNA-sensing pathway. Science (80- ). 2015;350(6260):568–71.
538. Tsang J, Chain BM, Miller RF, Webb BLJ, Barclay W, Towers GJ, Katz DR, Noursadeghi M. HIV-1 infection of macrophages is dependent on evasion of innate immune cellular activation. AIDS. 2009;23(17):2255–63.
539. Stacey AR, Norris PJ, Qin L, Haygreen EA, Taylor E, Heitman J, Lebedeva M, DeCamp A, Li D, Grove D, Self SG, Borrow P. Induction of a striking systemic cytokine cascade prior to peak viremia in acute human immunodeficiency virus type 1 infection, in contrast to more modest and delayed responses in acute hepatitis B and C virus infections. J Virol. 2009;83(8):3719–33.
540. Fitzgerald K a, McWhirter SM, Faia KL, Rowe DC, Latz E, Golenbock DT, Coyle AJ, Liao S-M, Maniatis T. IKKepsilon and TBK1 are essential components of the IRF3 signaling pathway. Nat Immunol [Internet]. 2003;4(5):491–6.
541. Schirrmacher V. Signaling through RIG-I and type I interferon receptor: Immune activation by Newcastle disease virus in man versus immune evasion by Ebola virus (Review). Int J Mol Med. 2015 Jul;36(1):3–10.
542. Lin R, Mamane Y, Hiscott J. Structural and functional analysis of interferon regulatory factor 3: localization of the transactivation and autoinhibitory domains. Mol Cell Biol. 1999;19(4):2465–74.
543. Trotard M, Tsopoulidis N, Tibroni N, Willemsen J, Binder M, Ruggieri A, Fackler OT. Sensing of hiv-1 infection in tzm-bl cells with reconstituted expression of sting. J Virol. 2016;90(4):2064–76.
544. Kogan M, Deshmane S, Sawaya BE, Gracely EJ, Khalili K, Rappaport J. Inhibition of NF-κB activity by HIV-1 Vpr is dependent on Vpr binding protein. J Cell Physiol. 2013;228(4):781–90.
545. Pollard H, Remy JS, Loussouarn G, Demolombe S, Behr JP, Escande D. Polyethylenimine but not cationic lipids promotes transgene delivery to the nucleus in mammalian cells. J Biol Chem. 1998;273(13):7507–11.
546. Zabner J, Fasbender AJ, Moninger T, Poellinger KA, Welsh MJ. Cellular and

molecular barriers to gene transfer by a cationic lipid. J Biol Chem. 1995;270(32):18997–9007.

547. De Noronha CMC, Sherman MP, Lin HW, Cavrois M V, Moir RD, Goldman RD, Greene WC. Dynamic disruptions in nuclear envelope architecture and integrity induced by HIV-1 Vpr. Science (80- ). 2001;294(5544):1105–8.
548. Fagerlund R, Melén K, Cao X, Julkunen I. NF-κB p52, RelB and c-Rel are transported into the nucleus via a subset of importin α molecules. Cell Signal. 2008;20(8):1442–51.
549. Liang P, Zhang H, Wang G, Li S, Cong S, Luo Y, Zhang B. KPNB1, XPO7 and IPO8 mediate the translocation ofNF-kappaB/p65 into the nucleus. Traffic. 2013 Nov;14(11):1132–43.
550. Fagerlund R, Kinnunen L, Kohler M, Julkunen I, Melen K. NF-{kappa}B is transported into the nucleus by importin {alpha}3 and importin {alpha}4. J Biol Chem. 2005 Apr;280(16):15942–51.
551. Kumar KP, McBride KM, Weaver BK, Dingwall C, Reich NC. Regulated Nuclear-Cytoplasmic Localization of Interferon Regulatory Factor 3, a Subunit of Double-Stranded RNA-Activated Factor 1. Mol Cell Biol. 2002;20(11):4159–68.
552. Sacramento CB, Moraes JZ, Denapolis PMA, Han SW. Gene expression promoted by the SV40 DNA targeting sequence and the hypoxia-responsive element under normoxia and hypoxia. Brazilian J Med Biol Res. 2010;43(8):722–7.
553. Ye J, Chen Z, Li Y, Zhao Z, He W, Zohaib A, Song Y, Deng C, Zhang B, Chen H, Cao S. Japanese Encephalitis Virus NS5 Inhibits Type I Interferon (IFN) Production by Blocking the Nuclear Translocation of IFN Regulatory Factor 3 and NF-κB. J Virol. 2017;91(8):e00039-17.
554. Taylor SL, Frias-Staheli N, Garcia-Sastre A, Schmaljohn CS. Hantaan Virus Nucleocapsid Protein Binds to Importin Proteins and Inhibits Tumor Necrosis Factor Alpha-Induced Activation of Nuclear Factor Kappa B. J Virol. 2009;83(3):1271–9.
555. Xu W, Edwards MR, Borek DM, Feagins AR, Mittal A, Alinger JB, Berry KN, Yen B, Hamilton J, Brett TJ, Pappu R V., Leung DW, Basler CF, Amarasinghe GK. Ebola virus VP24 targets a unique NLS binding site on karyopherin alpha 5 to selectively compete with nuclear import of phosphorylated STAT1. Cell Host Microbe. 2014;16(2):187–200.
556. Pallett MA, Ren H, Zhang R-Y, Scutts SR, Gonzalez L, Zhu Z, Maluquer de Motes C, Smith GL. Vaccinia Virus BBK E3 Ligase Adaptor A55 Targets Importin-Dependent NF-κB Activation and Inhibits CD8 + T-Cell Memory. J Virol. 2019;93(10):e00051-19.
557. Gagne B, Tremblay N, Park AY, Baril M, Lamarre D. Importin beta1 targeting by hepatitis C virus NS3/4A protein restricts IRF3 and NF-kappaB signaling of IFNB1 antiviral response. Traffic. 2017 Jun;18(6):362–77.

558. Hotter D, Krabbe T, Reith E, Gawanbacht A, Rahm N, Ayouba A, Van Driessche B, Van Lint C, Peeters M, Kirchhoff F, Sauter D. Primate lentiviruses use at least three alternative strategies to suppress NF-κB-mediated immune activation. PLoS Pathog. 2017;
559. Stacey AR, Norris PJ, Qin L, Haygreen EA, Taylor E, Heitman J, Lebedeva M, DeCamp A, Li D, Grove D, Self SG, Borrow P. Induction of a Striking Systemic Cytokine Cascade prior to Peak Viremia in Acute Human Immunodeficiency Virus Type 1 Infection, in Contrast to More Modest and Delayed Responses in Acute Hepatitis B and C Virus Infections. J Virol. 2009;83(8):3719–33.
560. Ross EK, Buckler-white AJ, Rabson AB, Englund G, Martin MA. Contribution of NF-KB and Spl Binding Motifs to the Replicative Capacity of Human Immunodeficiency Virus Type 1 : Distinct Patterns of Viral Growth Are Determined by T-Cell Types. J Virol. 1991;65(8):4350–8.
561. Chen BK, Feinberg MB, Baltimore D. The kappaB sites in the human immunodeficiency virus type 1 long terminal repeat enhance virus replication yet are not absolutely required for viral growth. J Virol. 1997;71(7):5495–504.
562. Greenwood EJD, Matheson NJ, Wals K, van den Boomen DJH, Antrobus R, Williamson JC, Lehner PJ. Temporal proteomic analysis of HIV infection reveals remodelling of the host phosphoproteome by lentiviral Vif variants. Elife. 2016;5(September2016):e18296.
563. Hilger M, Mann M. Triple SILAC to determine stimulus specific interactions in the Wnt pathway. J Proteome Res. 2012;